AD NUMBER

AD479833

NEW LIMITATION CHANGE

TO

Approved for public release, distribution unlimited

FROM

Distribution authorized to U.S. Gov't. agencies and their contractors; Administrative/Operational use; Mar 1966. Other requests shall be referred to Office of Naval Research, Arlington VA 22217-0000

AUTHORITY

ONR notice 27 Jul 1971.

479 833

(2)

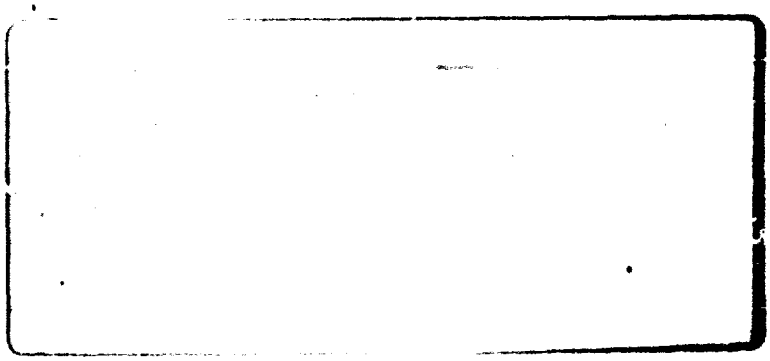

DECO Electronics, Inc.

Boston Boulder Leesburg Washington

VLF PROPAGATION AND NOISE MEASUREMENTS IN THE PACIFIC

REPORT NO. 30-F-12

AUTHOR

E. L. Maxwell

March 1966

Navy Department — Office of Naval Research

Washington, D. C.

Contract NOnr 3387(00) — Nr. 371-590 — Dated: 15 December 1960

COPY NO. 17

DECO ELECTRONICS, INC.

BOSTON BOULDER LEESBURG WASHINGTON, D.C.

TABLE OF CONTENTS

ABSTRACT

During May, June and July of 1965 the received field intensity from both VLF stations on Oahu Island, Hawaii were measured at Tokyo, Japan; Guam; and Boulder, Colorado. Atmospheric noise field intensities were also measured at all three sites and relative phase variations of the received signals were measured at Japan and Guam. This program presented a unique opportunity to study VLF propagation, since the paths from Oahu to Guam and Japan were almost the same length and were both all sea paths. The availability of two transmitters on Oahu which permitted simultaneous measurements at two VLF frequencies over the same path was also a unique opportunity. The results of this measurement program are presented in a number of ways in this report to afford maximum opportunity to study the propagation and atmospheric noise conditions.

The results show 22.3 and 24.0 kHz to be the best frequencies of those measured for the Oahu to Guam and Japan paths. Significantly, the diurnal variations of field intensity were very repeatable even during sunset and sunrise transition times which indicates that better predictions of VLF field intensities may be possible with an improved propagation model.

Means, medians, standard deviations, cumulative probabilities and diurnal variations of signal, noise and signal-to-noise-ratios have been computed, plotted and tabulated for all frequencies and for four hour time blocks and twenty-four hour periods. In addition, continuous plots of signal data for Japan and Guam are presented.

1. INTRODUCTION

Although many advances have recently been made in the science and art of predicting VLF propagation characteristics and atmospheric noise levels, there still exist unknown factors and discrepancies between predictions and results. The refinement of prediction techniques calls for refined field measurements to attempt to resolve some of the problems. This report presents the results of such a measurement program during May, June and July of 1965. The program, equipment, field operations, final results and analysis of results are presented herein.

2. DESCRIPTION OF PROGRAM AND EQUIPMENT

2.1 Transmitter and Receiver Locations

Figure 1 shows a map of the World indicating the location of transmitters and receiver sites. The location of two transmitting facilities on Oahu Island afforded the unique opportunity to measure propagation characteristics along identical paths at two frequencies. Receiving sites located both west and east of the transmitters offered opportunity to determine directional and latitude effects.

2.2 Frequencies and Parameters Measured

Frequencies of 16.6, 19.8, 22.3, 24.0 and 26.1 kHz were used at various times throughout the tests. The Haiku transmitting facility was primarily operated at 19.8 kHz as a means of providing a reference transmission for better delineation of effects seen at other frequencies. Some transmissions at 16.6 kHz were made from Haiku on a short term basis. The Lualualei transmitter facility transmitted on all of the frequencies at various times during the tests.

The receiving sites at Guam and Japan were equipped with identical equipment designed to measure the following:

1. The vertical electric field intensity from both transmitters.
2. Phase variations of the arriving signal from both transmitters.
3. The average vertical electric field intensity of the atmospheric noise at the frequencies of transmission.
4. Semi-automatic recording of atmospheric noise field intensities at frequencies from 30 Hz to 30 kHz.
5. Amplitude probability distributions of atmospheric noise at frequencies from 50 Hz to 30 kHz.
6. Direction of arrival of atmospheric noise.

At Boulder equipment was available only for measuring the vertical electric field intensity of the arriving signals and of the atmospheric noise at the frequency of transmission.

2.3 Equipment Description

Two Tracor VLF receivers were shipped to both Guam and Japan for amplitude and phase measurements. Ten foot whips and associated couplers were used with these receivers for measuring the vertical electric field. Rubidium frequency standards were used for the reference frequency of these instruments. Hewlett Packard 302-A Wave Analyzers were also shipped to each station as a back up instrument for obtaining vertical electric field intensities and for atmospheric noise measurements. These instruments were to be used with 30 foot whips and their associated coupler. Instrumentation for average noise measurements and amplitude probability distributions were included in the equipment at each station. Loop antennas and other associated equipment was available at each site for calibration checks and operational checks of the equipment. Esterline Angus Recorders were used to record vertical electric field intensities, atmospheric noise levels and phase variations. Amplitude probability distributions were recorded manually. The noise measuring instrumentation was semi-automatic providing for five minute integrations at twelve different frequencies which recycled automatically

every hour. An electronically advanced camera system with associated amplifiers and crossed loops was available at both sites for making direction of arrival measurements on the atmospheric noise.

3. FIELD OPERATIONS

The operation was beset with difficulties and delays from the outset. The normal problems of complex operations in the field were multiplied by the tight time schedule, power source problems in both Japan and Guam and shipping damage. The late arrival of the equipment at Boulder resulted in inadequate training of personnel and inadequate laboratory testing of the equipment prior to shipment. Some of the special equipment such as the semi-automatic noise measuring gear and the direction of arrival equipment had to be shipped unfinished for completion in the field. Some of the equipment was temporarily delayed in shipping overseas and much of it arrived in a somewhat damaged condition.

The final site locations selected at both Guam and Japan were little used airfields. Site location and quarters in Japan were excellent and once the 50 cycle power problem was compensated for, this field site was very adequate and provided good support. The field site at Guam required operation from a tent which presented some operational problems, but the most serious difficulty was involved with the portable 10 kilowatt generator provided for a power source. The equipment proved to be unreliable and on several occasions "ran away" causing difficulties with the equipment due to excessive voltage. Lack of protection for the equipment and lack of a reliable power source resulted in considerable loss in data since it was impossible to man the sites twenty-four hours a day for the entire measurement period. In other words, even though the equipment was capable of recording data in an unmanned operation this could not be done because of possible damage from a "run away" generator.

In part, because of the field conditions and in part because of inadequate preparations prior to going to the field, the data obtained from the operation at Guam consisted of continuous phase data from both transmitters and vertical electric field intensity data from one transmitter at a time. The vertical electric field intensity data was obtained with a 302-A wave analyzer since adequate calibration of the Tracors at this site for amplitude measurements was not accomplished. The automatic noise equipment was in operation for only the last few weeks and this data is in question and is not considered reliable. Because of the bandwidth of the 302-A wave analyzer, noise measurements during the open key operation for the transmitters were generally too low to obtain an accurate value. The field intensity data obtained at Guam appears to be very good, however, and the phase data will probably prove of value if completely analyzed at some later date.

At the Japan site some vertical electric field intensity data was obtained at two frequencies simultaneously and single frequency measurements were made for the greater percentage of time. Phase measurements at Japan also were obtained for most of the measurement period. The automatic noise equipment at Japan was put into operation during June and an adequate supply of noise data was obtained at this site. Amplitude probability distributions of the atmospheric noise were also obtained at this site. Noise measurements at the exact frequencies of transmission were also impossible at Japan because of the bandwidth problems.

Measurements of the inverse distance field of both transmitters were made in Hawaii as a means of determining close relationships between transmitter current and radiated power. This information was used to reduce and analyze the data obtained and is presented in Appendix B.

Both noise and vertical electric field intensity data were obtained at Boulder on a continuous basis with very little difficulty. The operation at Boulder was, of course, under laboratory conditions with a reduced number

of measurements. No direction of arrival data was obtained which was considered to be of sufficient quality for presentation in this report.

4. FINAL RESULTS

In spite of the many difficulties encountered the program produced a large amount of high quality data, the analysis of which, has proved to be most useful and of value to an understanding of VLF propagation and VLF-ELF atmospheric noise. The data will be presented in several different forms in this section as a means of gleaning the maximum amount of information from it.

4.1 Continuous Signal Plots

Data from Guam and Japan have been plotted together to provide a detailed study of the difference in the propagation characteristics along these two paths of almost identical length. Both paths are all sea paths, the only difference being in their direction of propagation. Figure 2 presents the data obtained at 16.6 kHz during the two, four day periods this frequency was transmitted. Such a small amount of data was obtained that very little can be said except that the results from the two paths appear to be similar.

Figure 3 presents the large volume of data obtained at 19.8 kHz. Although the mean field intensities at the two locations are very close to the same, a close examination of the data reveals significant differences. It should be remembered that the time for all of this data is Universal Time and the all daylight conditions for the propagation path occurs from approximately 2000 UT to 0600 UT. Although there is some fluctuation, there is generally close correlation between the field intensity at the two locations during all daylight path conditions. It is noted, however, that nighttime values at Japan were generally 2 to 5 db higher than the daytime values, whereas at Guam the nighttime field intensities at this frequency were from 1 to 10 db lower than the daytime values. Examination of Figure D-1

in Appendix D indicates rather stable conditions should exist at a distance of 6 megameters during daylight hours, but that considerable instability might be expected during the night. This is borne out by the results shown in Figure 3. In addition, since the difference in distance of the two paths is less than 100 kilometers we must assume that the difference in nighttime field intensities at the two sites must result from different phase velocities along the two paths. Examination of Figures 4, 5 and 6 and Figures D-2, D-3 and D-4 tend to further support this analysis. From Figure D-4 we note that we might expect greater variations between Japan and Guam during daytime hours than at night for 26.1 kHz. Figure 6 tends to bear this out since we observe that nighttime values at Japan and Guam, despite their scatter, are approximately the same whereas the daytime fields at Guam are 6 to 8 db higher than those at Japan. Intermediate conditions are seen to exist at 22.3 and 24.0 kHz.

At all frequencies it is noted that considerable stability exists during daylight hours.

Simultaneous measurements were made at Japan at two frequencies during the 16 days shown in Figure 7. Although normalized absolute field intensities may show as much as 10 db difference between the two frequencies, it is interesting to note that the variation in field intensity at the two frequencies is almost identical with the exception of nighttime hours when more scatter is seen at the higher of the two frequencies. With the two, eight day periods of data arranged one above the other, and since the same pairs of frequencies were used for the eight day periods, it is possible to compare results obtained two weeks apart. The repeatability of the results seen on this Figure indicates that with greater understanding of the earth ionospheric waveguide that calculations of expected VLF field intensities may be possible even during the nighttime and transitional periods. It appears that there is not so much a scattering of data as there is a lack of understanding of the variations seen.

4.2 Diurnal Signal Plots

Figures 8 through 12 are the plots of received signal field intensity at Japan as a function of time of day. It is important to note that these values are plotted against Universal Time and that local time is equal to UT + 9. The median for each group of hour and half hour values was computed and a line drawn between these median points. The zig zag effect which can be noted particularly for the results at 22.3 kHz and 26.1 kHz is the result of a change in propagation conditions during the two month period which shows up here because half hour values were obtained only during the first month. Similar results for Guam are shown in Figures 13 through 17 and the results for Boulder are shown in Figures 18 through 22. It is interesting to note that both Japan and Guam experienced changes in propagation characteristics from the first month to the second month whereas the Hawaii to Boulder path does not exhibit such a change. There are significant differences also which can be noted between the changes observed at Japan and Guam, such as at 22.3 kHz the half hour medians plot consistently higher than the hourly medians during the daytime at both Japan and Guam whereas during the night at Japan the half hour medians are still higher than the hourly medians, but at Guam they are lower. This indicates that during the first month of the measurements, propagation was better at all hours at Japan than during the second month, whereas at Guam propagation during the first month was better during the day and worse during the night. A considerable refinement in our understanding of ionospheric and latitude changes as a function of season will be required before our prediction capabilities can account for such variations. Sunrise and sunset times are at the surface and are for June 15.

4.3 Probability Distributions of Signal

Figures 23 through 37 give the plots of the probability distribution of the measured signal intensity at all three locations, Japan, Guam and Boulder.

Only hour data was used to prepare the probability distribution plots for Japan and Guam since inclusion of half hour data would tend to bias the results in favor of the conditions existing during the first month of the measurement period. The generally inverted S shape of these curves is expected because of the relative stability of the signal during a large portion of the day and the considerable instability experienced during the transition periods from day to night and night to day. The variation of the signal under such conditions is not random and we would not expect the straight line plot of a normal distribution.

4.4 Atmospheric Noise Measurements in Japan

Figures 38 through 43 present the results of atmospheric noise measurements obtained in Japan. A measurement was taken approximately once an hour at each frequency for a period of 31 days from June 14, 1965 to July 14, 1965. Each measurement consisted of a five minute integration of the noise in a 7 Hz bandwidth. Each of these five minute integrations have been plotted on the curves shown. The data has been presented in four hour time blocks rather than for hourly values for comparison with CCIR predictions and other measurements presented in a similar manner. The data has been normalized to a 1 Hz bandwidth for this presentation.

Continuous noise data was not obtained at the Guam site. The data which was obtained has been used only for the preparation of signal to noise probability distributions which will be presented in Section 5.

The atmospheric noise data obtained in Japan at 10, 20 and 30 kHz was also plotted versus time of day to determine diurnal variations. These plots are given in Figures 44 through 46. The reduction in local thunderstorm activity and activity in the Indonesian area is noted on these curves during the hours 2000 to 0400 UT. A slight dip can also be noted at about 1000 UT corresponding to the minimum worldwide thunderstorm activity. The data was normalized

to a 100 Hz bandwidth for this presentation.

Atmospheric noise measurements were also obtained at Boulder and the diurnal plots of the Boulder noise data at each of the transmitter frequencies are shown in Figures 47 through 51. It should be noted that local time in Boulder is given by UT - 7 hours. A decrease in local activity is noted for the hours 0800 to 1700 UT. The local activity tends to mask any evidence of the decrease in worldwide activity at 1000 UT. The bandwidth is 100 Hz.

The probability distributions of the rms atmospheric noise field intensities for Japan and Boulder are shown in Figures 52 through 67. It will be noted that this data more generally approaches a log normal distribution than did the signal data. There is still, however, some tendency for an inverted S shape indicating that the data is not entirely random. This may be due to the relatively small number of data points available. All of the probability plots of noise have been computed from all data obtained during the entire two month period. The Japan data is normalized to a 1 Hz bandwidth, Boulder to a 100 Hz bandwidth.

It will be noticed when examining the noise data for Boulder that there are abnormal differences in mean or median field intensities for the relatively slight difference in the frequencies measured. This is logically explained by noting that noise measurements at Boulder were not made continuously at each frequency, but rather were made in four day groups corresponding to the transmitted frequencies during which considerable change in local thunderstorm activity could occur.

4.5 Amplitude Probability Distributions

Amplitude Probability Distributions were obtained only in Japan during this program. In addition to providing information regarding the cumulative characteristics of the atmospheric noise at the frequencies studied, these APD's

(Amplitude Probability Distributions) provide the only measurement of the average to rms conversion factor necessary to convert the measurements of average electric field intensity to rms electric field intensity. The interim reports, prepared during the progress of the measurements, used CCIR predictions of the average to rms conversion factor, since, of course, the APD's were not available at the time. Over 100 APD's were taken during the two month measurement period and were reported in an interim report. Two samples at each of the frequencies used are included in this final report as examples of low and wide dynamic range conditions experienced during the measurement period. Table 1 shows the minimum and maximum dynamic range (90 percent to 0.0001 percent exceedance level) observed during the two month period in Japan. The sample APD's shown in Figures 68 through 85 are not necessarily those that gave the minimum and maximum dynamic ranges but are representative of the results obtained. A plot of rms to average conversion factors obtained from the APD's is given in Figure 86 along with values obtained at other locations at other times. The heavy curve shown indicates the values used for converting the average noise measurements to rms values. Since Malta, Summer and Japan, Summer, conditions are similar, and since the data obtained at Japan was limited in quantity, the results from both locations were considered in constructing the conversion curve.

5. ANALYSIS OF RESULTS

In addition to the reduction of the various collections of signal and noise data and their presentation in various forms individually, signal-to-noise-ratios have been computed from the data and are presented in this section. Since the variations of signal and atmospheric noise field intensities are both functions of time of day and other propagation variables, they cannot be treated as being non-correlated. It is important, therefore, when computing the diurnal pattern and cumulative distribution of signal-to-noise-ratios, that the signal and noise field intensities used, be only those measured at or near the same real time.

Since the Japan noise data was obtained with instrumentation completely separate from that used for determining signal field intensities, the analysis of the data in terms of signal-to-noise-ratios required the selection of signal data and noise data which had been measured within 30 minutes of each other. Although this resulted in a reduction in the number of data points for signal-to-noise-ratios compared to the total number of data for signal or noise separately, it was considered necessary to analyse the data in this manner to obtain valid results.

As was mentioned earlier, much of the noise data at Guam did not yield absolute field intensities because of the dynamic range limitations of the field intensity equipment and/or equipment noise levels. Therefore, diurnal plots of signal-to-noise-ratios for Guam are not available. The chart recordings obtained, however, do provide measurements of the low signal-to-noise-ratios and also permit the assignment of greater than values to signal-to-noise-ratios. It was possible, therefore, to manually tabulate the low signal-to-noise-ratios and greater than values. The collection of these data permitted the calculation and plotting of the cumulative distribution of the low signal-to-noise-ratios or high probability values. All of the results presented in the following sub sections have been normalized to a bandwidth of 100 Hs and a transmitter radiated power of 1 kilowatt.

Appendix C describes methods used to compute the signal-to-noise-ratios described herein.

5.1 Diurnal Signal-to-Noise Plots

Figures 87 through 91 are diurnal plots of signal-to-noise-ratios for Japan and Figures 92 through 96 are diurnal plots of signal-to-noise-ratios as measured at Boulder. Sunrise and sunset times were computed at the earth's surface on June 15.

An examination of Figures 87 through 91 shows very similar diurnal

variations of the signal-to-noise-ratios with the exception of 16.6 kHz which indicates a generally poor signal-to-noise-ratio from sunset to sunrise. The results for 19.8, 22.3 and 24.0 kHz are especially similar and in this normalised form indicate that for a given power radiated equivalent communications might be expected at these frequencies. Reference to Appendix B, however, which shows a general increase in radiated power with an increase in frequency would indicate that better results might be obtained at the two higher frequencies. At 26.1 kHz, generally lower normalized signal-to-noise-ratios are indicated.

When examining Figures 92 through 96 for Boulder it should be noted that local time is now UT - 7 not UT + 9 as was the case for the Japan data. The data for 16.6 and 19.8 kHz show a reduced diurnal variation with a broad sunset effect from 0200 to 0500 UT and a short sunrise dip at 1500 UT. The higher frequencies show an increasingly greater reduction in signal during the sunrise and sunset periods with markedly higher signal-to-noise-ratios during nighttime hours. The sunset effect is consistently spread over a number of hours from 0200 to 0500 with the minimum signal-to-noise-ratio changing with frequency from 0330 at 19.8 to 0500 at 22.3 kHz. The sunrise effect is the same at all frequencies with a sharp dip in signal-to-noise-ratio occurring consistently at 1500 UT. The saw tooth effect or peaks or valleys occurring on the half hour and hour for the plot of median signal-to-noise-ratios is in this case an indication of a change in atmospheric noise conditions from the first half of this two month period relative to the second half since such a sig zag effect was not noted for signal data at Boulder. Increased local thunderstorm activity for the second 30 day period resulted in a lower signal-to-noise-ratio as expected.

5.2 Probability Distributions of Signal-to-Noise-Ratio

Figures 97 through 101 are plots of the cumulative distribution of measured signal-to-noise-ratios for Japan, Figures 102 through 108 are similar figures for Guam and Figures 109 through 113 are for Boulder. It is important

to remember that the Japan data was obtained by interpolation of noise data measured at 10, 20 and 30 kHz to the frequencies of interest and by selecting signal and noise data measured during the same half hour period. Figures 102 through 108 for Guam were manually computed as previously described and it should be noted that data for Lualualei and Haiku have been presented separately to provide a comparison of the results with this technique. It is encouraging to note that Lualualei and Haiku are in close agreement. The data for Boulder includes all data collected during the two month period and it is noted that with this very much greater number of data points, approximately 10 times the data available from Japan, that the plots are very nearly log normal.

These plots permit the determination of the percentage of time that a communications system requiring a given signal-to-noise-ratio will be effective in these areas.

Complete details on the methods of computation for these cumulative distributions is given in Appendix C.

5.3 Means, Medians and Standard Deviations

Tables 2 through 12 give the computed values for the mean, median and standard deviation of signal, noise and signal-to-noise-ratio for Japan, Guam and Boulder. Four hour time block presentations are included along with the values for all twenty-four hours combined. There were no computations for noise and signal-to-noise-ratio for Guam since the noise data collected at that location was incomplete. For Japan and Guam the half hour data was omitted from computations for the signal values since its inclusion would have weighted the results in favor of the first half of the two month period. The Japan noise and signal-to-noise computations were, of course, the selected data as previously described which covered a 31 day period. All data collected at Boulder was used in the Boulder computations.

Tables 13 and 14 give the computations of standard deviation, mean and median values for the atmospheric noise data obtained in Japan at frequencies

from 20 Hz to 30 kHz. In contrast to the noise data used to obtain signal-to-noise-ratios, this data has been normalized to a 1 Hz bandwidth instead of a 100 Hz bandwidth.

The equations and methods used in computing the standard deviation, mean and medians as given in these tables are described in detail in Appendix C.

6. RESULTS OF PHASE MEASUREMENTS

The analysis of the phase data to date has been very time consuming and disappointing. Phase jumps and excessive phase drift of the transmitter frequency standard, the receiver frequency standard or both has rendered much of the data extremely difficult, if not impossible to analyze. In addition, we find numerous occasions when the Tracor phase receivers lost tract or were shut down for one reason or another, including primary power failures. Given sufficient time to compare results between measurements made at the same time with different pieces of equipment and to correlate phase discontinuities with transmitter records, a large quantity of good and useful phase data could be obtained from the raw data in hand. Since it was considered that the phase data was of lesser importance than the amplitude and signal-to-noise-ratios, the analysis of the phase data was left until last. Time and fiscal limitations and the difficulties described above have limited the amount of data available for presentation in this report.

Figures 114 through 118 present the results of the data analyzed at this time. Figures 114 and 115 show the diurnal phase variations as measured at Japan and Guam during the four day period from 26 June to 29 June 1965. The phase variations at Japan are reversed from those at Guam and are reversed from those predicted by theory. Although this could have been caused by improper connections of the equipment there is no record to indicate that such was the case. We are not discounting the fact that this could have

happened, however. The discontinuity indicated on Figure 115 indicates a phase jump which could not be accurately determined. The phase plot from 0800 to 2400 on the 28th of June was arbitrarily positioned such that the relative phase observed at 2400 hours on the 27th of June was identical to that at 2400 hours on the 28th of June.

Figure 116 shows the diurnal variation of phase occurring on the 17th of June at a frequency of 22.3 kHz in Japan. Assuming the plotting of the phase variations following the discontinuity has been accurately positioned, it appears that phase lags occur at sunrise and sunset but the phase during the nighttime and daytime periods is approximately the same.

Figures 117 and 118 present the diurnal variation of phase at 26.1 kHz for the period 22 June to 25 June. A much greater diurnal variation is noted at Japan than at Guam. It is particularly interesting to note that this four day period immediately preceding the four day period presented in Figure 114 and that a normal diurnal variation of phase was obtained at 26.1 kHz whereas a reversed diurnal variation was obtained at 19.8 kHz. There is no reason to believe that any changes in the equipment connections were made between these two four day records. Further comparisons of Figures 114, 116 and 117 would lead one to believe that at 19.8 kHz in Japan a reversed phase variation was obtained, at 22.3 kHz no significant nighttime to daytime variation in phase was observed and that at 26.1 kHz a significant and normal phase variation was observed.

As mentioned above the examination of considerable additional data should be done before any conclusions are reached concerning the diurnal phase variations at these locations.

7. CONCLUSIONS

The primary conclusion which this data leads one to make is simply that the state-of-the-art today is not adequate for accurately predicting diurnal

variations of VLF field intensities. In fact, it is barely accurate for the prediction of monthly means and medians. This is especially true at frequencies above 20 kHz.

This measurement program has resulted in a significantly greater understanding of field intensities and signal-to-noise-ratios in the western Pacific region. For communications between NPM and this western Pacific area, either of the frequencies 22.3 or 24.0 kHz should result in significantly improved communications during this season than 16.6, 19.8 or 26.1 kHz. It should not be assumed that this will be true for other seasons.

The opportunity to simultaneously measure field intensities over identical or similar paths at identical frequencies and to make measurements at different frequencies over the same path simultaneously has proven to be of significant value. The repeatability of diurnal variations over long periods of time and some significant differences noted over very similar paths as a function of frequency provide an unparalleled opportunity for improving our understanding of VLF propagation.

It is interesting to note that a change in procedure (eliminating half hour measurements) from the first 30 day period to the second 30 day period accentuated changes in propagation characteristics and atmospheric noise levels. These differences might never have been noted without this fortuitous change in operation. This should be kept in mind for future programs.

Finally it can be stated without reservation that, although very significant results have been forthcoming from this program, that they could have been obtained with much less difficulty and in the long run, in less time had the operational schedule been planned more realistically or the number of measurement programs reduced significantly. This too should provide guidance for future programs.

It is recommended that further analysis of this data be made, in

particular, the phase data available and that comparisons of the data be made with more rigorous computations of field intensity including the effects of mode conversion at the sunrise-sunset interfaces. It is obvious that some variation in the characteristics of the ionosphere for the paths must also be considered.

8. ACKNOWLEDGEMENTS

The author wishes to acknowledge the considerable effort put forth by all personnel involved in the field measurements, in particular the following individuals: Robert R. Morgan, David B. Reimer, Harvey D. Runty, Edward H. Whelan, Dennis Smith, Thomas Burdick and Roland D. Croghan, all of DECO; Fred Williams and Edward Bourque of USNUSL and various other Naval personnel stationed at Japan and Guam. Acknowledgement is also given to Donald L. Stone for his efforts in data reduction and data preparation. I also want to express my thanks to Bill Garner, Frank Rhoads, Frank Malone, Commander Stephan and Ed Wolkoff for extremely useful consultations held at various times and the several recommendations made by them.

TABLE 1

Dynamic Range (90% to 0.0001% Exceedance Levels) of Atmospheric Noise Observed in Japan.

Freq. Hz	Minimum	Maximum
140	47	61
320	39	61
520	43	68
1 K	43	68
3 K	36	62
5 K	36	72
10 K	37	73
20 K	41	67
30 K	41	60

TABLE 2

Standard Deviation, Mean and Median of All Hourly Signal Data
From Japan For Four Hour Time Blocks.

Freq. (kHz)		00-04	04-08	08-12	12-16	16-20	20-24
16.6	STD DEV=	2.77	4.66	6.06	5.08	3.07	0.91
	NO. PTS.=	14	19	11	10	7	5
	MEAN/MEDIAN=	31.5/31.0	25.9/26.1	23.1/21.7	24.3/23.4	24.4/24.7	28.2/27.9
19.8	STD DEV=	1.66	5.90	4.71	4.02	5.65	2.28
	NO. PTS.=	99	98	104	109	104	116
	MEAN/MEDIAN=	29.1/28.9	23.8/24.2	25.6/24.2	30.8/30.6	23.0/23.2	27.3/27.1
22.3	STD DEV=	2.86	4.02	5.81	3.81	6.52	2.40
	NO. PTS.=	36	30	25	25	20	30
	MEAN/MEDIAN=	30.1/28.3	25.3/25.1	28.4/28.6	34.1/33.6	26.8/25.8	27.4/26.5
24.0	STD DEV=	1.80	9.07	7.14	2.60	8.15	1.90
	NO. PTS.=	39	41	37	36	37	41
	MEAN/MEDIAN=	24.7/24.9	23.2/19.9	24.5/20.7	29.5/29.9	21.4/20.9	23.1/22.9
26.1	STD DEV=	0.91	5.90	4.98	5.21	5.63	1.30
	NO. PTS.=	36	35	30	35	34	42
	MEAN/MEDIAN=	20.0/19.9	15.2/16.3	16.3/14.7	24.6/23.9	15.0/14.1	18.9/18.9

Normalized to 1 KW power.
Mean/Median in db rel to 1 μv/m.
Standard Deviation in db.

TABLE 3

Standard Deviation, Mean and Median of Selected Noise From Japan For Four Hour Time Blocks.

Freq. (kHz)		00-04	04-08	08-12	12-16	16-20	20-24
16.6	STD DEV=	2.88	1.51	2.05	0.58	2.05	1.84
	NO. PTS. =	6	8	10	4	4	5
	MEAN/MEDIAN=	38.7/37.1	44.0/44.3	45.8/45.6	46.1/46.2	45.9/44.5	43.3/44.0
19.8	STD DEV=	2.34	2.68	2.96	2.03	2.13	2.07
	NO. PTS. =	22	22	29	30	25	33
	MEAN/MEDIAN=	36.2/35.8	41.0/40.9	39.8/39.4	41.5/41.6	39.5/39.2	35.6/35.0
22.3	STD DEV=	5.70	5.98	2.31	1.65	3.23	3.03
	NO. PTS. =	8	8	8	8	10	16
	MEAN/MEDIAN =	41.2/39.3	44.2/42.8	38.4/38.1	41.1/40.6	40.0/38.8	35.6/33.9
24.0	STD DEV=	0.66	1.48	1.65	3.15	1.68	1.96
	NO. PTS. =	6	7	4	5	5	8
	MEAN/MEDIAN=	32.3/32.0	37.6/37.5	37.2/37.8	36.7/37.5	36.9/36.7	33.2/32.8
26.1	STD DEV=	1.41	2.98	3.51	1.63	1.59	1.55
	NO. PTS. =	10	4	2	7	7	7
	MEAN/MEDIAN =	32.4/32.0	38.8/38.7	41.0/40.3	40.9/41.0	36.3/36.3	32.7/32.3

Normalized to 100 Hz BW.
Mean/Median in db rel to 1 μv/m.
Standard Deviation in db.

TABLE 4

Standard Deviation, Mean and Median of Signal to Noise Ratio
From Japan For Four Hour Time Blocks.

Freq. (kHz)		00-04	04-08	08-12	12-16	16-20	20-24
16.6	STD DEV=	2.19	5.70	5.24	4.20	3.08	2.71
	NO. PTS. =	6	8	10	4	4	5
	MEAN/MEDIAN=	-7.7/-7.6	-16.7/-15.8	-22.3/-22.6	-26.0/-27.0	-19.8/-19.4	-14.5/-16.1
19.8	STD DEV=	2.73	9.28	6.92	3.93	5.53	2.65
	NO. PTS. =	22	22	29	30	25	33
	MEAN/MEDIAN=	-7.7/-7.7	-16.6/-18.9	-13.5/-15.8	-10.4/-11.1	-16.1/-15.9	-8.8/-8.7
22.3	STD DEV=	5.06	6.81	5.50	2.83	4.29	3.25
	NO. PTS. =	8	8	8	8	10	16
	MEAN/MEDIAN=	-10.8/-11.2	-15.1/-16.6	-8.8/-8.3	-9.7/-11.3	-12.2/-12.0	-8.8/-8.1
24.0	STD DEV=	1.25	4.91	10.17	4.12	1.60	2.47
	NO. PTS. =	6	7	4	5	5	8
	MEAN/MEDIAN=	-9.5/-9.5	-19.4/-20.9	-11.0/-15.8	-8.4/-8.6	-15.6/-15.0	-10.2/-9.9
26.1	STD DEV=	1.76	7.48	3.51	3.13	3.72	2.62
	NO. PTS. =	10	4	2	7	7	7
	MEAN/MEDIAN=	-11.7/-11.4	-21.3/-22.9	-28.8/-29.4	-14.3/-16.2	-22.7/-24.0	-13.4/-13.3

31 Days of Interpolated Data.
Normalized to 100 Hz BW and 1 KW Power.
Mean/Median in db.
Standard Deviation in db.

TABLE 5

Standard Deviation, Mean and Median of Signal, Noise, and Signal to Noise Ratio From Japan.

Freq. (kHz)	Number of Data Pts.	Standard Deviation of Signal	Noise	S/N Ratio	Mean	Median
16.6	62	5.71			26.9	26.0
	37		3.32		44.3	44.3
	37			7.82	-15.9	-17.4
19.8	223	5.73			26.6	26.3
	161		3.34		39.2	38.7
	161			7.03	-11.4	-12.1
22.3	66	4.76			27.5	27.0
	33		5.16		41.6	40.8
	33			6.09	-11.1	-11.8
24.0	81	5.68			23.1	22.4
	35		2.86		35.7	35.8
	35			6.34	-11.7	-11.5
26.1	83	5.53			19.3	18.9
	37		4.01		36.7	35.0
	37			6.88	-15.3	-16.0

31 Days of Selected Data
Normalized to 1 KW Power and 100 Hz BW.
All in db or db rel to 1 μv/m.

TABLE 6

Standard Deviation, Mean and Median
For All Hourly Signal Data From Japan.

Freq. (kHz)	Number of Data Pts.	Standard Deviation	Mean	Median
16.6	66	5.58	26.9	26.3
19.8	630	5.42	27.1	26.8
22.3	166	5.24	29.2	27.5
24.0	231	6.83	24.7	23.4
26.1	212	5.77	19.1	18.4

Normalized to 1 KW Power.
All in db or db rel to 1 μv/m.

TABLE 7

Standard Deviation, Mean and Median of Hourly Signal Data From Guam For Four Hour Time Blocks.

Freq. (kHz)		00-04	04-08	08-12	12-16	16-20	20-24
16.6	STD DEV=	1.78	6.46	3.29	5.76	4.60	3.66
	NO. PTS. =	18	17	16	17	14	17
	MEAN/MEDIAN =	30.0/30.0	25.4/23.7	19.8/19.6	19.1/19.5	21.3/22.5	26.5/26.3
19.8	STD DEV=	2.78	7.08	5.89	7.24	5.08	3.74
	NO. PTS.=	73	86	84	86	78	88
	MEAN/MEDIAN=	31.4/30.6	27.1/26.6	26.3/24.9	28.8/26.6	23.5/22.2	30.3/29.0
22.3	STD DEV=	3.48	8.20	4.67	3.55	3.86	2.63
	NO. PTS. =	55	62	51	53	47	54
	MEAN/MEDIAN=	30.3/30.0	25.9/26.5	23.7/23.8	23.7/23.3	24.2/23.2	29.4/29.0
24.0	STD DEV=	1.67	6.60	7.33	5.21	6.59	7.04
	NO. PTS. =	54	65	83	89	70	69
	MEAN/MEDIAN=	30.1/30.3	24.4/24.4	22.5/21.3	26.1/24.9	22.7/20.6	28.5/27.4
26.1	STD DEV=	3.77	6.81	7.79	5.09	6.83	6.90
	NO. PTS. =	45	53	53	61	54	64
	MEAN/MEDIAN=	26.7/26.9	21.1/21.7	26.4/26.2	29.2/29.9	22.7/18.9	23.5/22.6

Normalized to 1 KW Power and 100 Hz BW.
Mean/Median in db rel to 1 μv/m.
Standard Deviation in db.

TABLE 8

Standard Deviation, Mean and Median of Signal
For All Hourly Data From Guam.

Freq. (kHz)	Number of Data Pts.	Standard Deviation	Mean	Median
16.6	99	6.38	24.8	23.4
19.8	406	6.34	27.5	26.5
22.3	242	5.64	26.4	25.8
24.0	241	6.69	25.6	24.7
26.1	232	7.09	25.1	24.2

Normalized to 1 KW Power.
Mean/Median in db rel to 1 μv/m.
Standard Deviation in db.

TABLE 9

Standard Deviation, Mean and Median of all Signal Data
From Boulder For Four Hour Time Blocks.

Freq. (kHz)		00-04	04-08	08-12	12-16	16-20	20-24
16.6	STD DEV=	1.46	4.30	7.53	6.32	6.01	2.99
	NO. PTS. =	26	25	24	22	25	22
	MEAN/MEDIAN=	37.2/37.0	38.6/37.8	40.9/42.3	32.2/31.9	36.1/37.0	38.6/38.2
19.8	STD DEV=	2.29	4.85	3.50	5.59	1.46	1.16
	NO. PTS. =	169	184	196	185	206	228
	MEAN/MEDIAN=	33.4/33.6	35.0/35.0	34.5/34.2	33.5/32.3	33.3/33.5	34.9/34.8
22.3	STD DEV=	1.26	5.40	1.07	6.98	1.87	0.89
	NO. PTS. =	73	82	82	77	70	82
	MEAN/MEDIAN=	30.5/30.5	32.2/29.1	37.8/37.9	29.7/30.6	29.9/30.0	32.4/32.3
24.0	STD DEV=	1.20	6.27	3.18	5.26	1.48	1.09
	NO. PTS. =	86	91	106	96	97	107
	MEAN/MEDIAN=	28.6/28.7	30.8/32.3	32.4/32.5	29.5/29.5	27.9/27.9	29.6/29.4
26.1	STD DEV=	1.72	10.07	0.93	6.11	2.12	0.81
	NO. PTS. =	51	48	53	55	56	61
	MEAN/MEDIAN=	28.3/28.3	34.1/36.4	39.1/39.0	27.4/26.5	27.9/28.0	30.6/30.6

Normalized to 1 KW Power.
Mean/Median in db rel to 1 μv/m.
Standard Deviation in db.

TABLE 10

Standard Deviation, Mean and Median of all Noise Data From Boulder For Four Hour Time Blocks.

Freq. (kHz)		00-04	04-08	08-12	12-16	16-20	20-24
16.6	STD DEV=	6.24	3.90	4.71	5.17	6.08	5.68
	NO. PTS. =	26	25	24	22	25	22
	MEAN/MEDIAN=	52.0/50.1	48.2/46.1	45.5/43.3	42.5/39.1	48.7/48.1	54.6/53.6
19.8	STD DEV=	4.24	5.39	4.73	4.13	4.70	3.54
	NO. PTS. =	125	138	151	150	157	175
	MEAN/MEDIAN=	52.4/51.6	52.3/52.6	49.6/49.1	47.2/45.6	48.6/47.6	53.5/52.6
22.3	STD DEV=	5.62	4.66	4.41	3.78	4.50	4.37
	NO. PTS. =	73	82	82	77	70	82
	MEAN/MEDIAN=	50.6/48.7	49.6/49.7	45.2/43.5	39.3/37.7	42.0/40.7	50.6/49.7
24.0	STD DEV=	4.12	5.32	4.87	4.63	5.11	3.80
	NO. PTS. =	86	91	106	96	97	107
	MEAN/MEDIAN=	48.4/46.6	49.2/48.1	44.9/42.6	38.0/36.6	40.8/38.6	47.4/46.6
26.1	STD DEV=	3.43	3.16	4.27	3.90	4.43	4.81
	NO. PTS. =	51	48	53	55	56	61
	MEAN/MEDIAN=	49.9/50.0	48.1/47.5	46.5/45.5	39.8/38.0	42.7/40.5	49.9/49.5

Normalized to 100 Hz BW.
Mean/Median in db rel to 1 μv/m.
Standard Deviation in db.

TABLE 11

Standard Deviation, Mean and Median of Signal to Noise Ratio
From Boulder For Four Hour Time Blocks.

Freq. (kHz)		00-04	04-08	08-12	12-16	16-20	20-24
16.6	STD DEV=	6.12	6.40	8.53	6.91	4.80	5.24
	NO. PTS. =	26	25	24	22	25	22
	MEAN/MEDIAN=	-11.2/-11.2	-7.6/-9.6	-2.3/-2.3	-7.9/-10.1	-11.0/-15.4	-13.4/-15.6
19.8	STD DEV=	3.42	5.96	4.24	5.42	4.52	3.50
	NO. PTS. =	125	138	151	150	157	175
	MEAN/MEDIAN=	-17.7/-18.4	-14.4/-16.3	-13.2/-15.0	-12.1/-13.7	-13.2/-13.7	-17.4/-18.4
22.3	STD DEV=	5.03	8.70	4.36	7.81	3.61	3.85
	NO. PTS. =	73	82	82	77	70	82
	MEAN/MEDIAN=	-17.2/-18.2	-14.3/-17.6	-5.3/-5.6	-8.3/-8.7	-10.4/-11.7	-16.4/-17.4
24.0	STD DEV=	4.48	8.30	5.17	5.98	4.51	3.90
	NO. PTS. =	86	91	106	96	97	107
	MEAN/MEDIAN=	-17.8/-18.3	-15.3/-17.5	-10.2/-11.2	-6.9/-8.1	-10.5/-10.7	-16.3/-16.9
26.1	STD DEV=	3.78	11.34	4.45	6.59	3.40	4.28
	NO. PTS. =	51	48	53	55	56	61
	MEAN/MEDIAN=	-20.4/-21.7	-12.4/-12.8	-5.4/-6.0	-11.1/-13.1	-13.3/-13.1	-17.2/-18.9

Normalized to 1 KW Power and 100 Hz BW.
All in db or db rel to 1 μv/m.

TABLE 12

Standard Deviation, Mean and Median of Signal, Noise, and Signal to Noise Ratio
For All Data From Boulder.

Freq. (kHz)	Number of Data Pts.	Standard Deviation of Signal	Noise	S/N Ratio	Mean	Median
16.6	144	5.93			37.7	37.2
	144		6.88		49.5	46.6
	144			7.33	-8.1	-11.5
19.8	1168	3.56			34.1	34.2
	896		5.13		50.9	50.1
	896			5.00	-14.4	-16.3
22.3	466	4.98			32.7	31.6
	466		6.49		47.3	44.7
	466			7.74	-10.9	-13.8
24.0	583	3.88			30.0	29.3
	583		6.43		45.6	43.6
	583			6.98	-11.9	-14.3
26.1	324	6.53			32.3	29.7
	324		5.78		46.9	45.5
	324			7.90	-12.1	-14.1

Normalized to 1 KW Power and 100 Hz BW.
All in db or db rel to 1 μv/m.

TABLE 13

Standard Deviation, Mean and Median for Various Frequencies From the Automatic Noise System From Japan for Four Hour Time Blocks.

Freq. (Hz)		00-04	04-08	08-12	12-16	16-20	20-24
20	STD DEV=	5.80	5.28	6.02	5.14	7.47	5.91
	NO. PTS. =	66	77	75	78	91	84
	MEAN/MEDIAN=	48.9/45.8	48.1/46.0	47.2/45.3	46.4/44.7	46.7/44.7	46.3/45.6
75	STD DEV=	5.29	2.29	3.21	3.14	4.45	3.82
	NO. PTS. =	71	72	78	86	87	91
	MEAN/MEDIAN=	46.6/43.3	44.6/44.3	44.8/44.8	44.1/43.6	42.9/42.9	43.4/43.2
140	STD DEV=	4.85	2.92	2.50	2.64	3.76	2.24
	NO. PTS. =	81	79	84	86	90	90
	MEAN/MEDIAN=	44.6/42.1	43.9/43.6	44.5/44.2	43.9/44.0	40.6/40.0	42.3/42.1
320	STD DEV=	2.68	2.46	3.52	3.76	3.63	2.66
	NO. PTS. =	83	84	75	95	93	89
	MEAN/MEDIAN=	43.0/42.2	42.8/42.4	44.0/42.5	43.0/42.8	36.9/36.5	12.2/41.7
510	STD DEV=	2.83	2.54	2.36	3.65	3.74	2.79
	NO. PTS. =	81	81	74	94	93	84
	MEAN/MEDIAN=	42.2/41.3	42.4/41.8	42.0/41.8	41.6/41.8	35.1/34.1	41.6/41.1

Normalized to 1 Hz BW.
Mean/Median in db rel to 1 μv/m.
Standard Deviation in db.

TABLE 13
Contd.

Freq. (Hz)		00-04	04-08	08-12	12-16	16-20	20-24
1 K	STD DEV=	3.37	2.48	2.21	2.78	4.58	2.72
	NO. PTS. =	84	79	73	89	95	82
	MEAN/MEDIAN=	36.4/34.9	36.3/35.7	34.9/34.3	34.7/34.4	30.0/28.3	34.6/33.6
3 K	STD DEV=	4.25	3.23	2.66	3.37	4.52	2.95
	NO. PTS. =	81	77	71	88	97	90
	MEAN/MEDIAN=	27.0/25.0	26.6/25.9	26.2/25.5	27.8/27.3	24.7/23.4	25.6/24.7
5 K	STD DEV=	5.05	3.55	2.92	2.96	2.90	3.70
	NO. PTS. =	73	77	68	81	99	90
	MEAN/MEDIAN=	28.7/26.3	29.3/28.9	32.8/32.3	32.5/32.5	30.4/29.8	27.9/26.5
10 K	STD DEV=	3.89	3.12	2.37	2.55	2.05	2.85
	NO. PTS. =	75	71	74	80	103	94
	MEAN/MEDIAN=	23.9/22.1	29.1/29.4	29.6/29.4	29.4/29.0	27.2/27.0	24.5/23.7
20 K	STD DEV=	4.74	3.21	3.20	5.14	3.66	4.14
	NO. PTS. =	65	80	81	74	102	98
	MEAN/MEDIAN=	18.4/15.5	21.9/21.4	20.8/20.2	24.6/21.8	20.8/19.6	17.2/14.8
30 K	STD DEV=	4.50	3.39	3.58	3.62	3.53	3.72
	NO. PTS. =	70	79	78	74	103	98
	MEAN/MEDIAN=	14.6/12.2	17.2/15.8	16.0/14.9	19.4/18.3	16.9/15.8	13.3/11.8

Normalized to 1 Hz BW.
Mean/Median in db rel to 1 μv/m.
Standard Deviation in db.

TABLE 14

Standard Deviation, Mean and Median For Various Frequencies From The Automatic Noise System From Japan.

Freq. (Hz)	Number of Data Pts.	Standard Deviation	Mean	Median
20	473	6.21	47.4	45.6
75	486	3.91	44.4	43.7
140	511	3.55	43.4	42.8
320	520	4.00	42.2	41.8
510	508	4.21	41.1	41.1
1 K	503	4.08	34.6	34.3
3 K	506	3.95	26.3	25.0
5 K	489	4.16	30.4	29.4
10 K	498	3.78	27.4	27.0
20 K	502	4.70	20.9	19.3
30 K	503	4.31	16.4	14.9

Normalized to 1 Hz BW.
Mean/Median in db rel to 1 μv/m.
Standard Deviation in db.

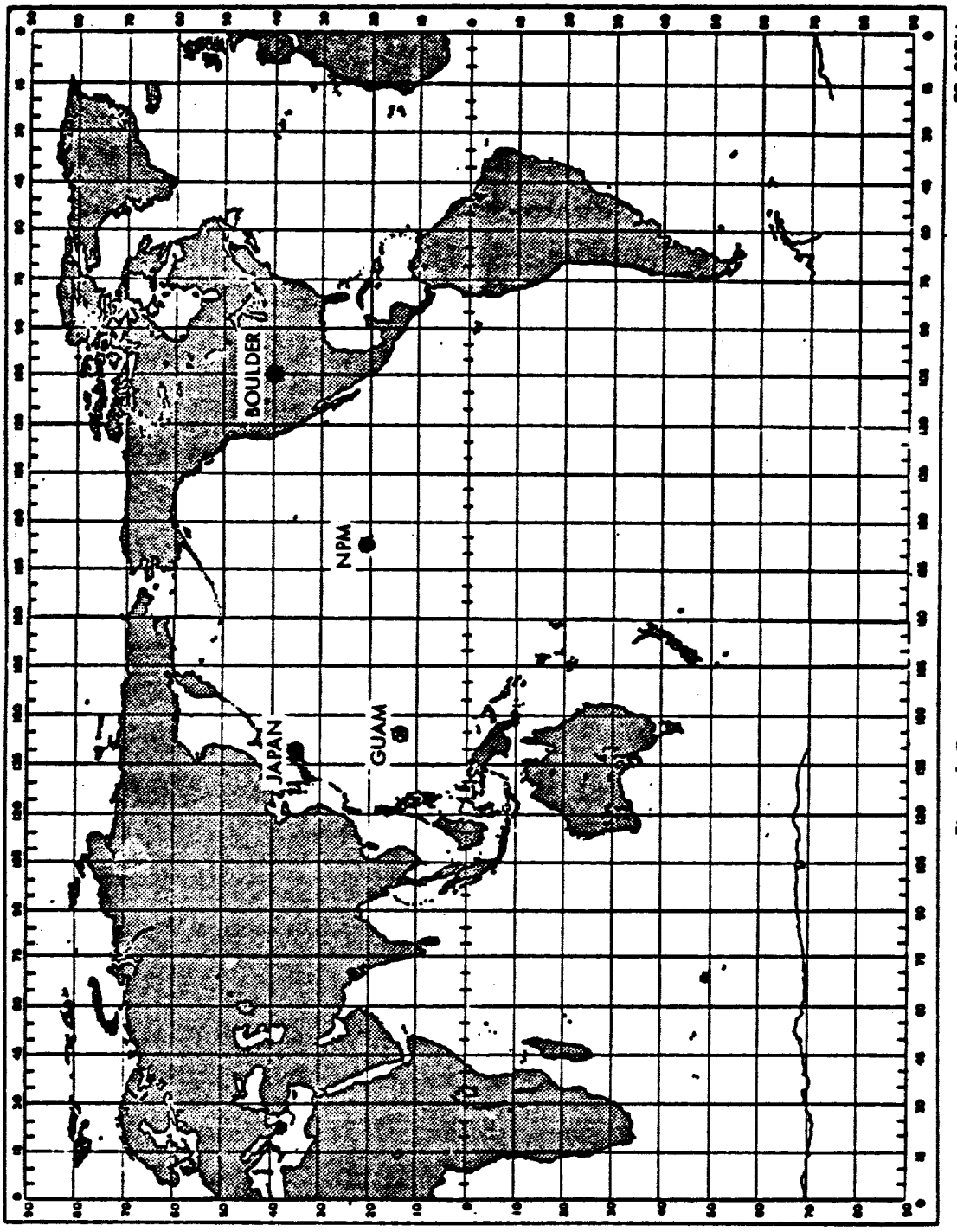

Figure 1 Transmitter and Receiver Locations for Tests

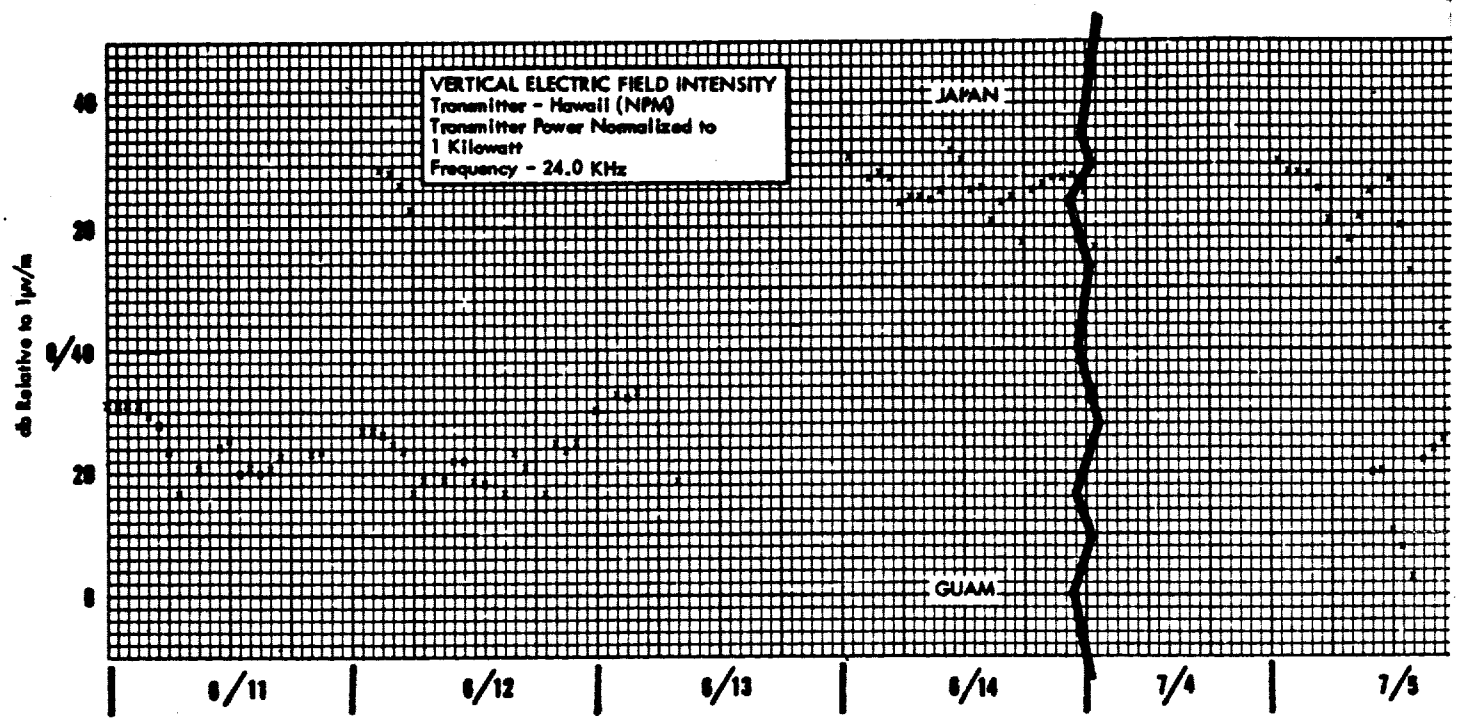

Figure 2 Simultaneous Measurements of Field Intensity at Japan and Guam

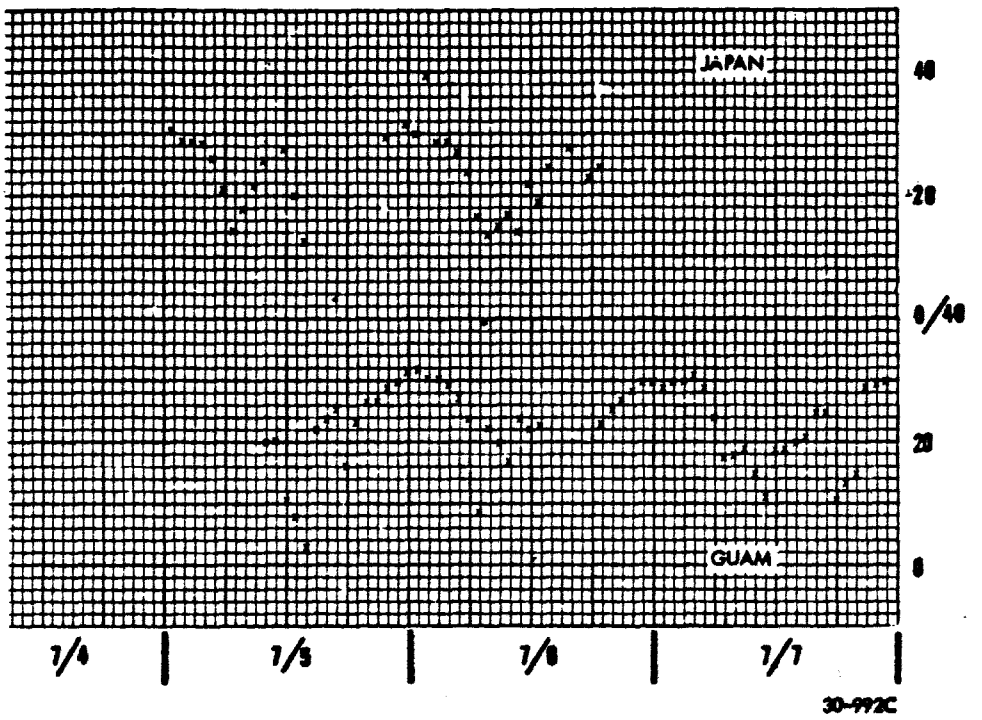
JAPAN
GUAM
40
20
0/40
20
0
7/4
7/5
7/6
7/7
30-992C

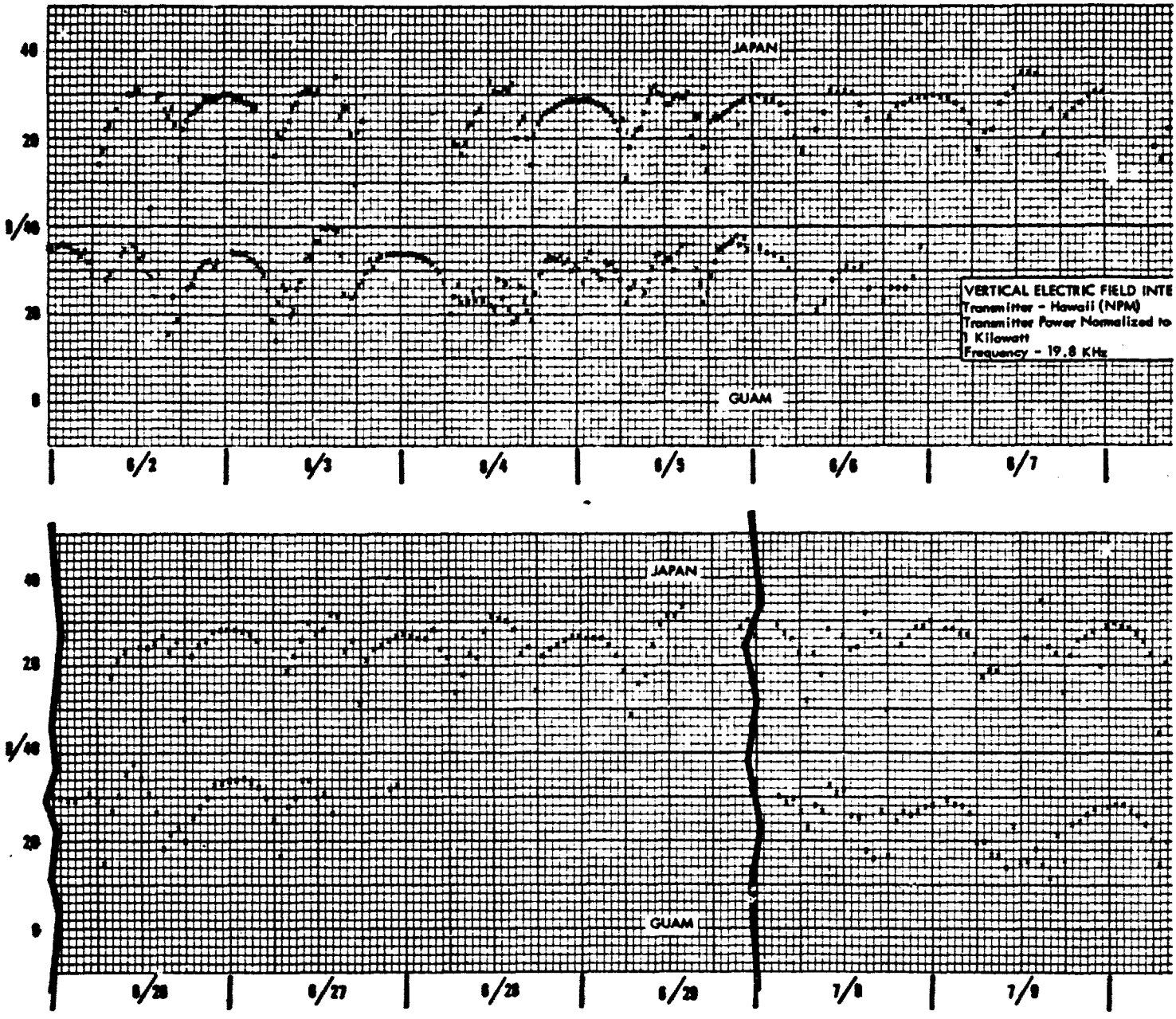

Figure 3 Simultaneous Measurements of Field Intensity at Japan and Guam

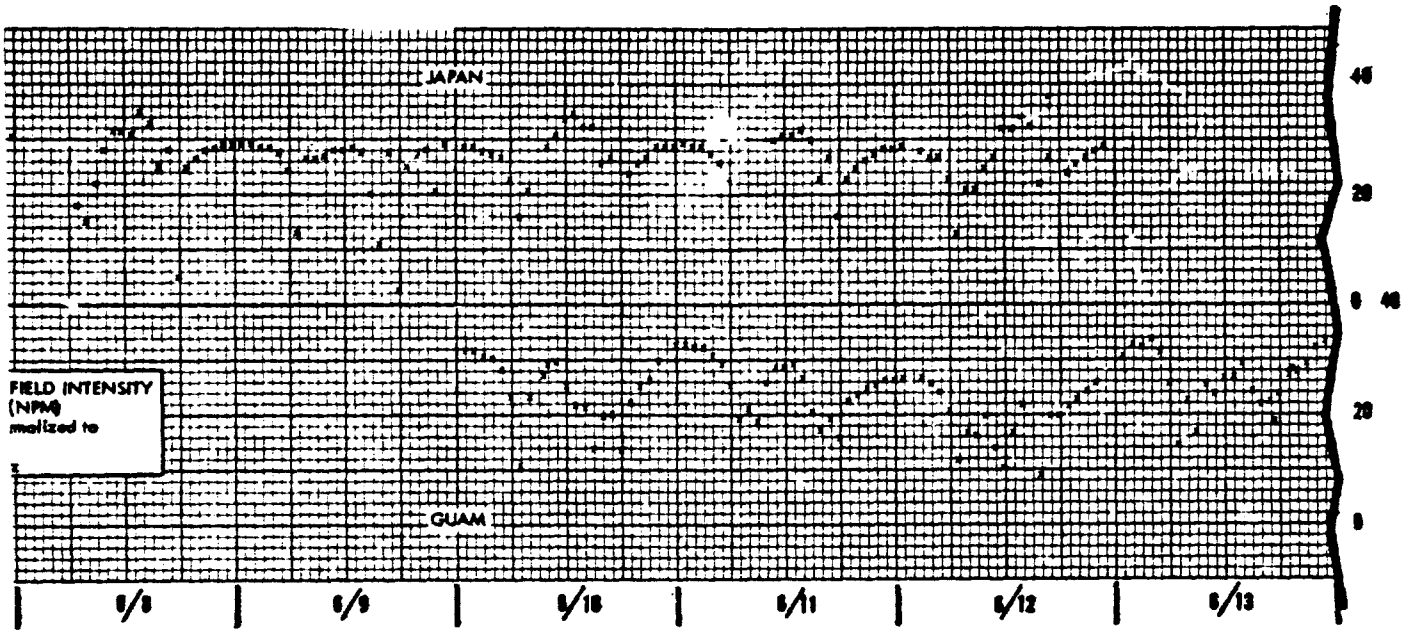
JAPAN
GUAM
FIELD INTENSITY
(NPM)
malized to
40
20
0
40
20
0
6/8
6/9
6/10
6/11
6/12
6/13

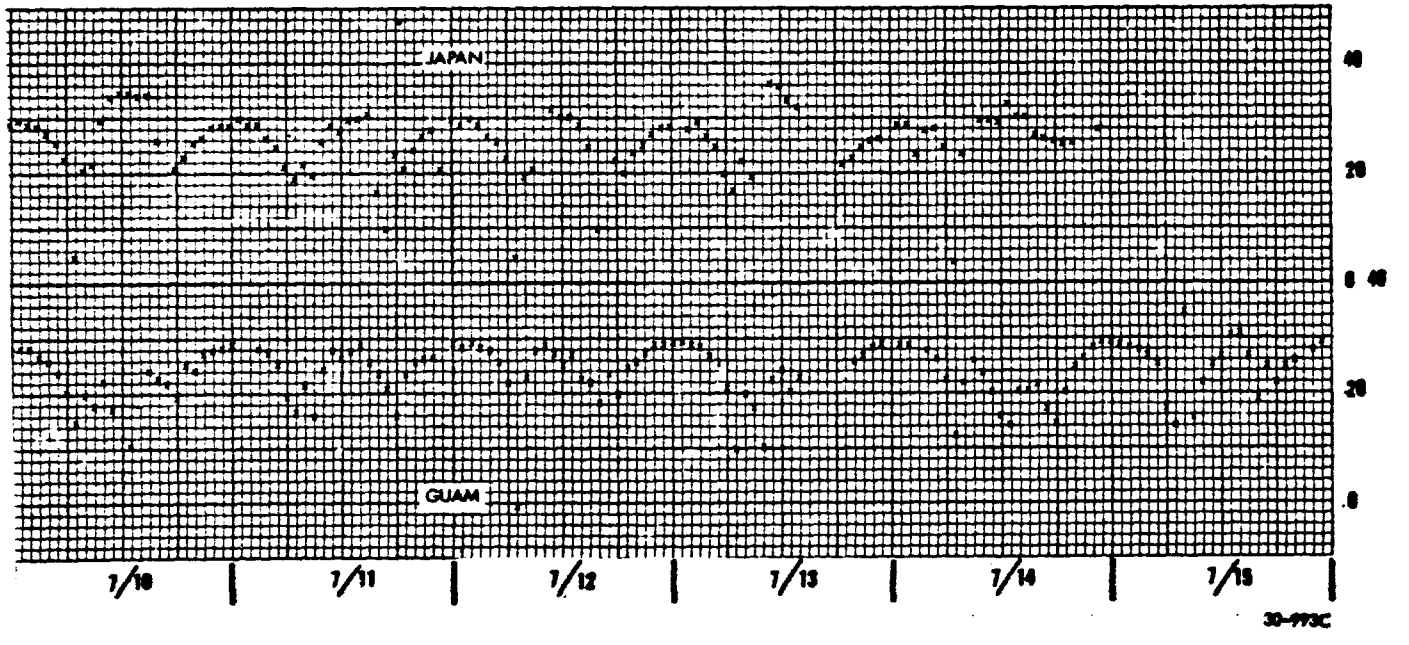
JAPAN
GUAM
40
20
0
40
20
0
7/10
7/11
7/12
7/13
7/14
7/15

30-993C

2

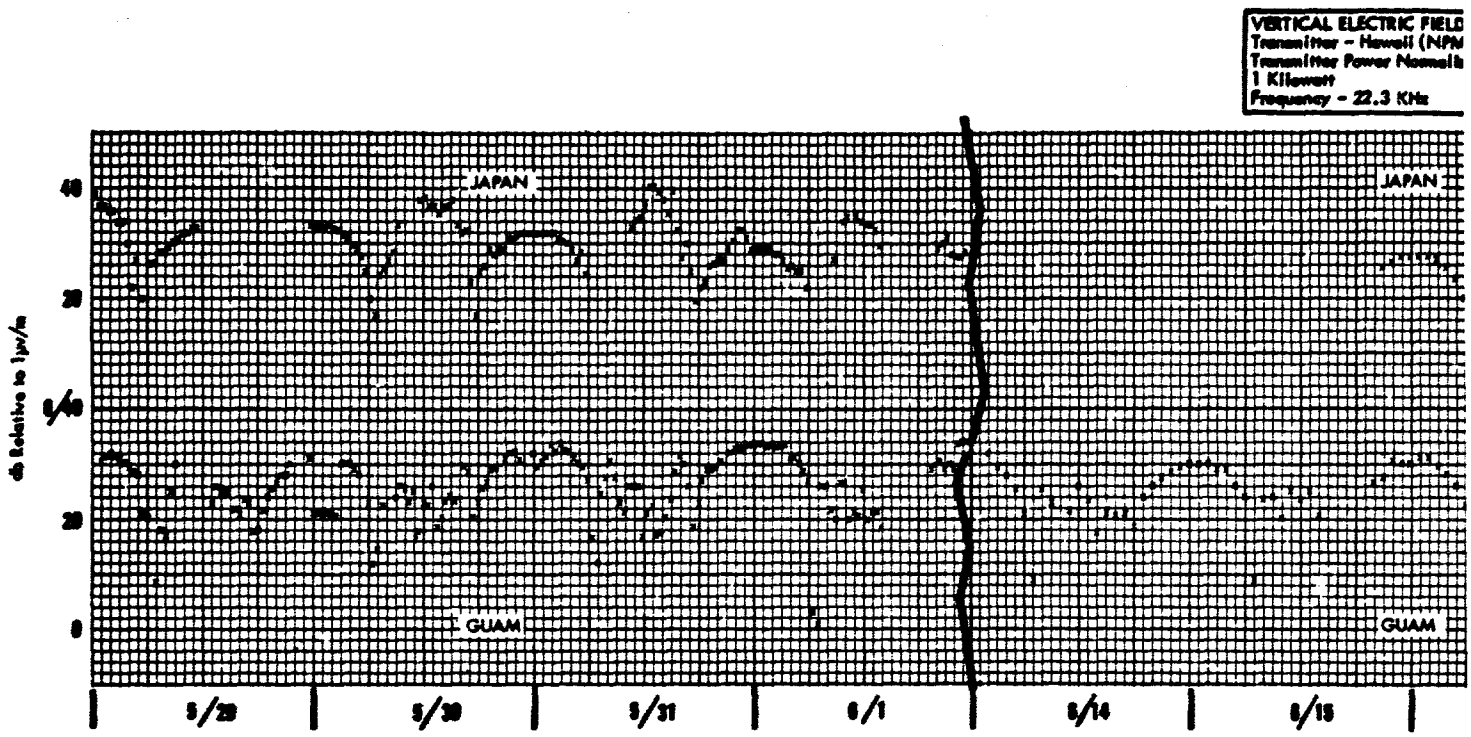

Figure 4 Simultaneous Measurements of Field Intensity at Japan and Guam

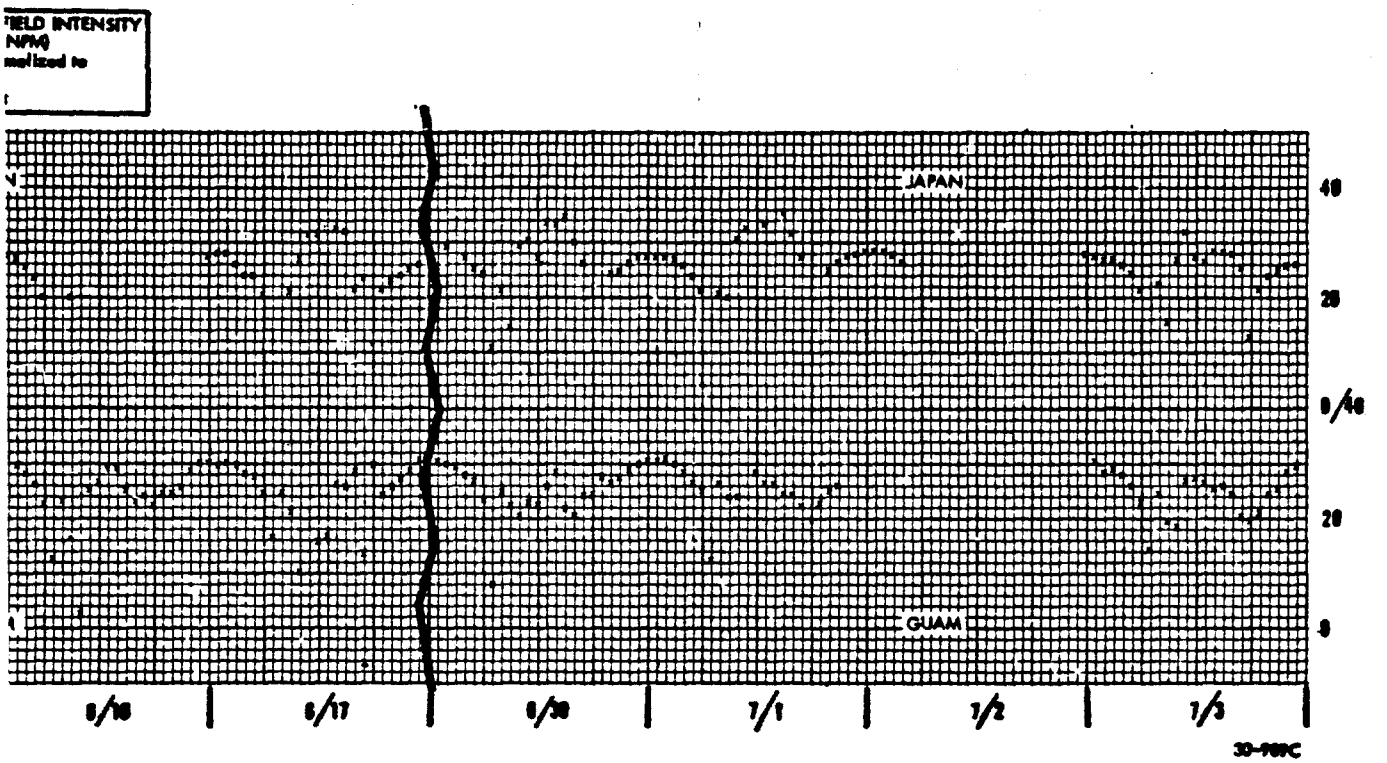

2

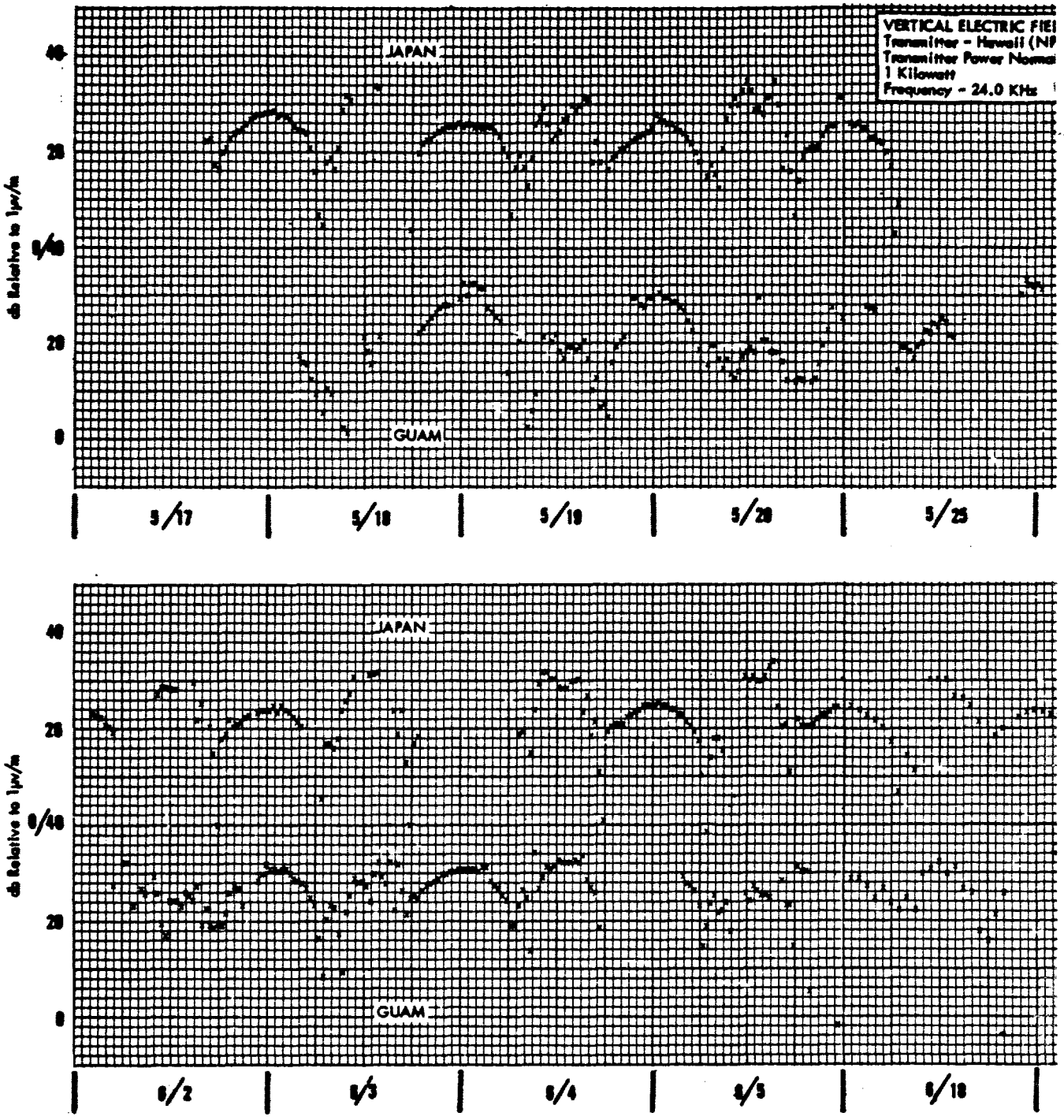

Figure 5 Simultaneous Measurements of Field Intensity at Japan and Guam

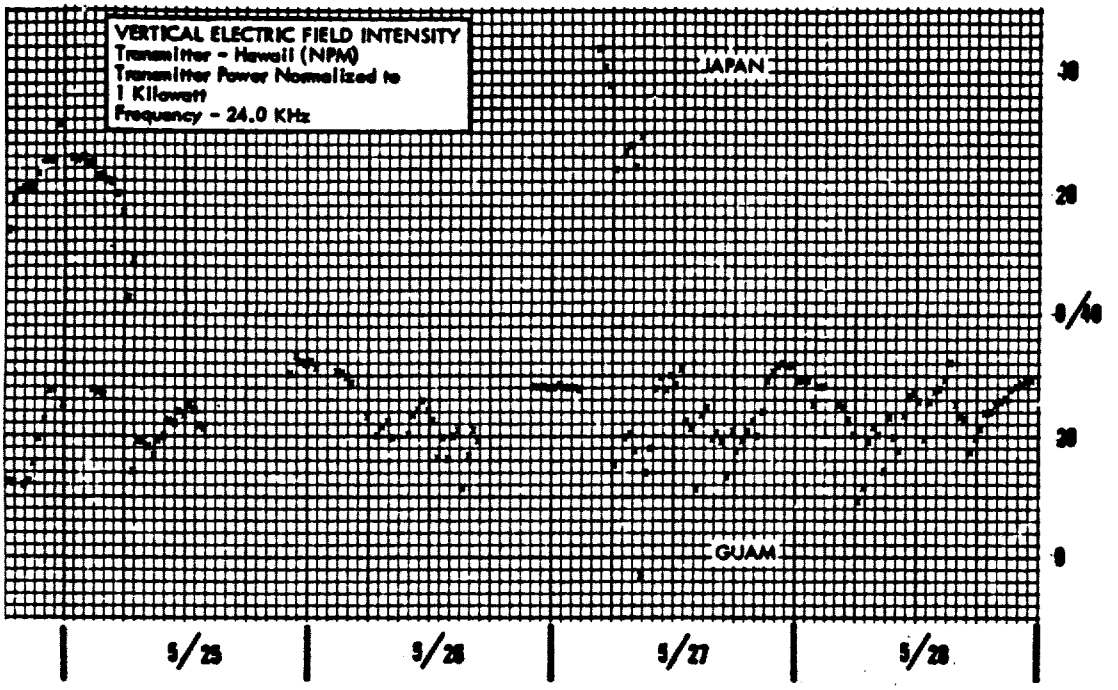
VERTICAL ELECTRIC FIELD INTENSITY
Transmitter - Hawaii (NPM)
Transmitter Power Normalized to
1 Kilowatt
Frequency - 24.0 KHz
JAPAN
GUAM
30
20
0/40
20
0
5/25
5/26
5/27
5/28

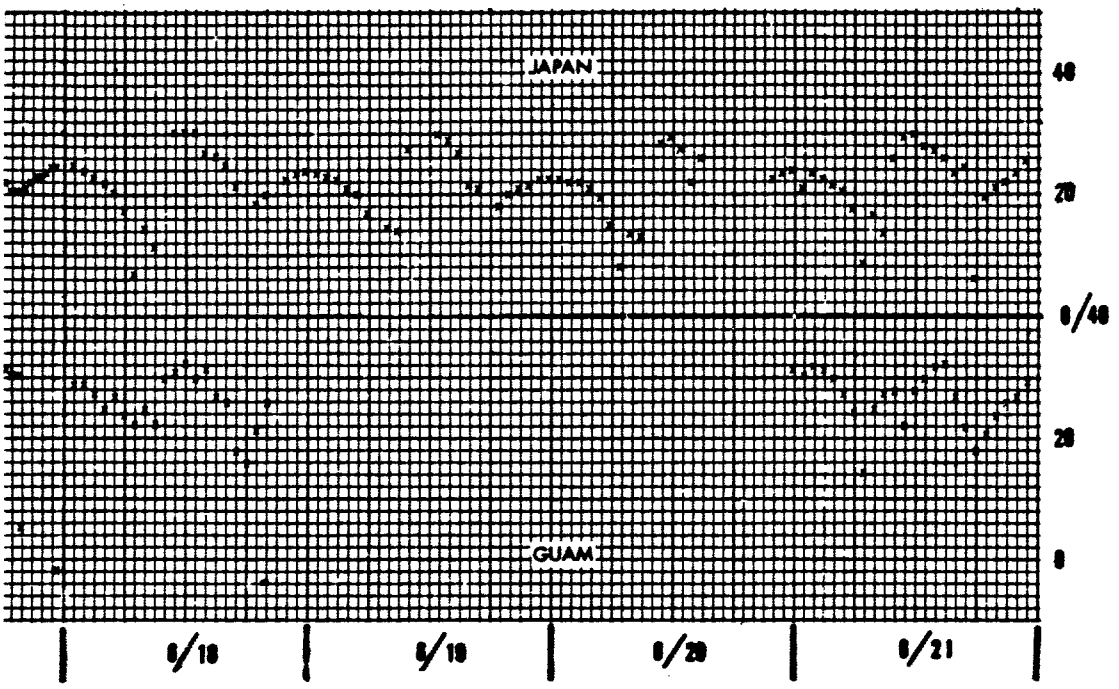
JAPAN
GUAM
40
20
0/40
20
0
6/18
6/19
6/20
6/21

30-990C

2

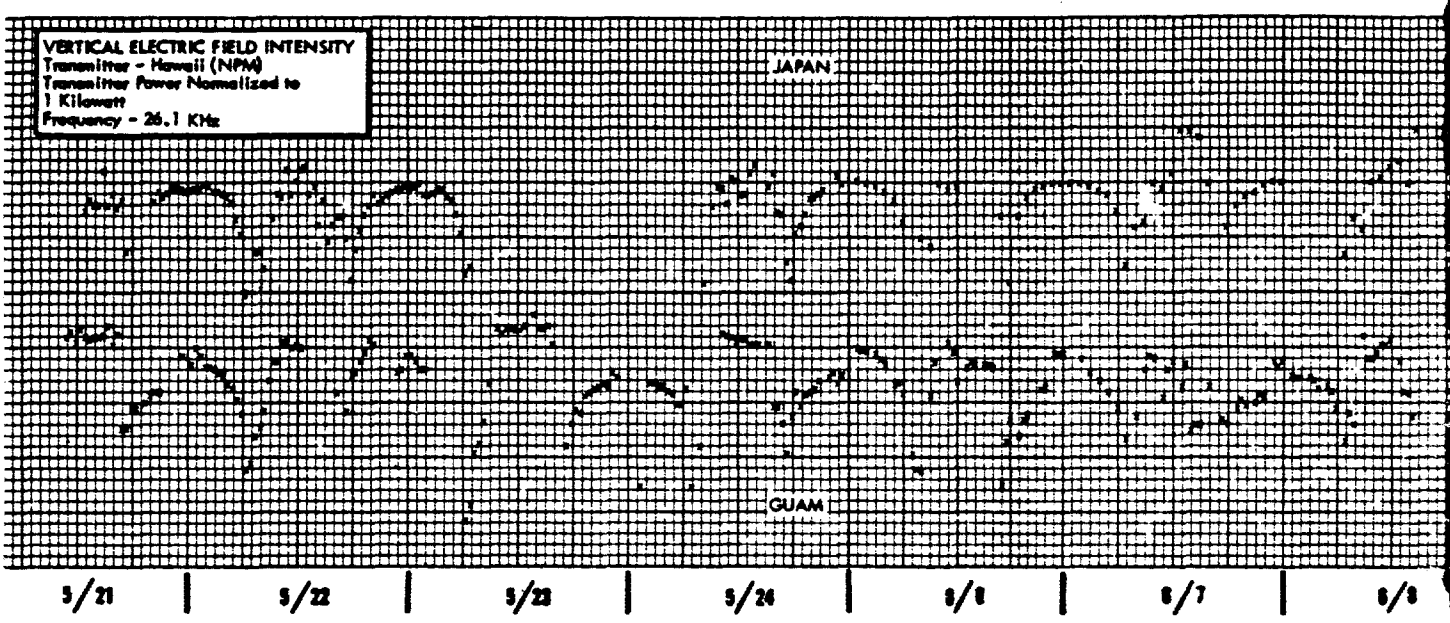

Figure 6 Simultaneous Measurements of Field Intensity at Japan and Guam

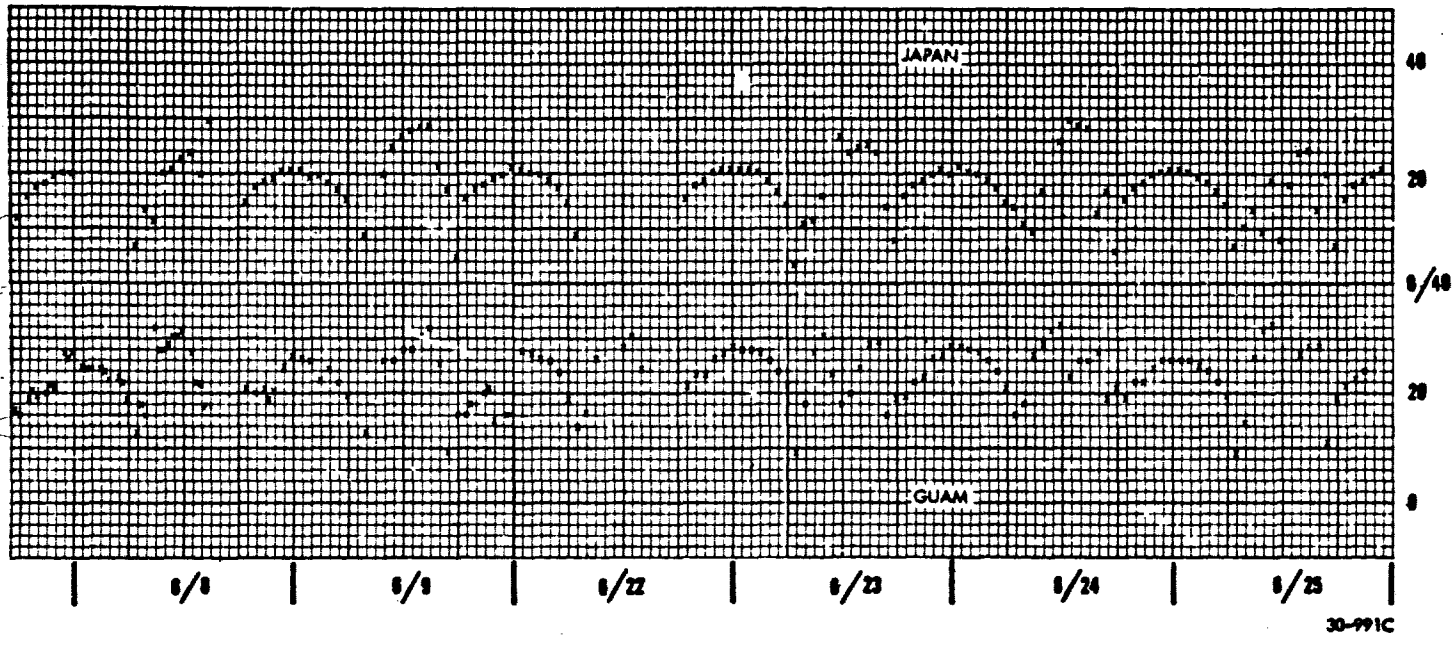

2

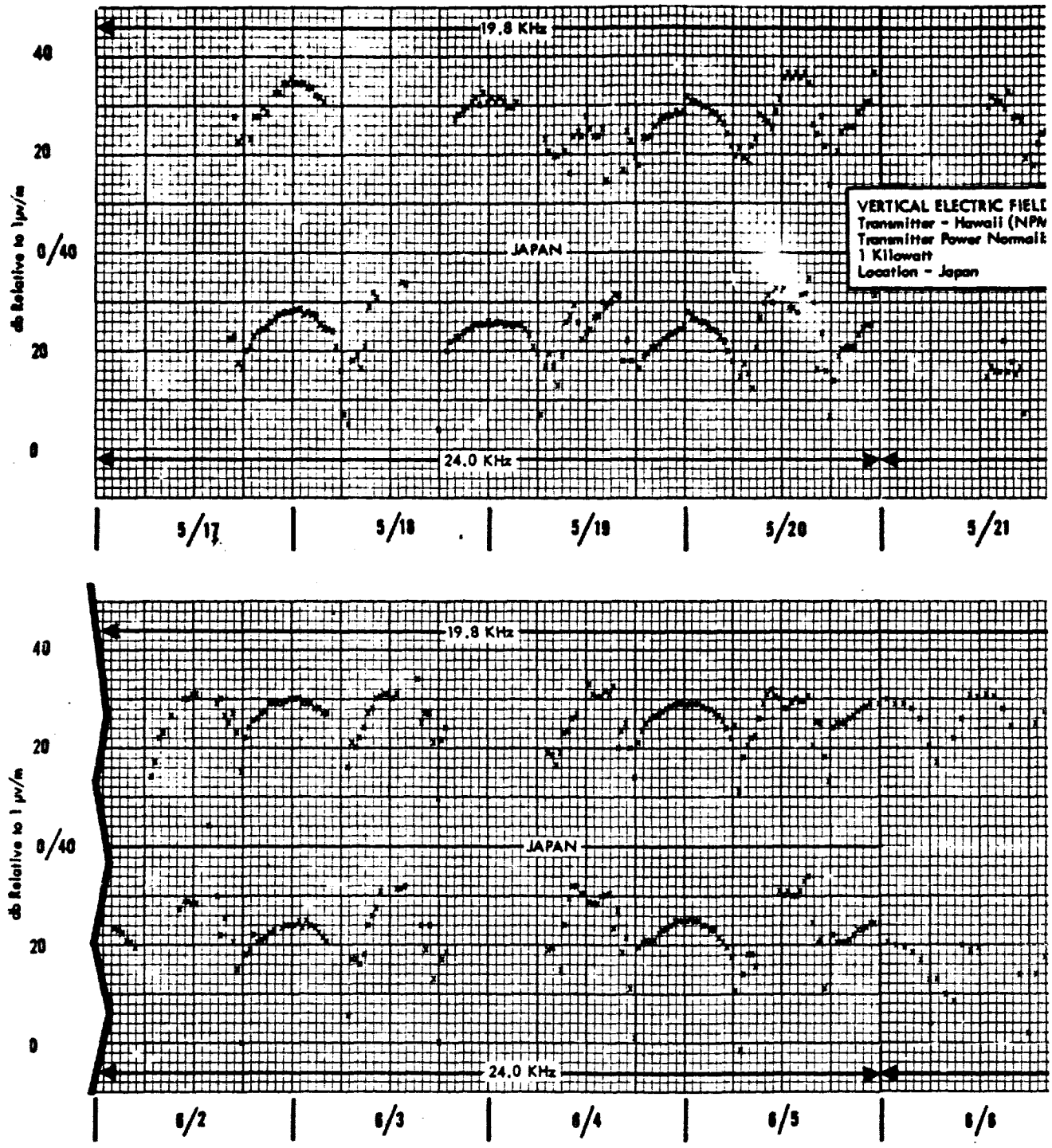

Figure 7 Simultaneous Measurements of Field Intensity at Two Frequencies

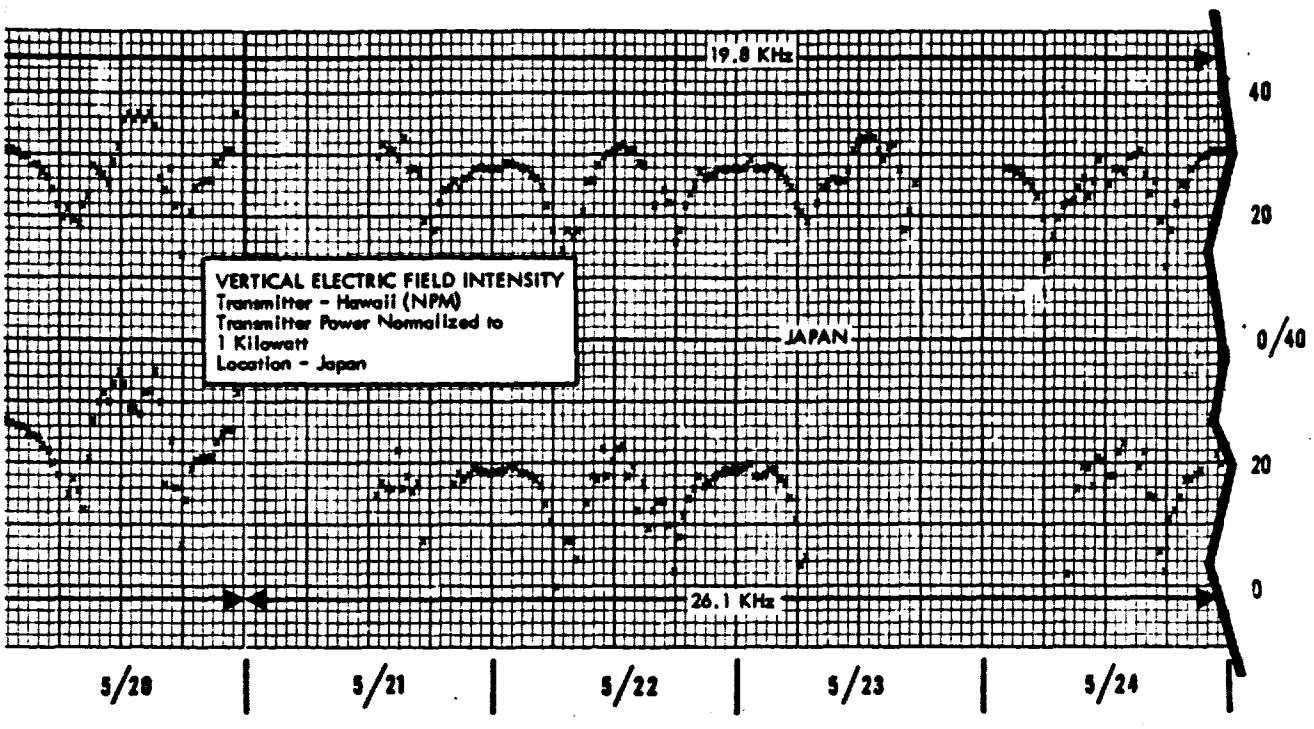

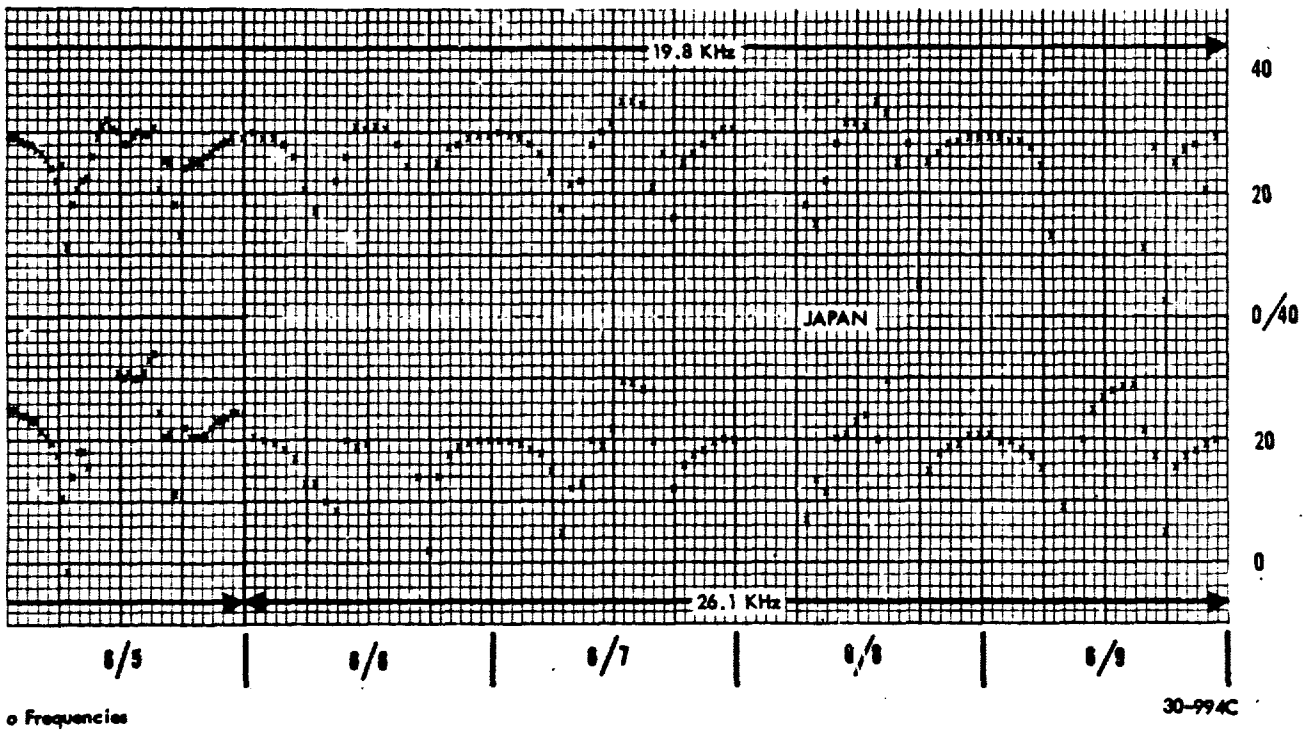

o Frequencies

30-994C

2

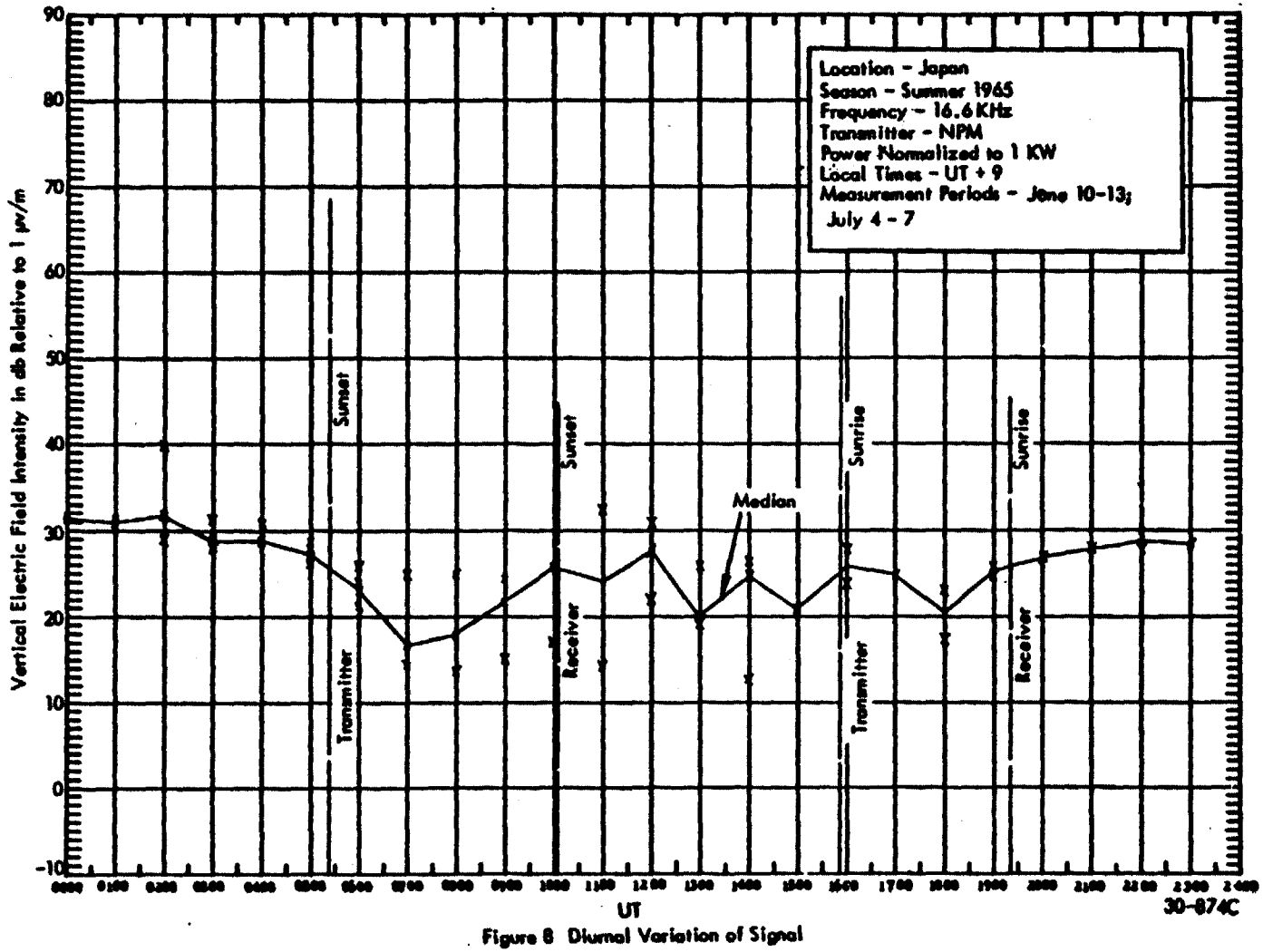

Figure 8 Diurnal Variation of Signal

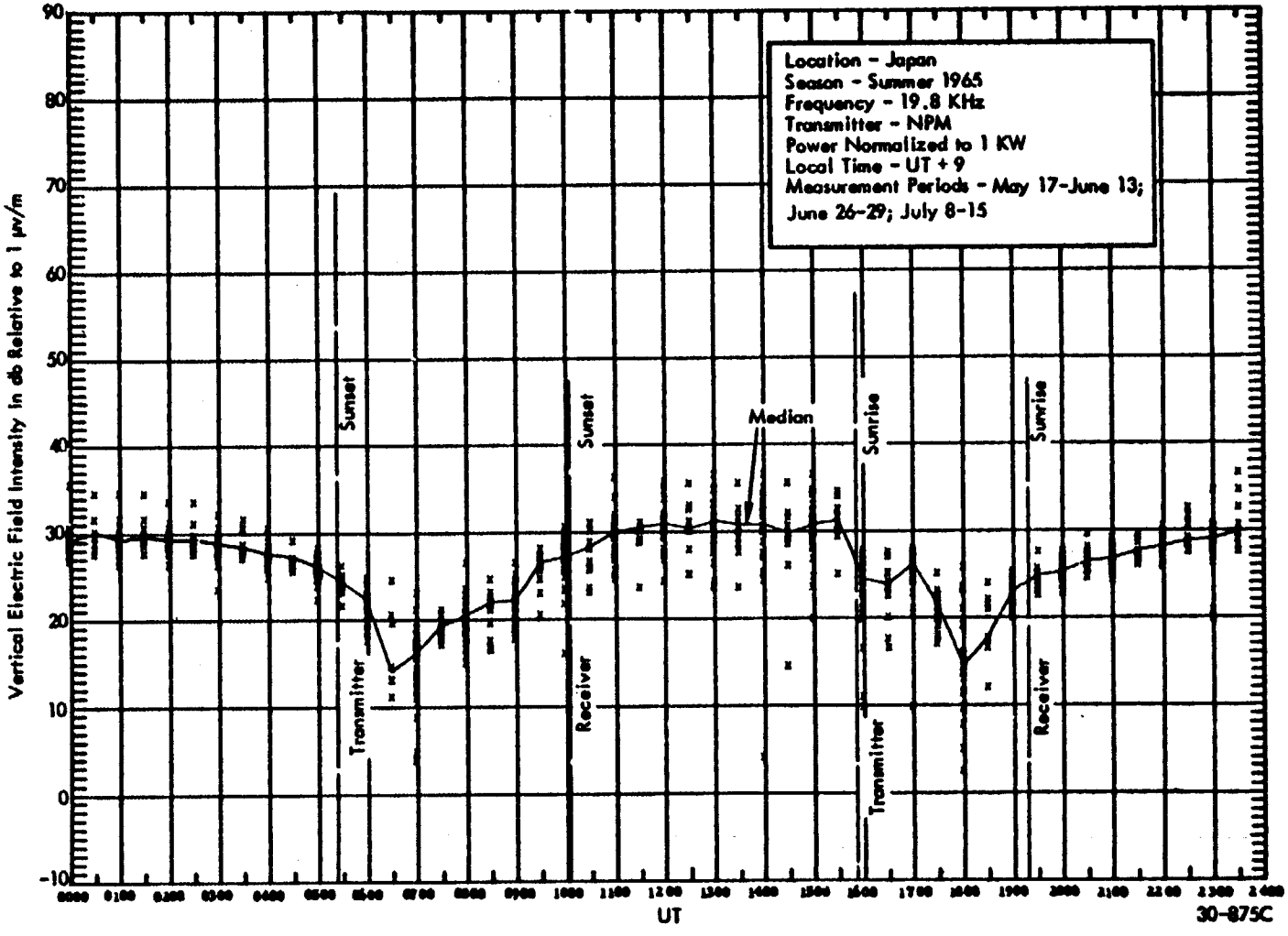

Figure 9 Diurnal Variation of Signal

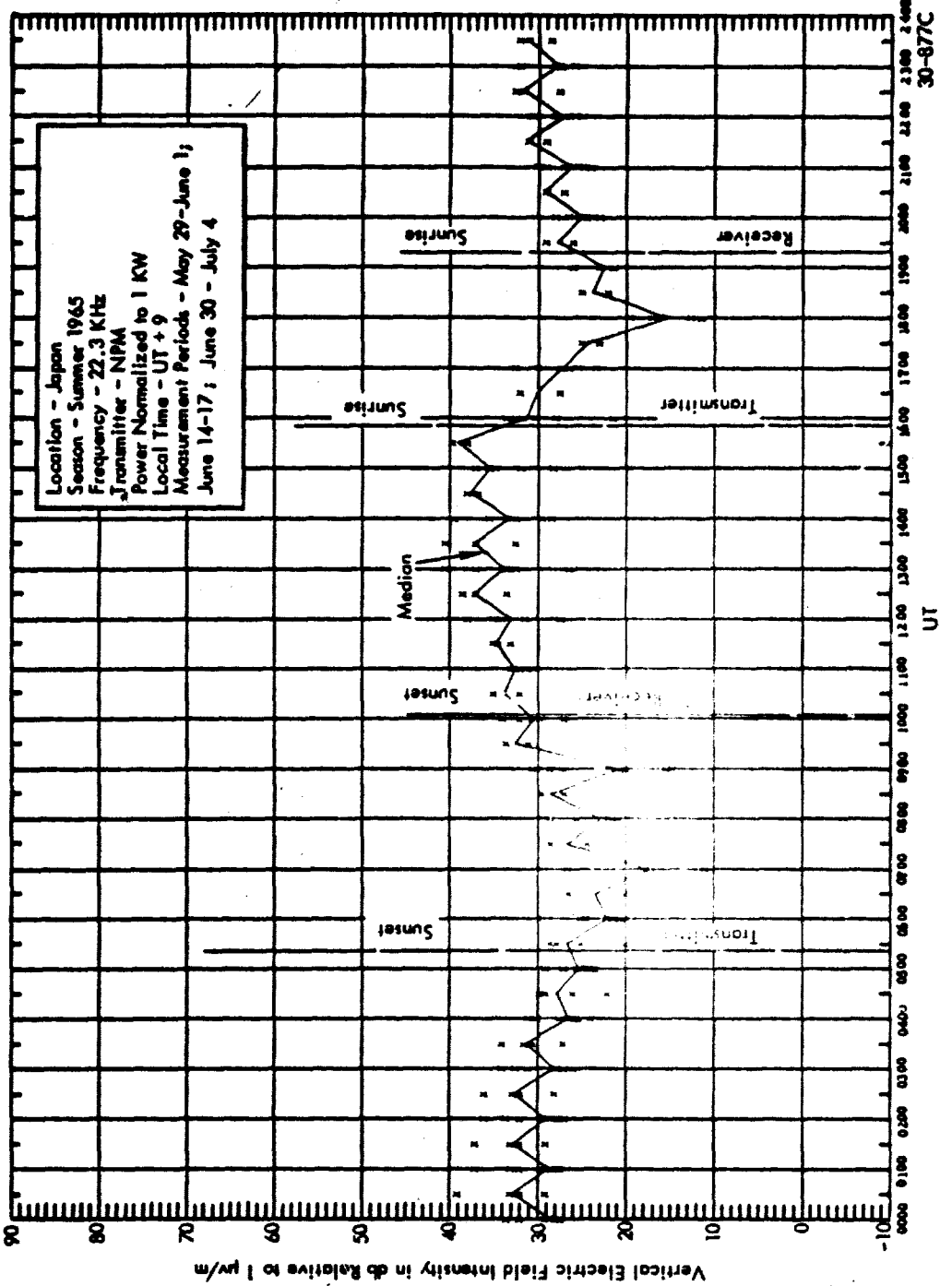

Figure 10 Diurnal Variation of Signal

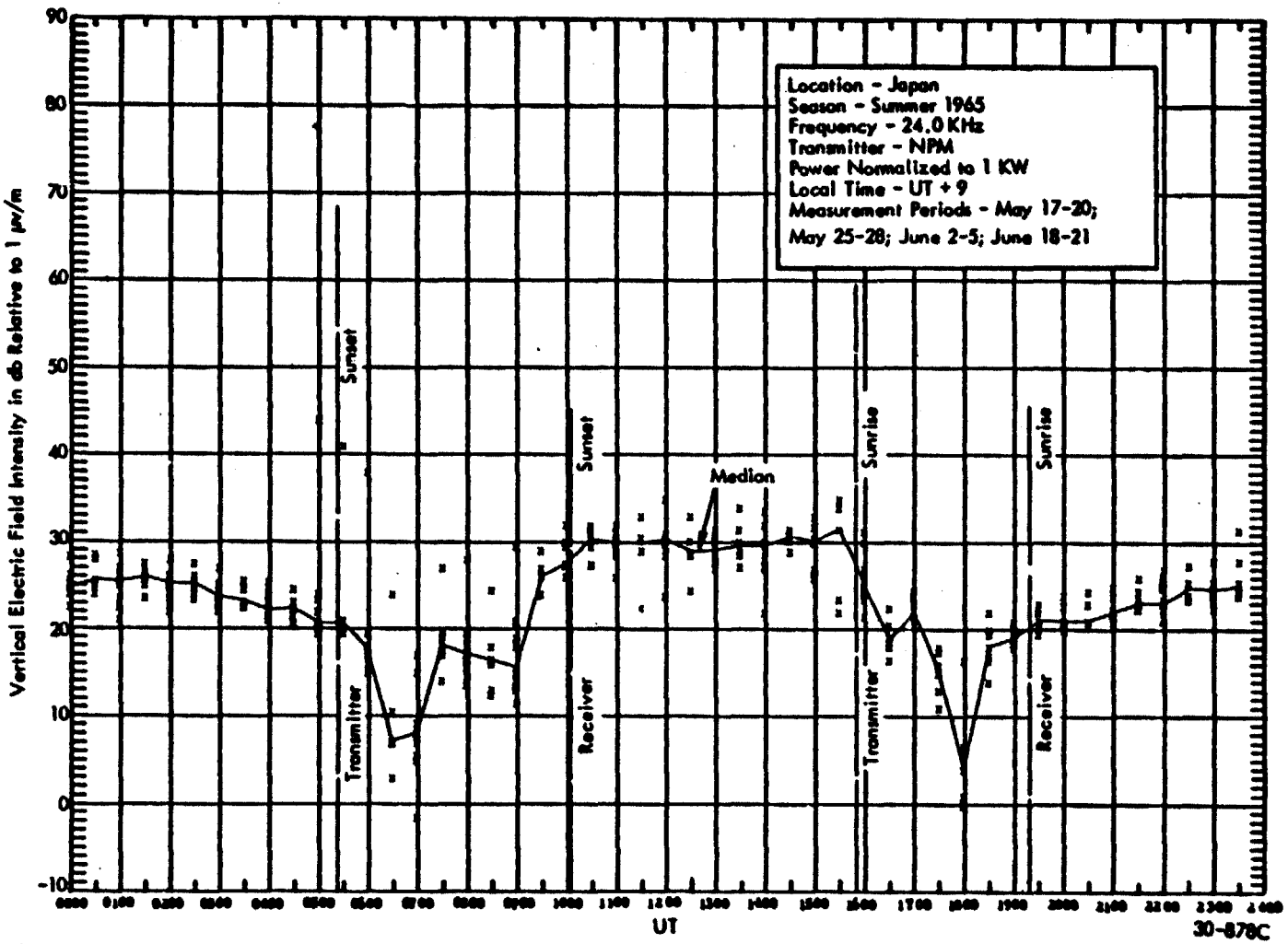

Figure 11 Diurnal Variation of Signal

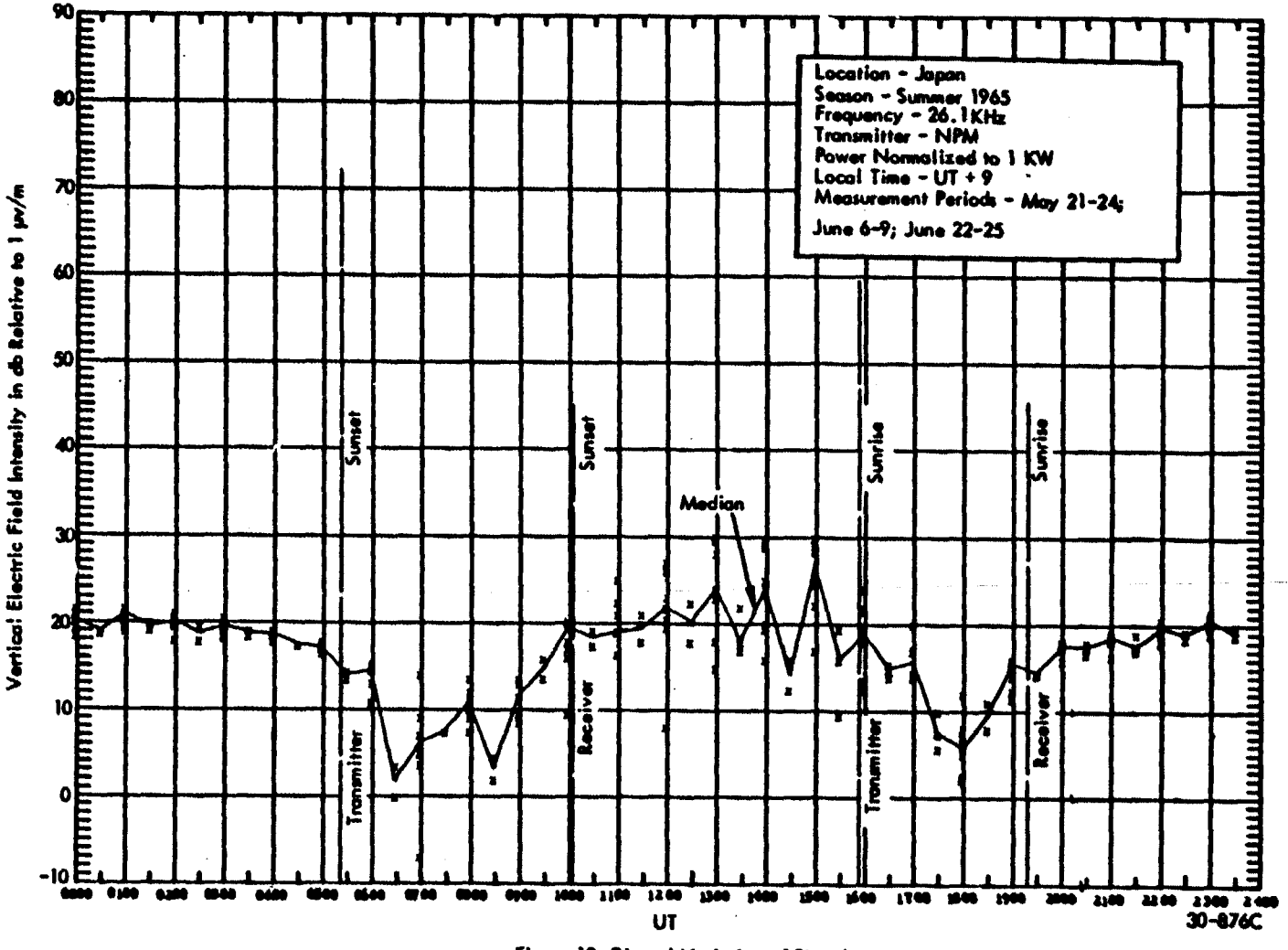

Figure 12 Diurnal Variation of Signal

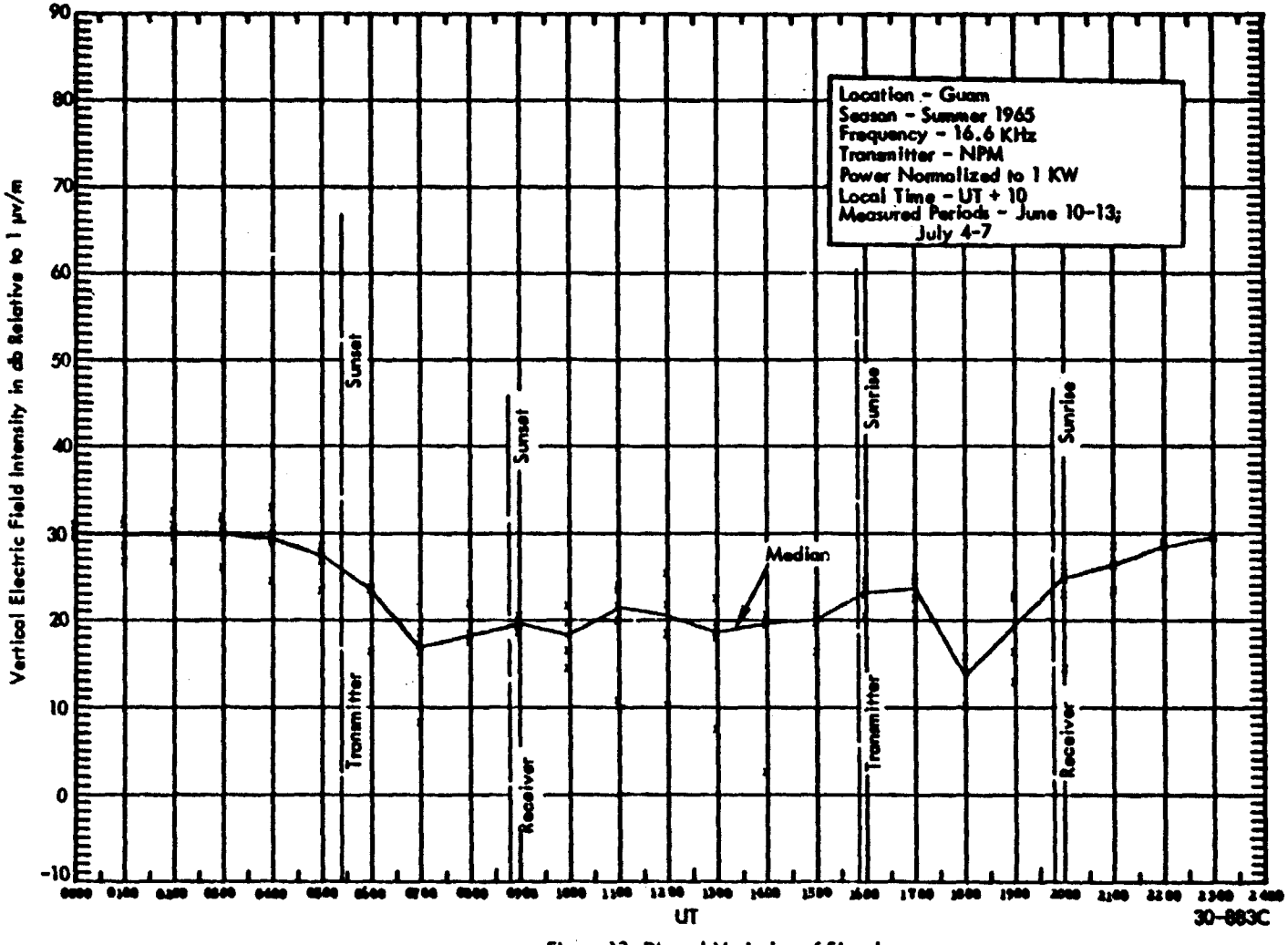

Figure 13 Diurnal Variation of Signal

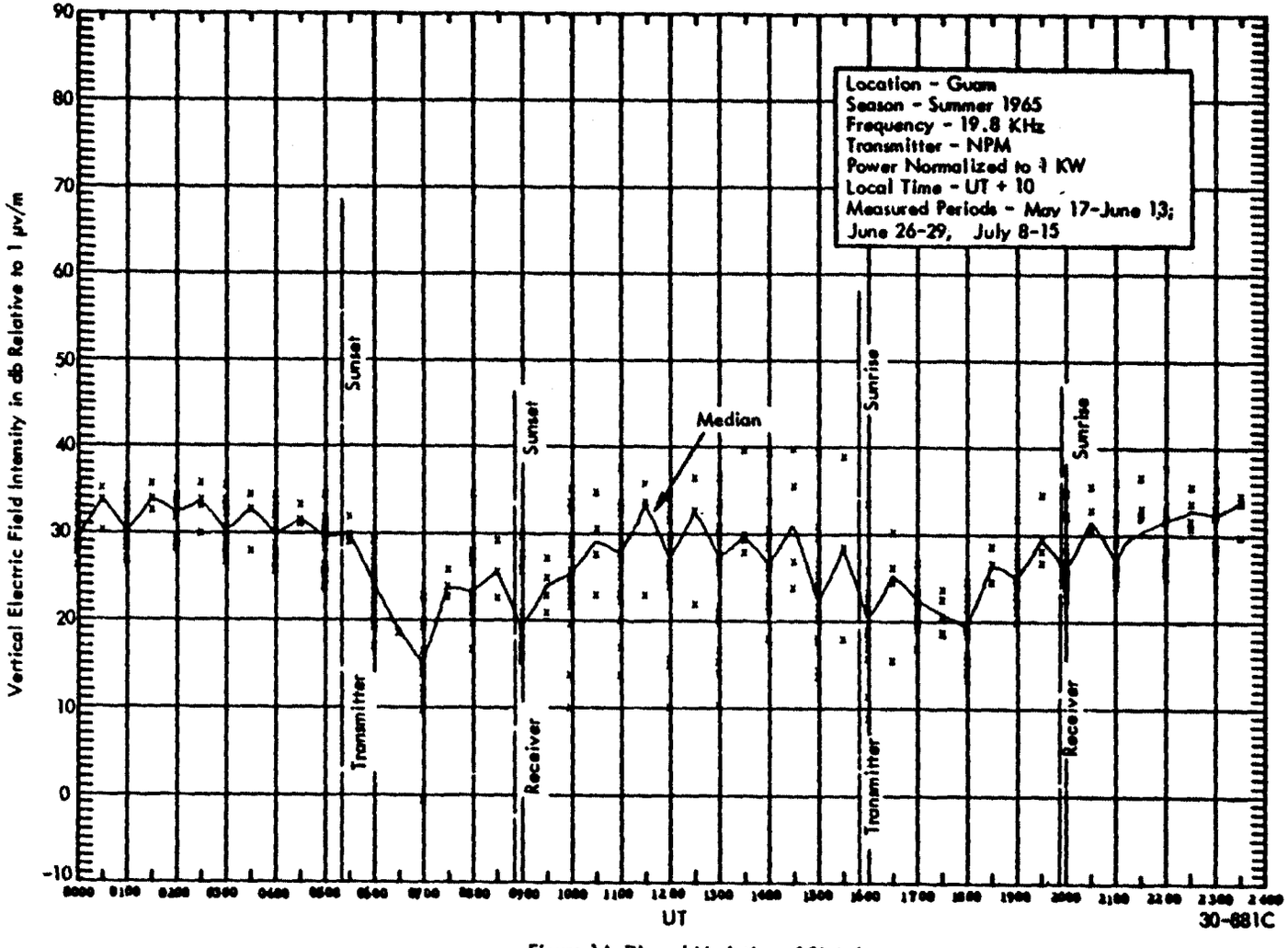

Figure 14 Diurnal Variation of Signal

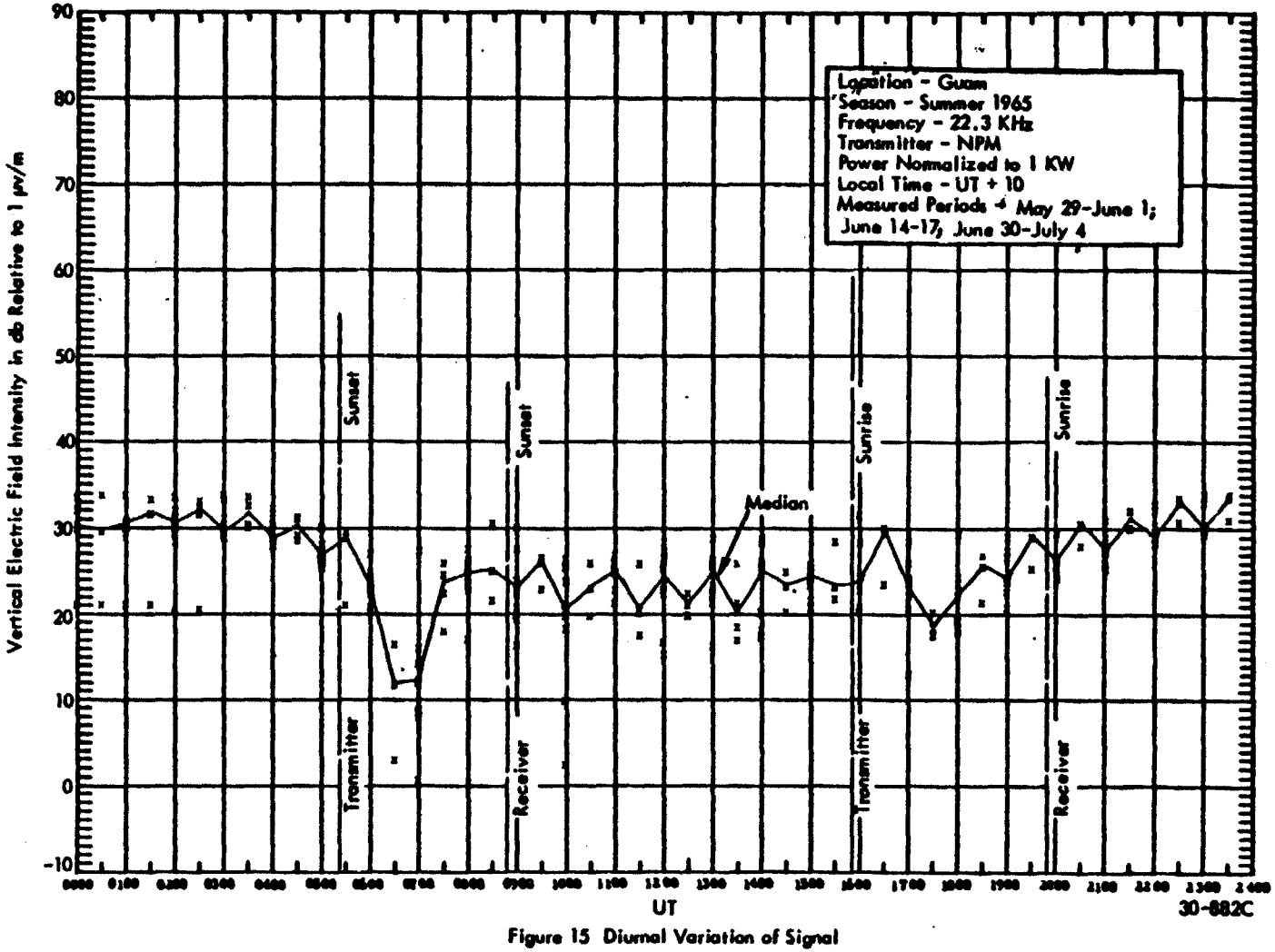

Figure 15 Diurnal Variation of Signal

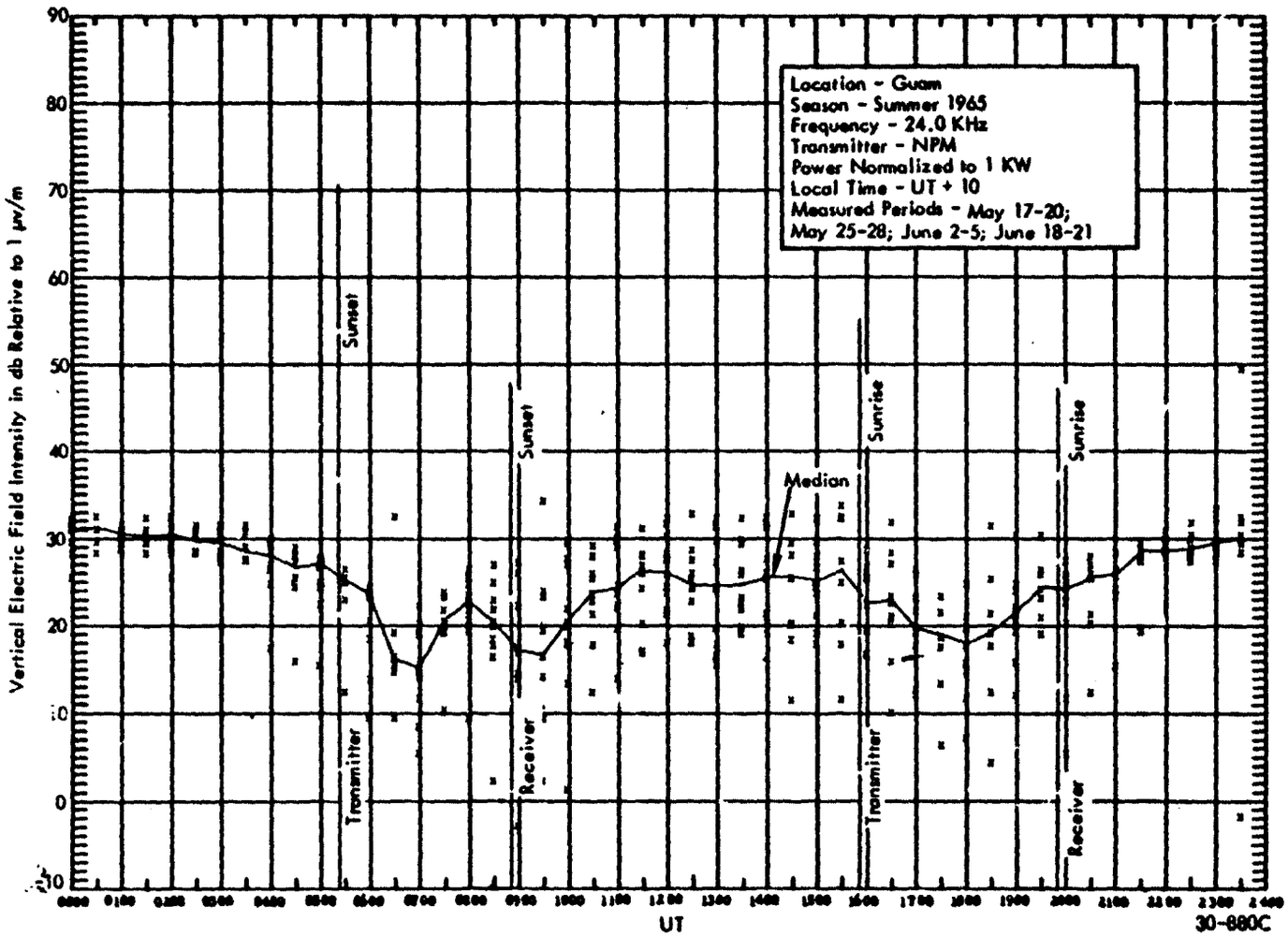

Figure 16 Diumal Variation of Signal

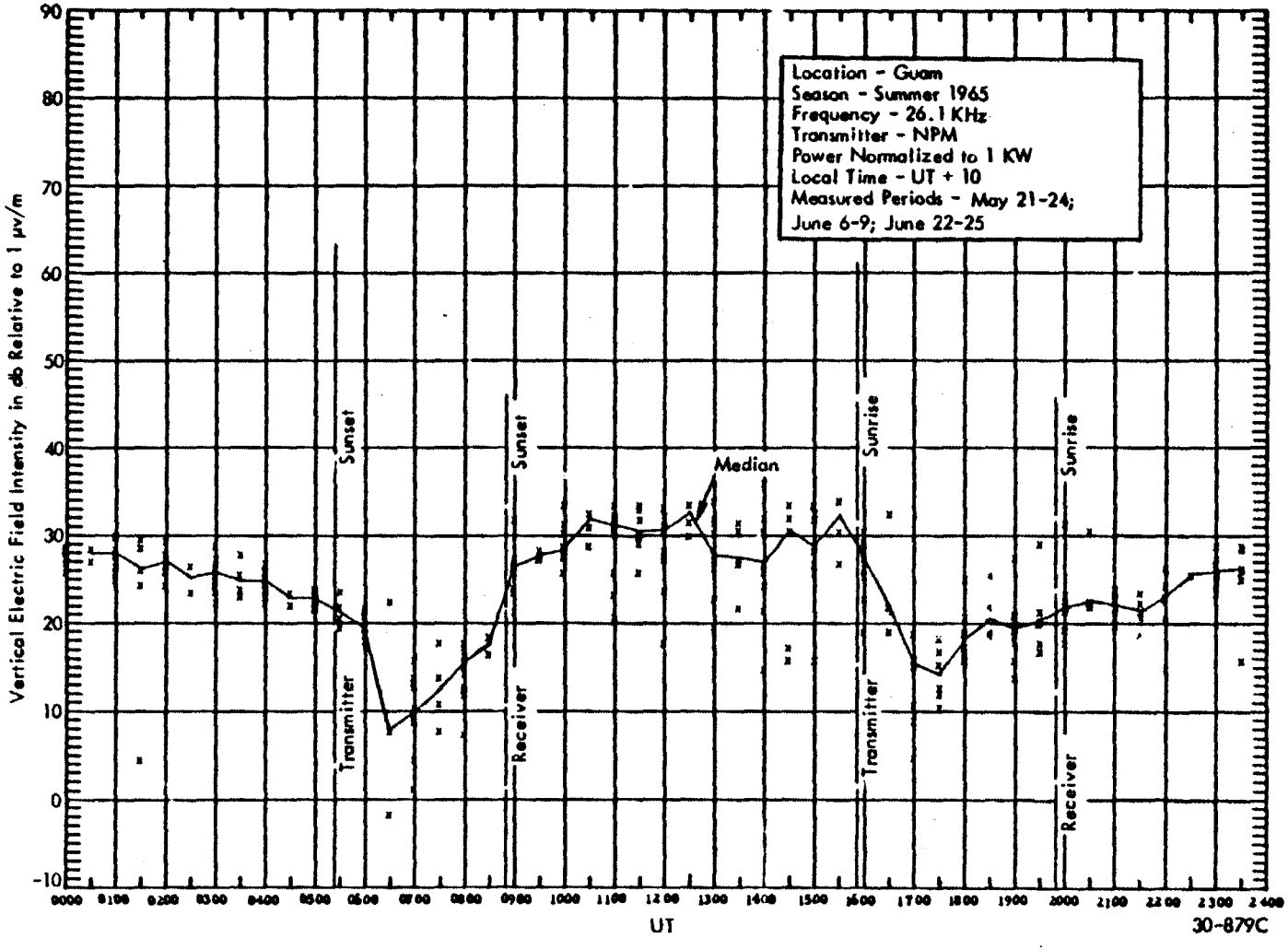

Figure 17 Diurnal Variation of Signal

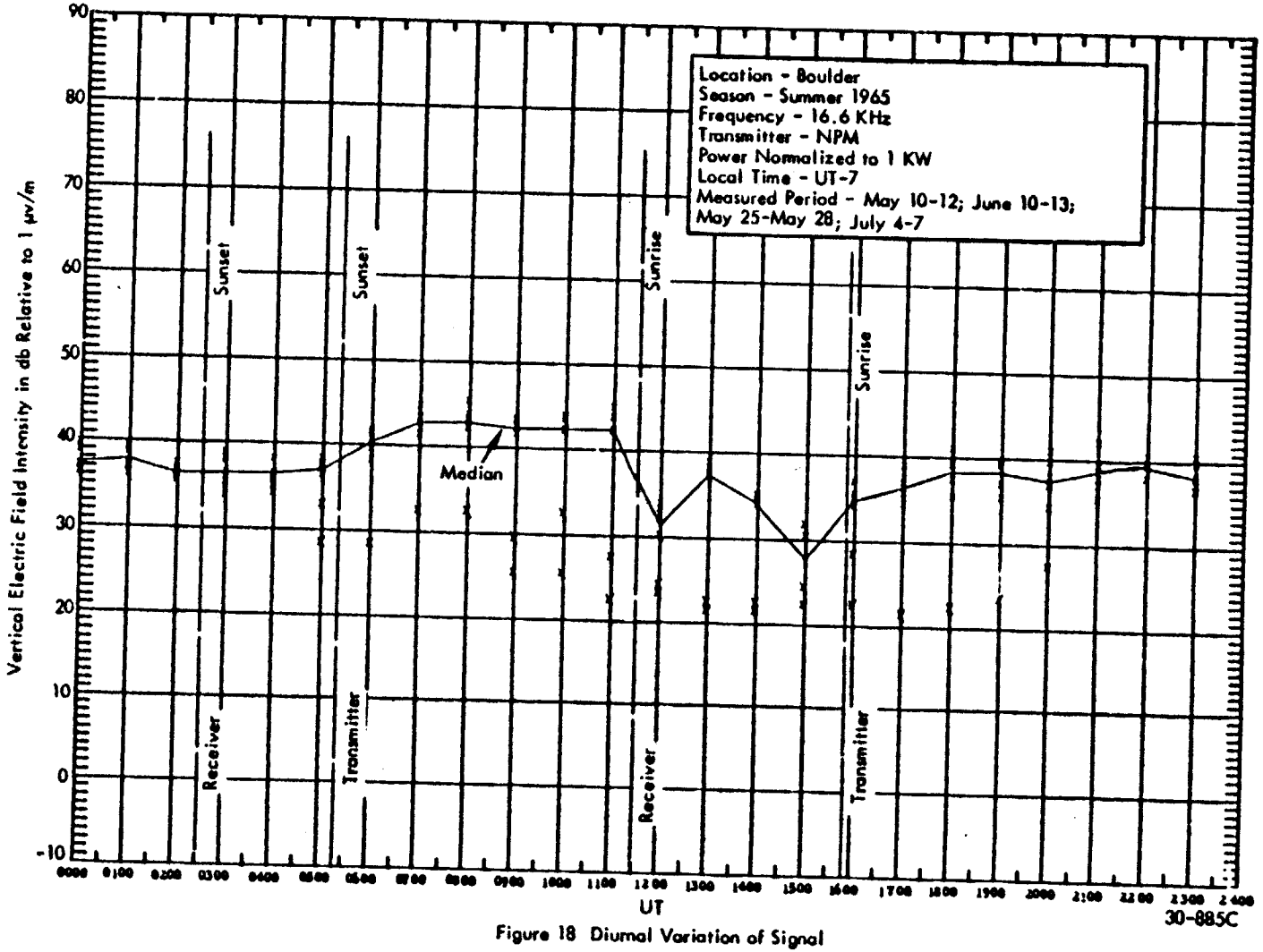

Figure 18 Diumal Variation of Signal

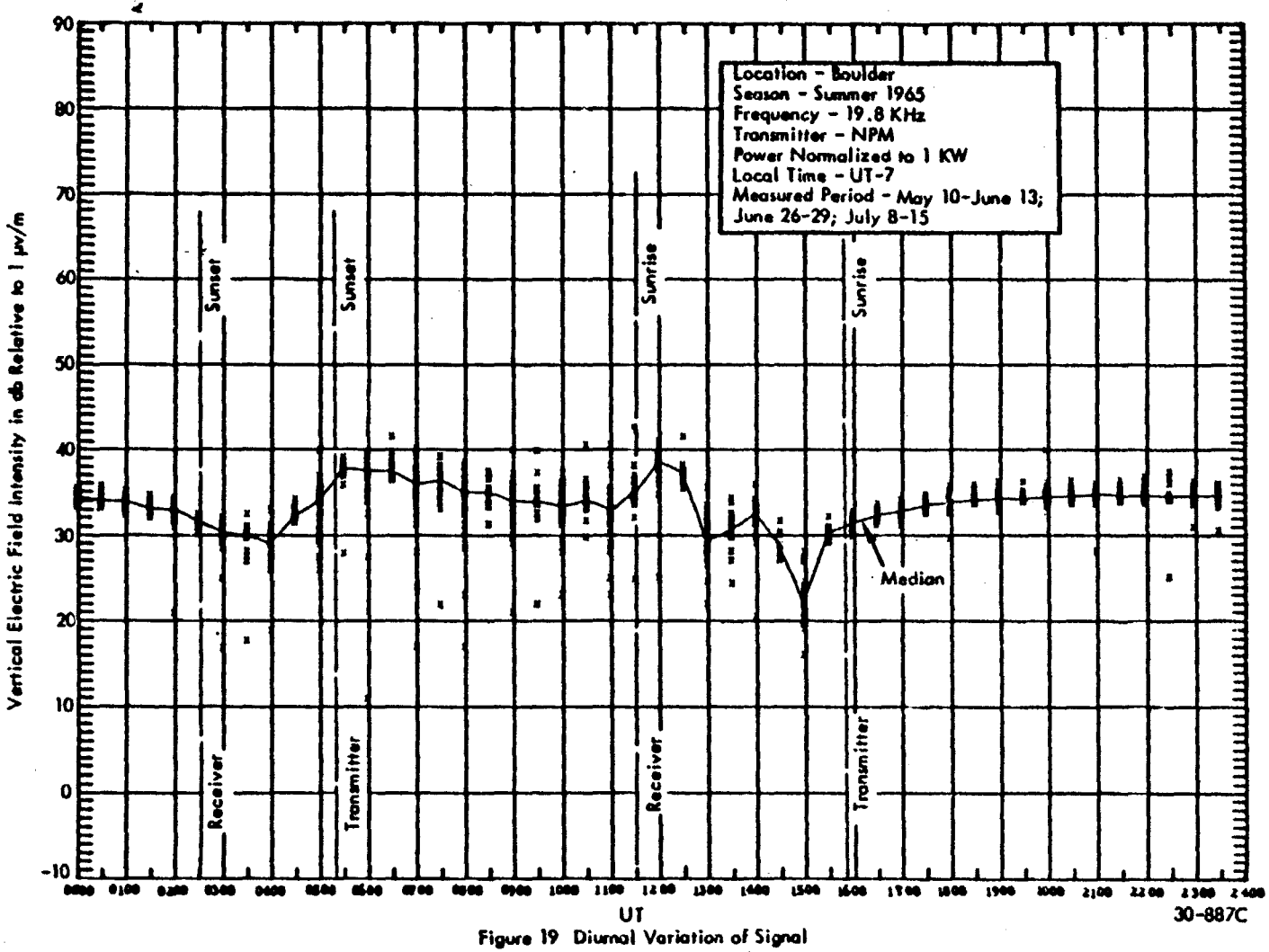

Figure 19 Diurnal Variation of Signal

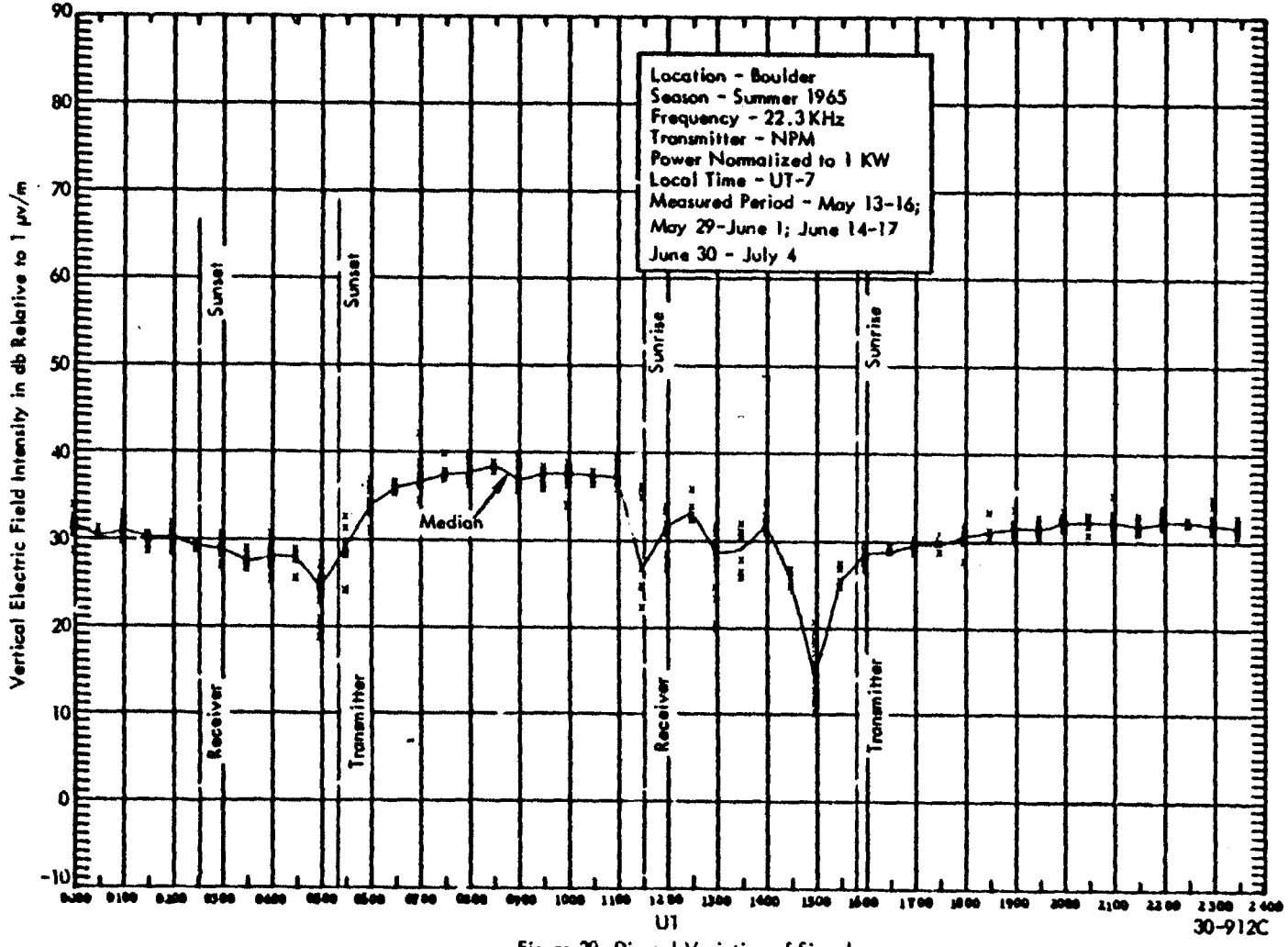

Figure 20 Diurnal Variation of Signal

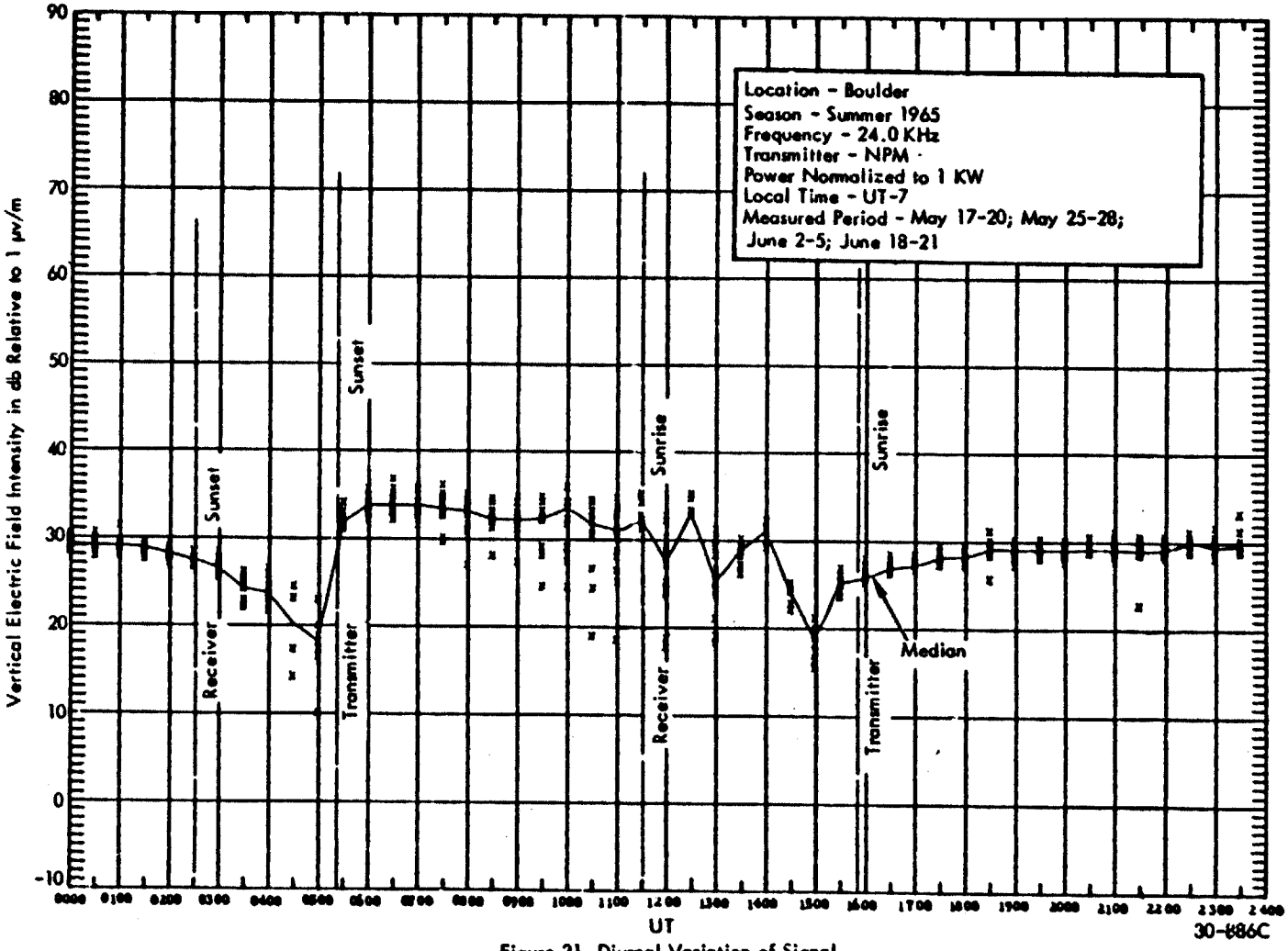

Figure 21 Diurnal Variation of Signal

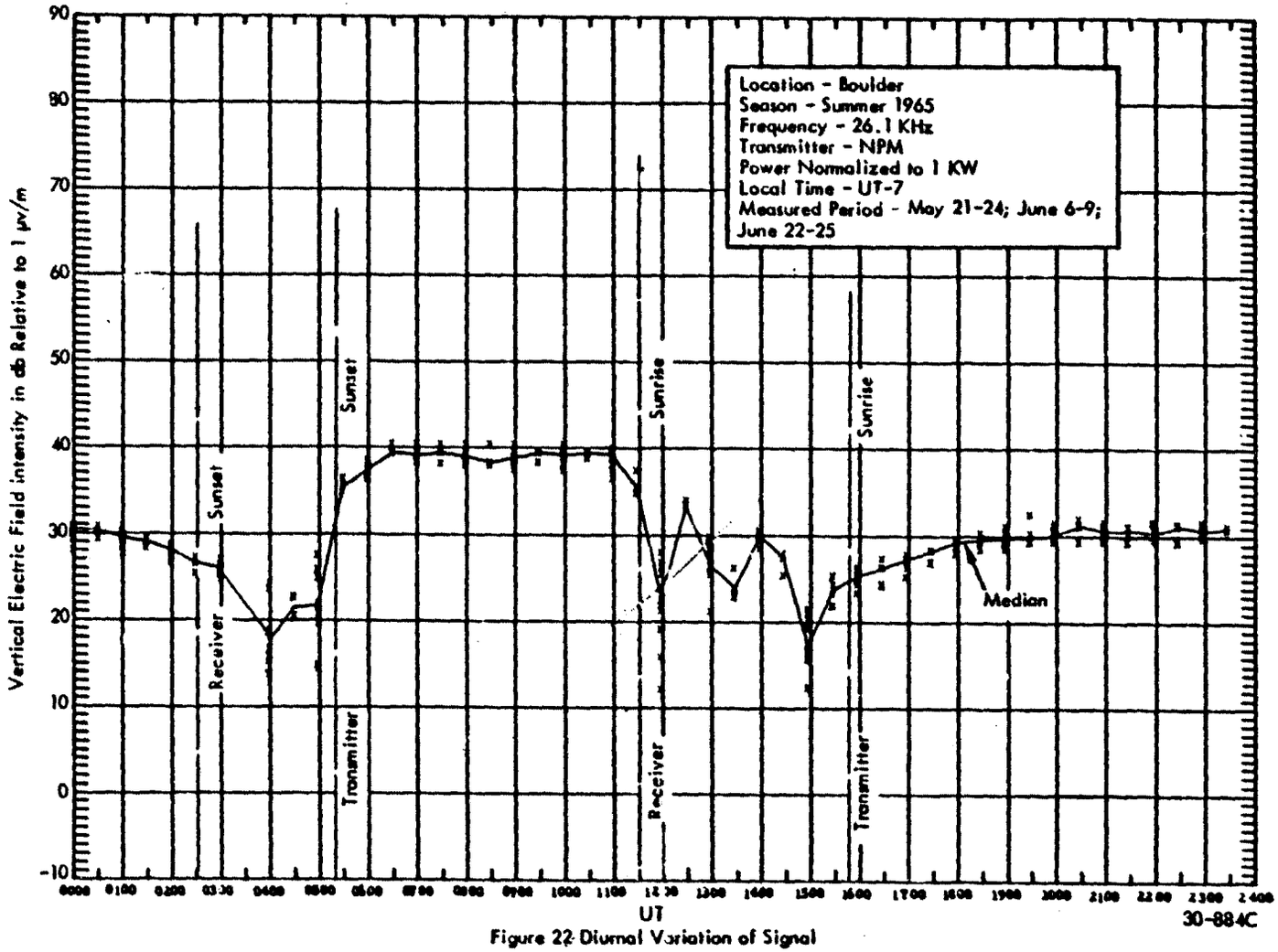

Figure 22 Diurnal Variation of Signal

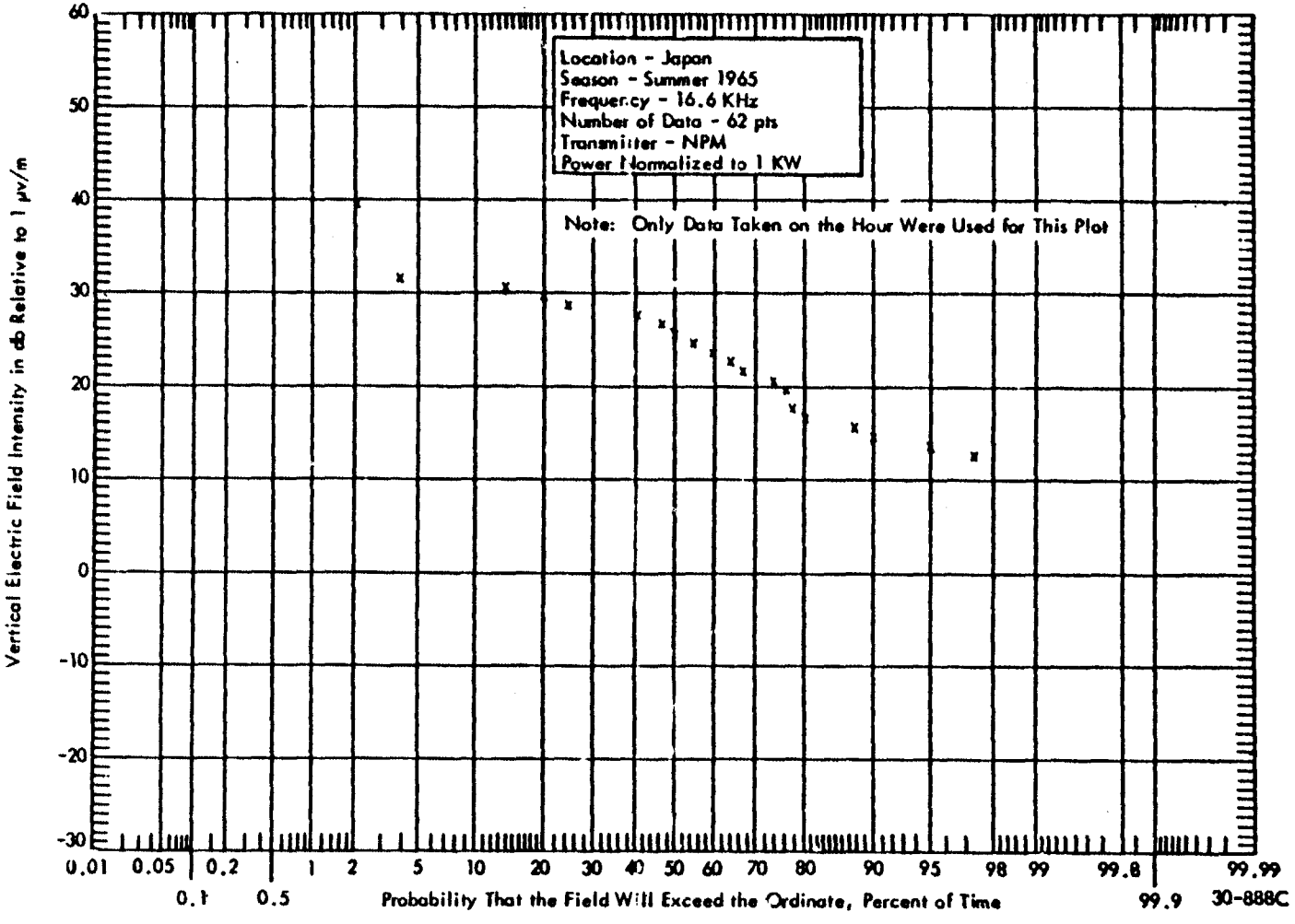

Figure 23 Probability Distribution of Measured Signal Intensity

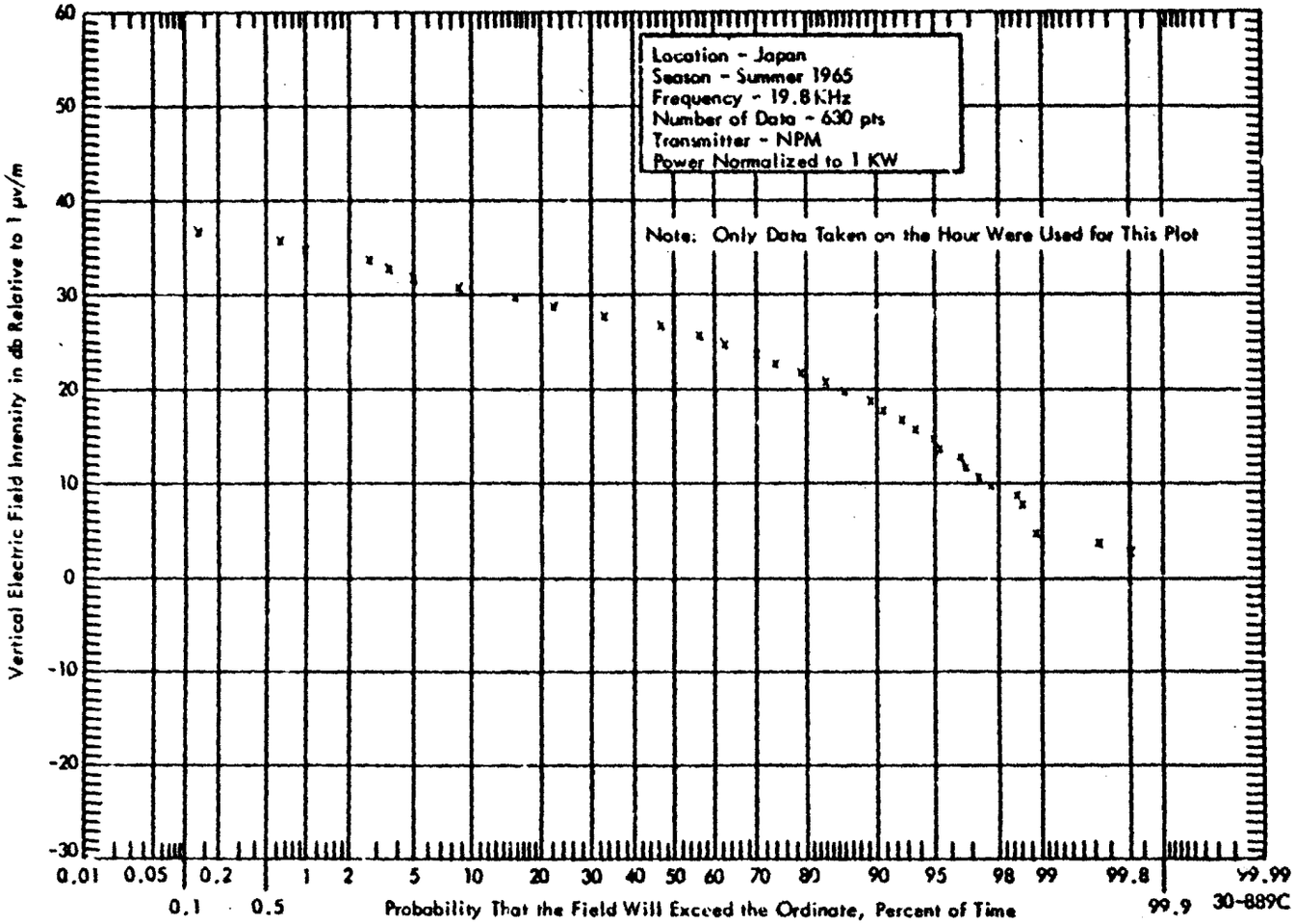

Figure 24 Probability Distribution of Measured Signal Intensity

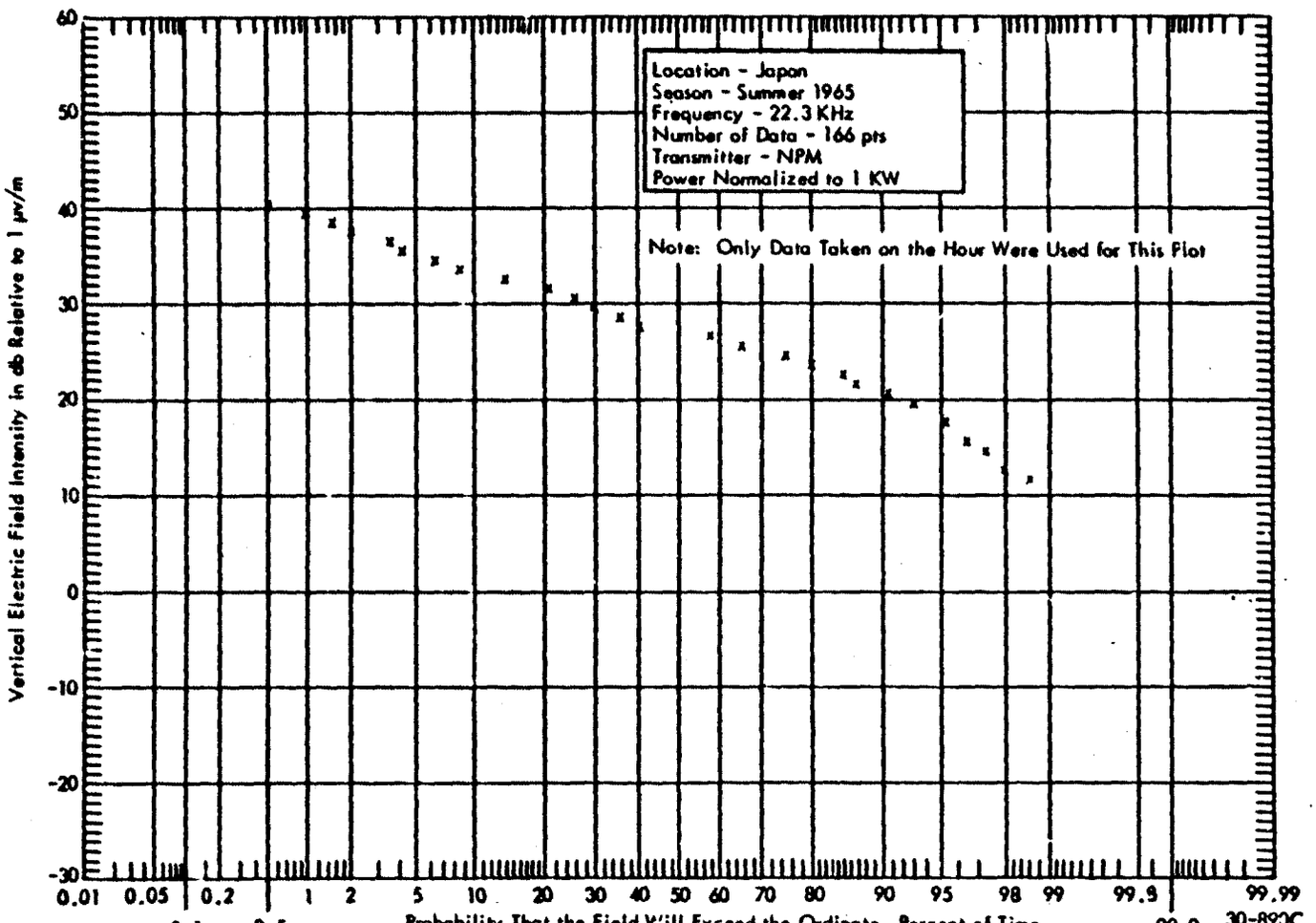

Figure 25 Probability Distribution of Measured Signal Intensity

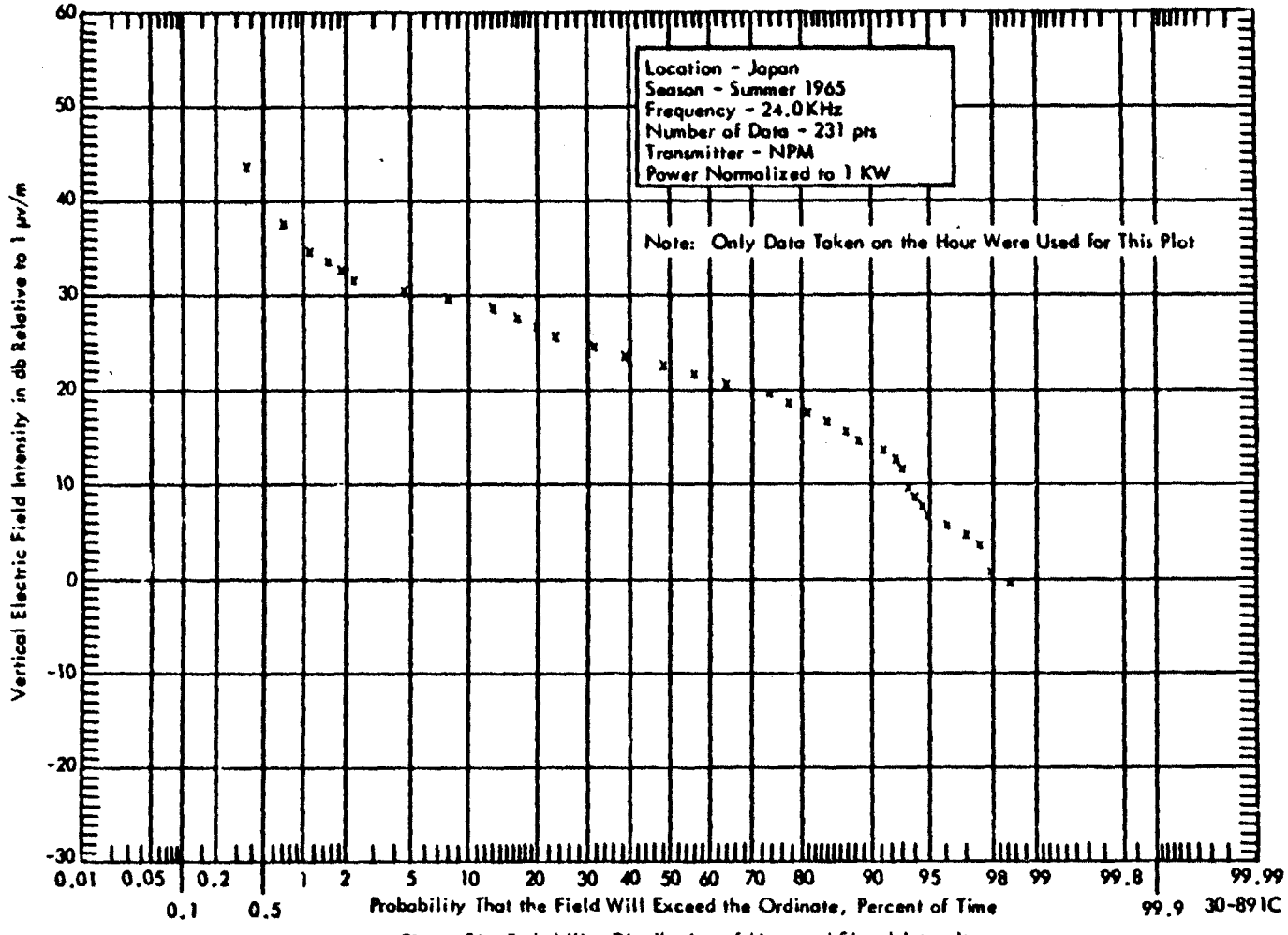

Figure 26 Probability Distribution of Measured Signal Intensity

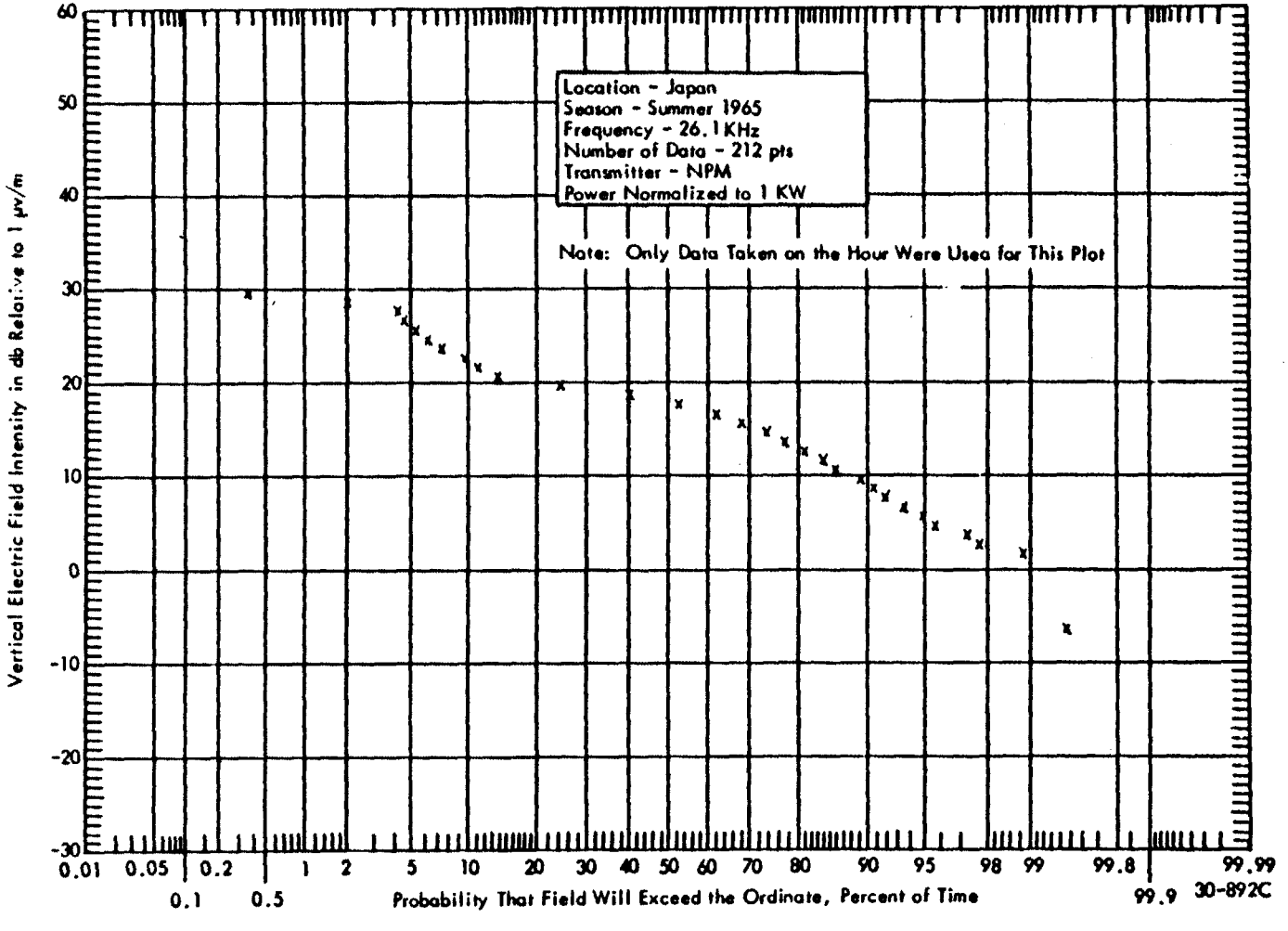

Figure 27 Probability Distribution of Measured Signal Intensity

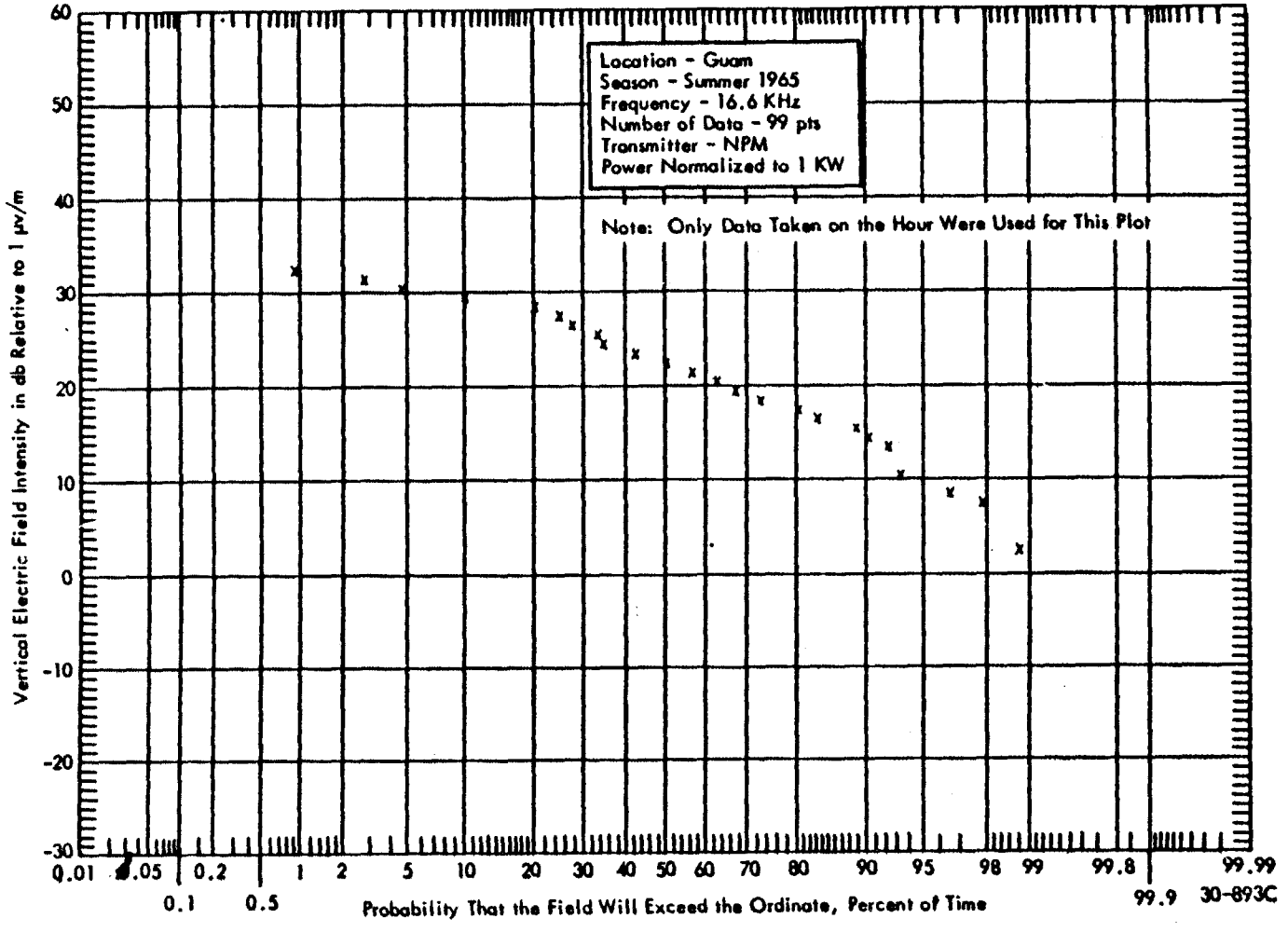

Figure 28 Probability Distribution of Measured Signal Intensity

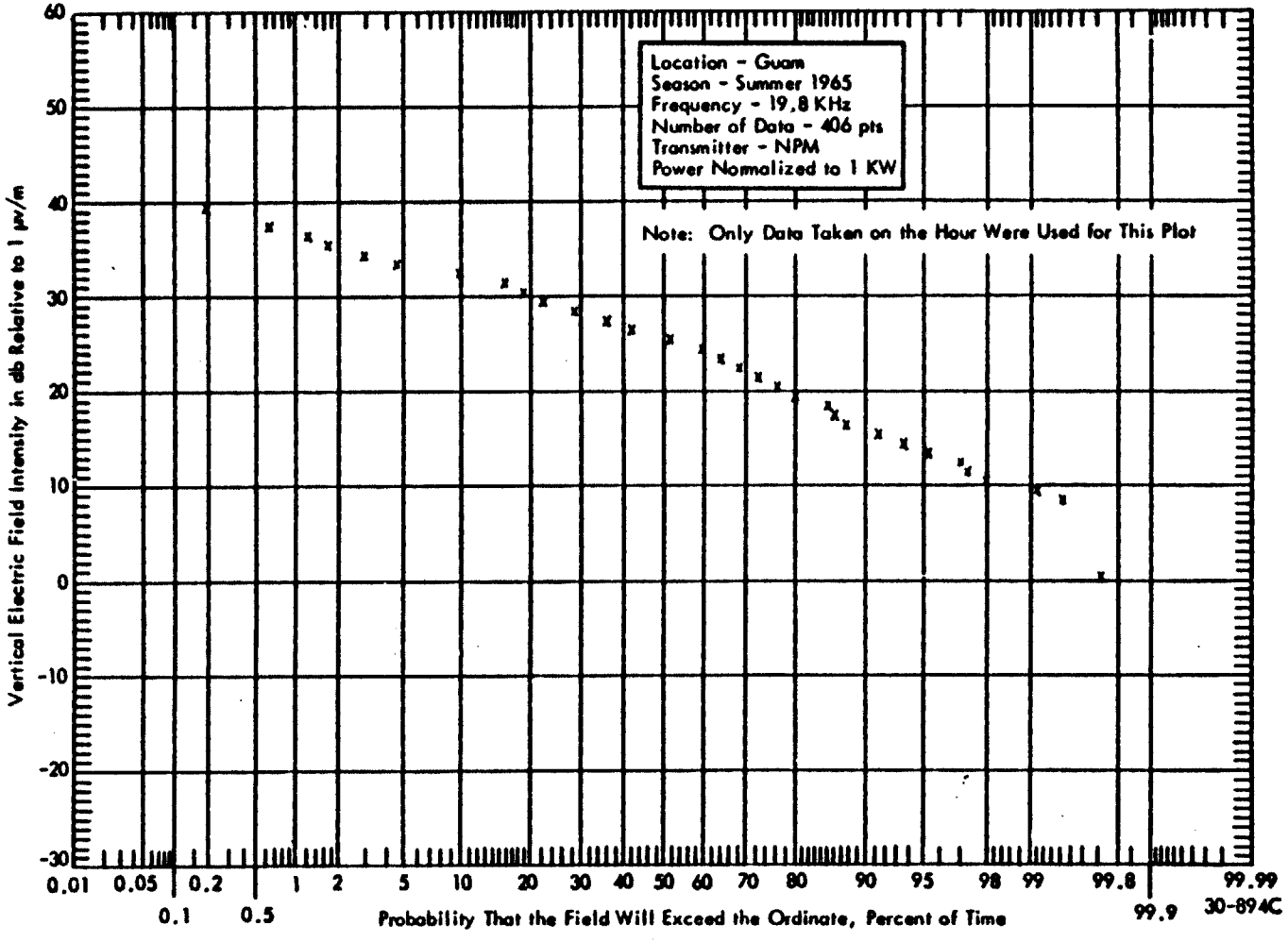

Figure 29 Probability Distribution of Measured Signal Intensity

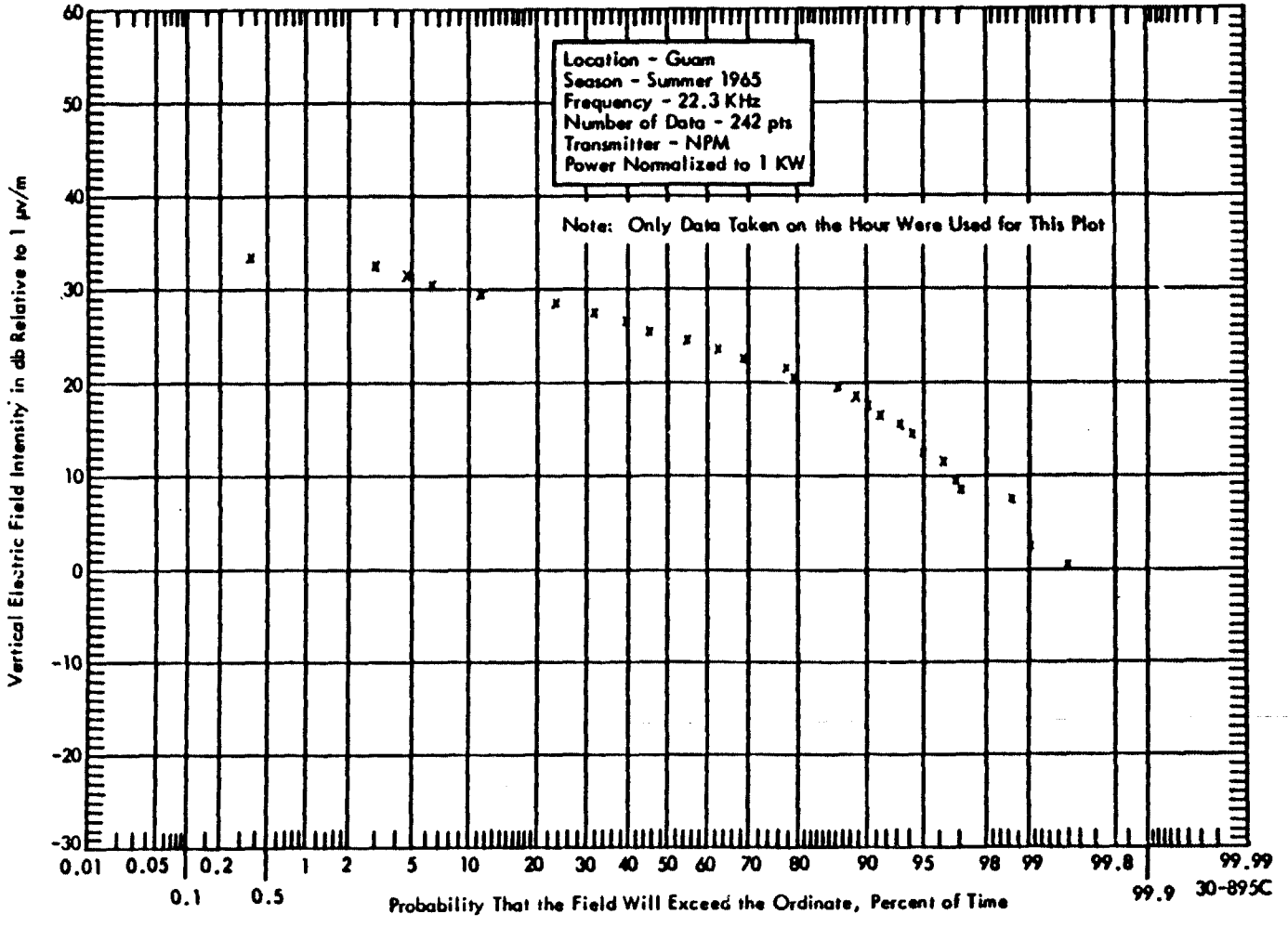

Figure 30 Probability Distribution of Measured Signal Intensity

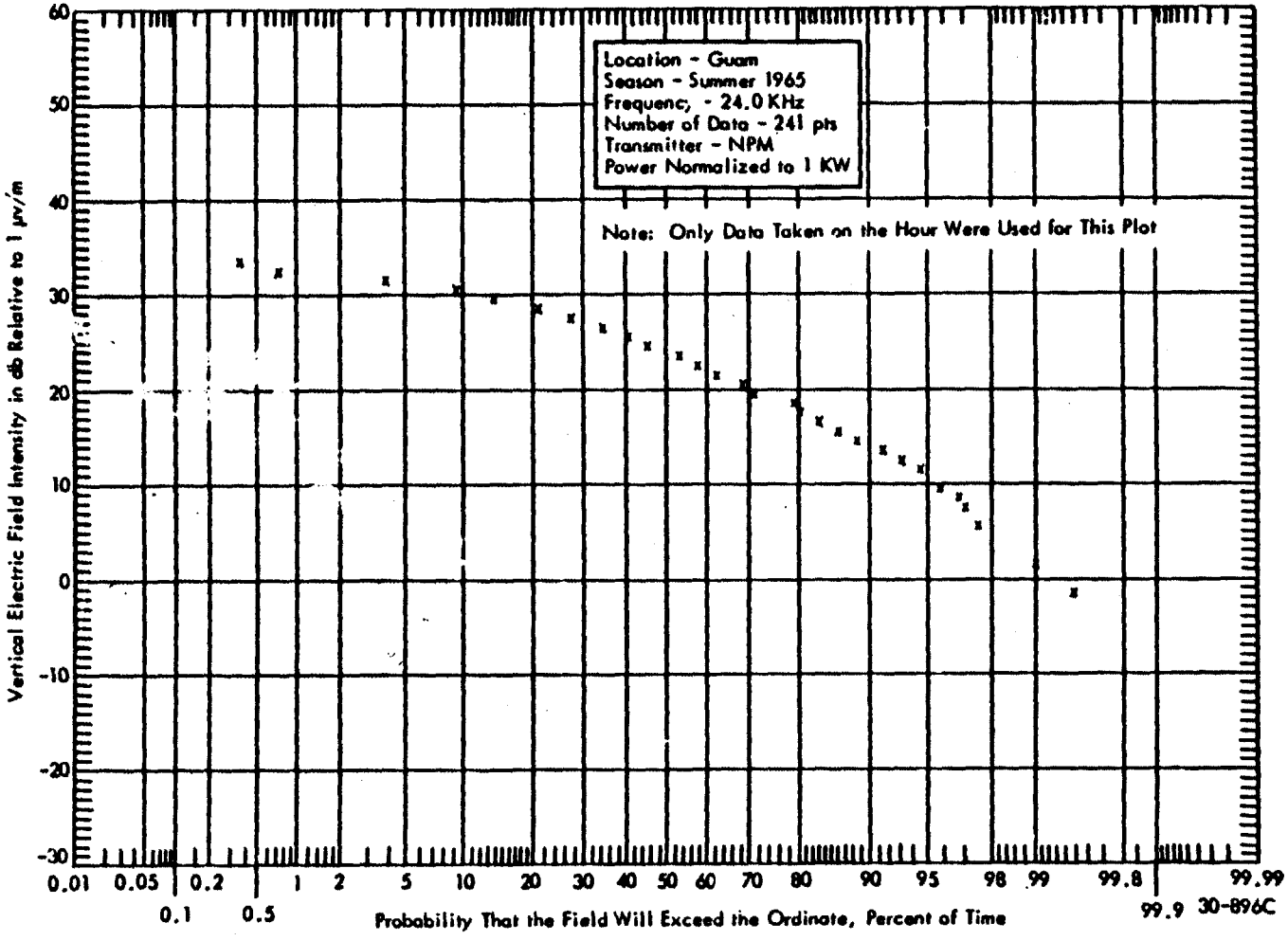

Figure 31 Probability Distribution of Measured Signal Intensity

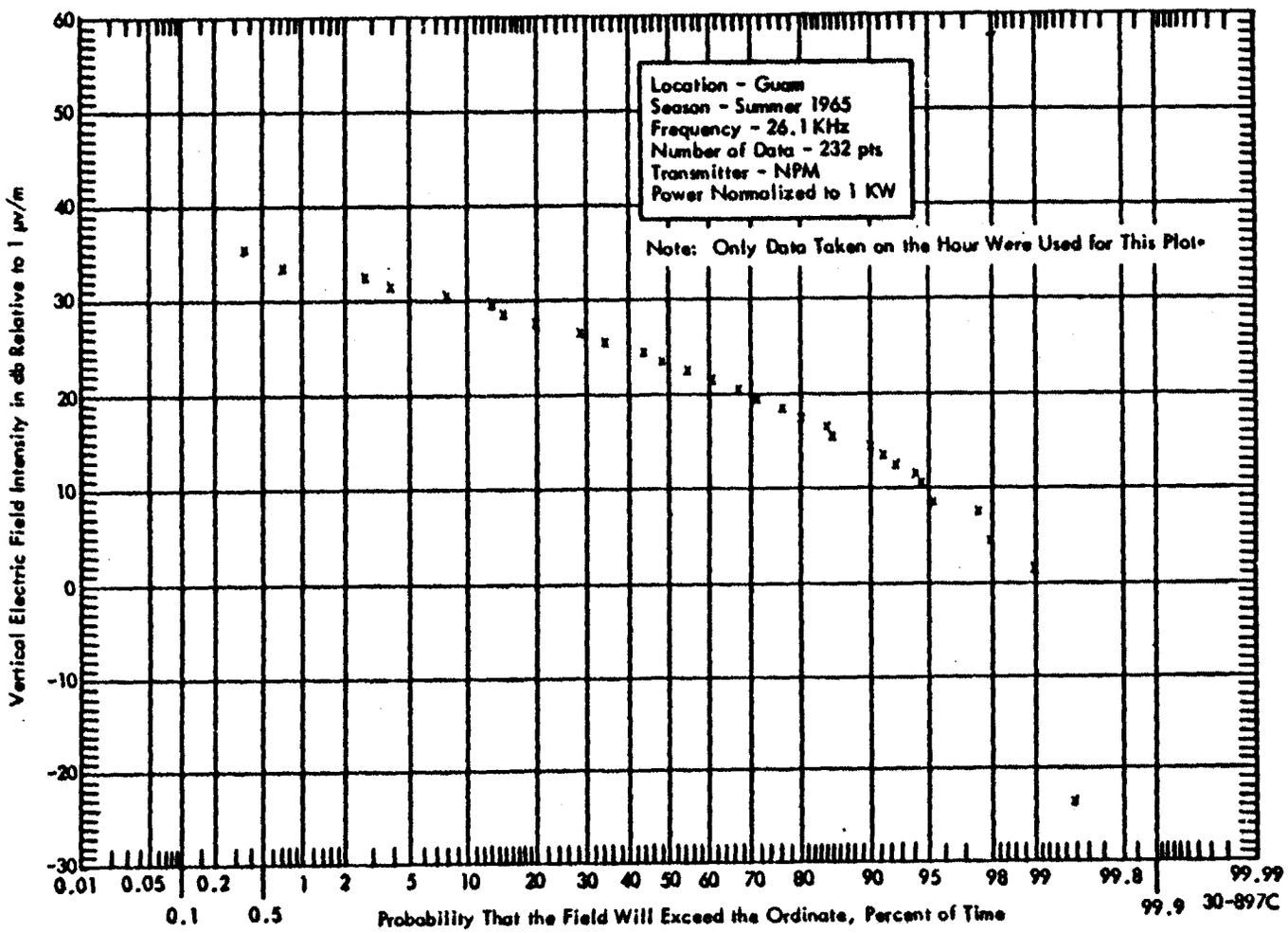

Figure 32 Probability Distribution of Measured Signal Intensity

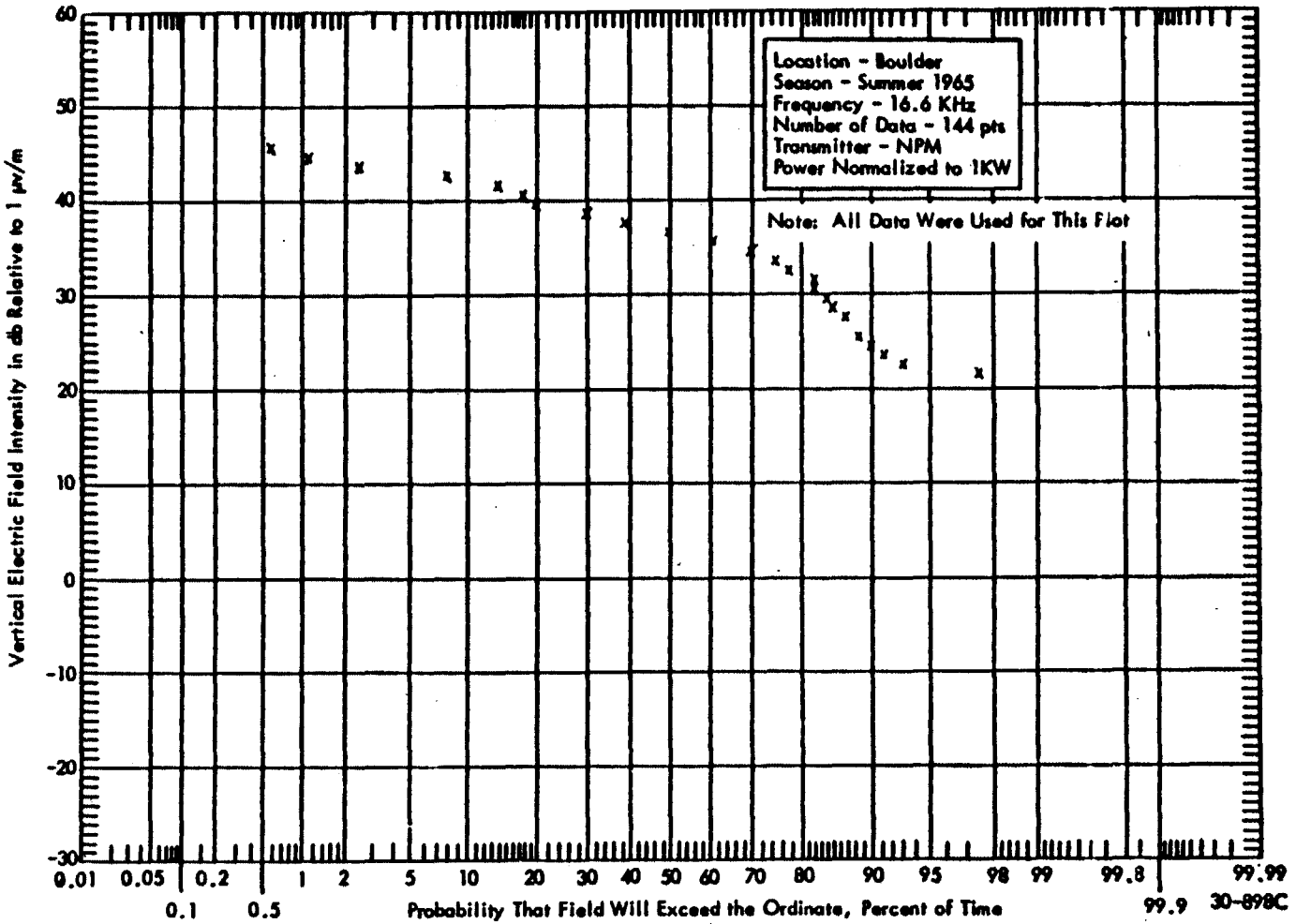

Figure 33 Probability Distribution of Measured Signal Intensity

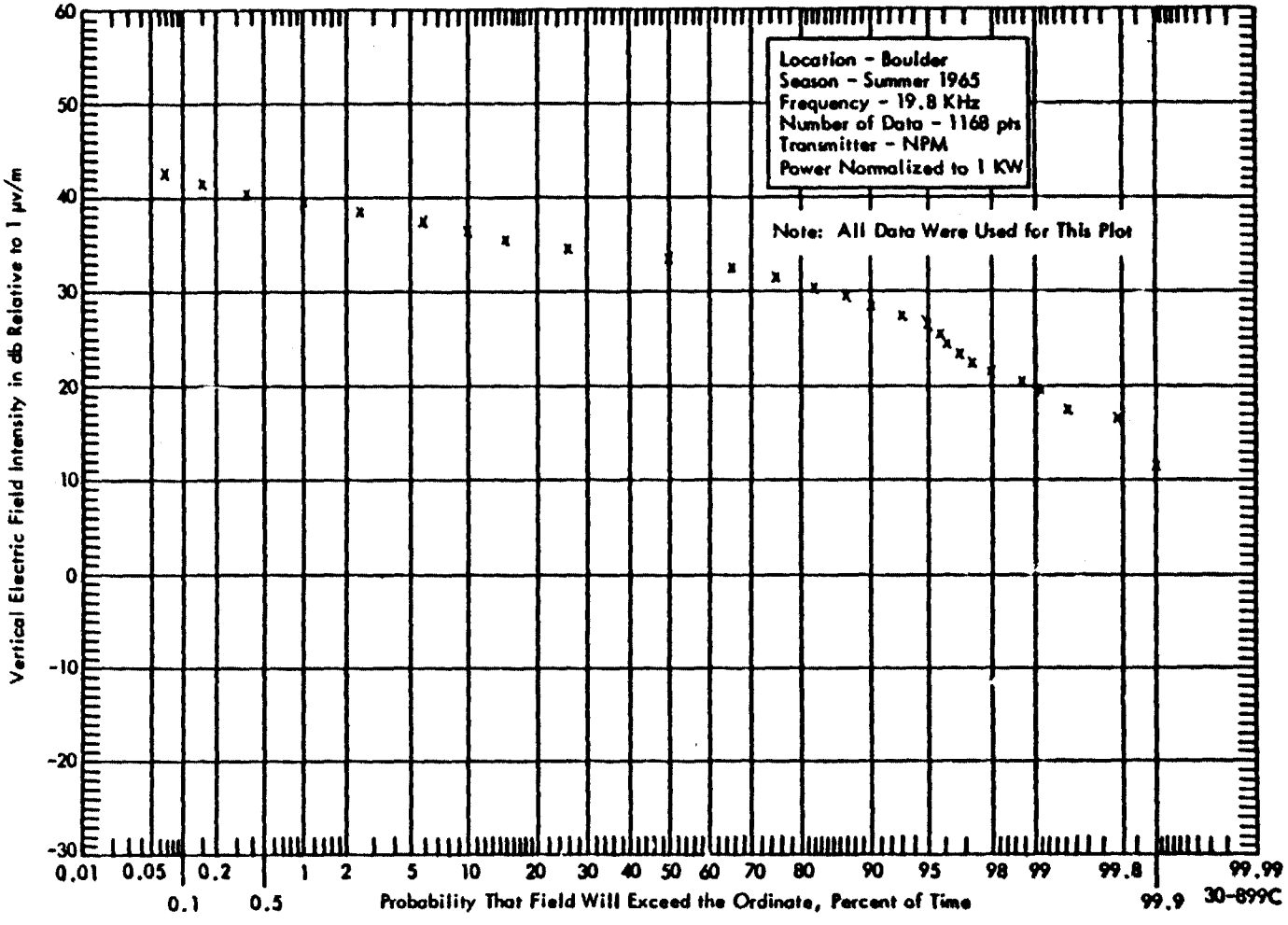

Figure 34 Probability Distribution of Measured Signal Intensity

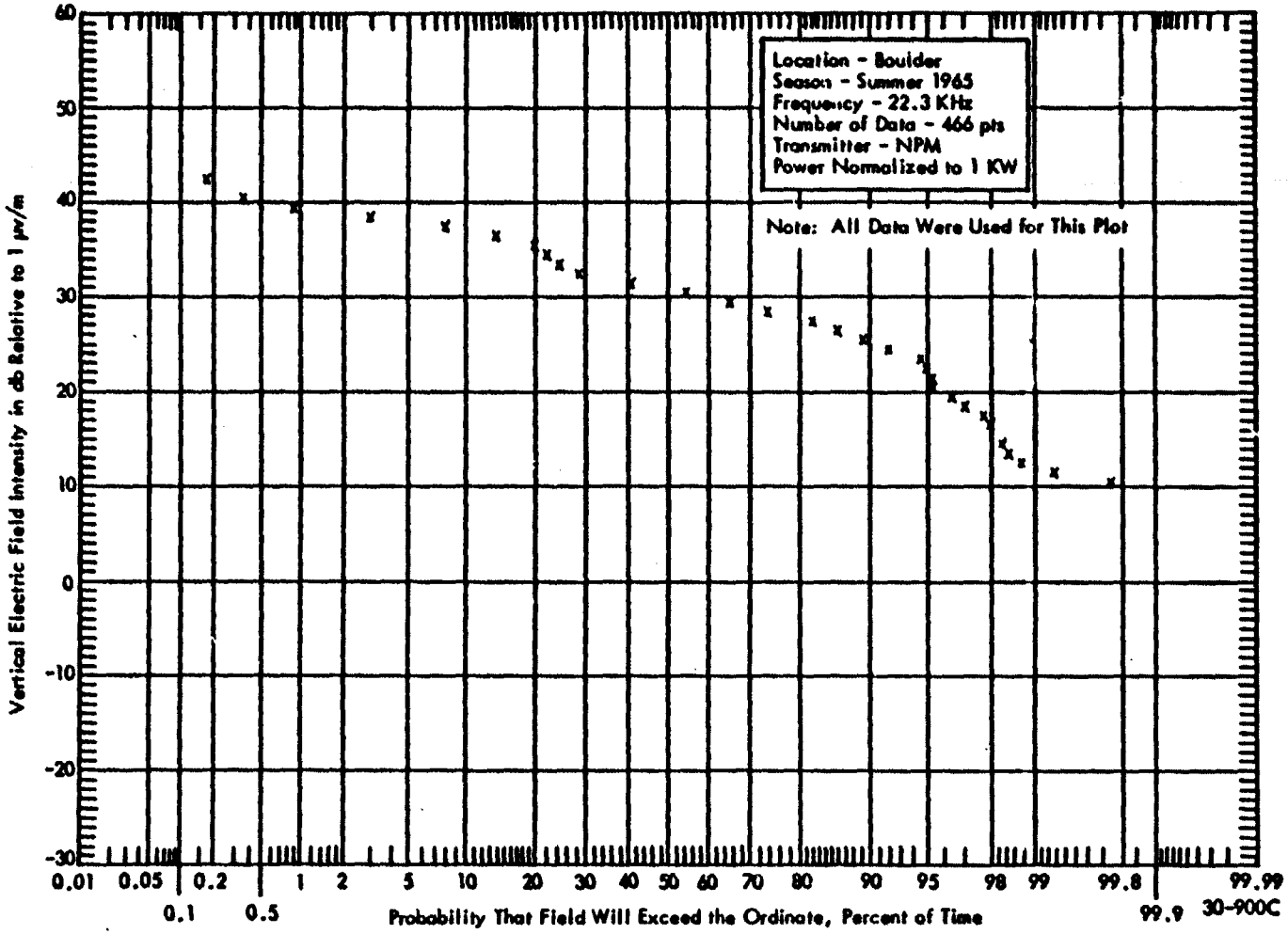

Figure 35 Probability Distribution of Measured Signal Intensity

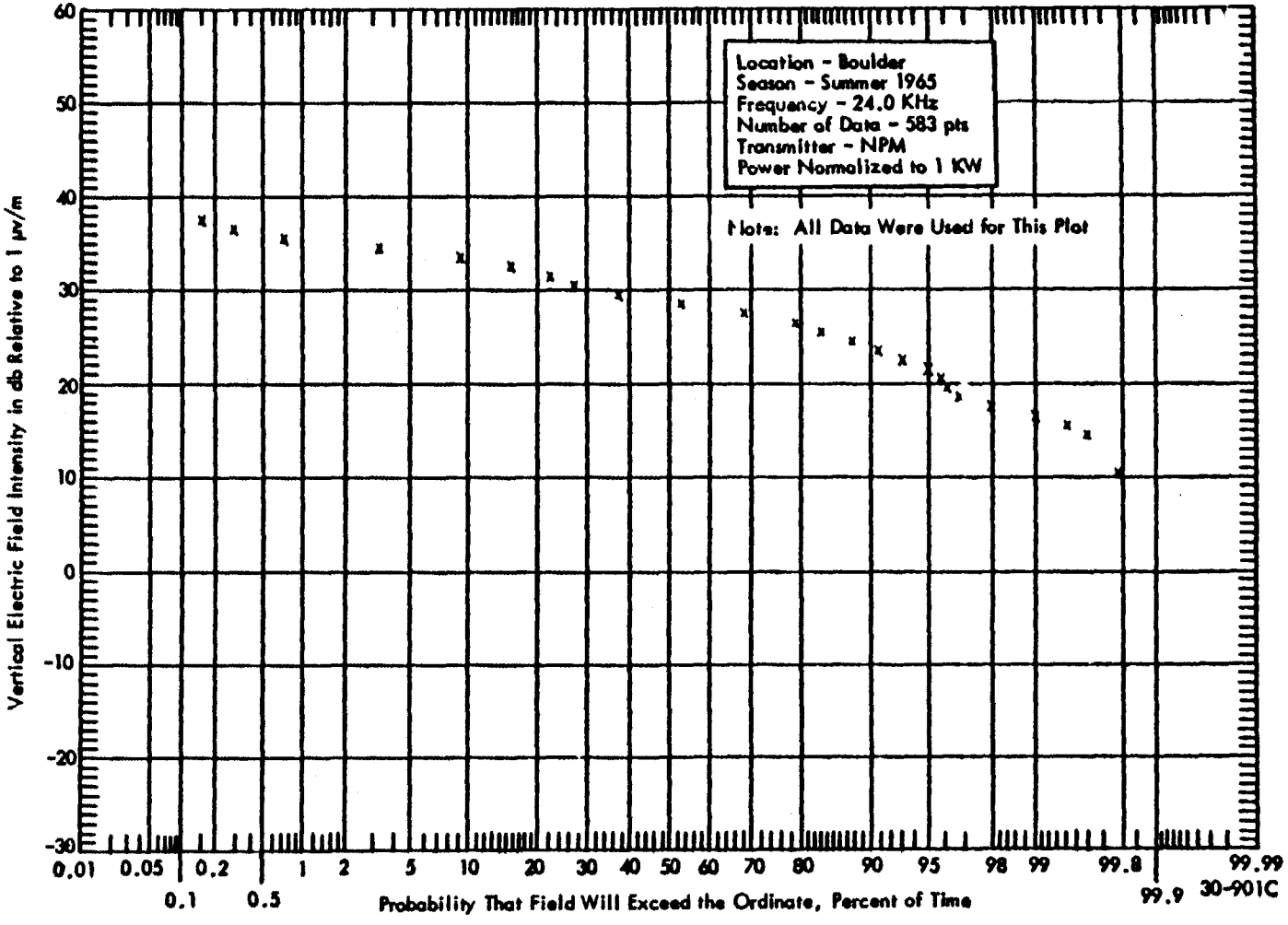

Figure 36 Probability Distribution of Measured Signal Intensity

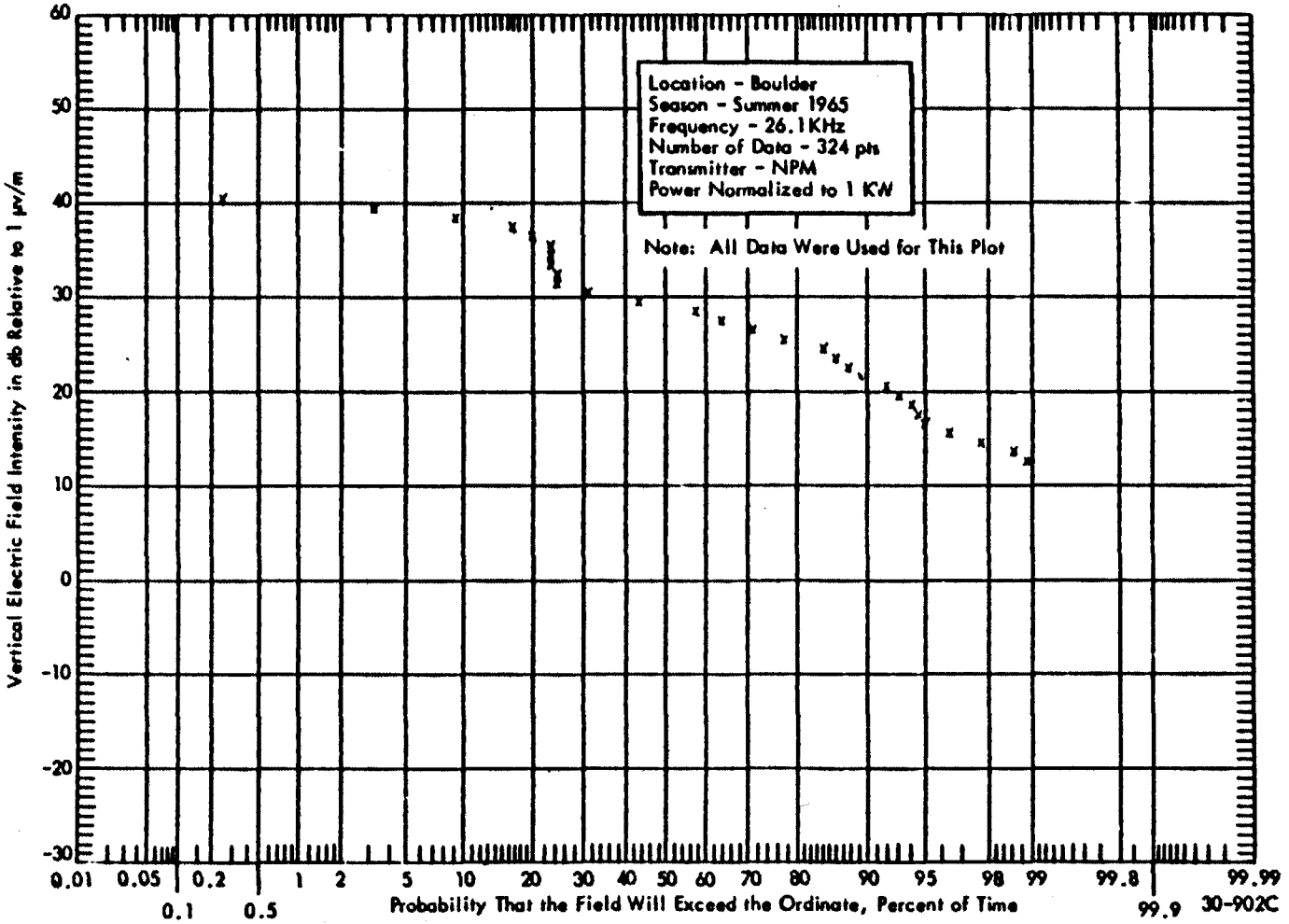

Figure 37 Probability Distribution of Measured Signal Intensity

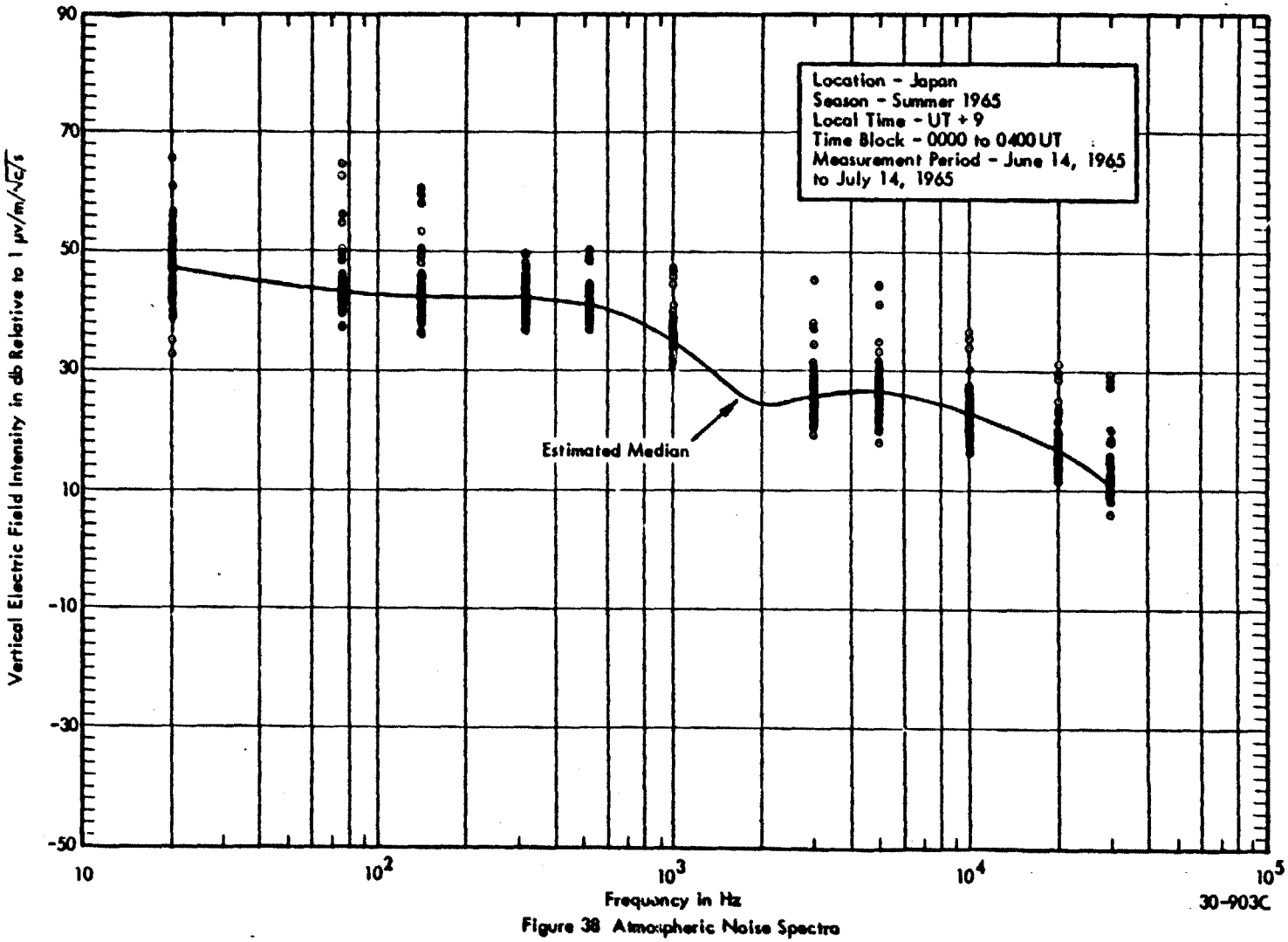

Figure 38 Atmospheric Noise Spectra

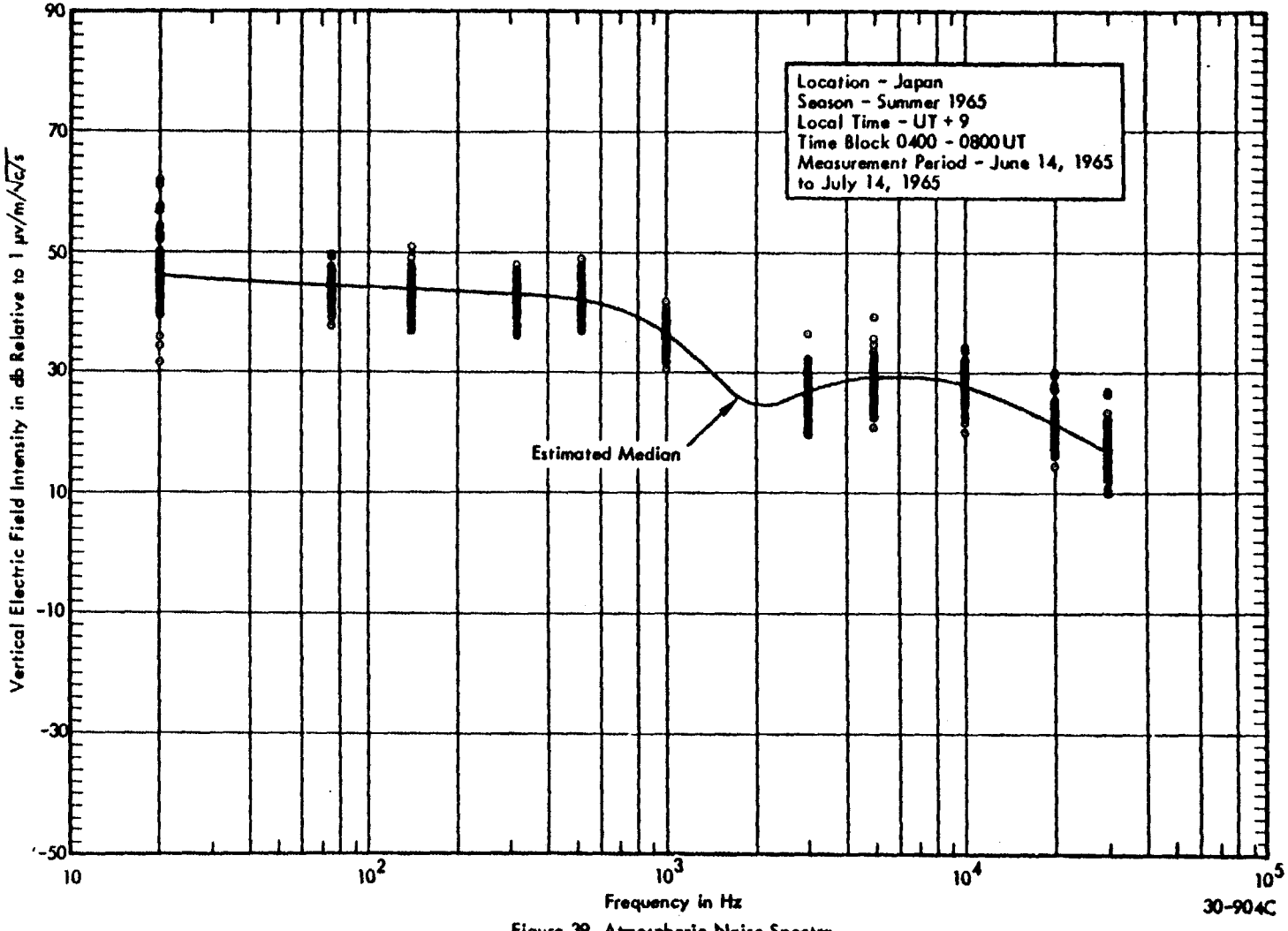

Figure 39 Atmospheric Noise Spectra

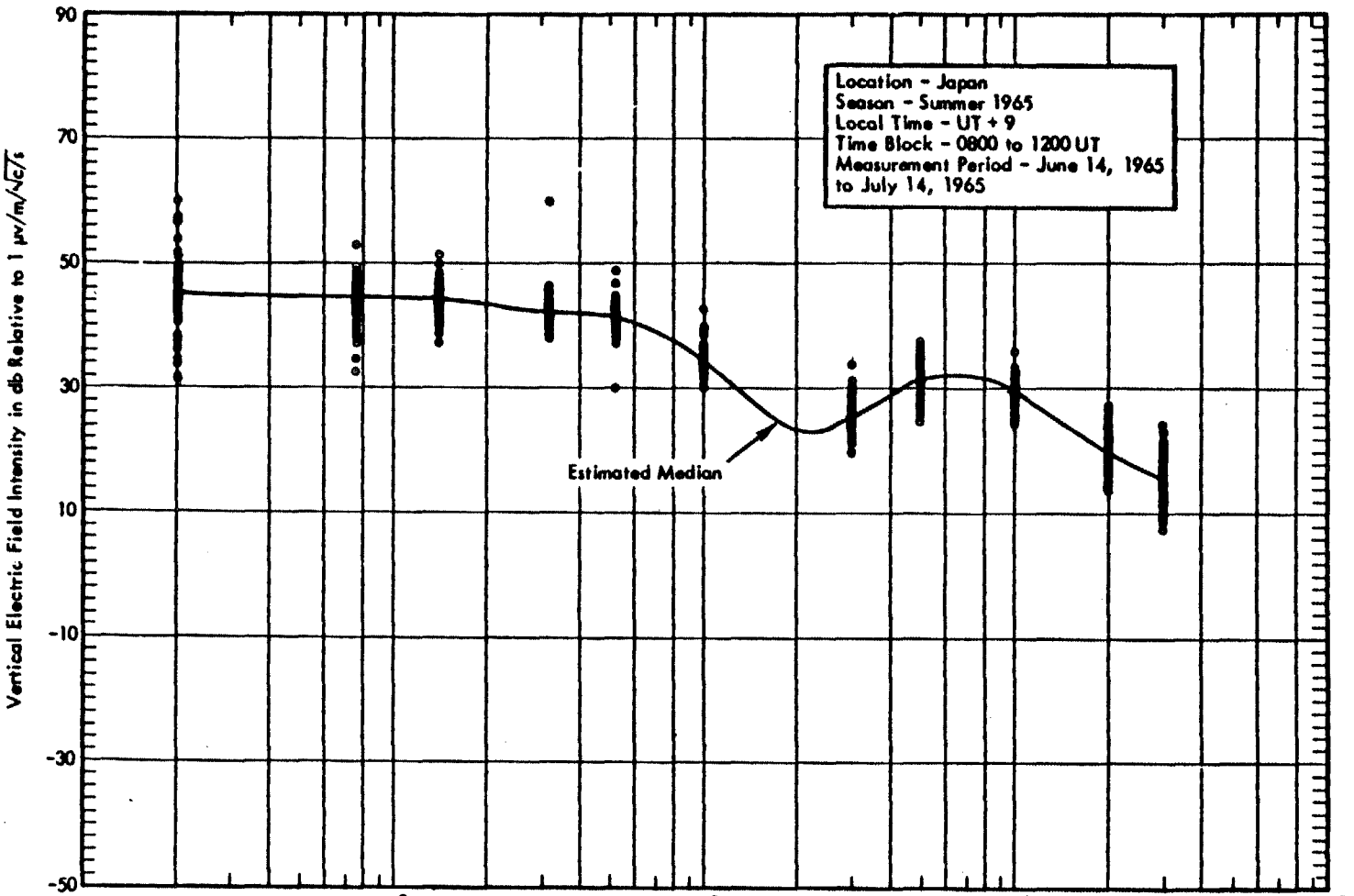

Figure 40 Atmospheric Noise Spectra

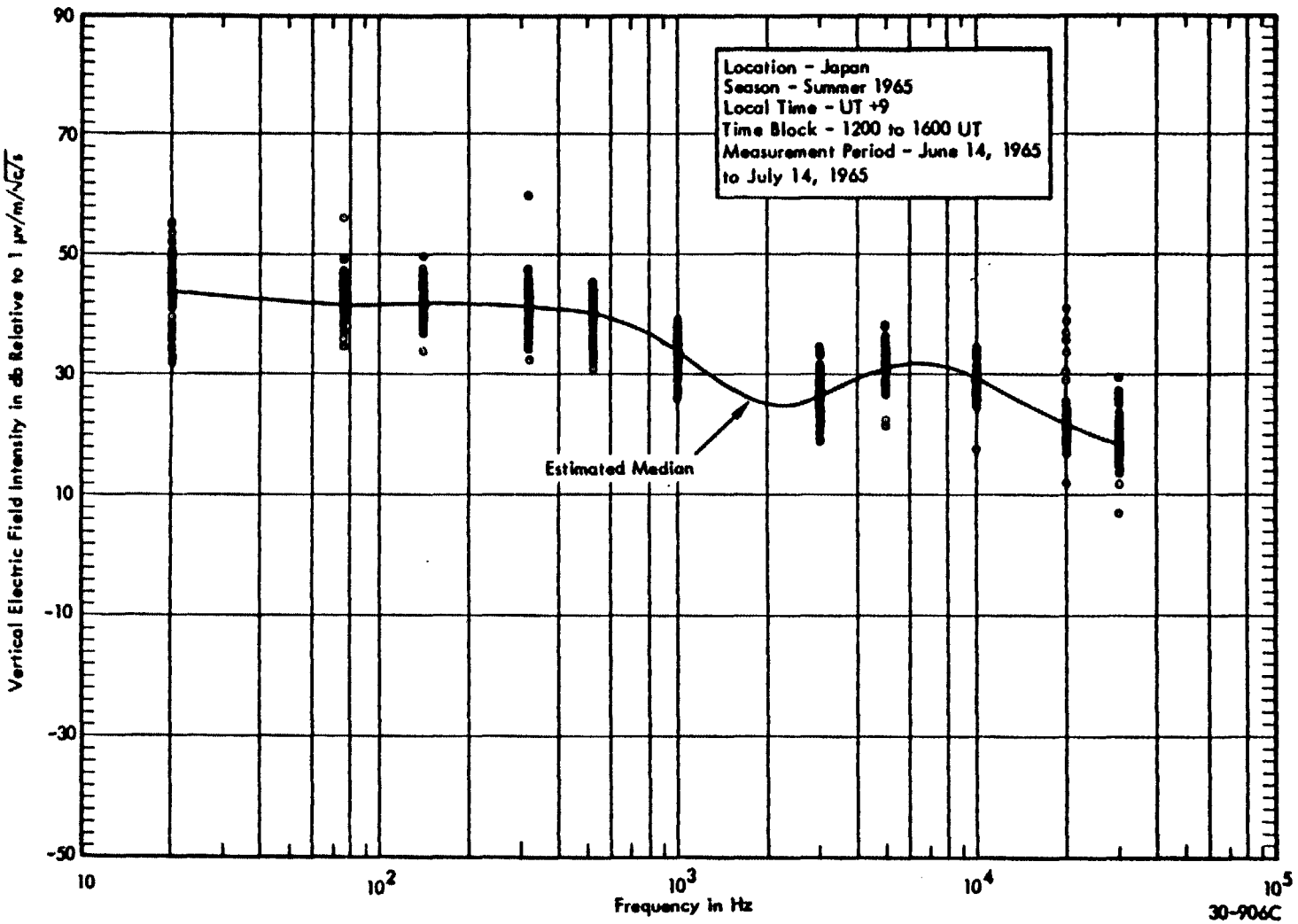

Figure 41 Atmospheric Noise Spectra

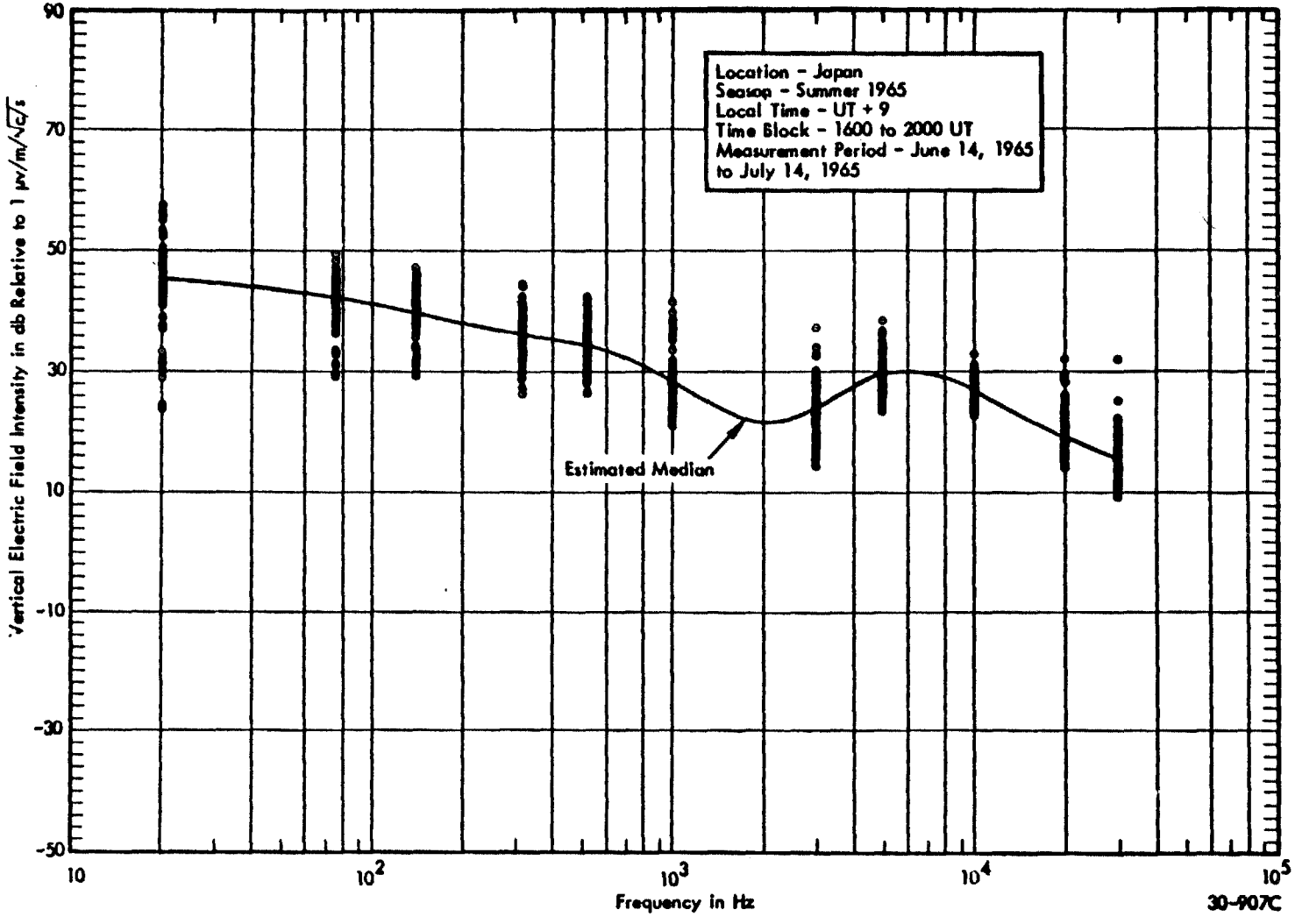

Figure 42 Atmospheric Noise Spectra

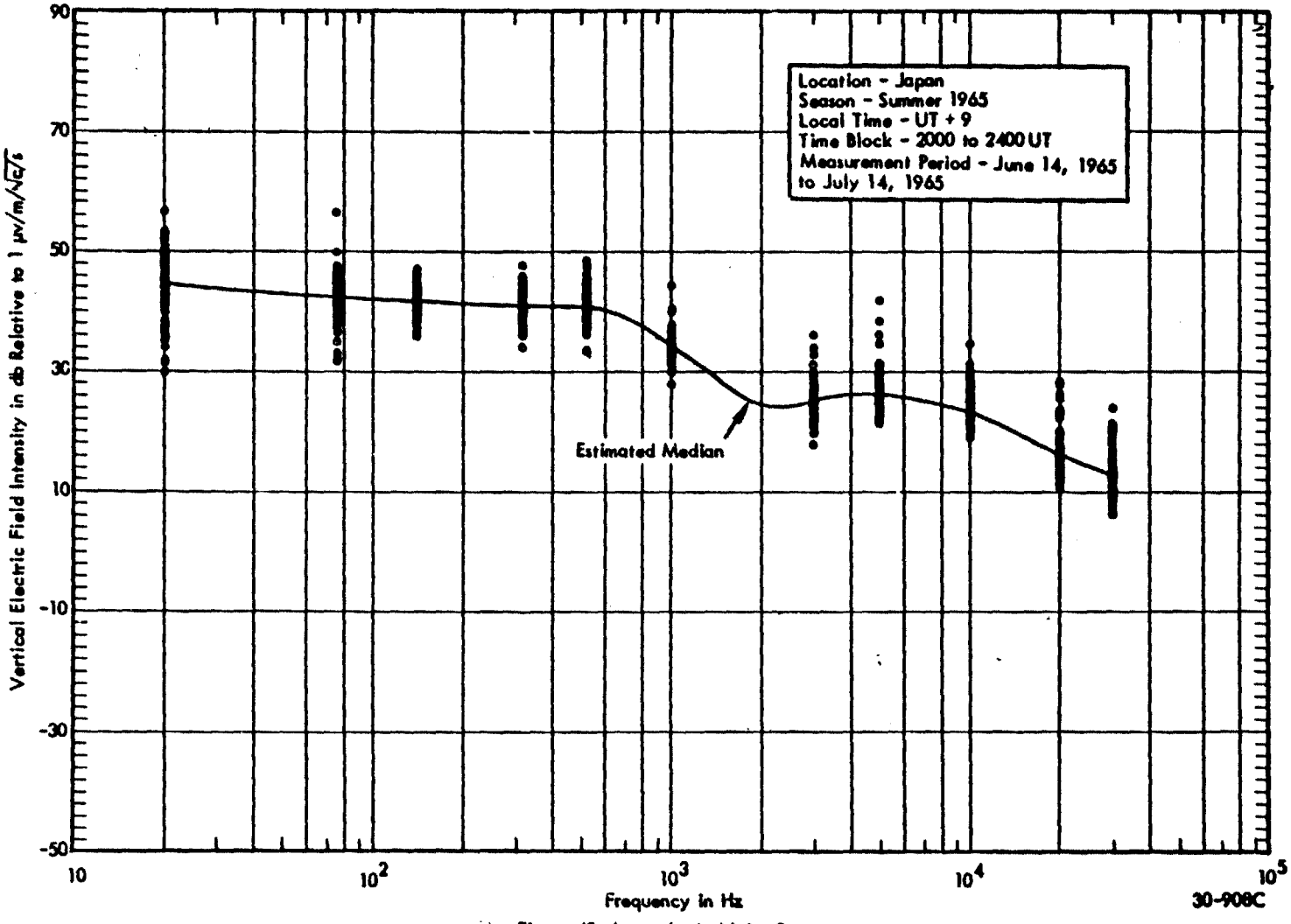

Figure 43 Atmospheric Noise Spectra

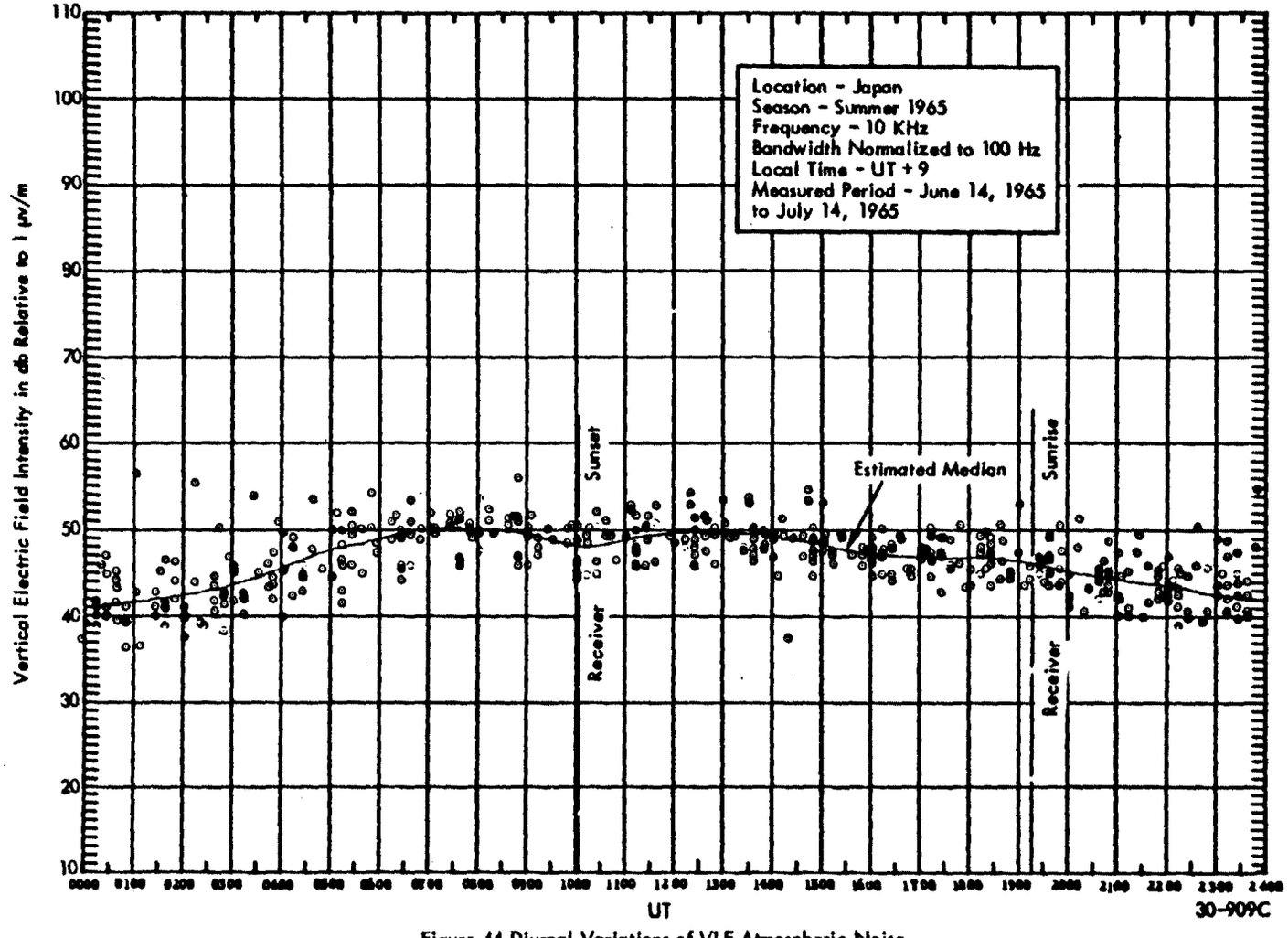

Figure 44 Diurnal Variations of VLF Atmospheric Noise

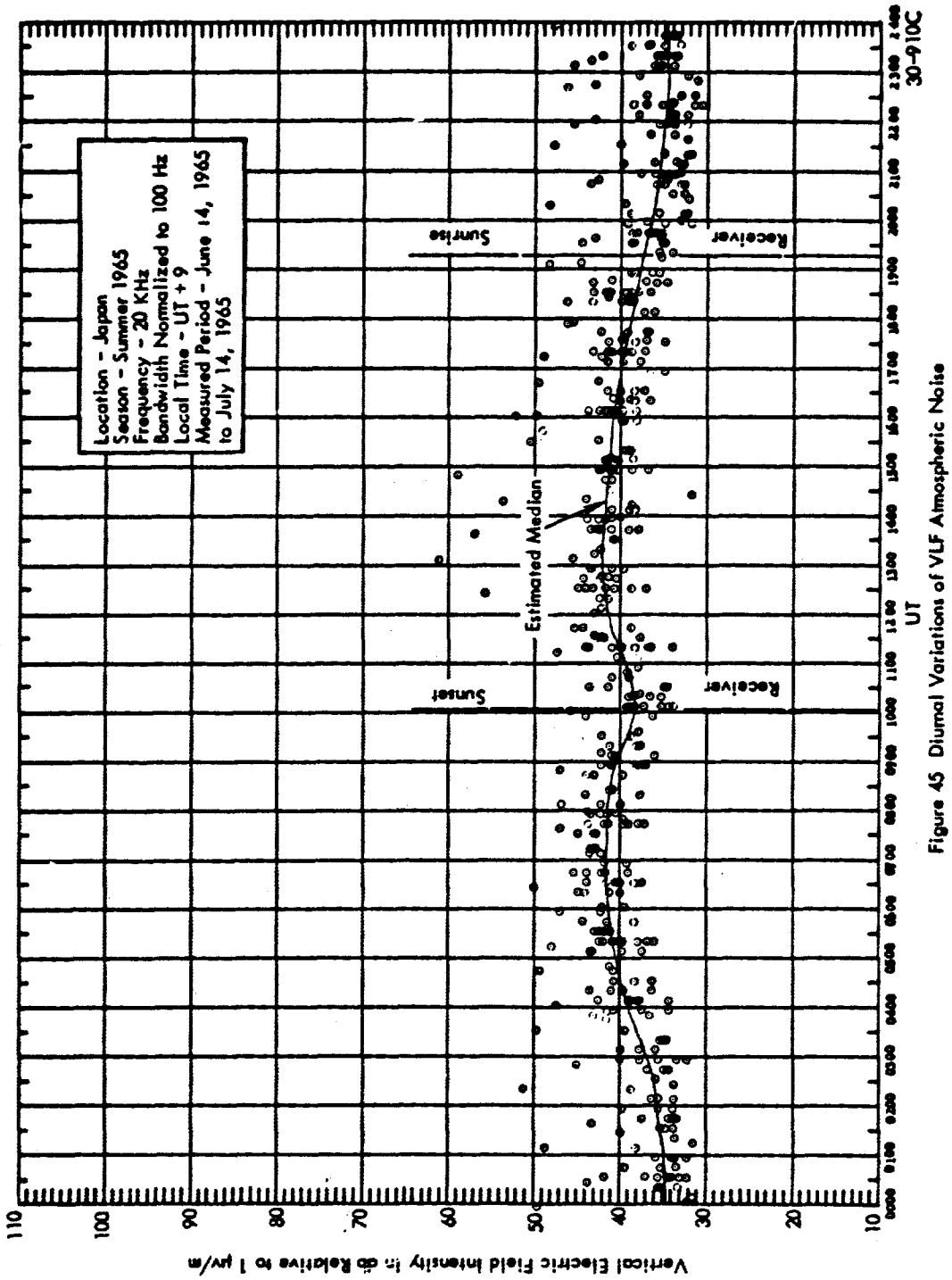

Figure 45 Diurnal Variations of VLF Atmospheric Noise

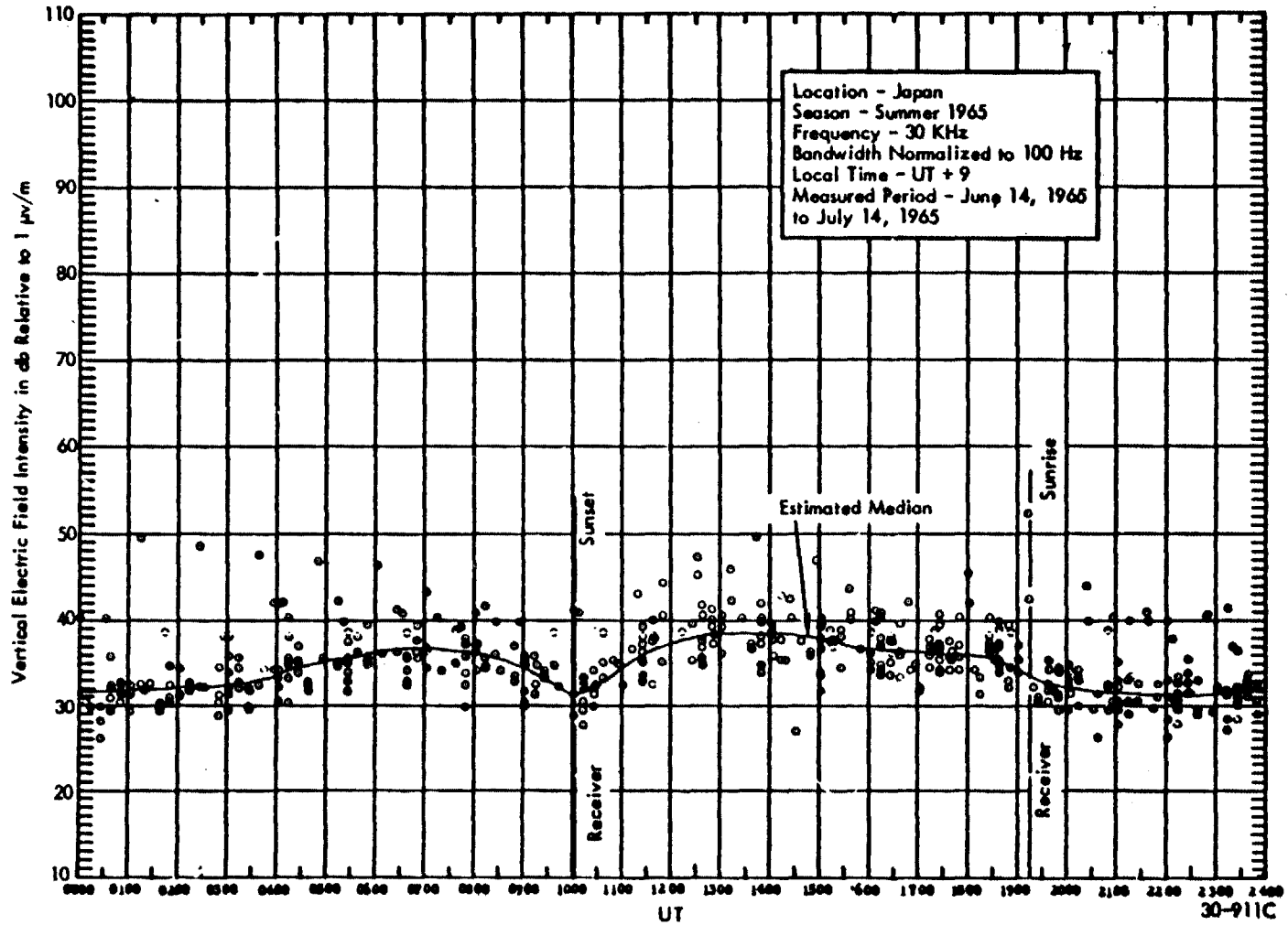

Figure 46 Diurnal Variations of VLF Atmospheric Noise

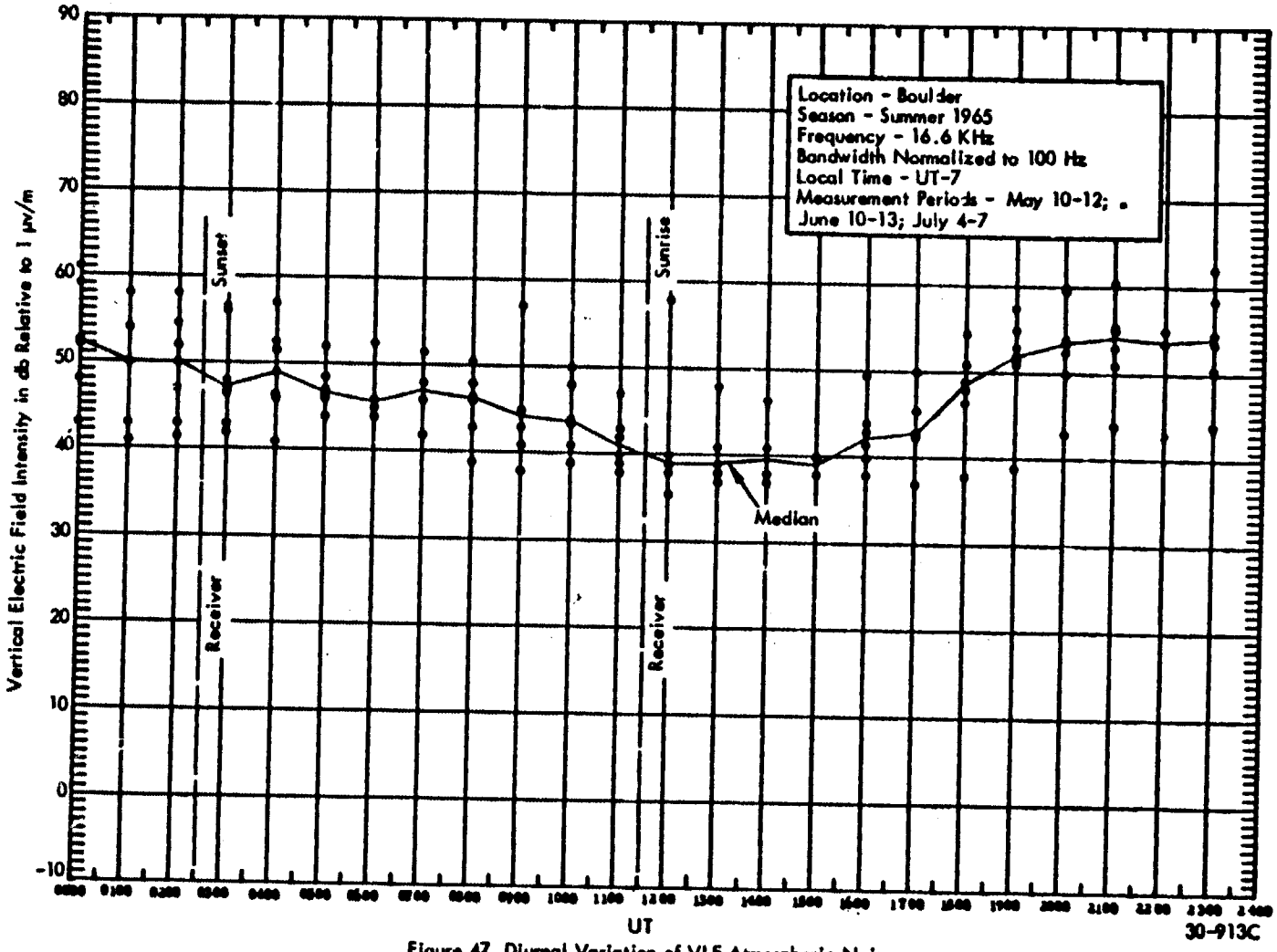

Figure 47 Diurnal Variation of VLF Atmospheric Noise

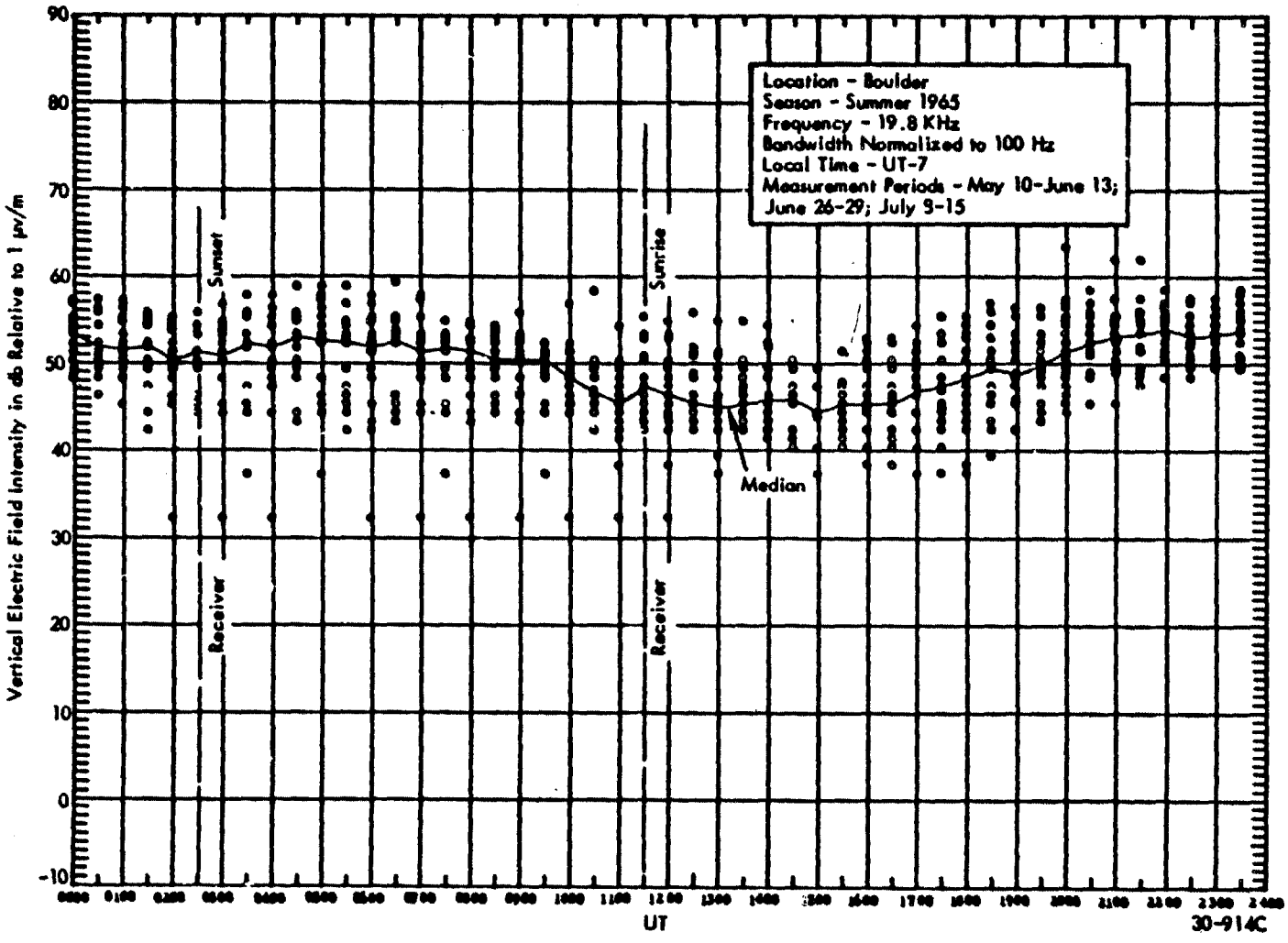

Figure 48 Diurnal Variation of VLF Atmospheric Noise

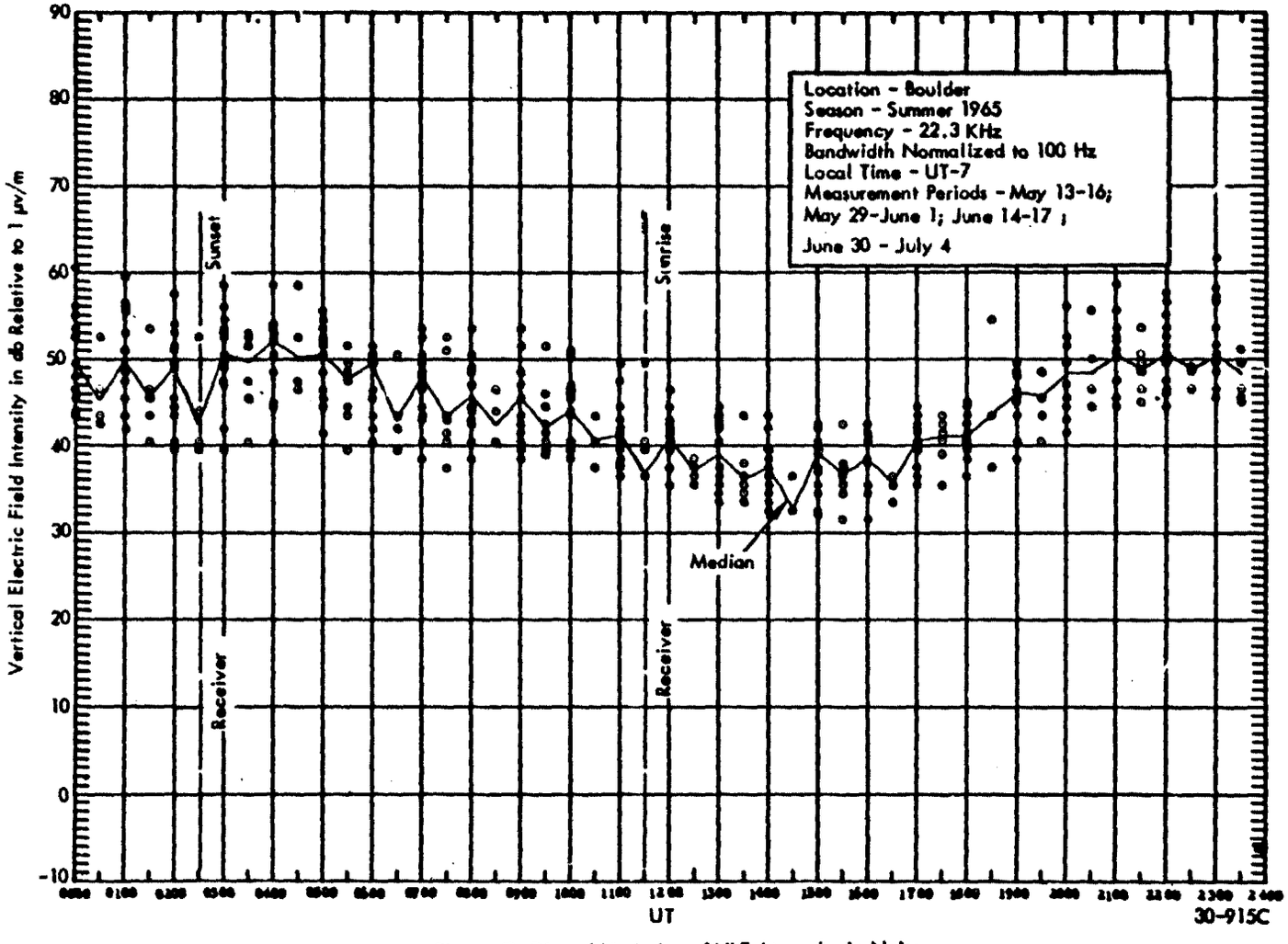

Figure 49 Diurnal Variation of VLF Atmospheric Noise

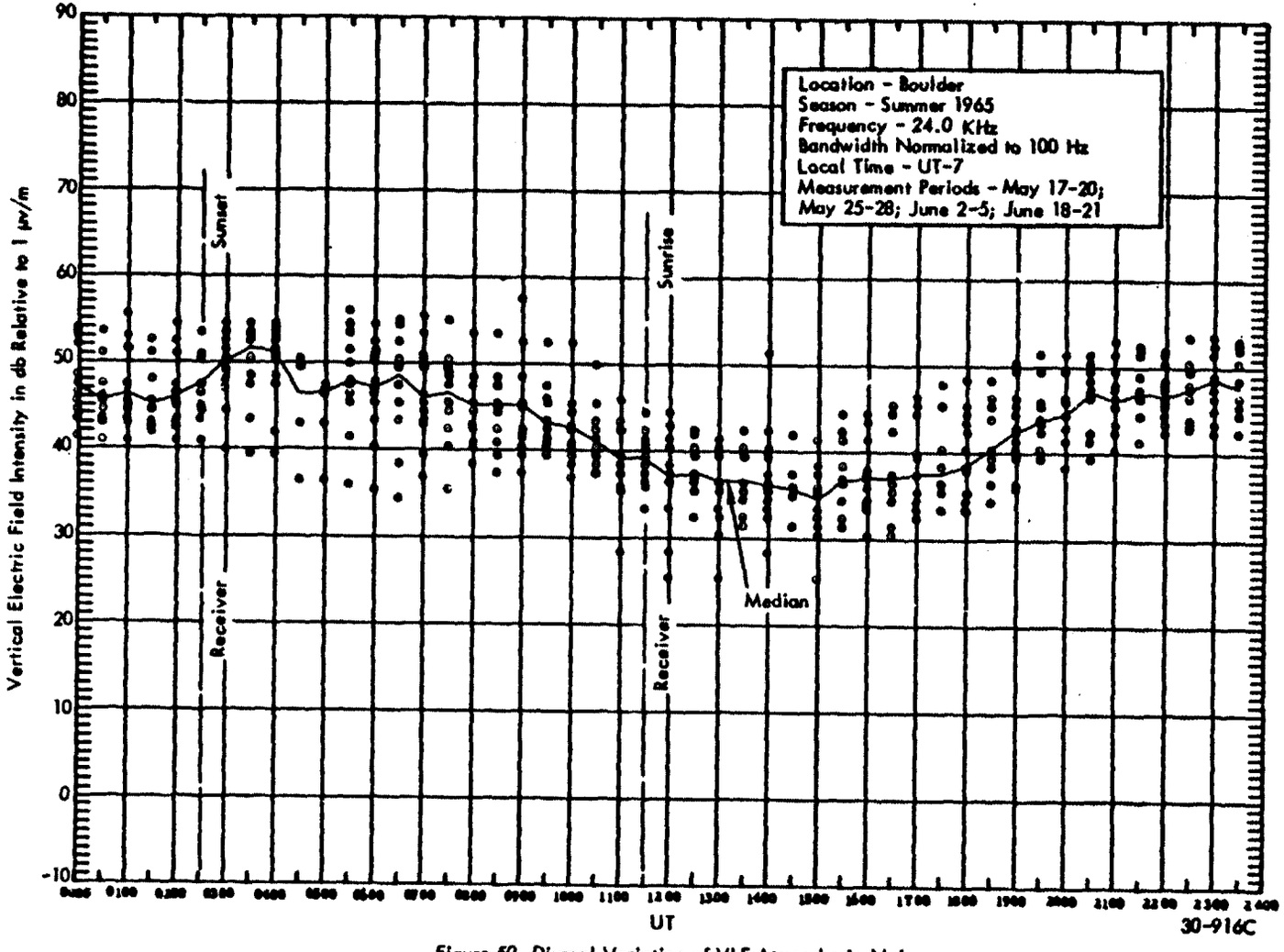

Figure 50 Diurnal Variation of VLF Atmospheric Noise

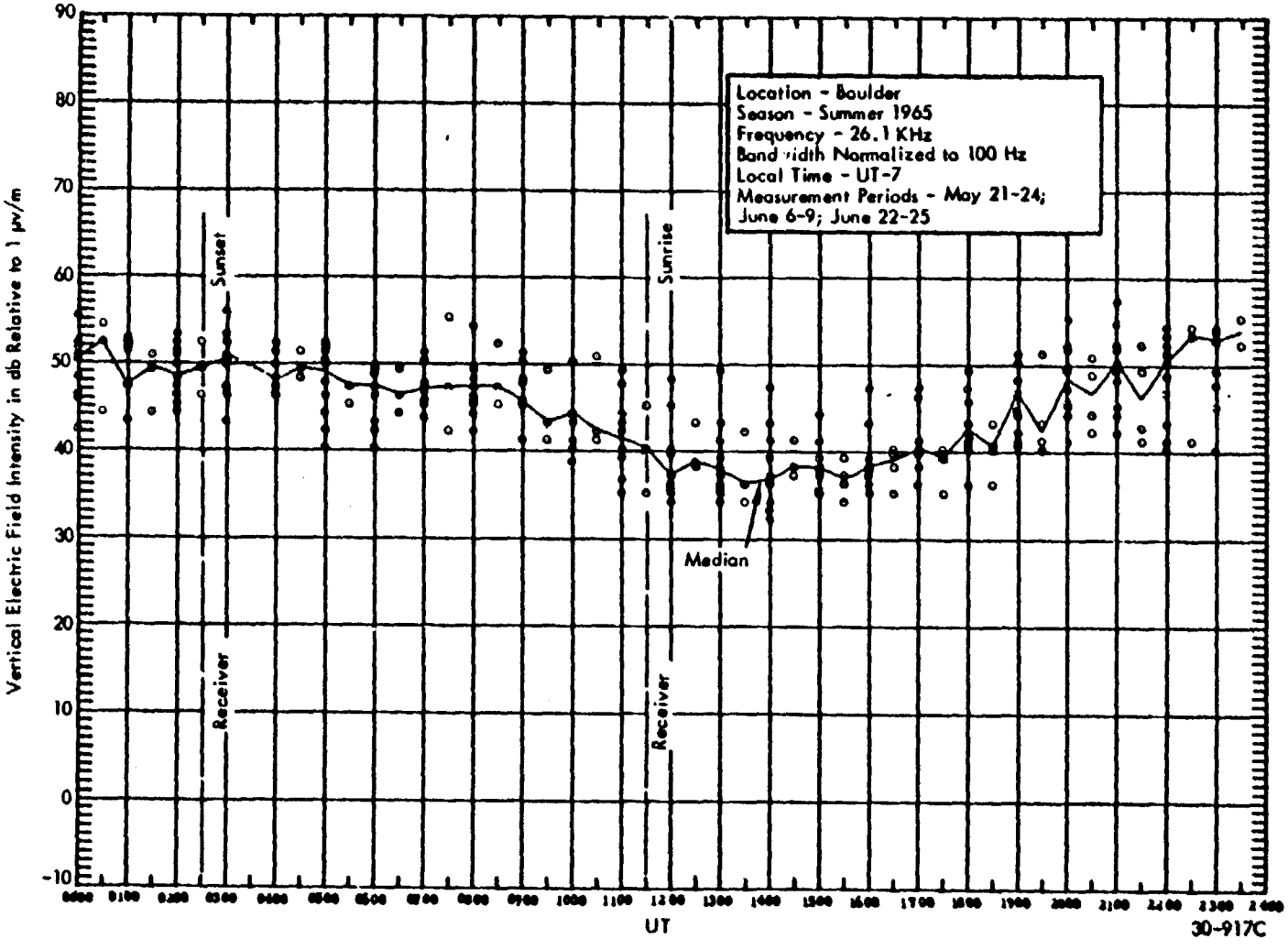

Figure 51 Diurnal Variation of VLF Atmospheric Noise

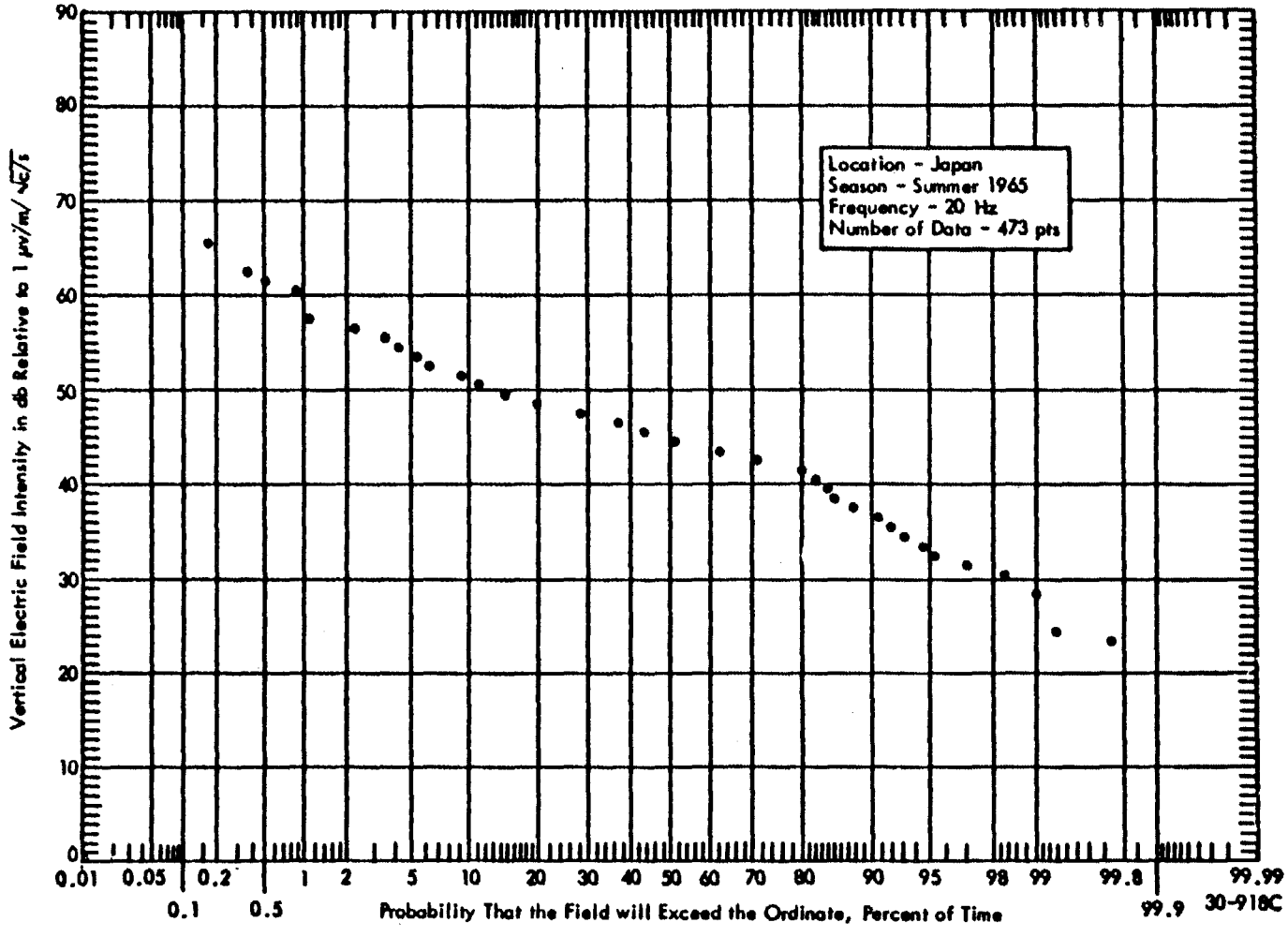

Figure 52 Cumulative Distribution of RMS Atmospheric Noise Intensity

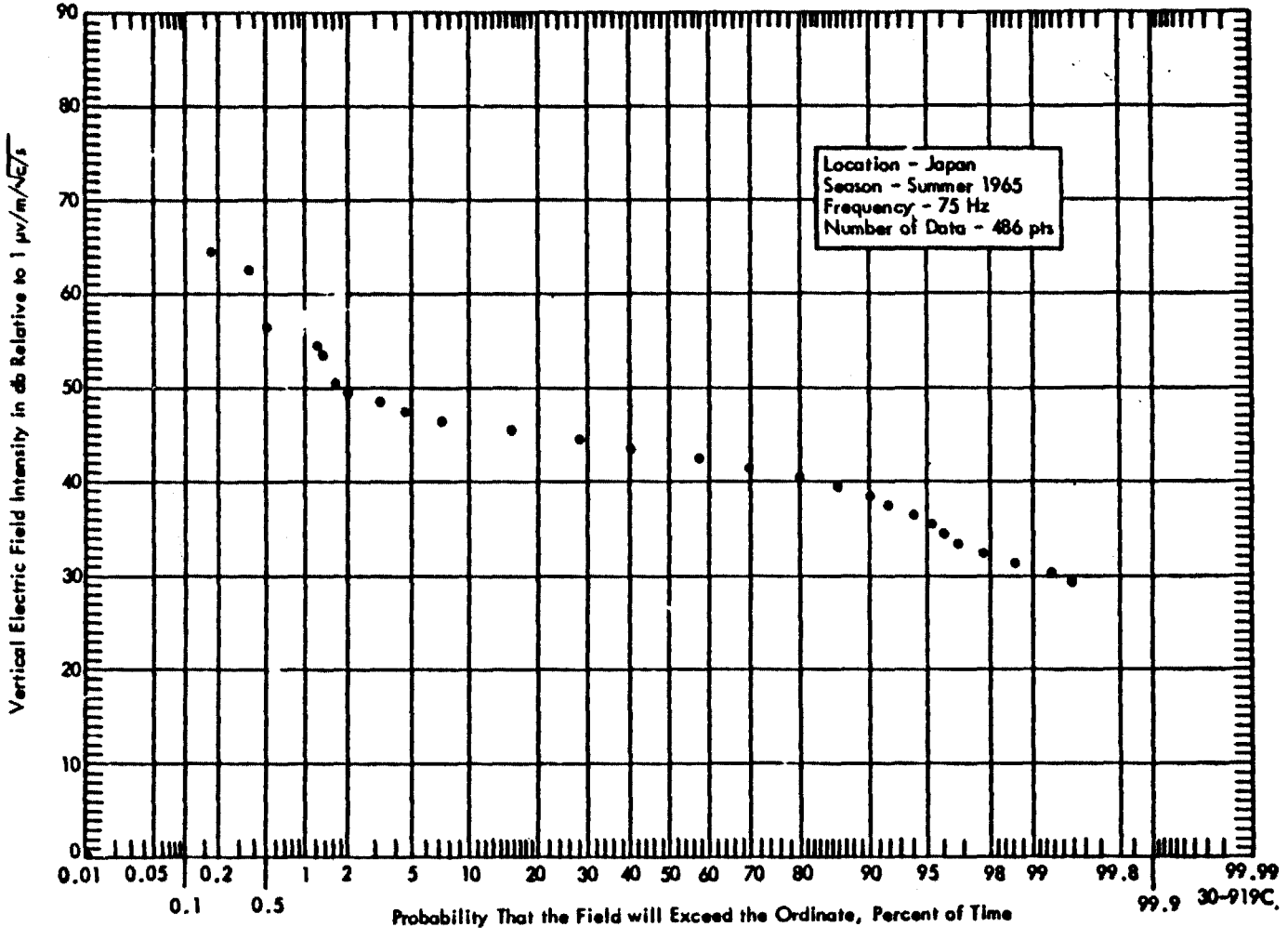

Figure 53 Cumulative Distribution of RMS Atmospheric Noise Intensity

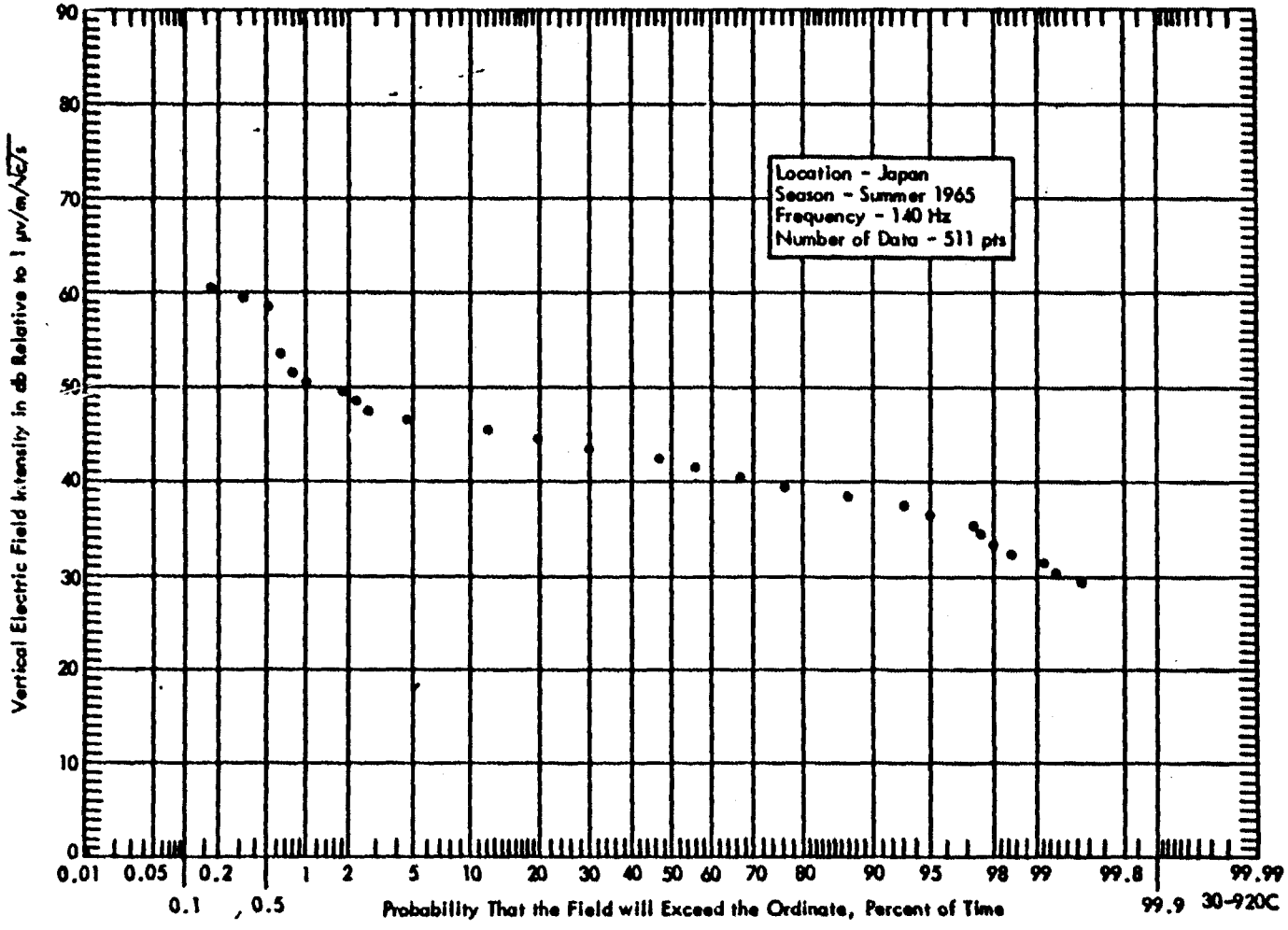

Figure 54 Cumulative Distribution of RMS Atmospheric Noise Intensity

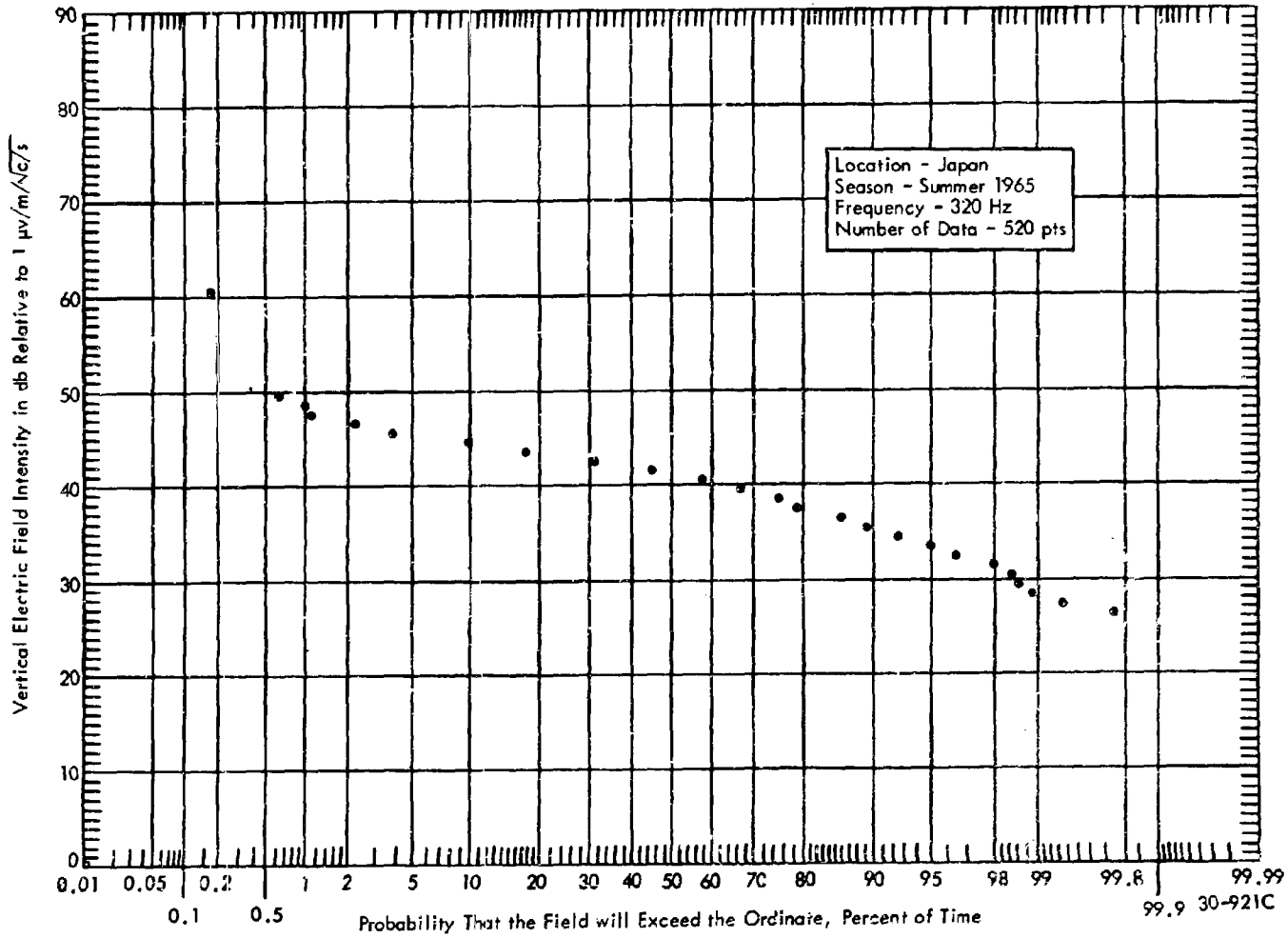

Figure 55 Cumulative Distribution of RMS Atmospheric Noise Intensity

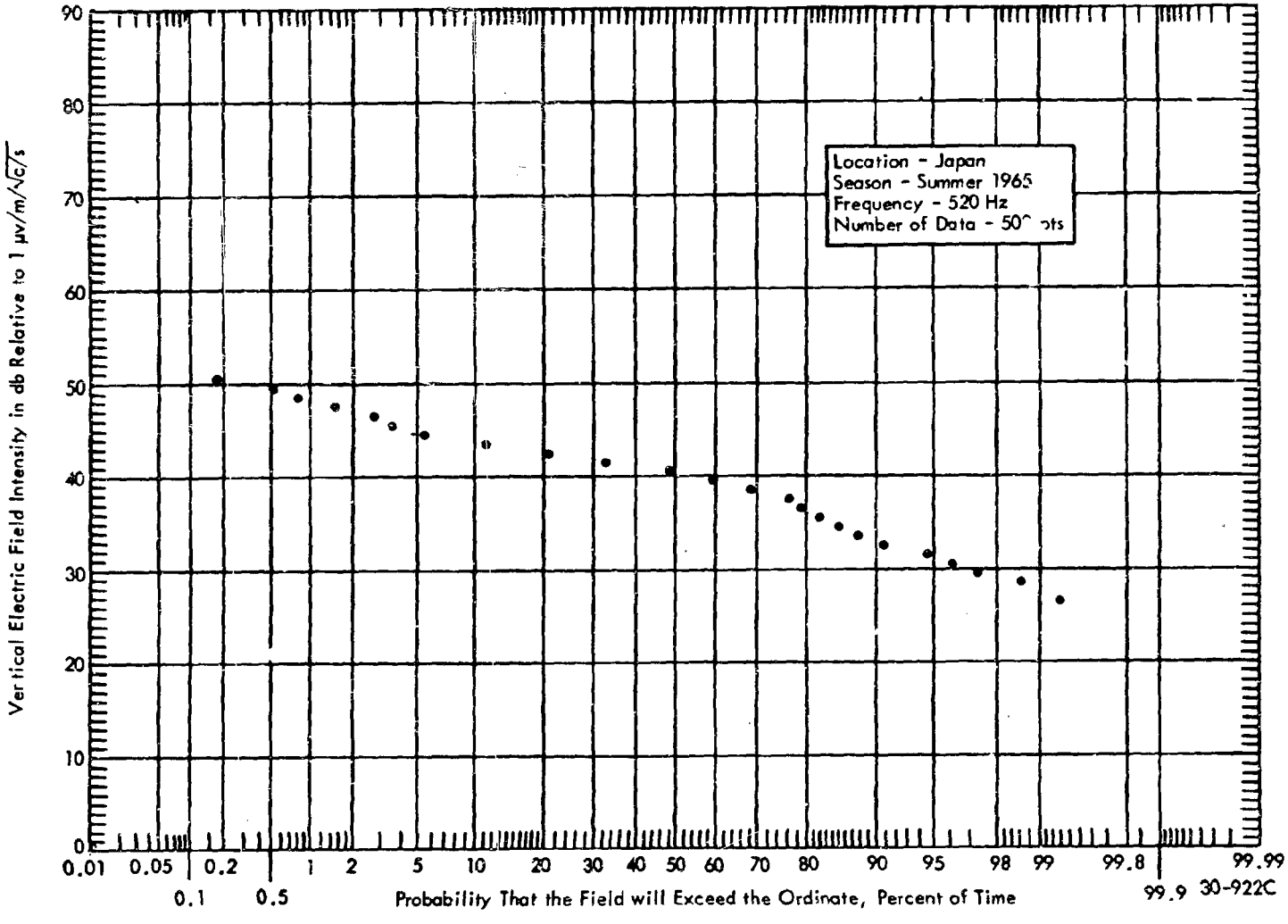

Figure 56 Cumulative Distribution of RMS Atmospheric Noise Intensity

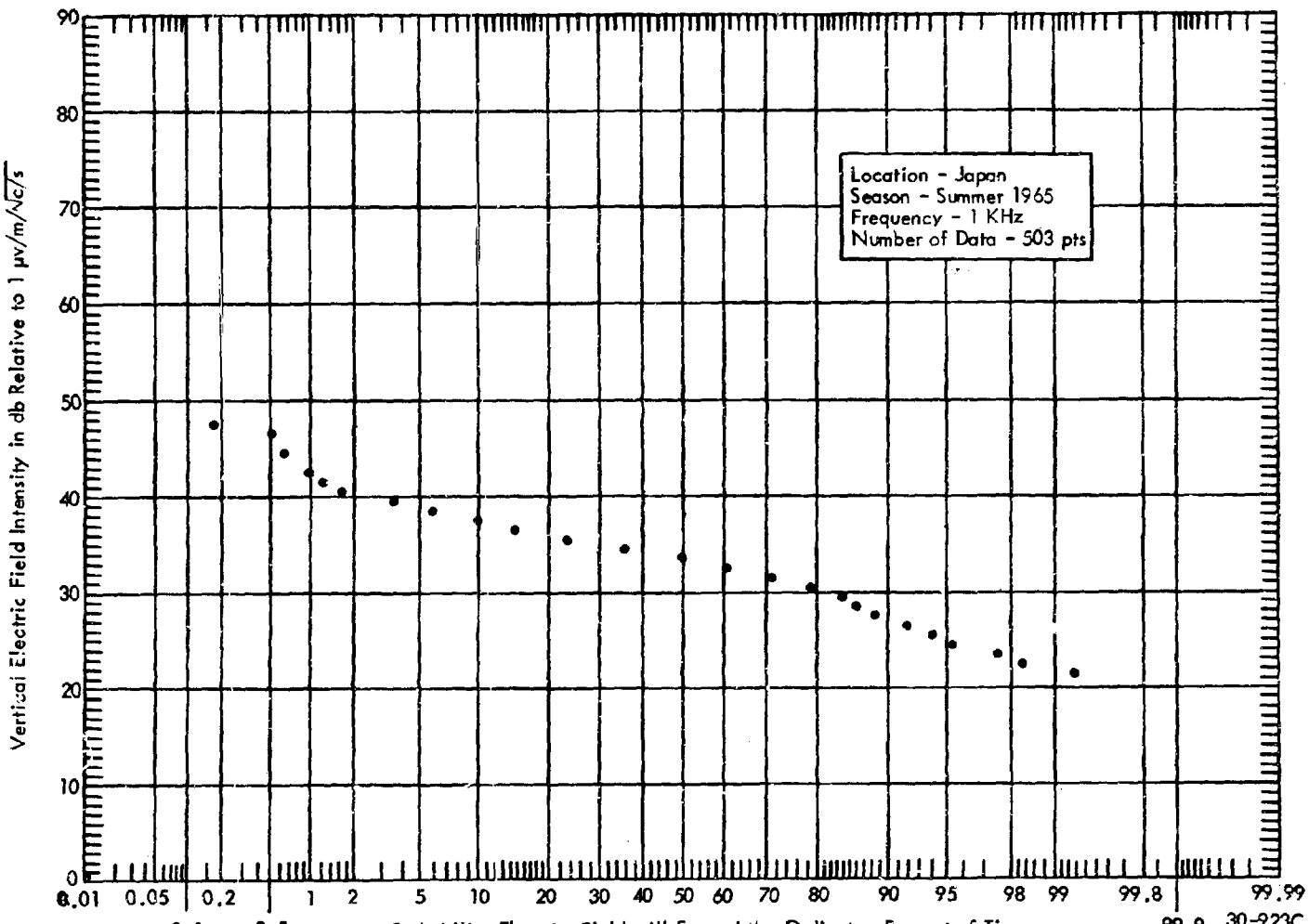

Figure 57 Cumulative Distribution of RMS Atmospheric Noise intensity

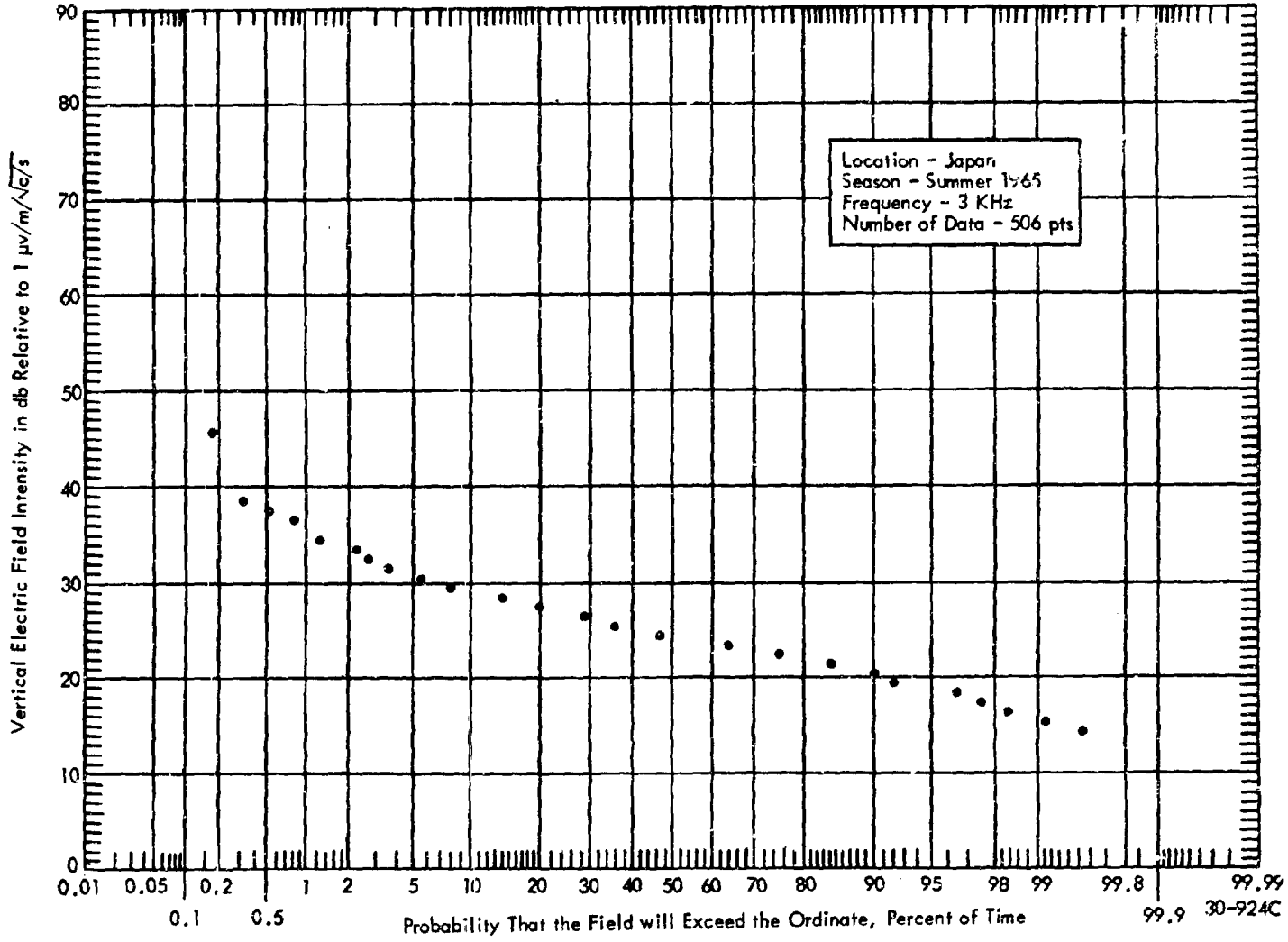

Figure 58 Cumulative Distribution of RMS Atmospheric Noise Intensity

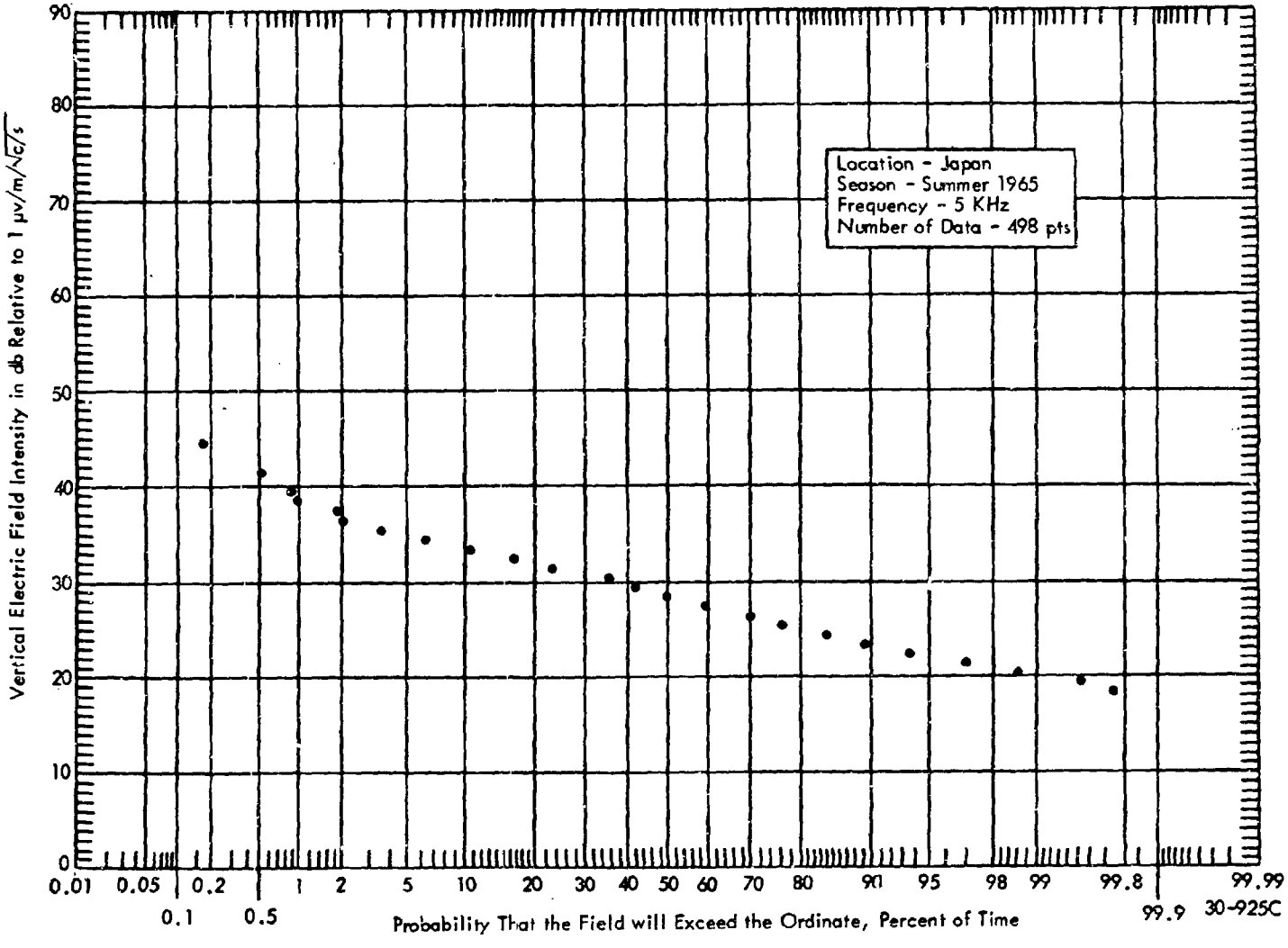

Figure 59 Cumulative Distribution of RMS Atmospheric Noise Intensity

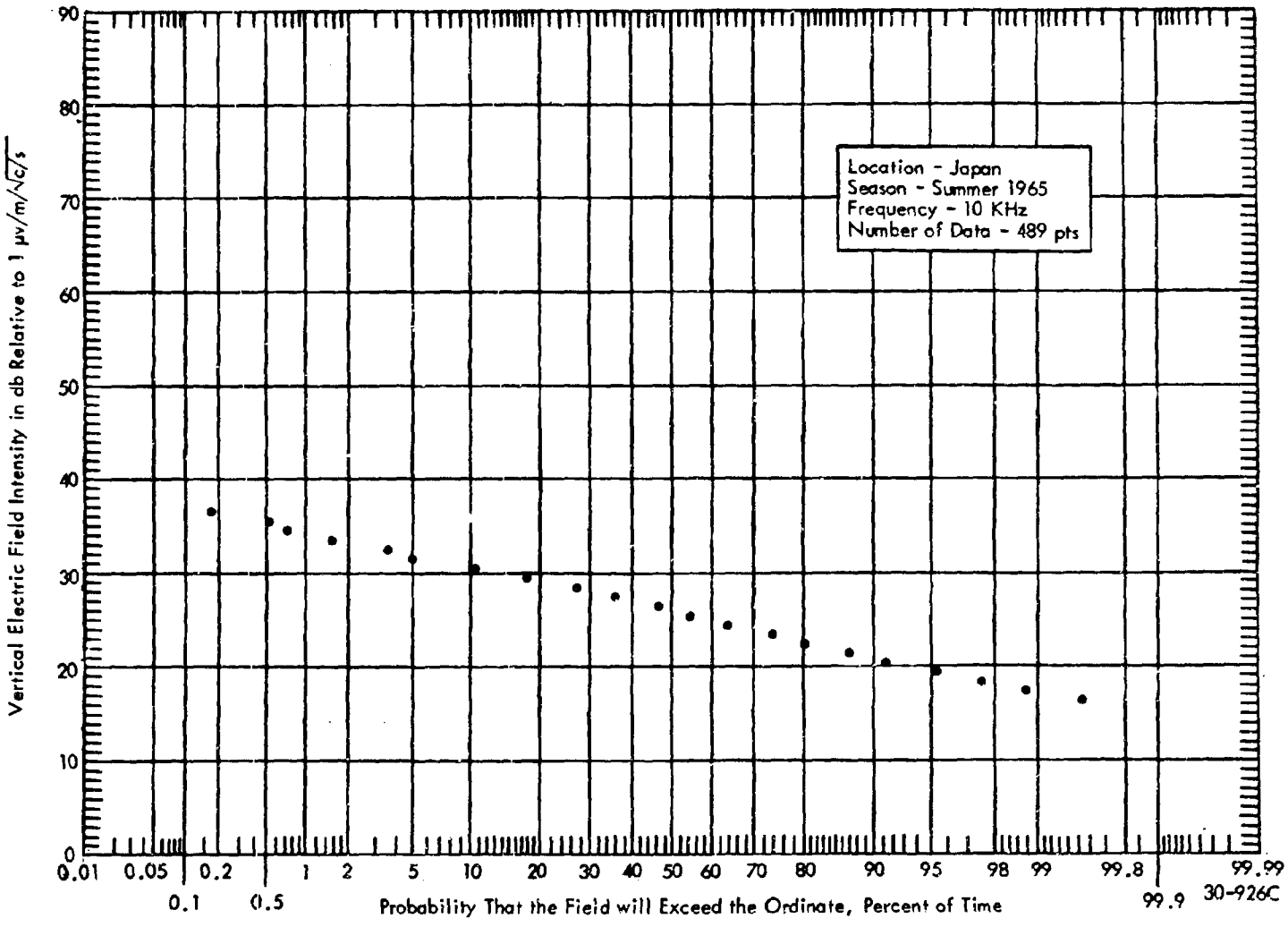

Figure 60 Cumulative Distribution of RMS Atmospheric Noise Intensity

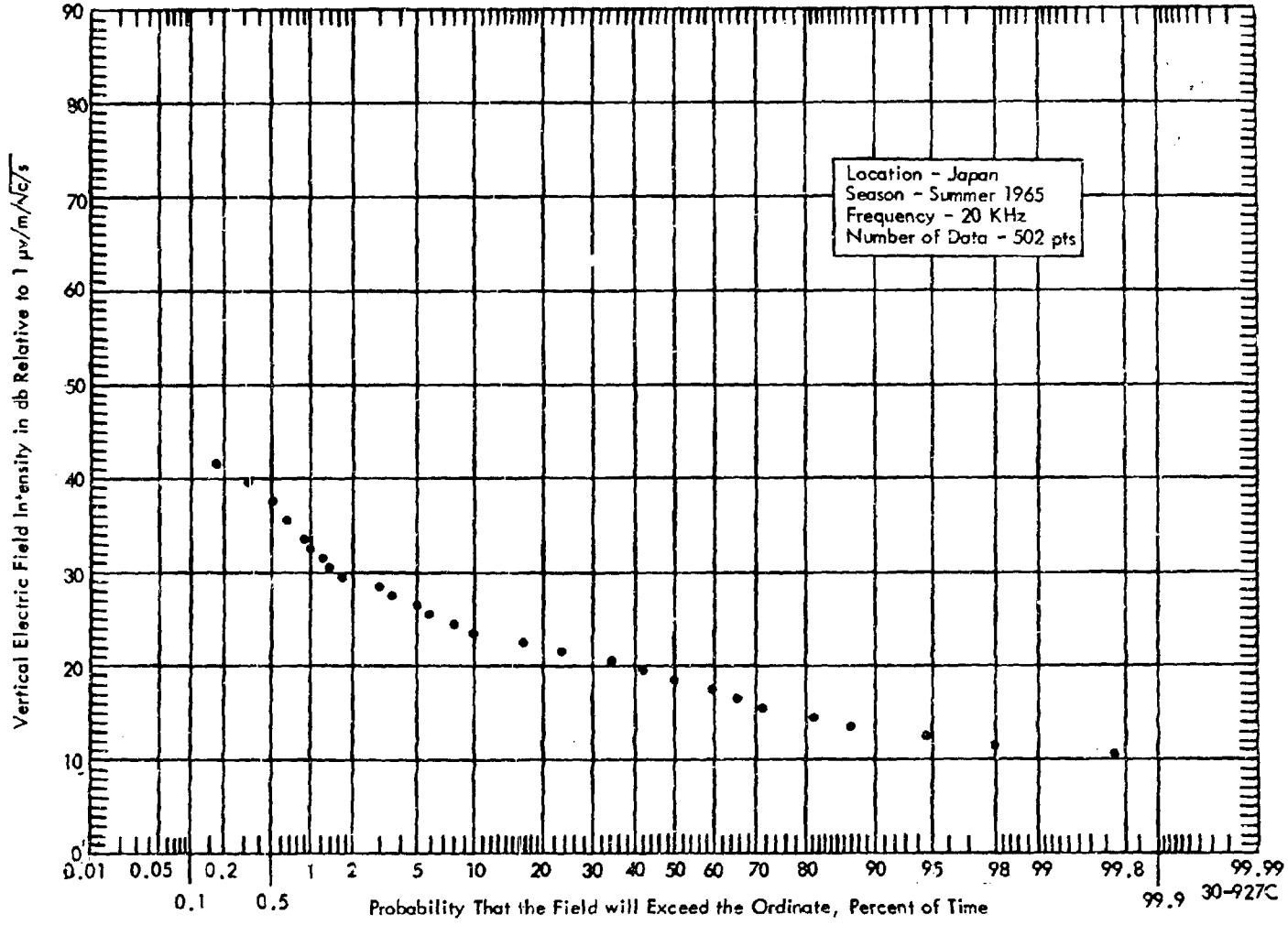

Figure 61 Cumulative Distribution of RMS Atmospheric Noise Intensity

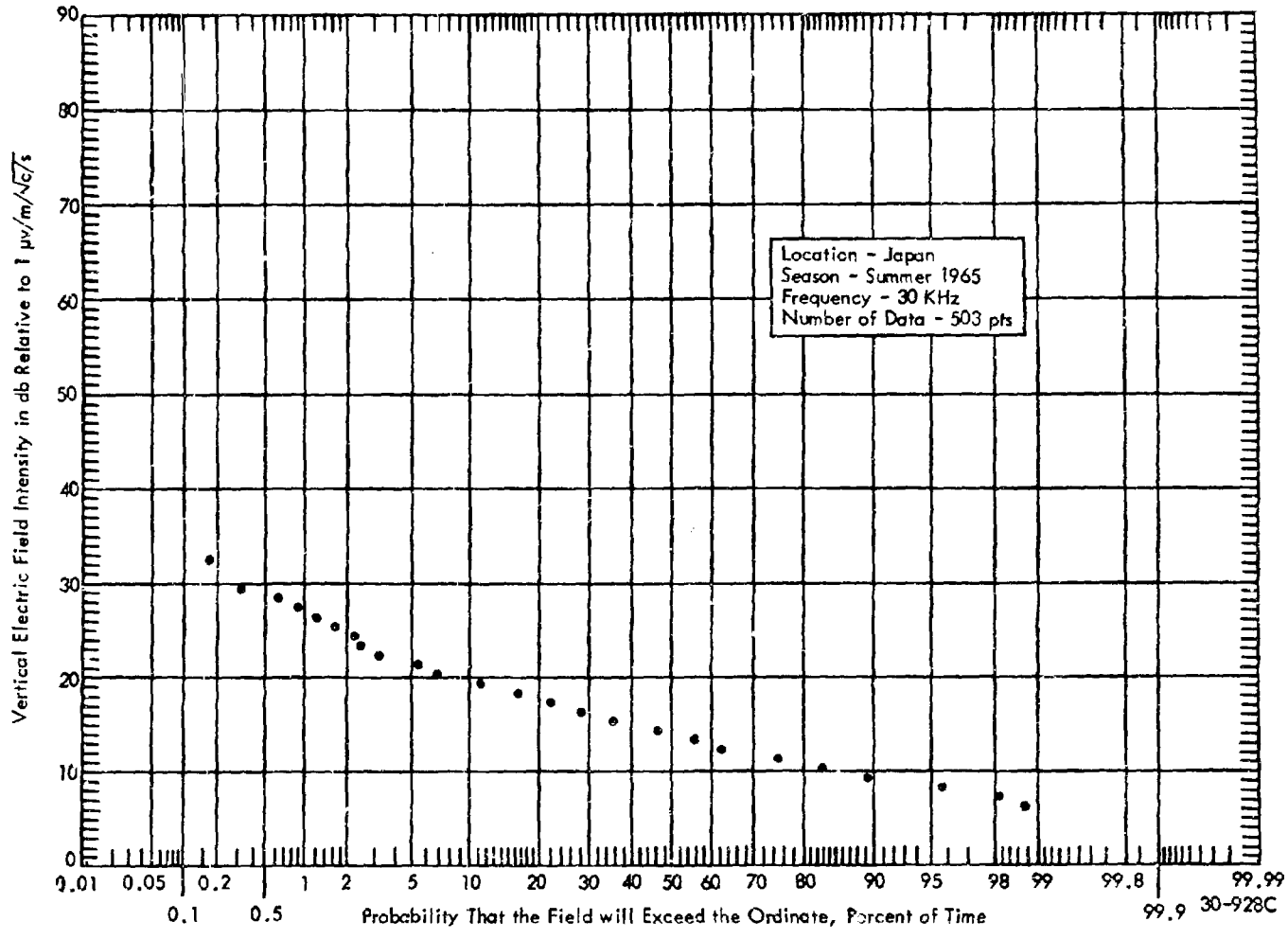

Figure 62 Cumulative Distribution of RMS Atmospheric Noise Intensity

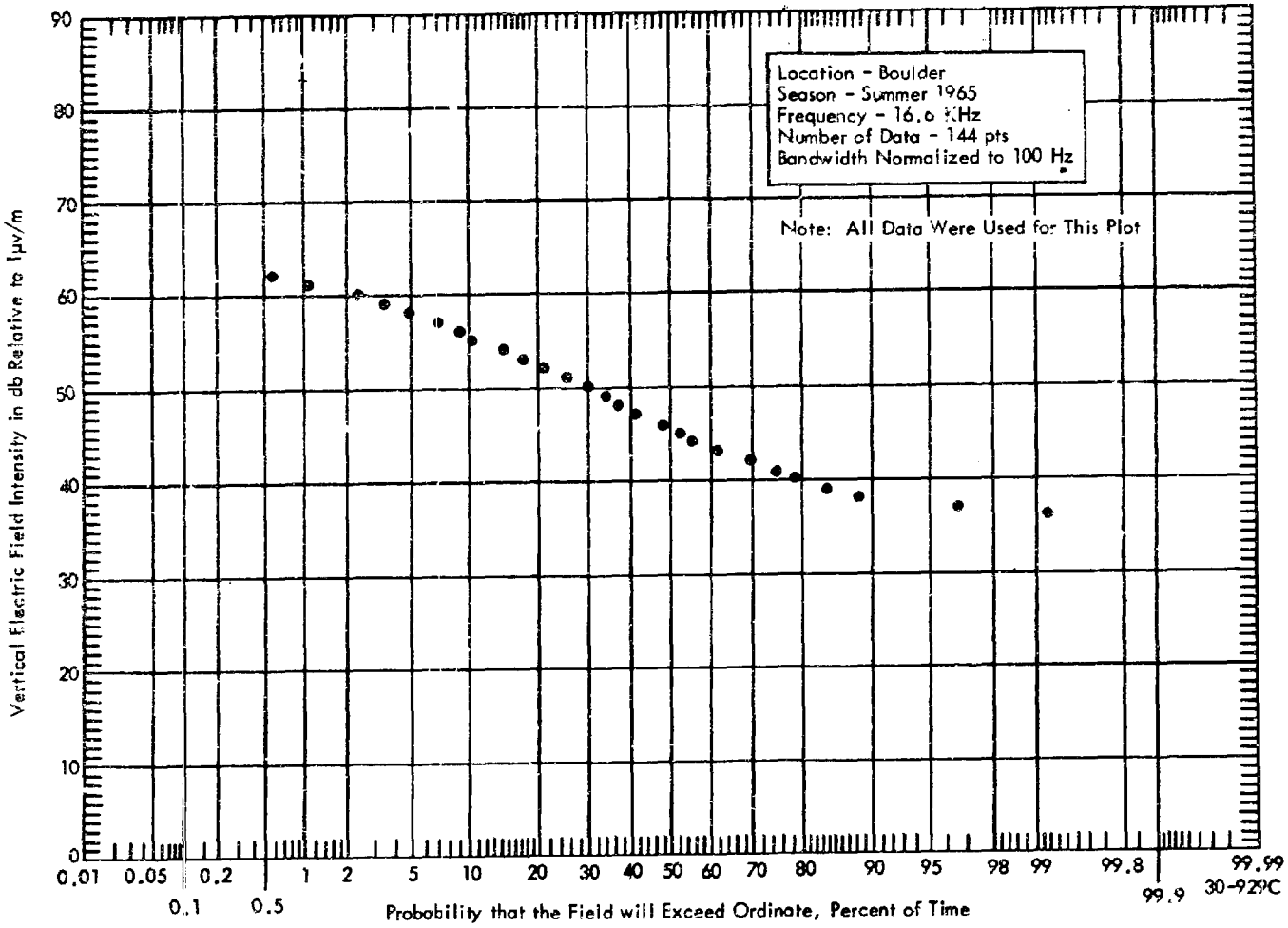

Figure 63 Cumulative Distribution of Measured RMS Atmospheric Noise

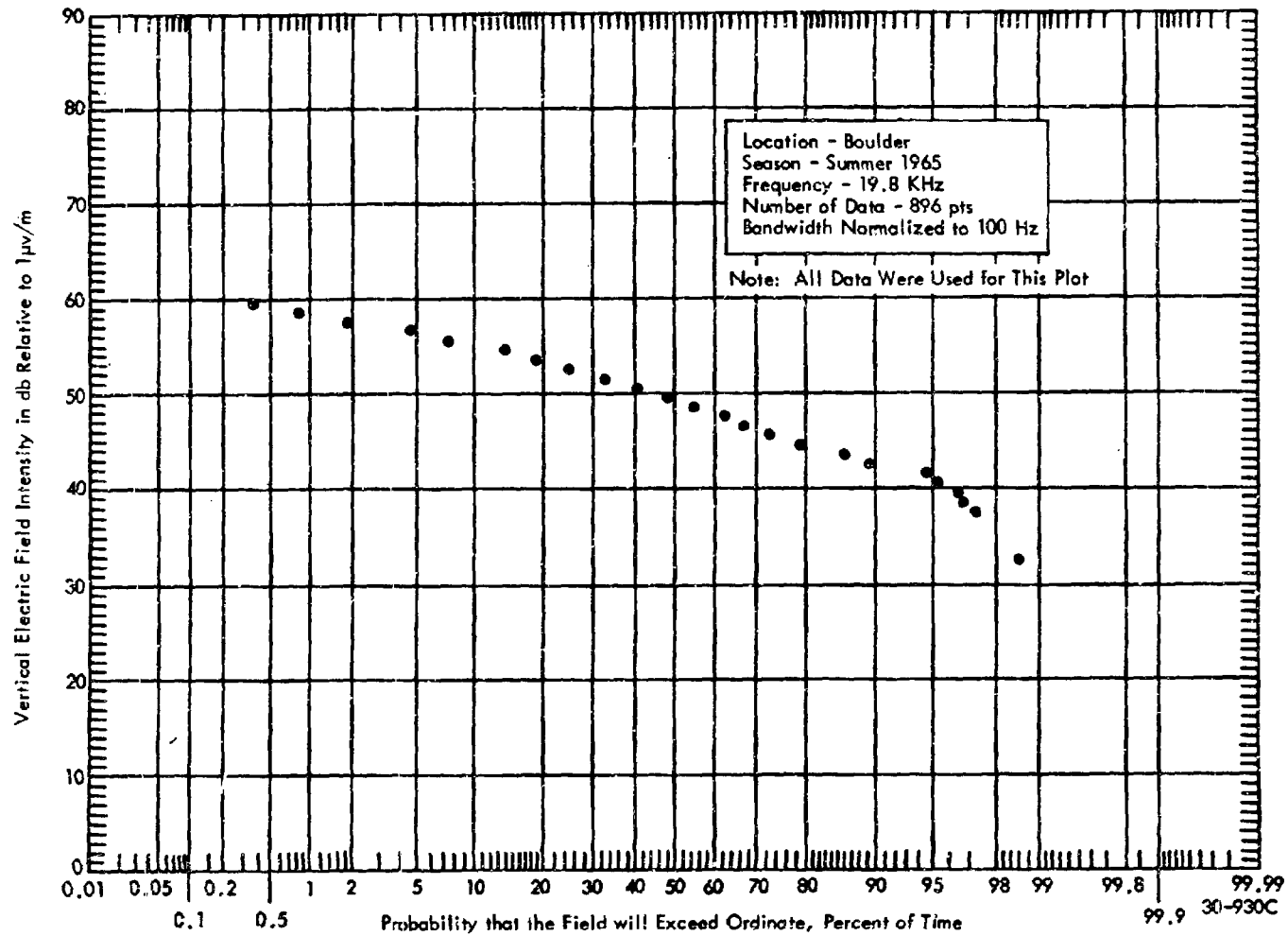

Figure 64 Cumulative Distribution of Measured RMS Atmospheric Noise

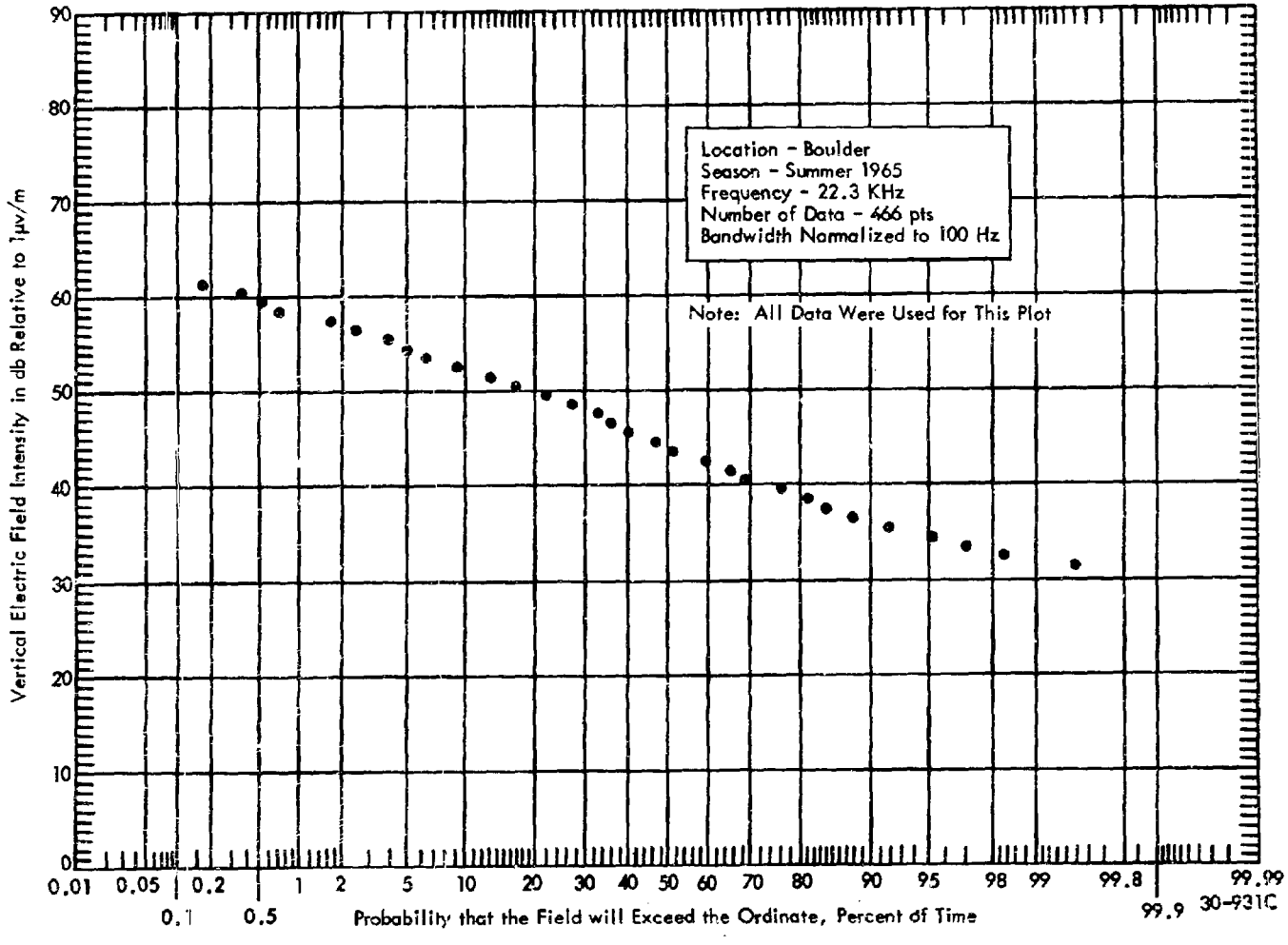

Figure 65 Cumulative Distribution of Measured RMS Atmospheric Noise

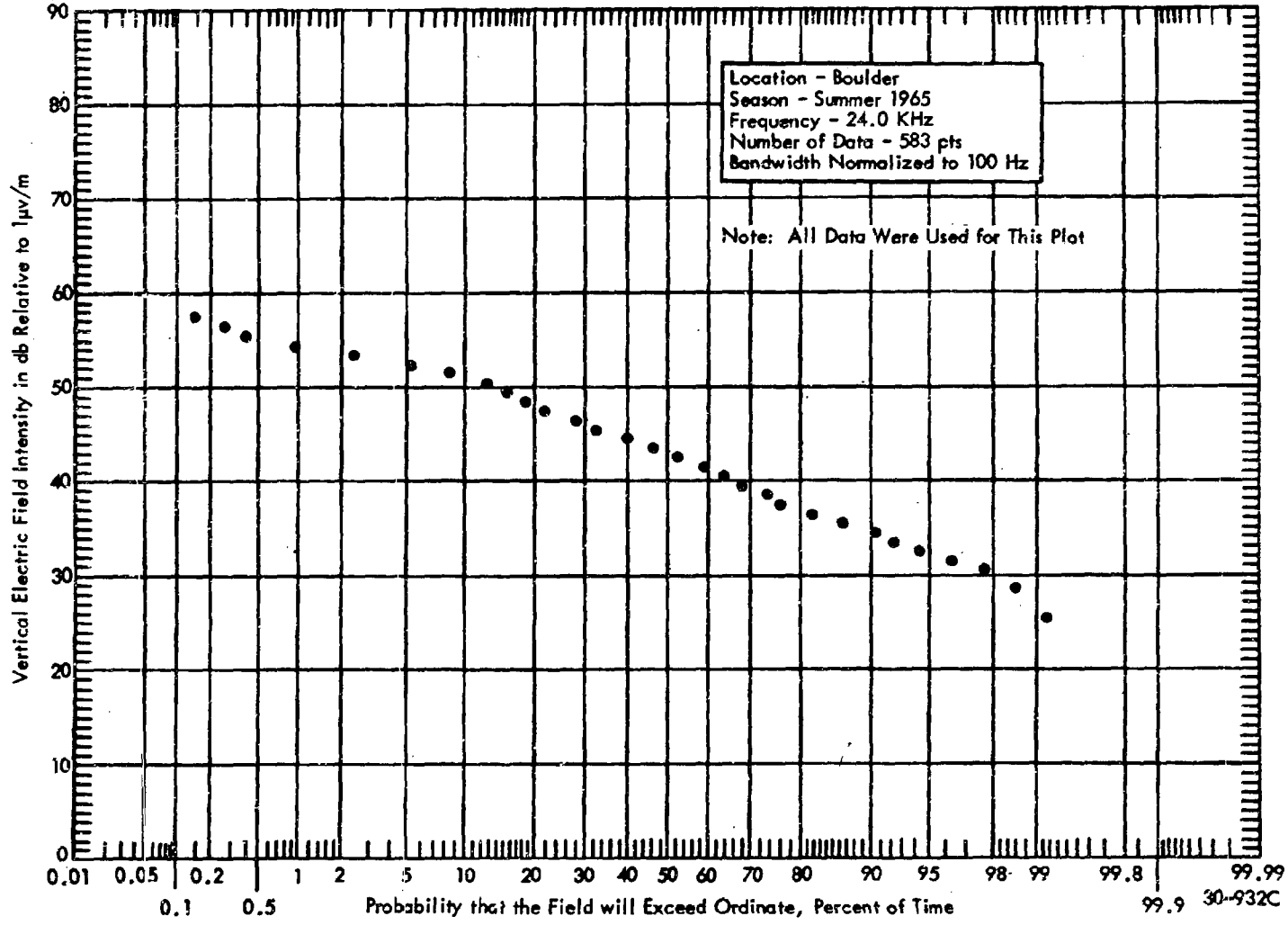

Figure 66 Cumulative Distribution of Measured RMS Atmospheric Noise

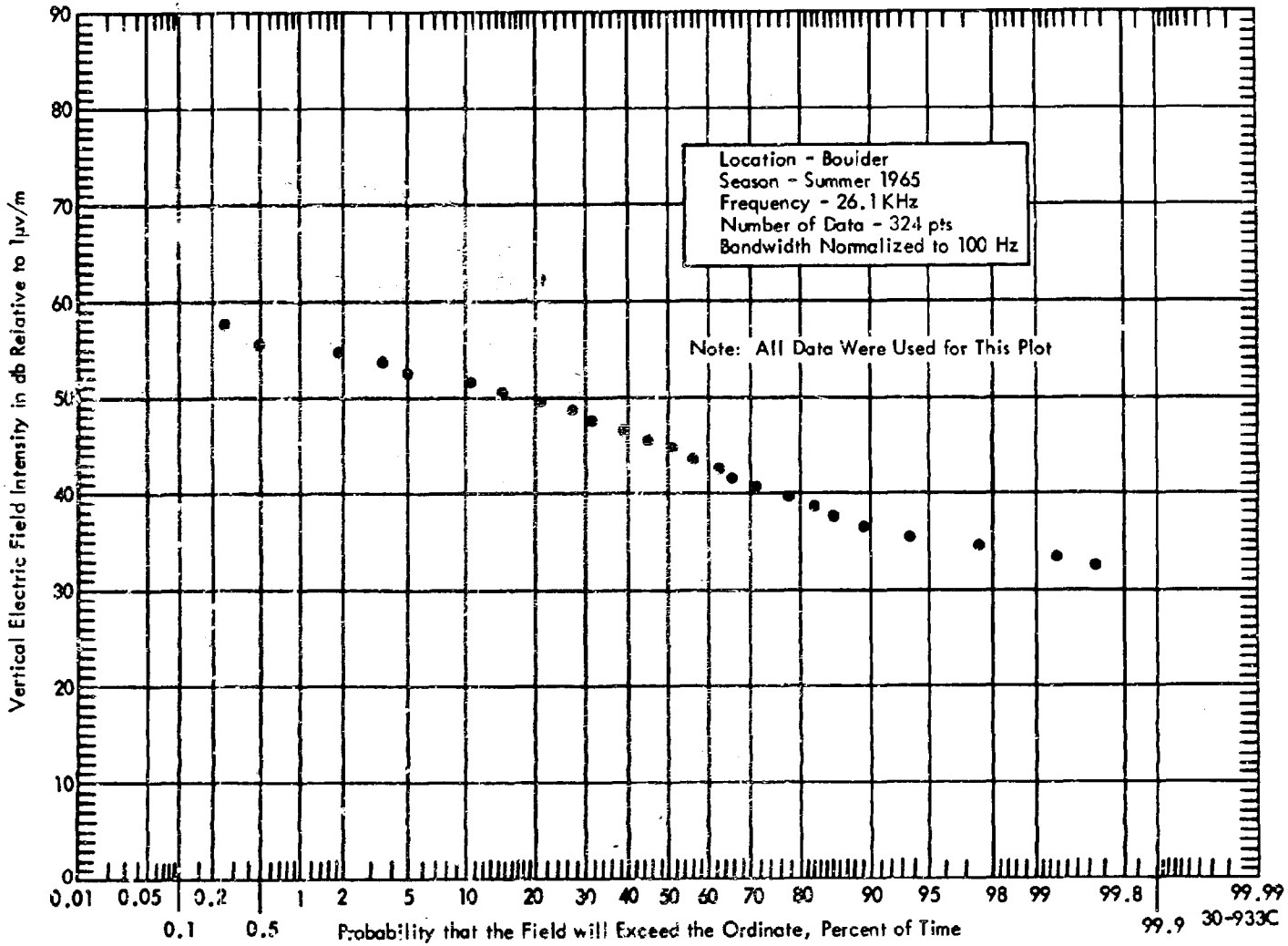

Figure 67 Cumulative Distribution of Measured RMS Atmospheric Noise

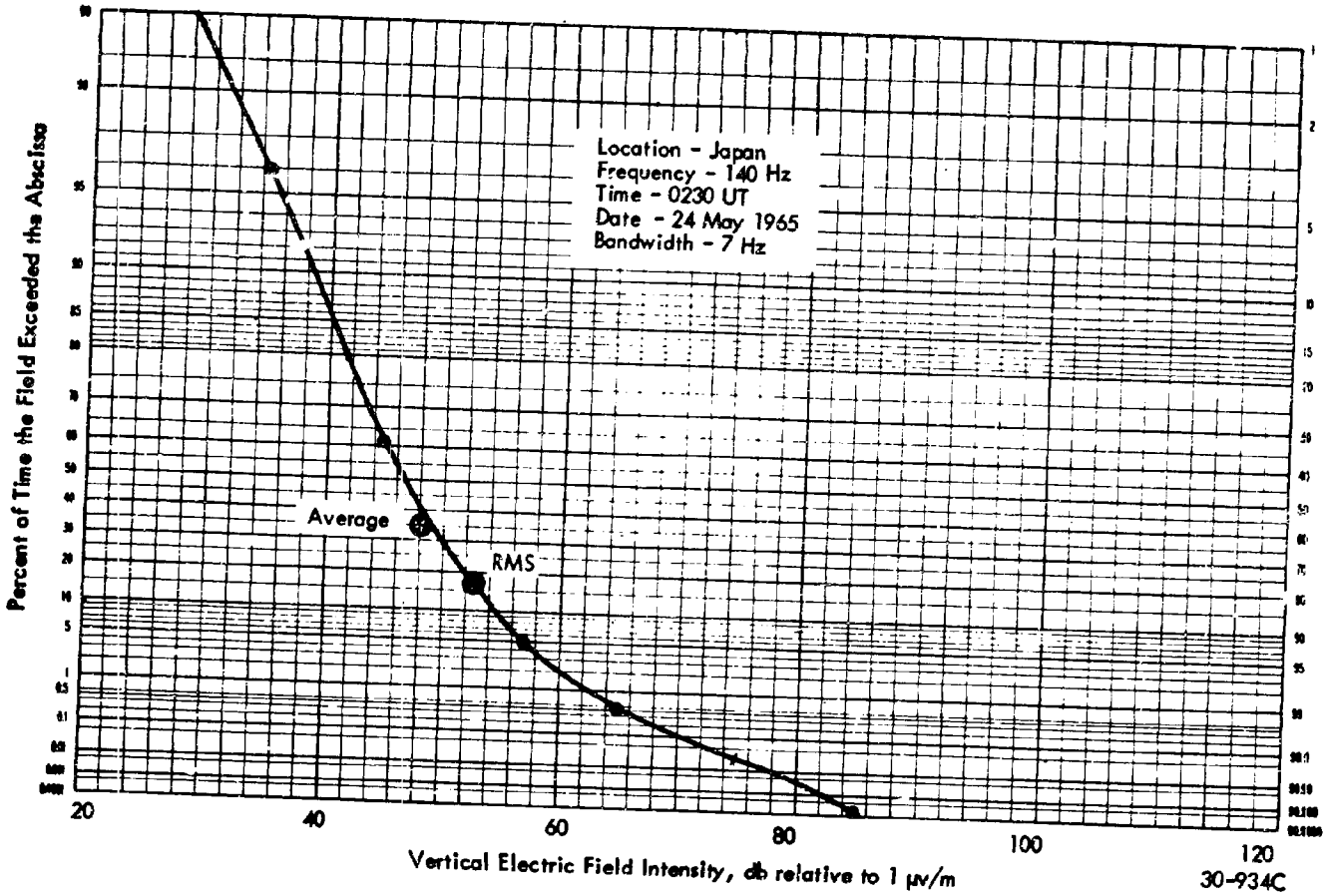

Figure 68 Amplitude Probability Distribution for Atmospheric Noise

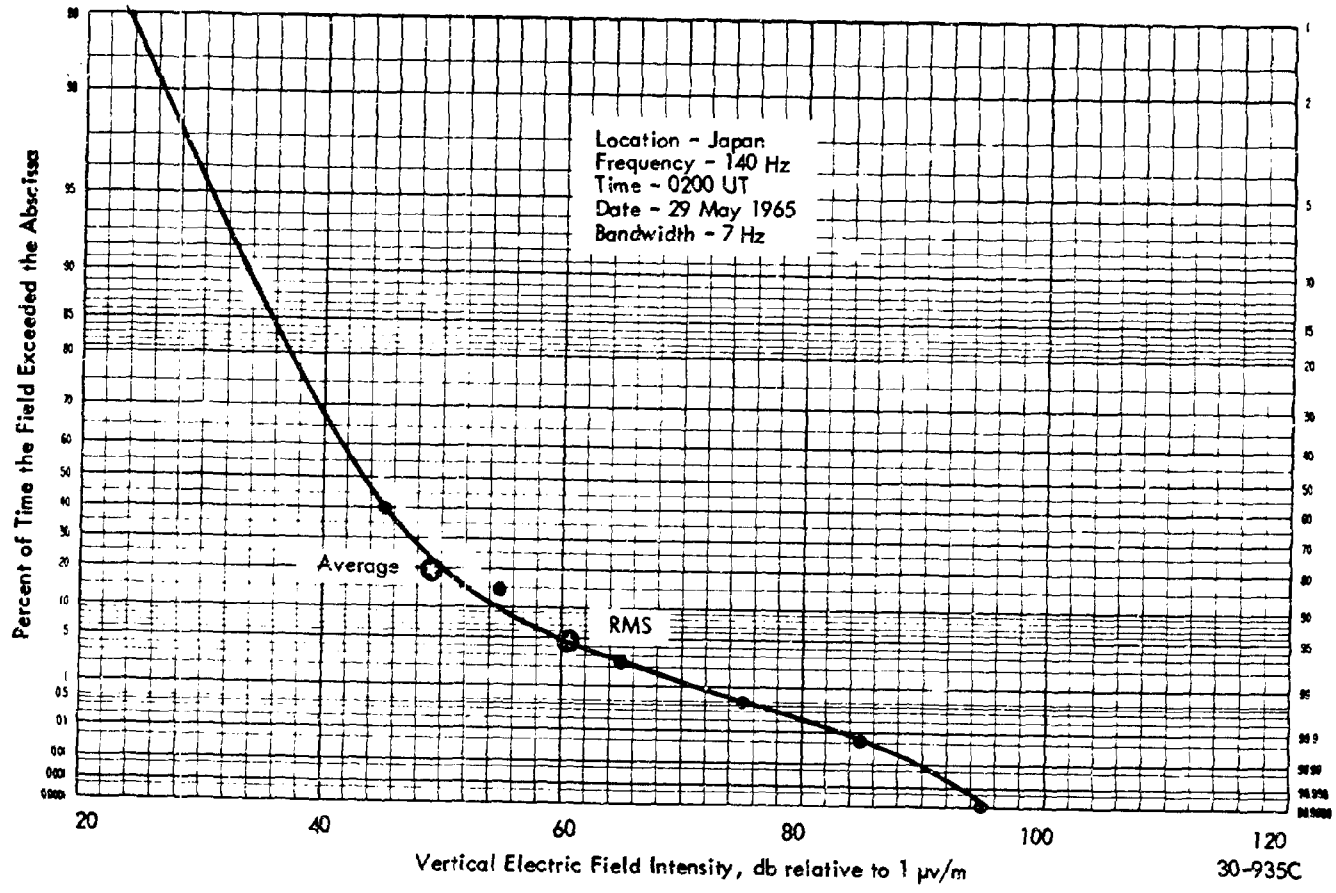

Figure 69 Amplitude Probability Distribution for Atmospheric Noise

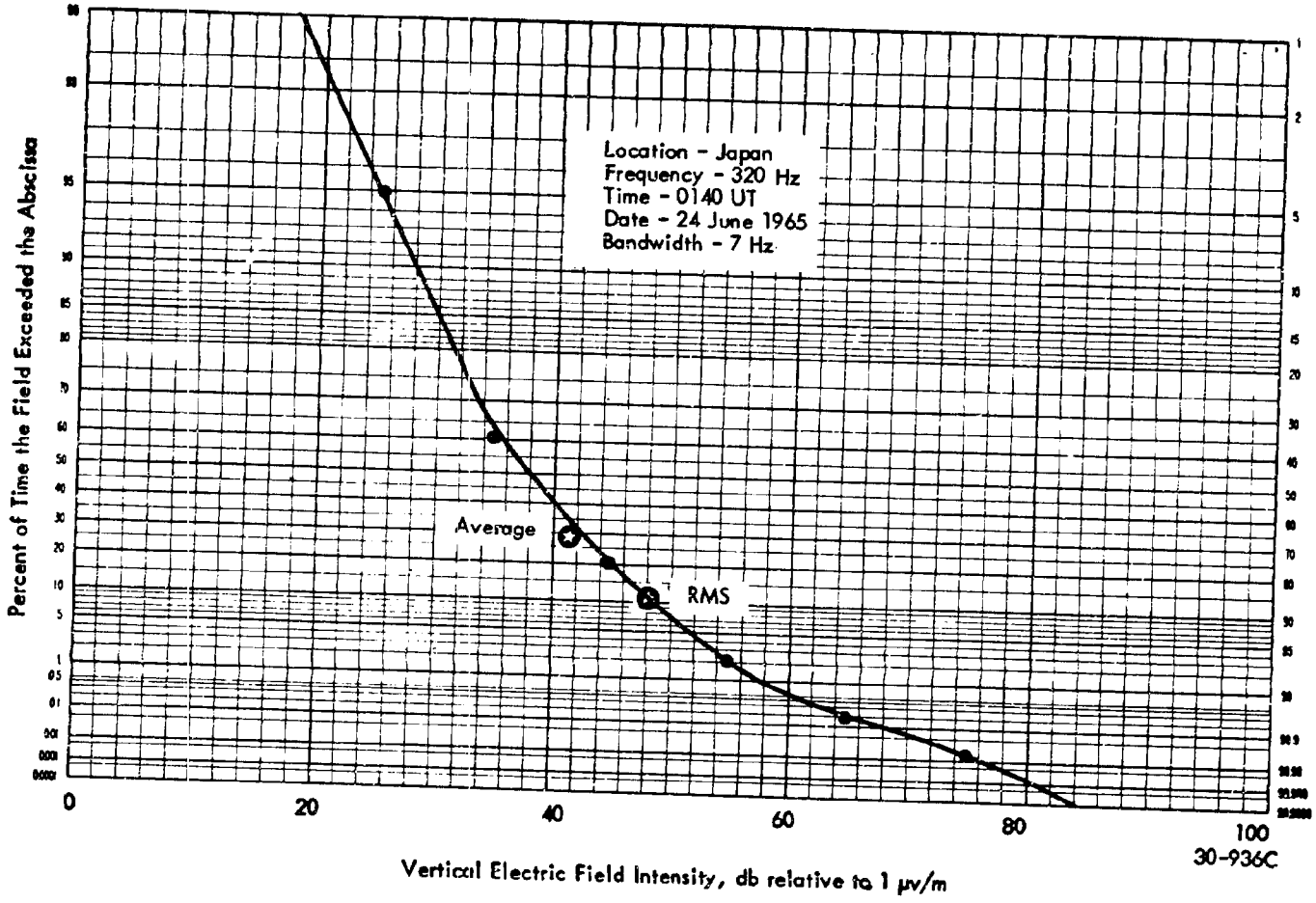

Figure 70 Amplitude Probability Distribution for Atmospheric Noise

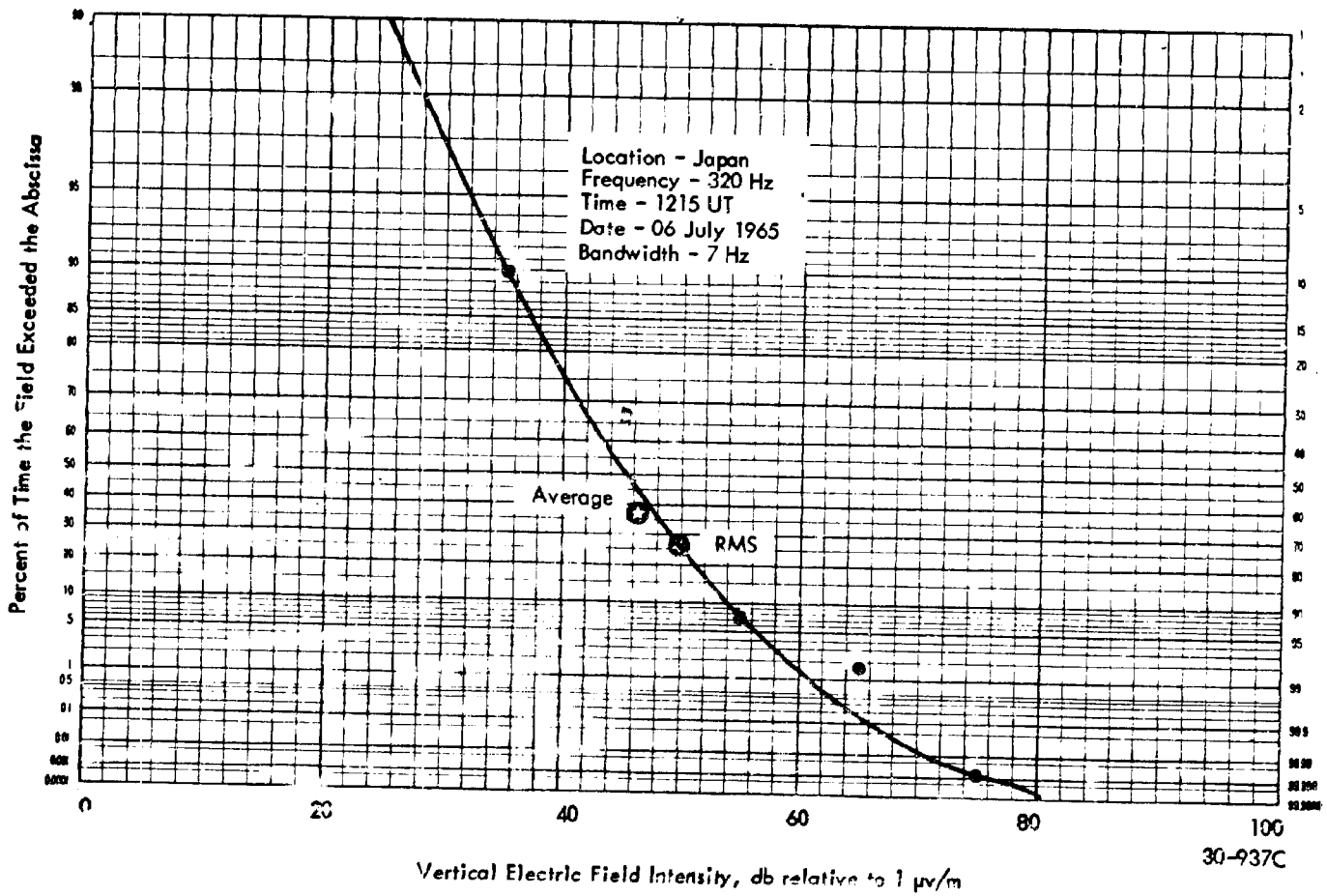

Figure 71 Amplitude Probability Distribution for Atmospheric Noise

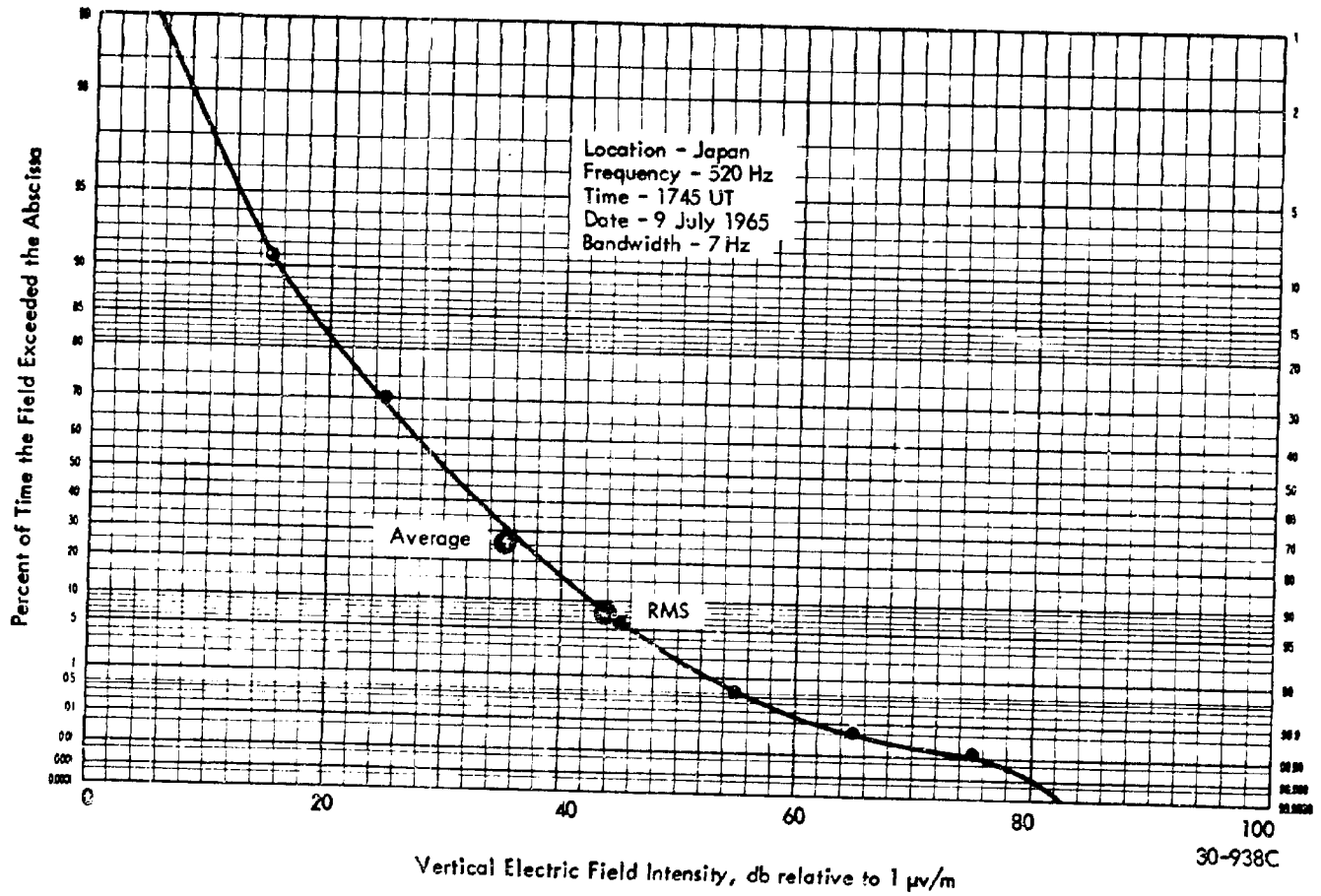

Figure 72 Amplitude Probability Distribution for Atmospheric Noise

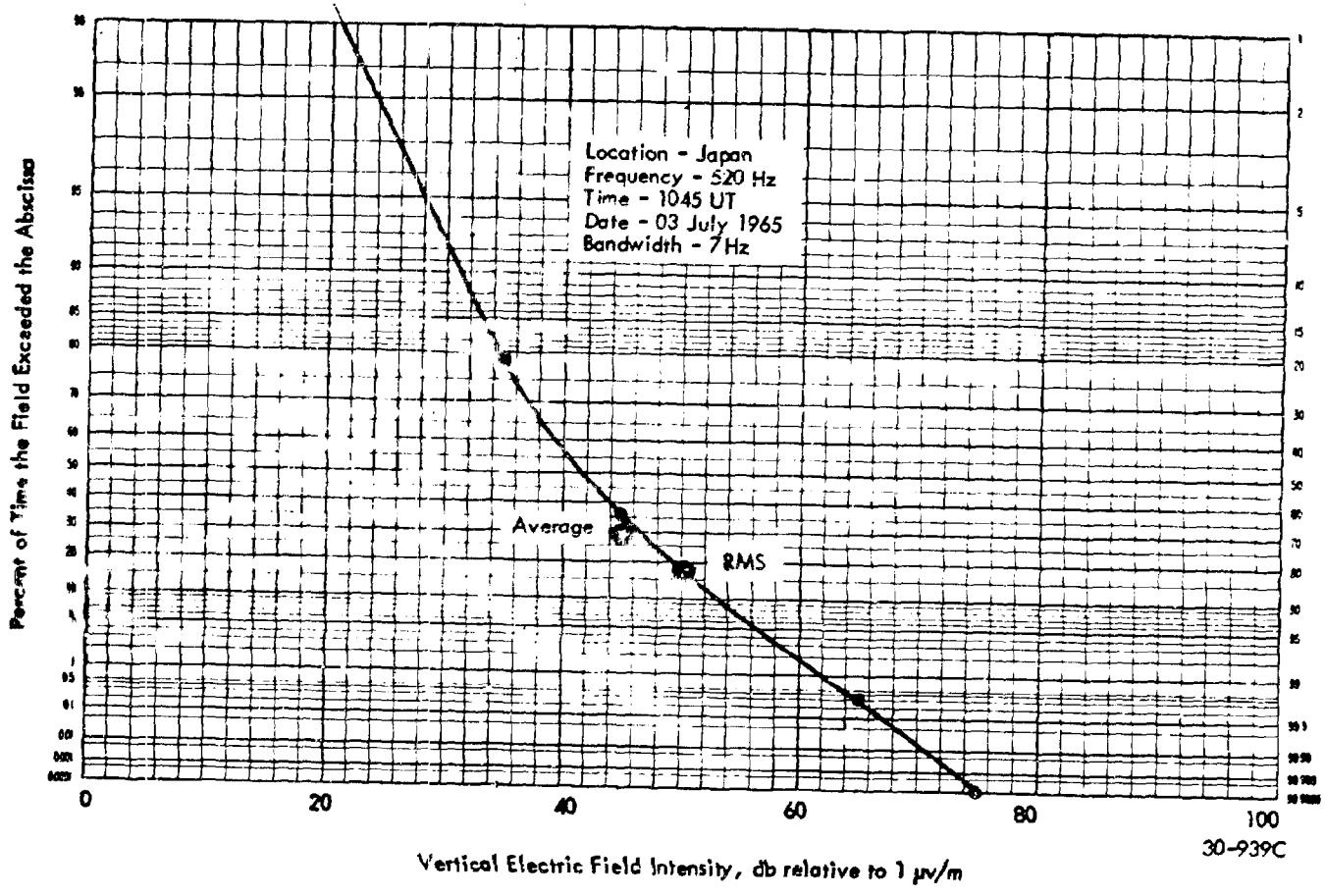

Figure 73 Amplitude Probability Distribution for Atmospheric Noise

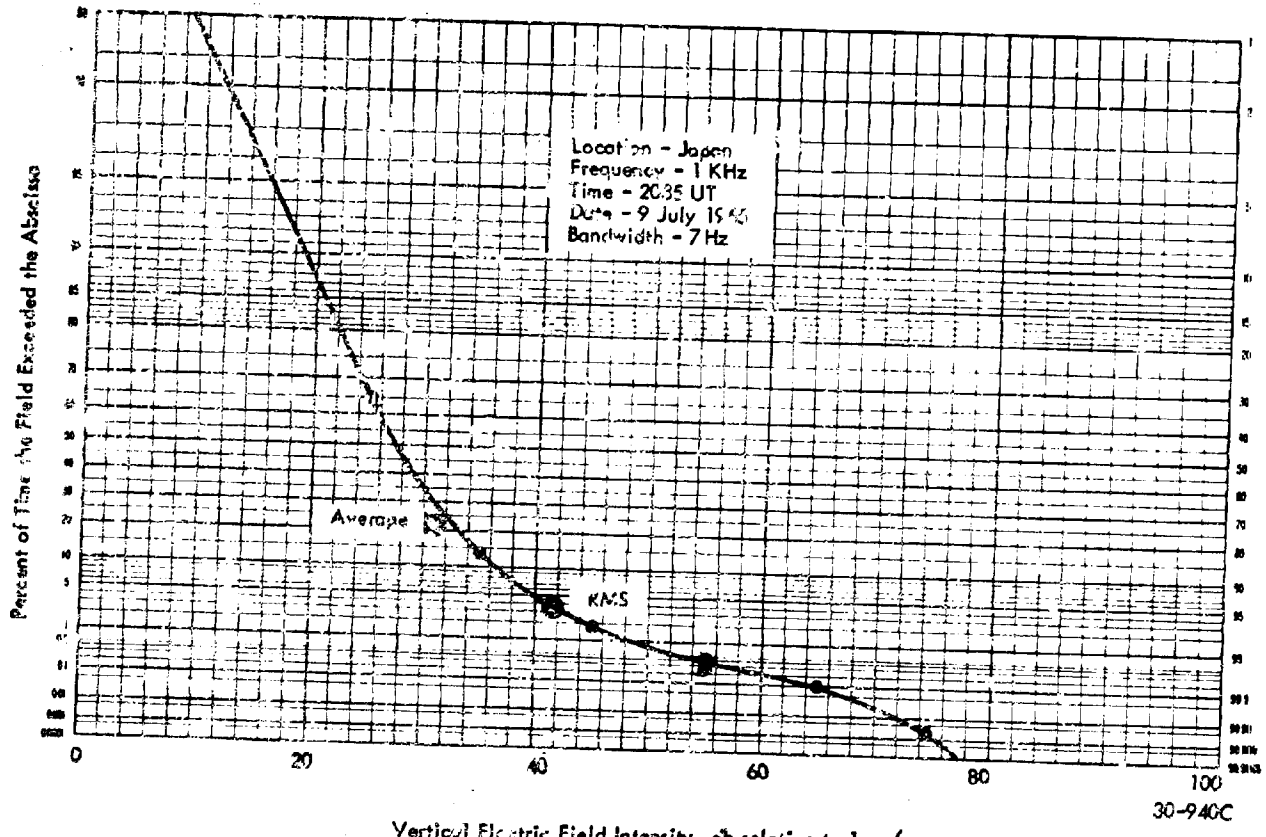

Figure 74 Amplitude Probability Distribution for Atmospheric Noise

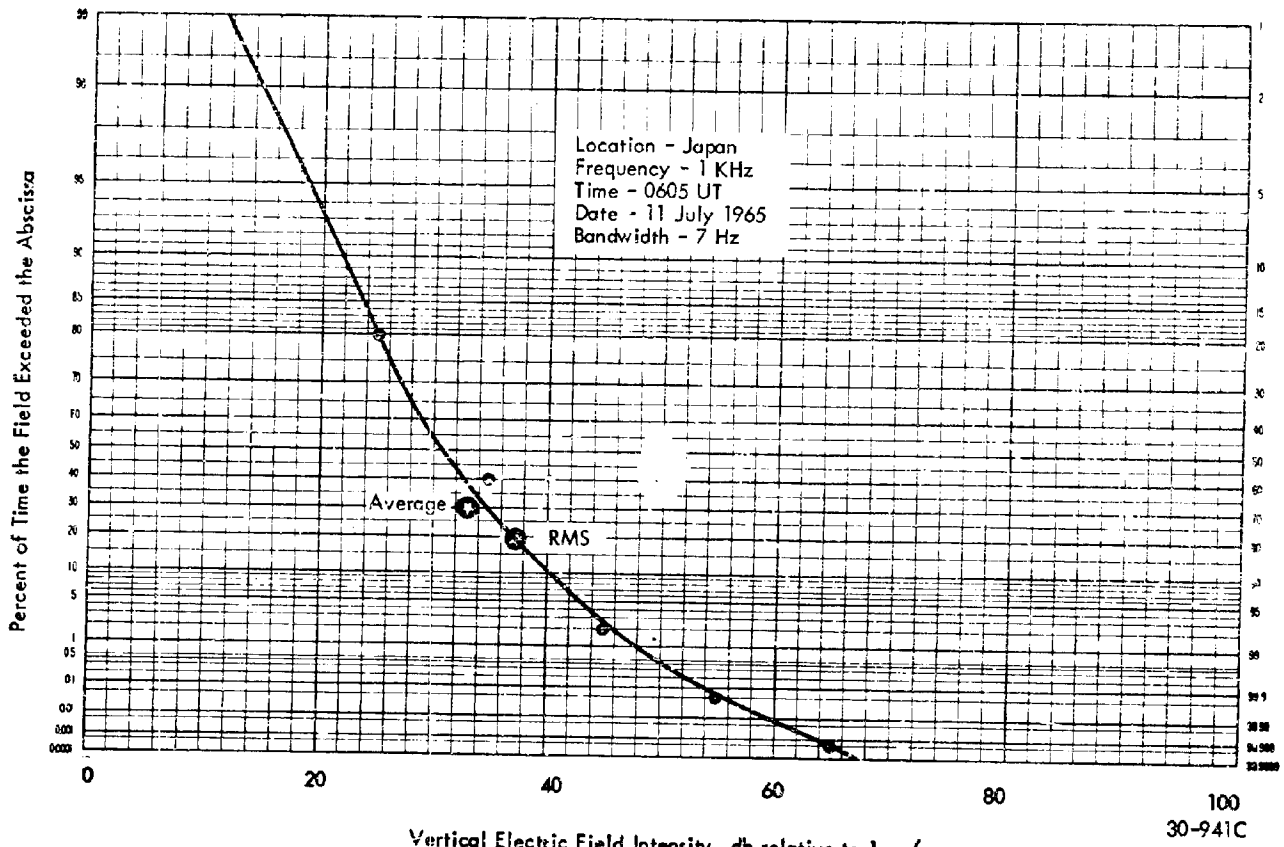

Figure 75 Amplitude Probability Distribution for Atmospheric Noise

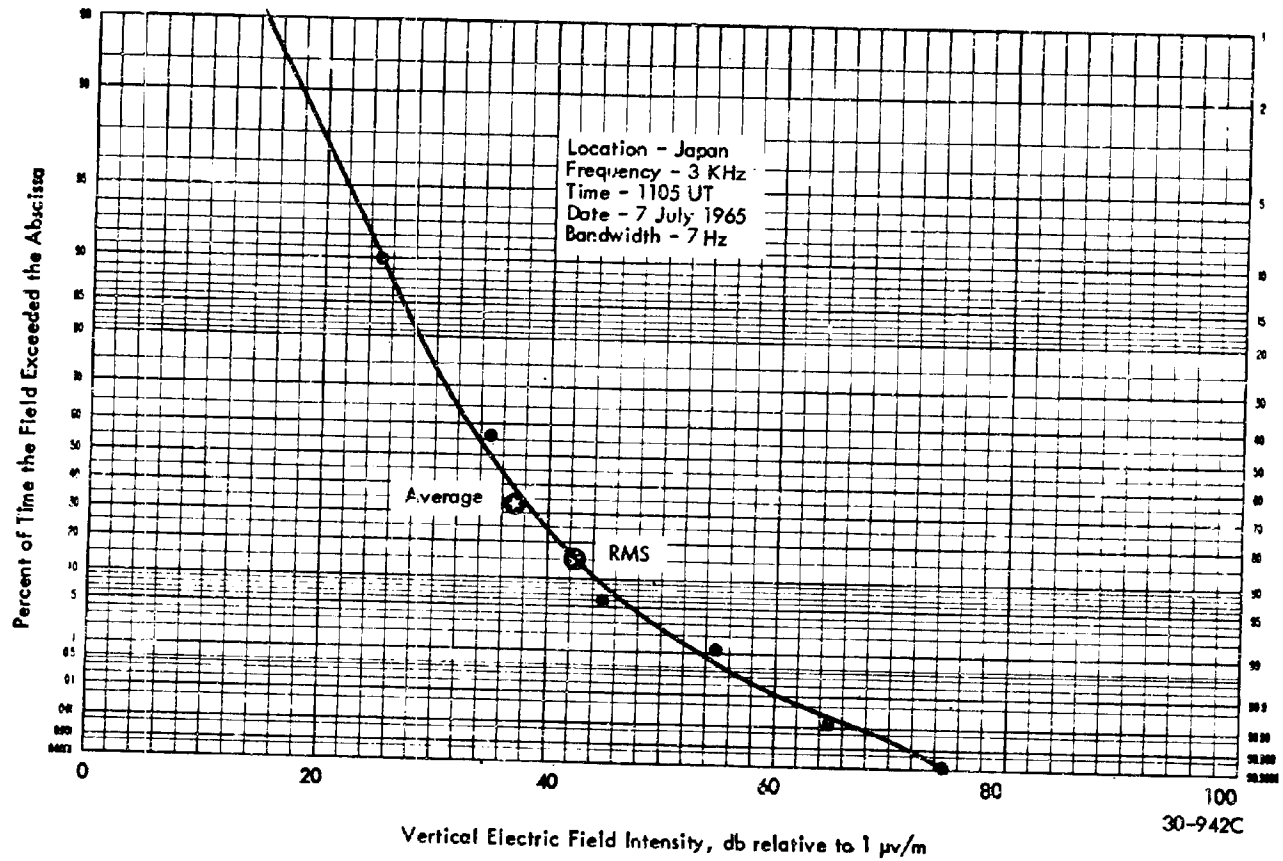

Figure 76 Amplitude Probability Distribution for Atmospheric Noise

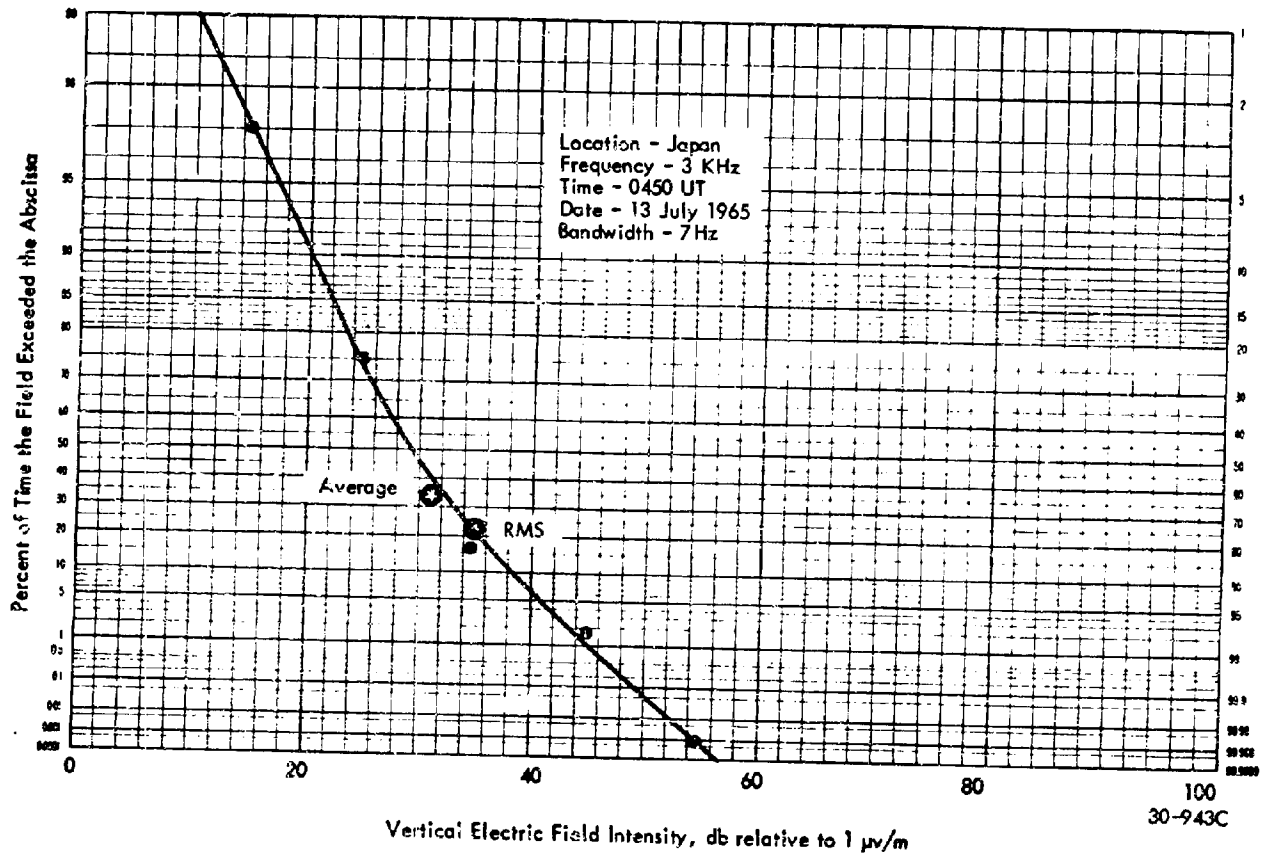

Figure 77 Amplitude Probability Distribution for Atmospheric Noise

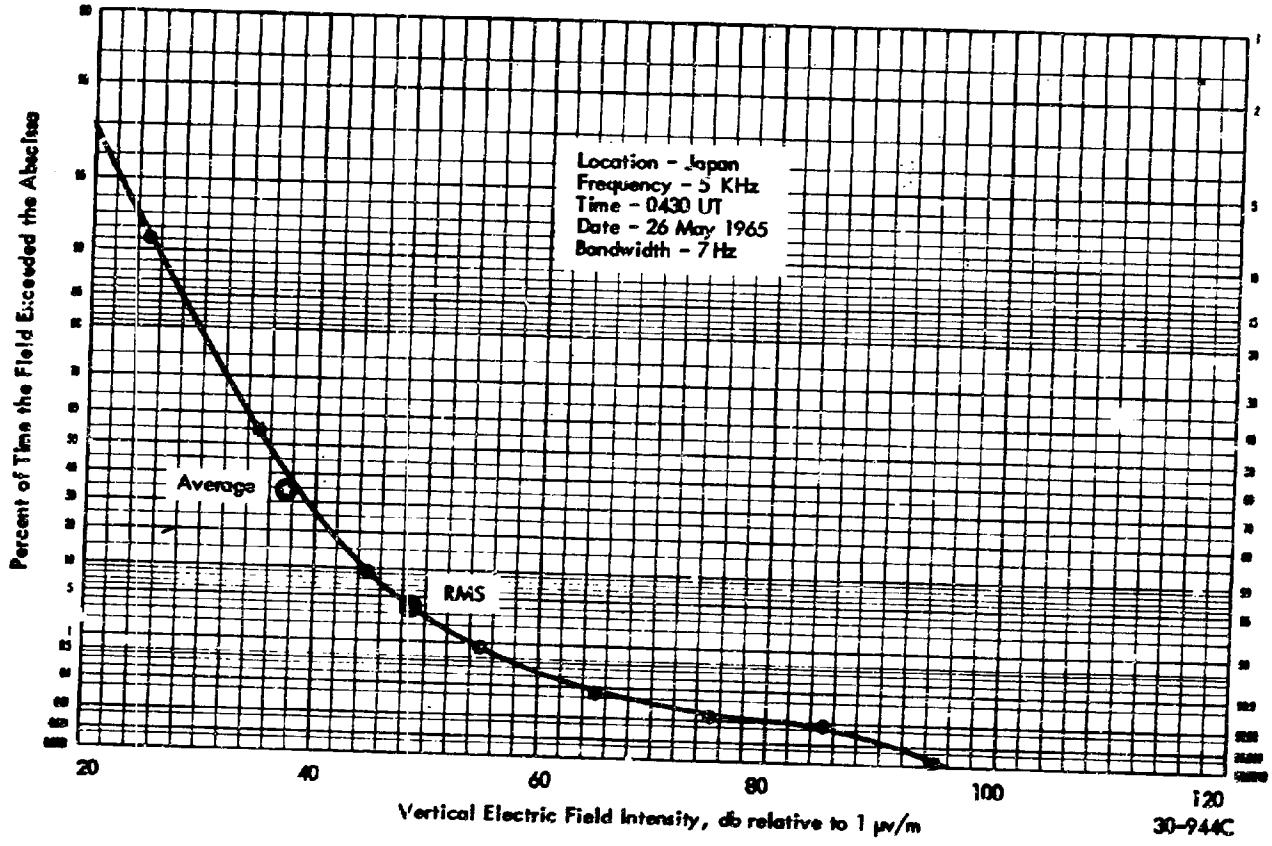

Figure 78 Amplitude Probability Distribution for Atmospheric Noise

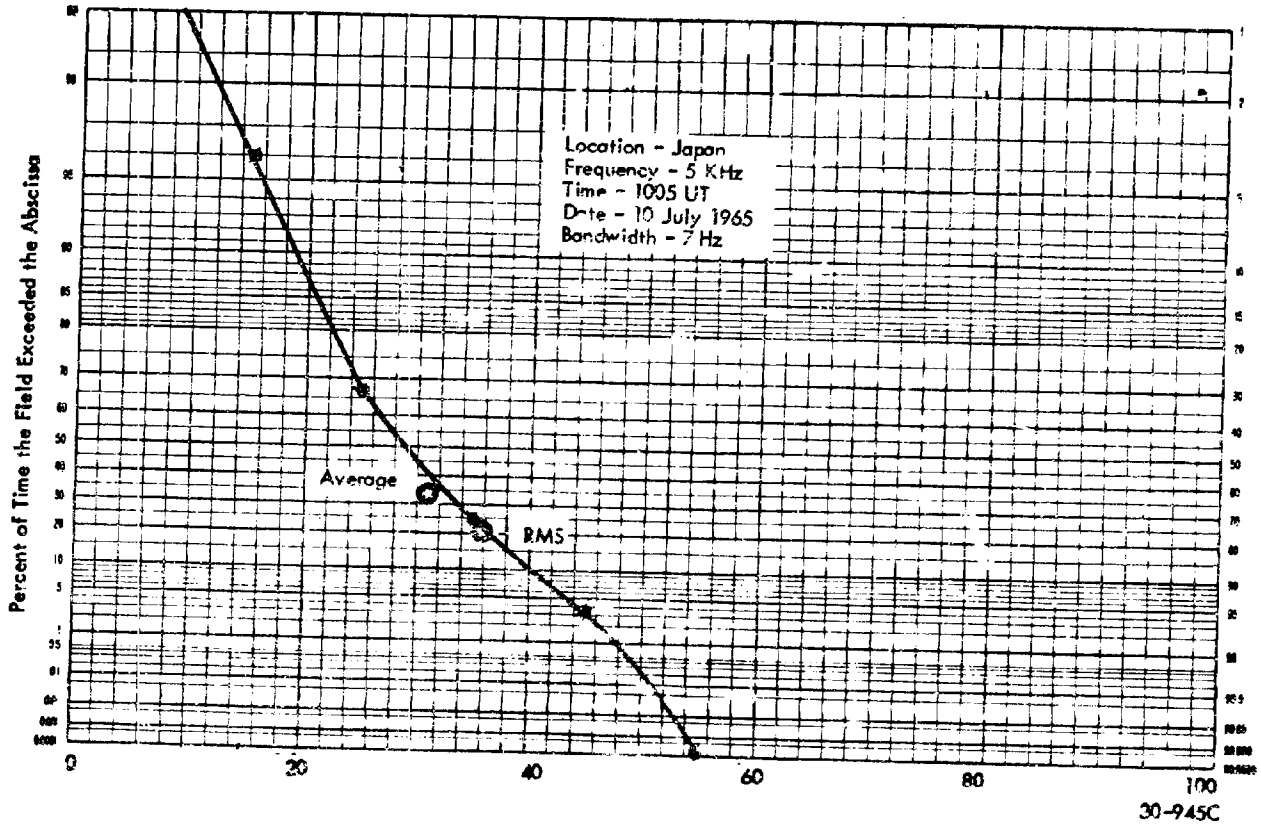

Vertical Electric Field Intensity, db relative to 1 μv/m

Figure 79 Amplitude Probability Distribution for Atmospheric Noise

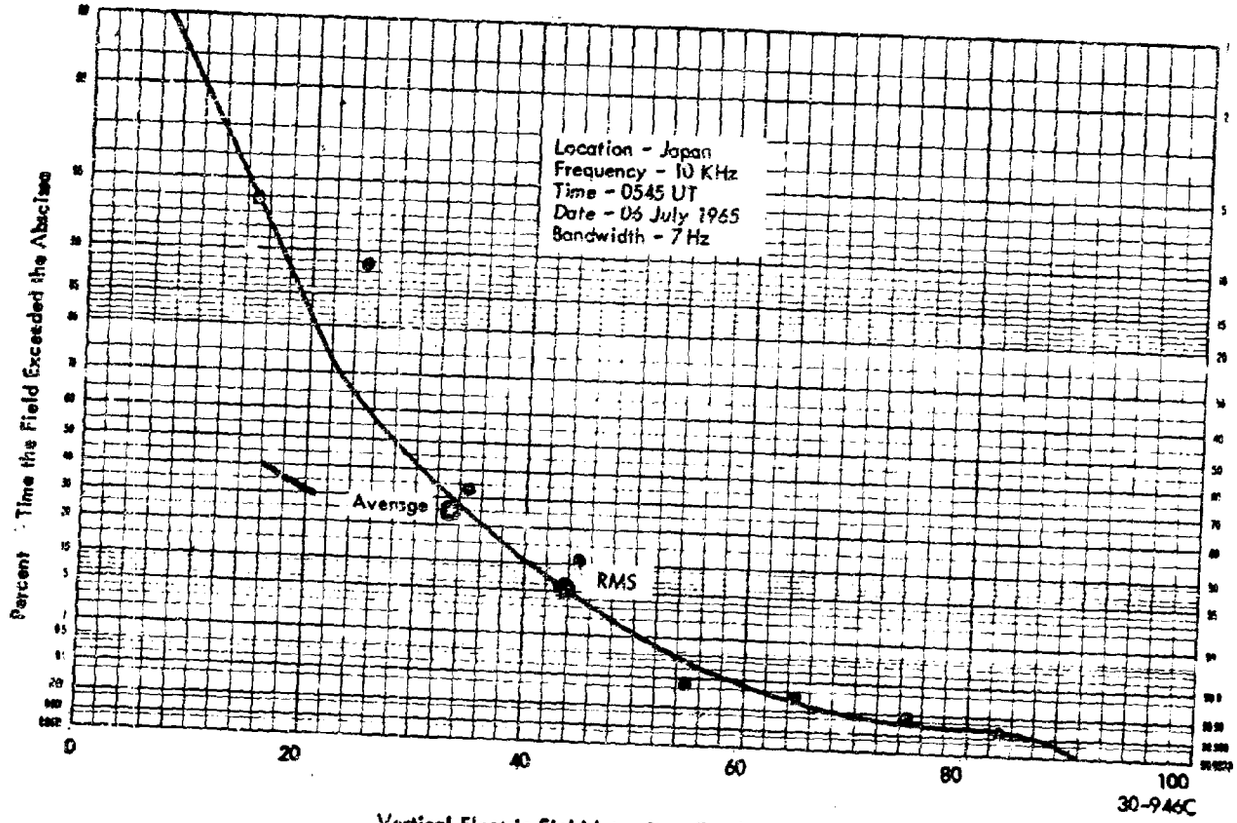

Figure 80 Amplitude Probability Distribution for Atmospheric Noise

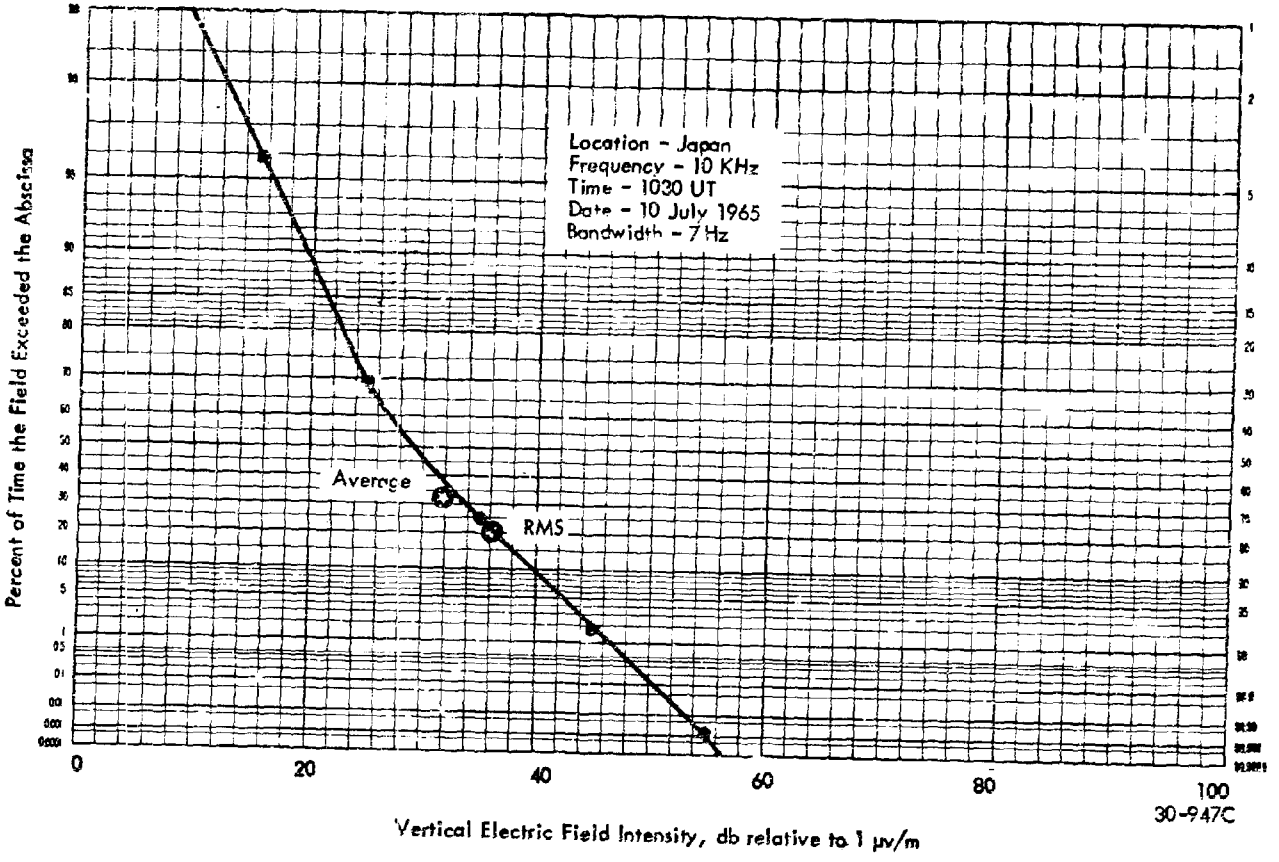

Figure 81 Amplitude Probability Distribution for Atmospheric Noise

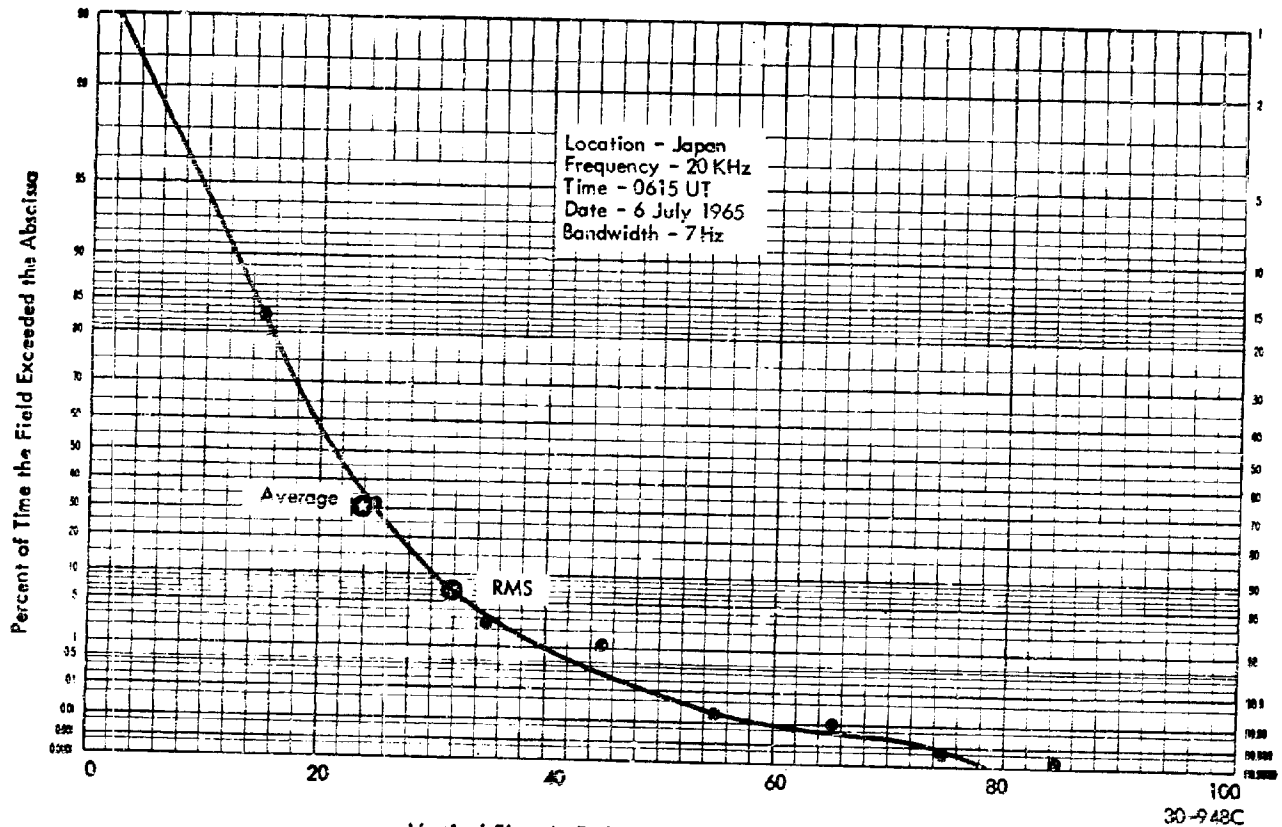

Figure 82 Amplitude Probability Distribution for Atmospheric Noise

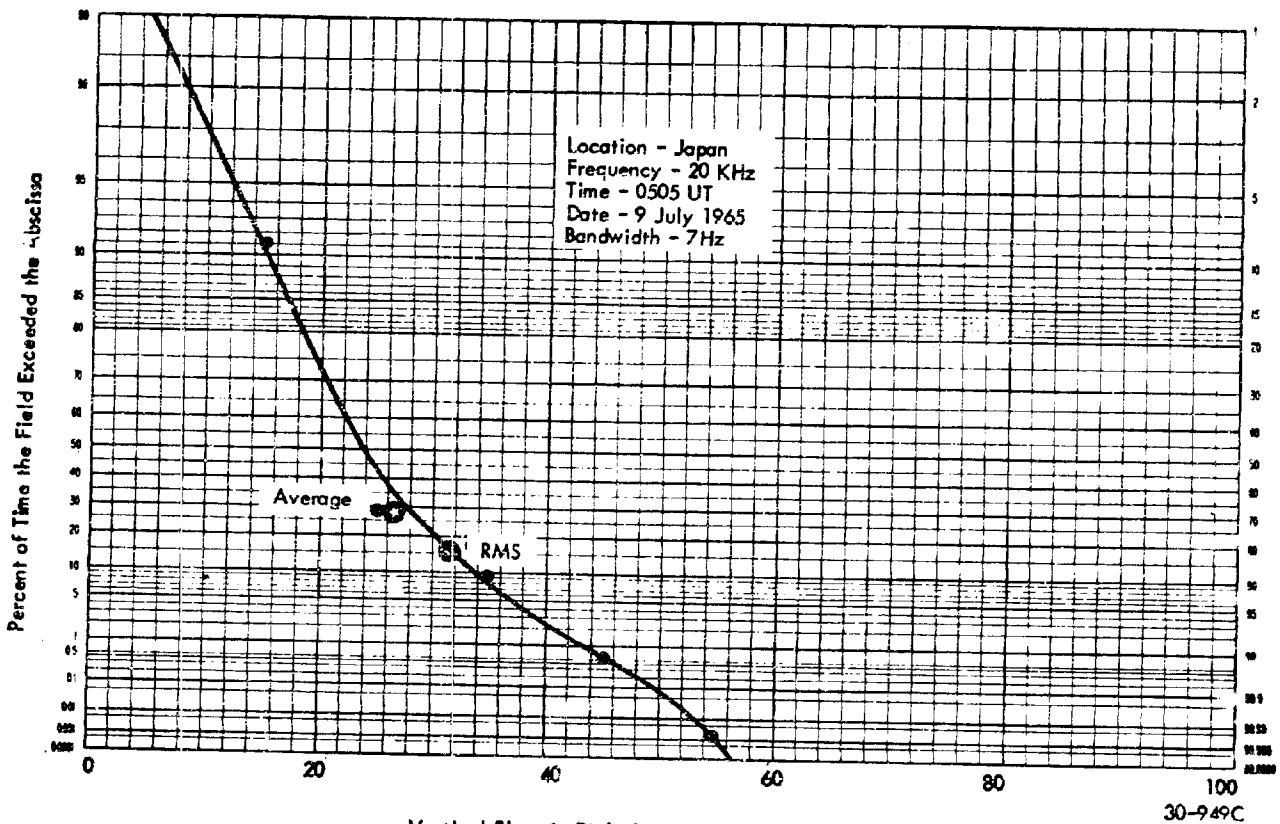

Figure 83 Amplitude Probability Distribution for Atmospheric Noise

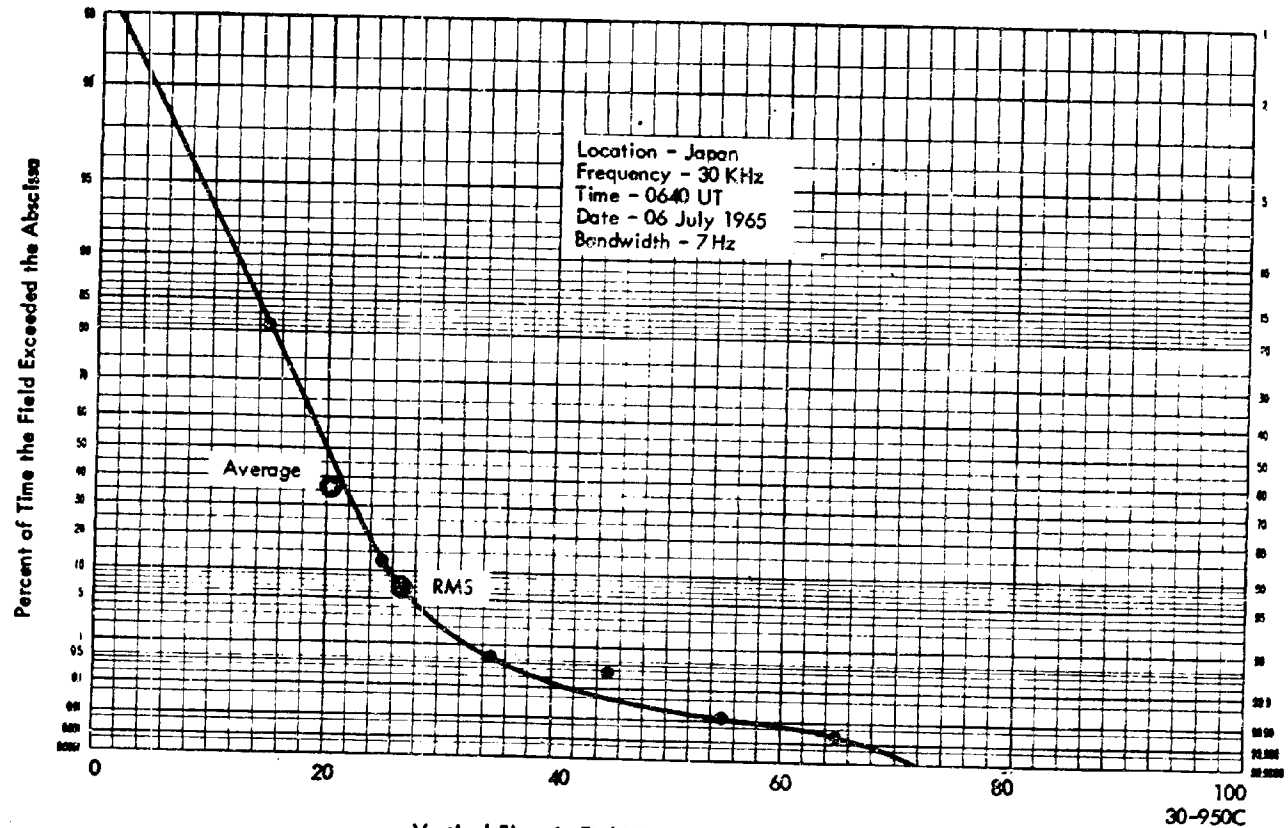

Figure 8-4 Amplitude Probability Distribution for Atmospheric Noise

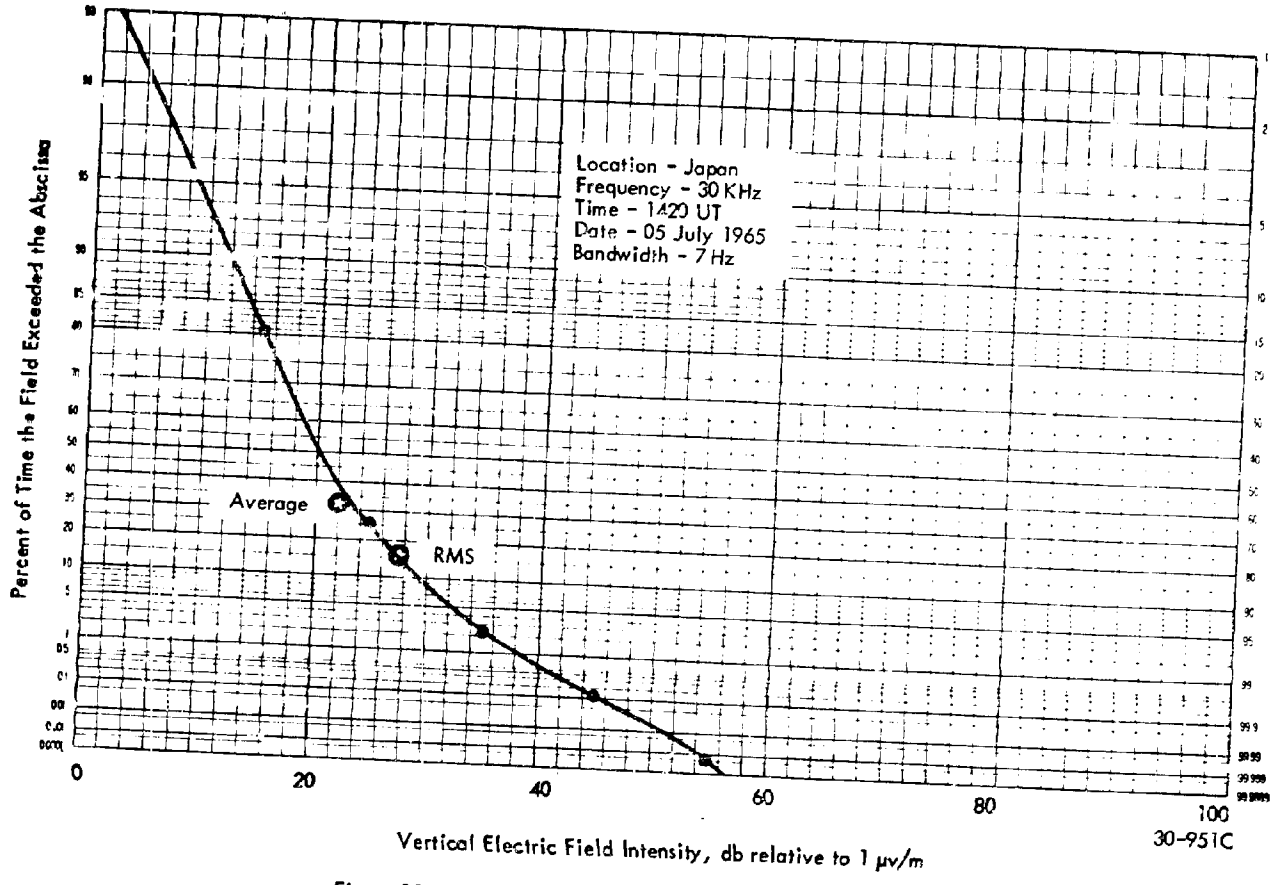

Figure 85 Amplitude Probability Distribution for Atmospheric Noise

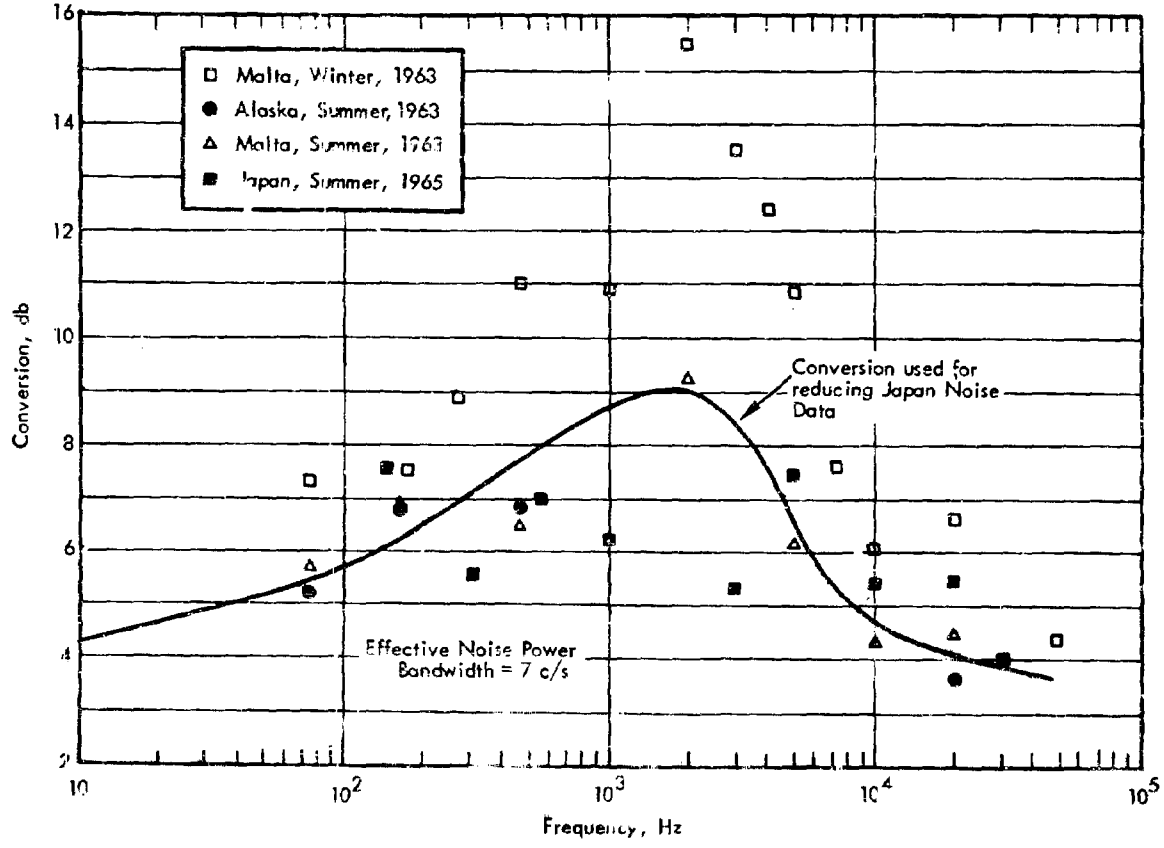

Figure 84 Average to RMS Conversion Factors as Measured

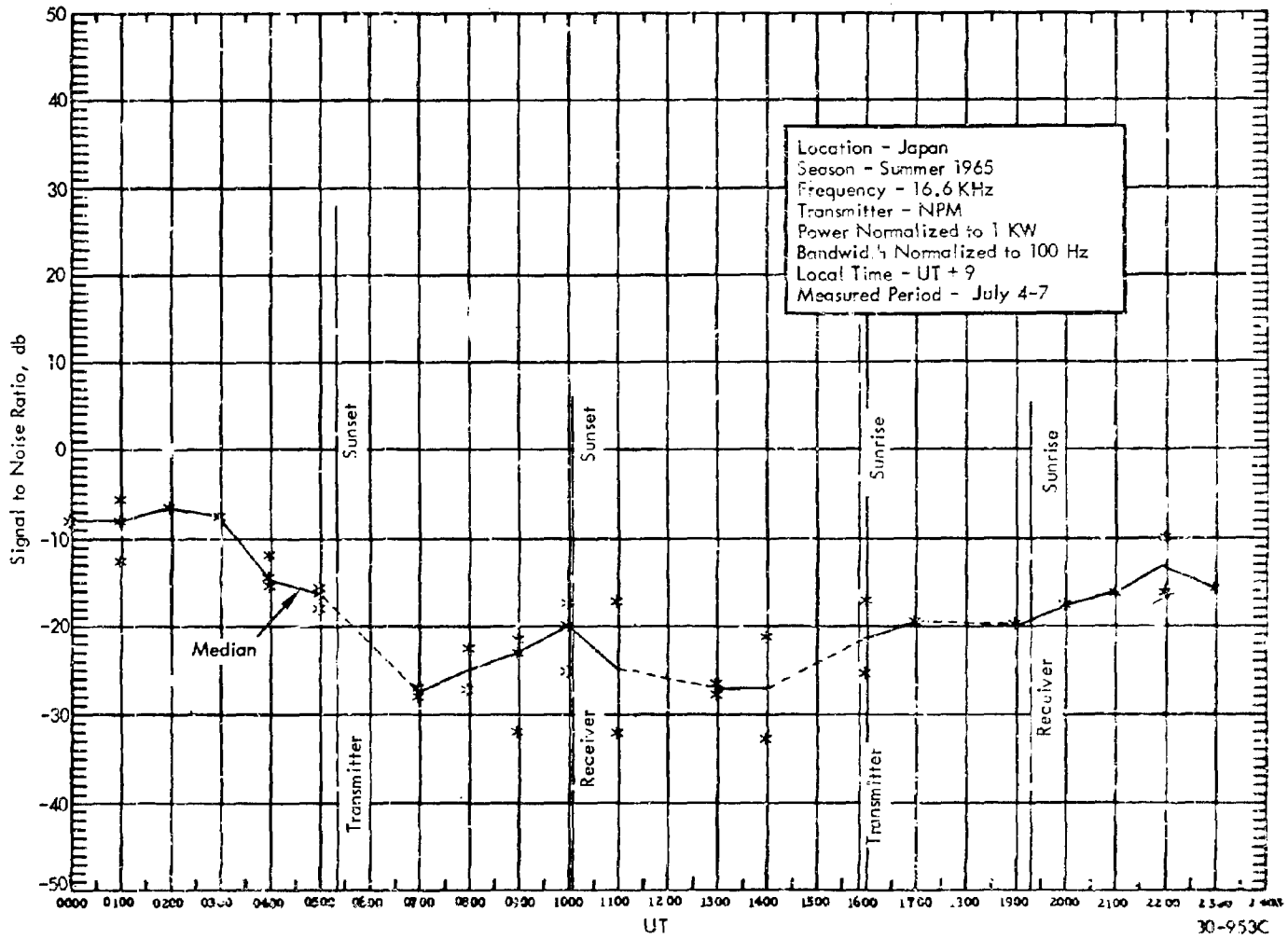

Figure 87 Measured Signal to Noise Ratio

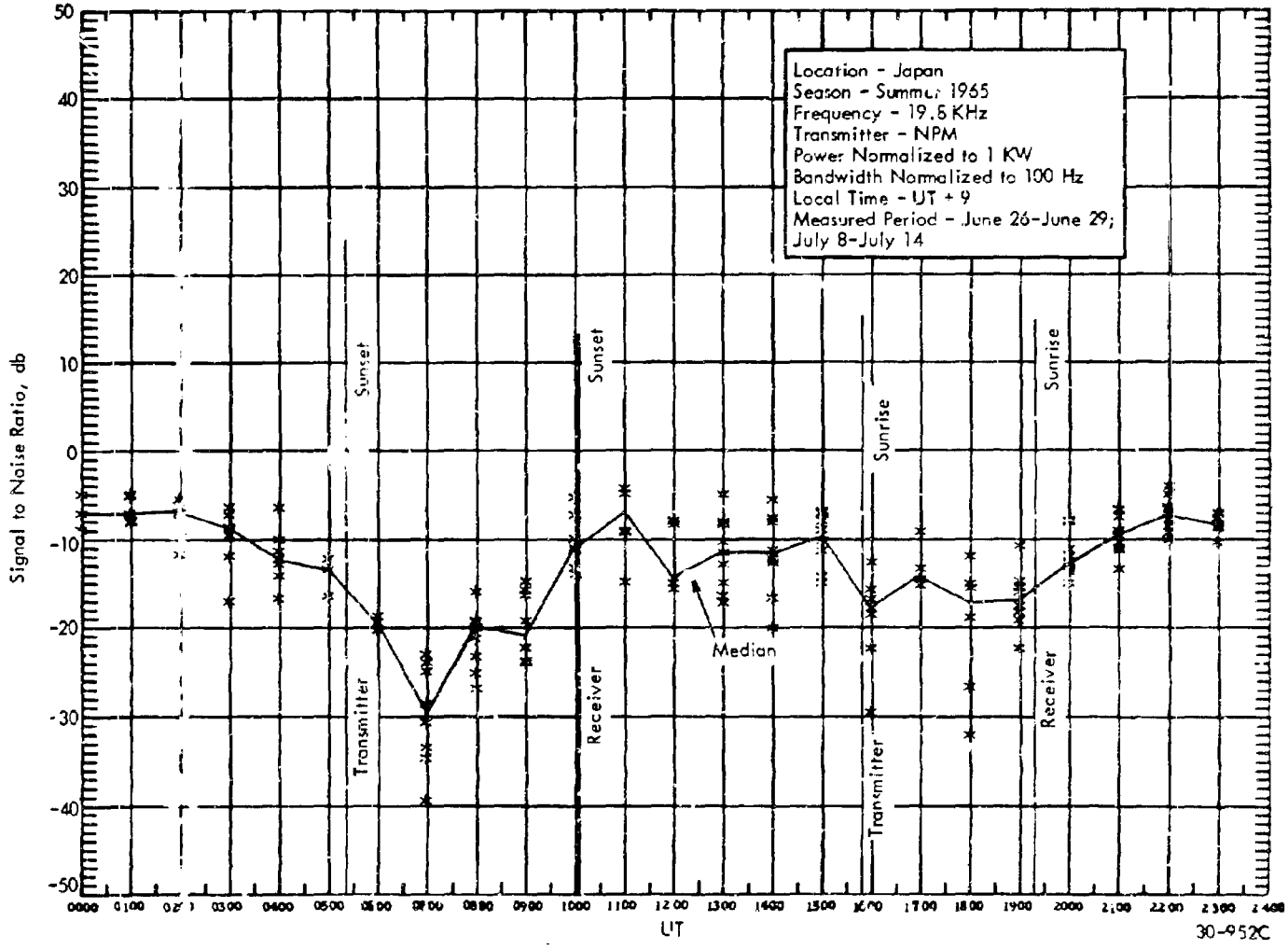

Figure 88 Measured Signal to Noise Ratio

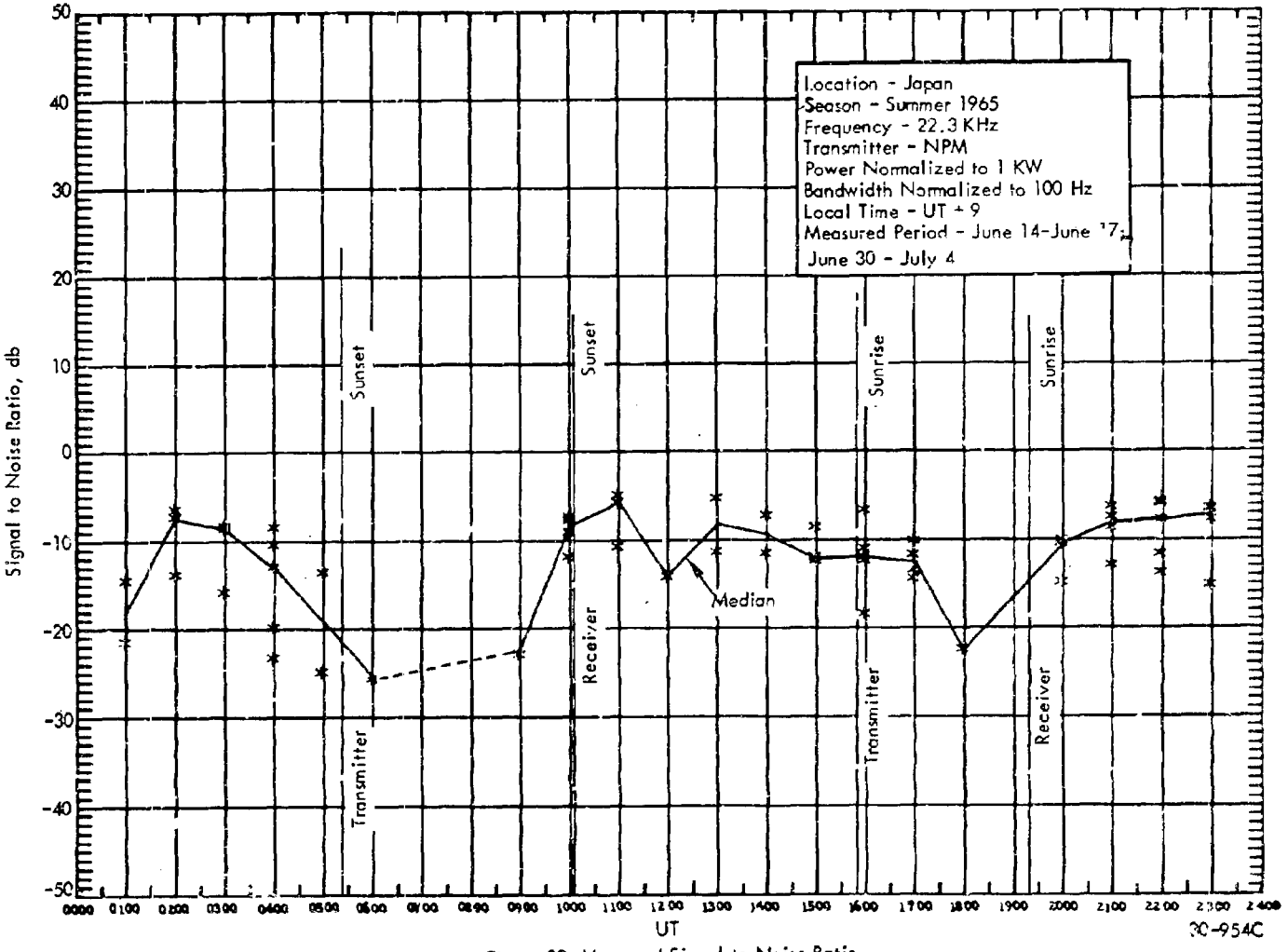

Figure 89 Measured Signal to Noise Ratio

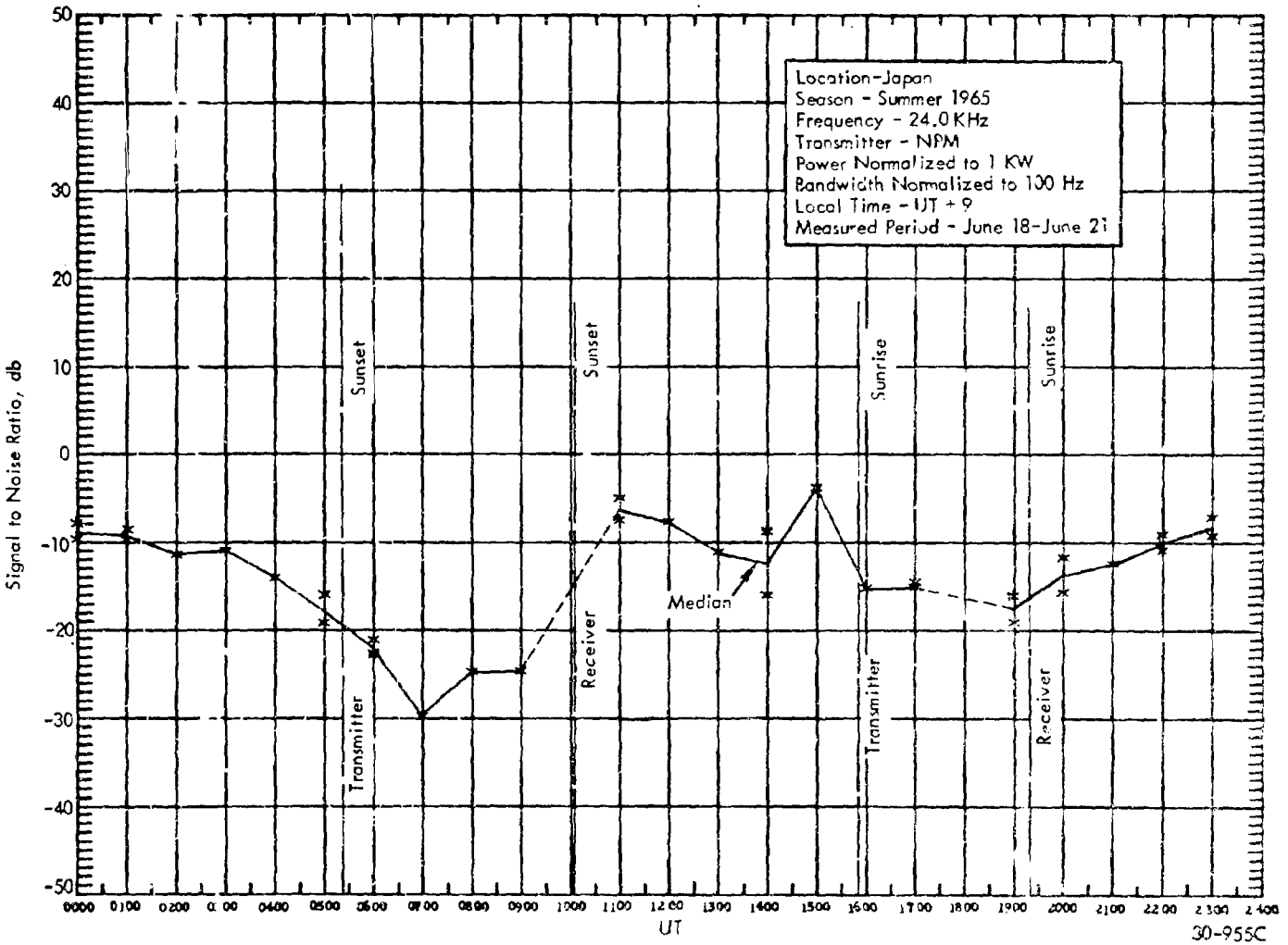

Figure 90 Measured Signal to Noise Ratio

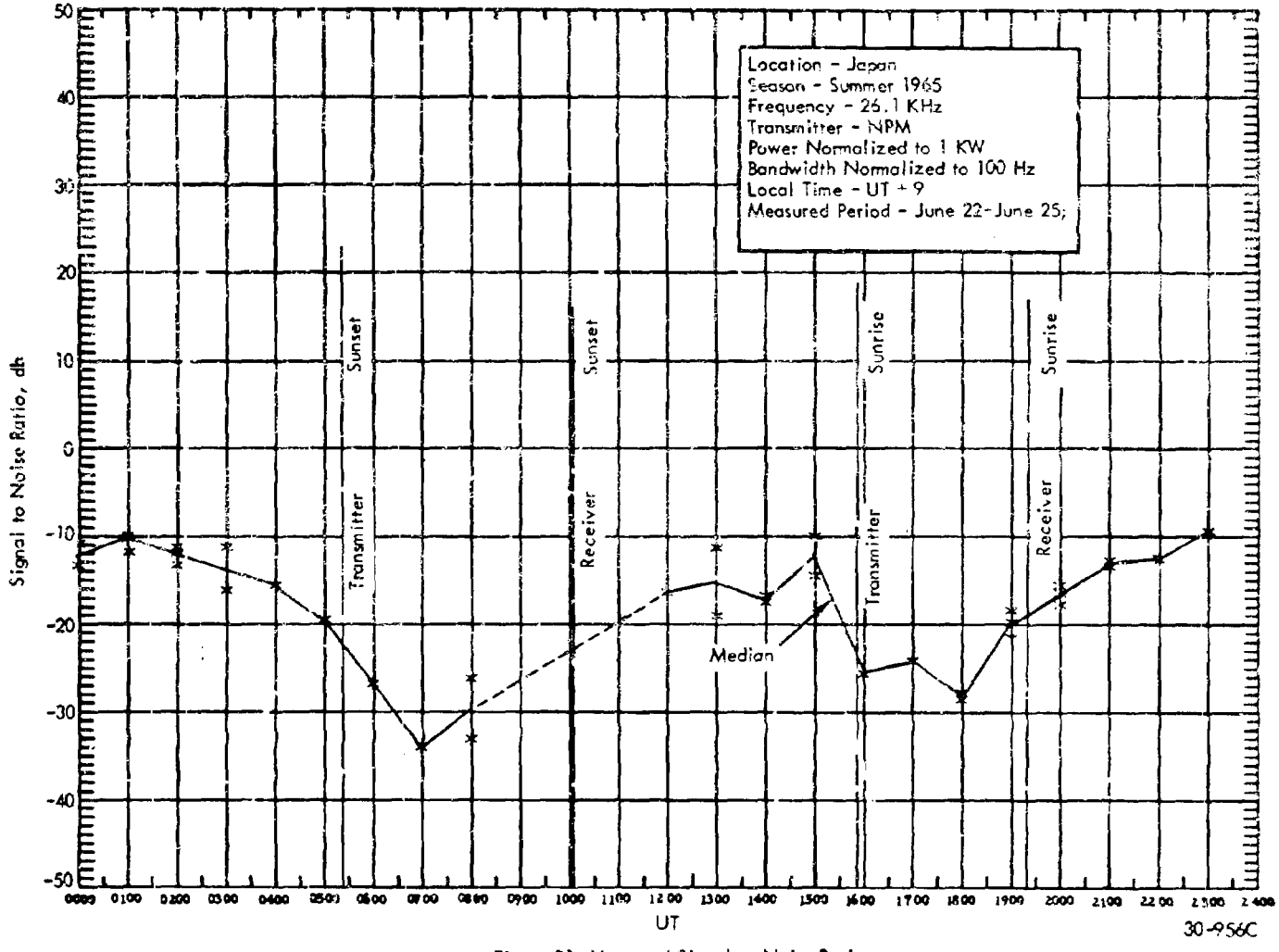

Figure 91 Measured Signal to Noise Ratio

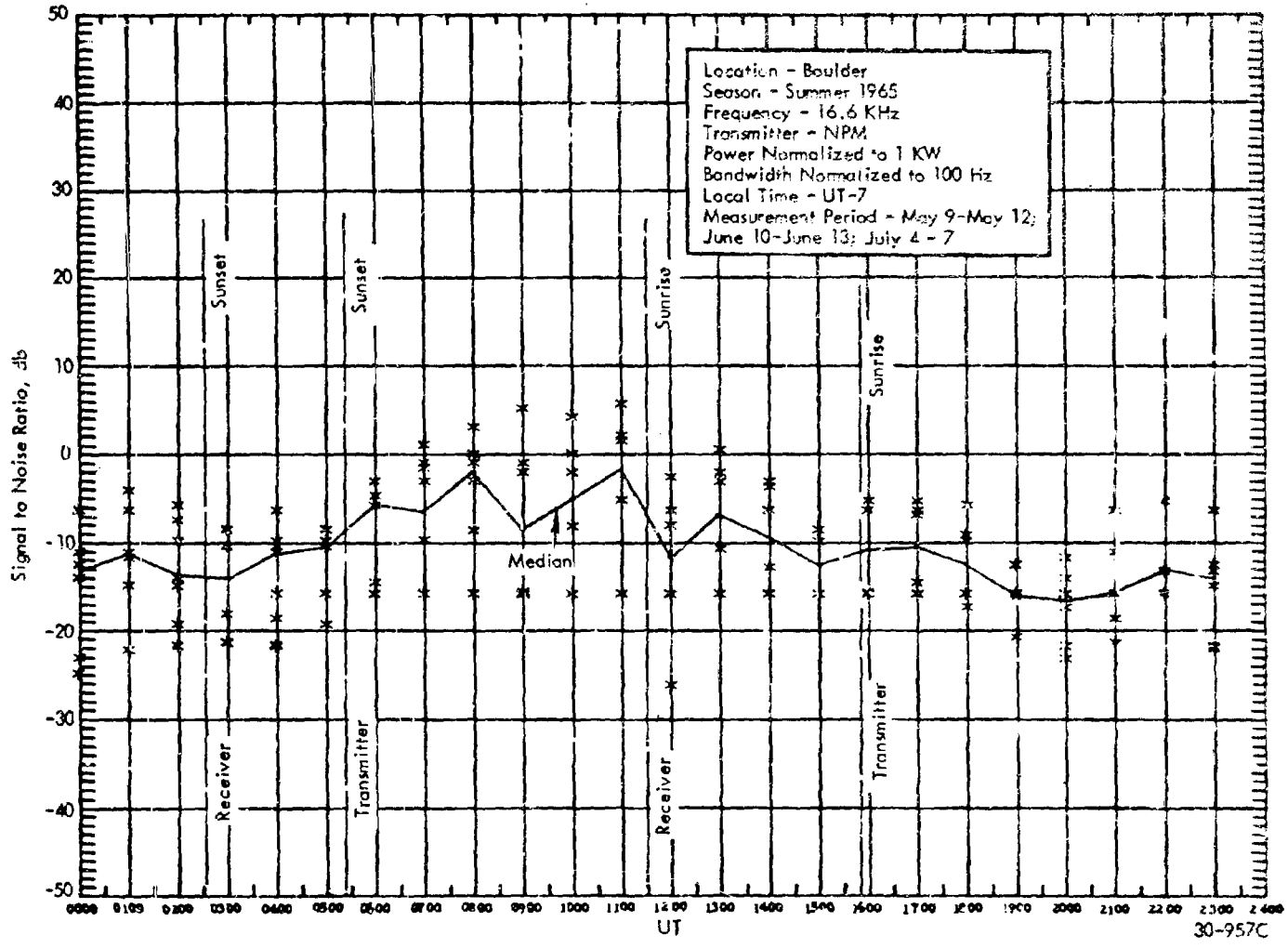

Figure 92 Measured Signal to Noise Ratio

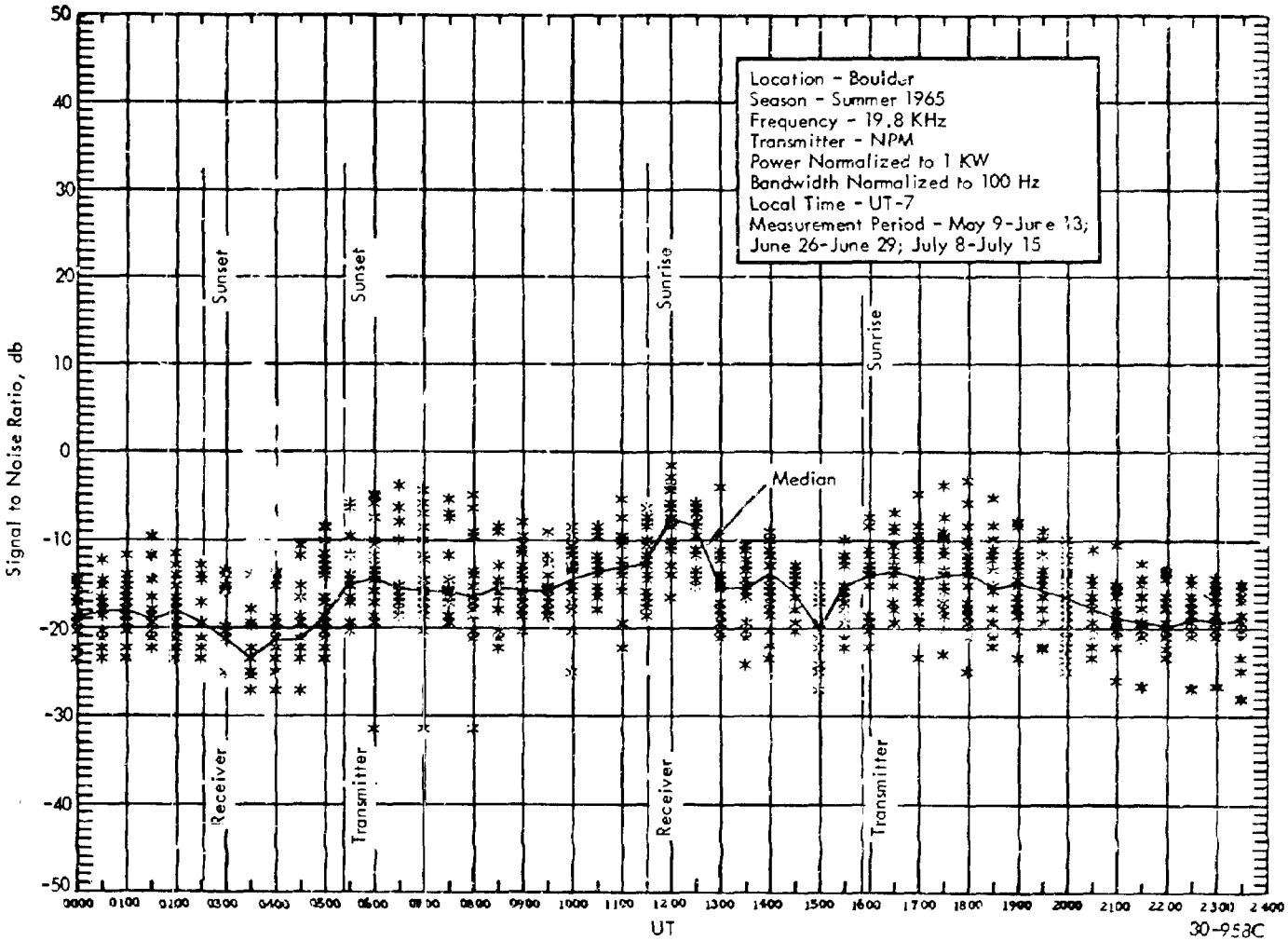

Figure 93 Measured Signal to Noise Ratio

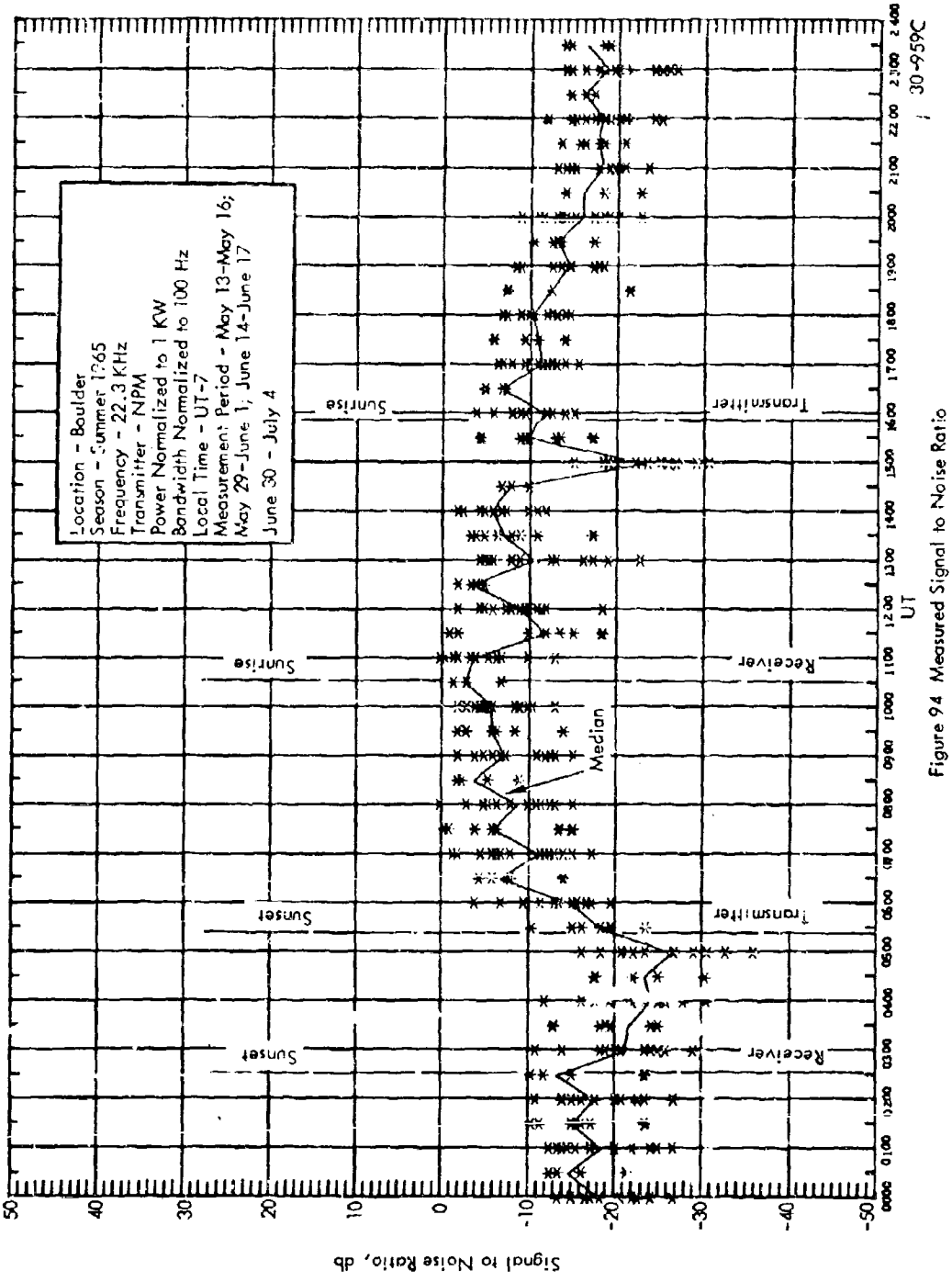

Figure 94 Measured Signal to Noise Ratio

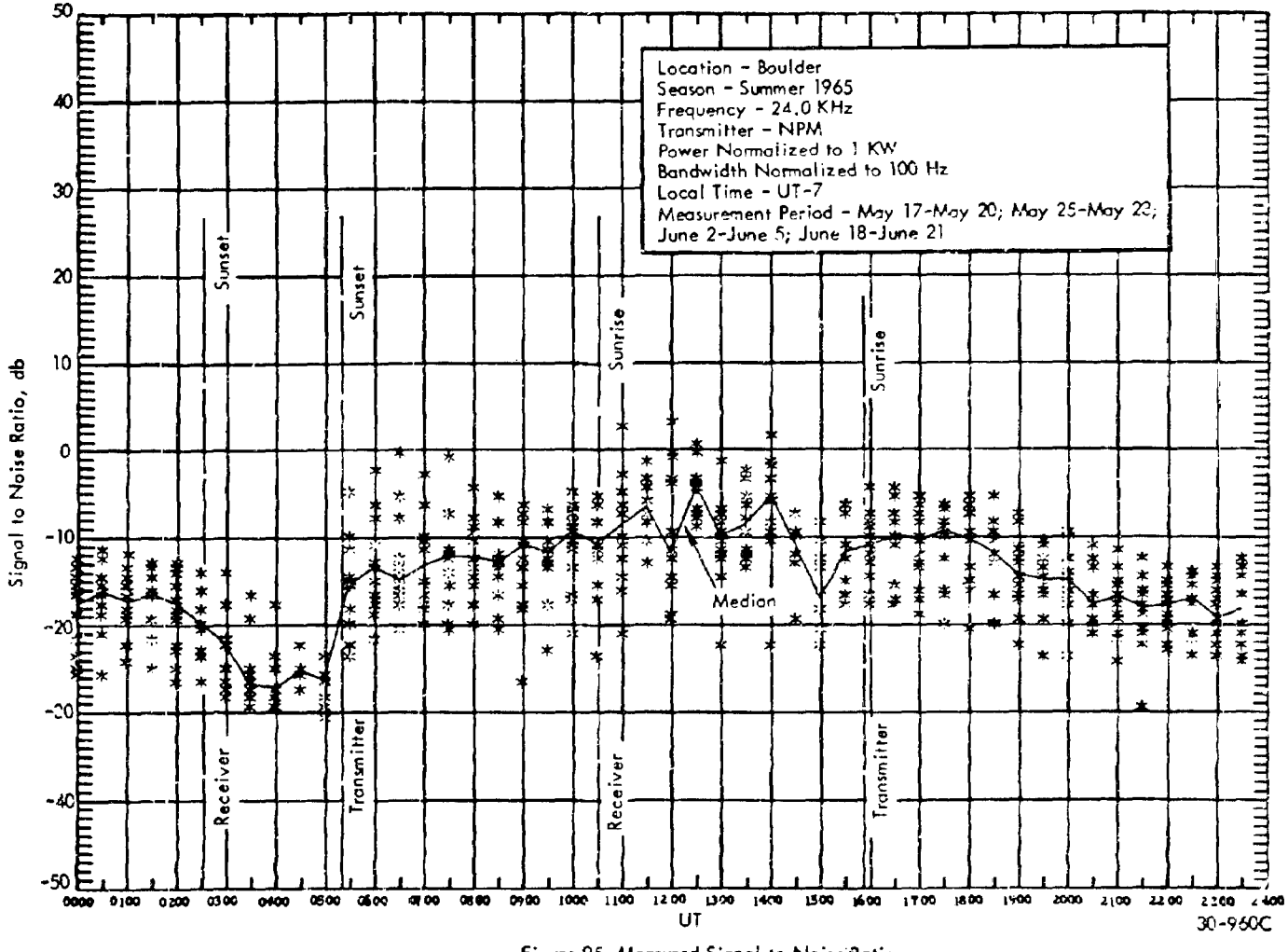

Figure 95 Measured Signal to Noise Ratio

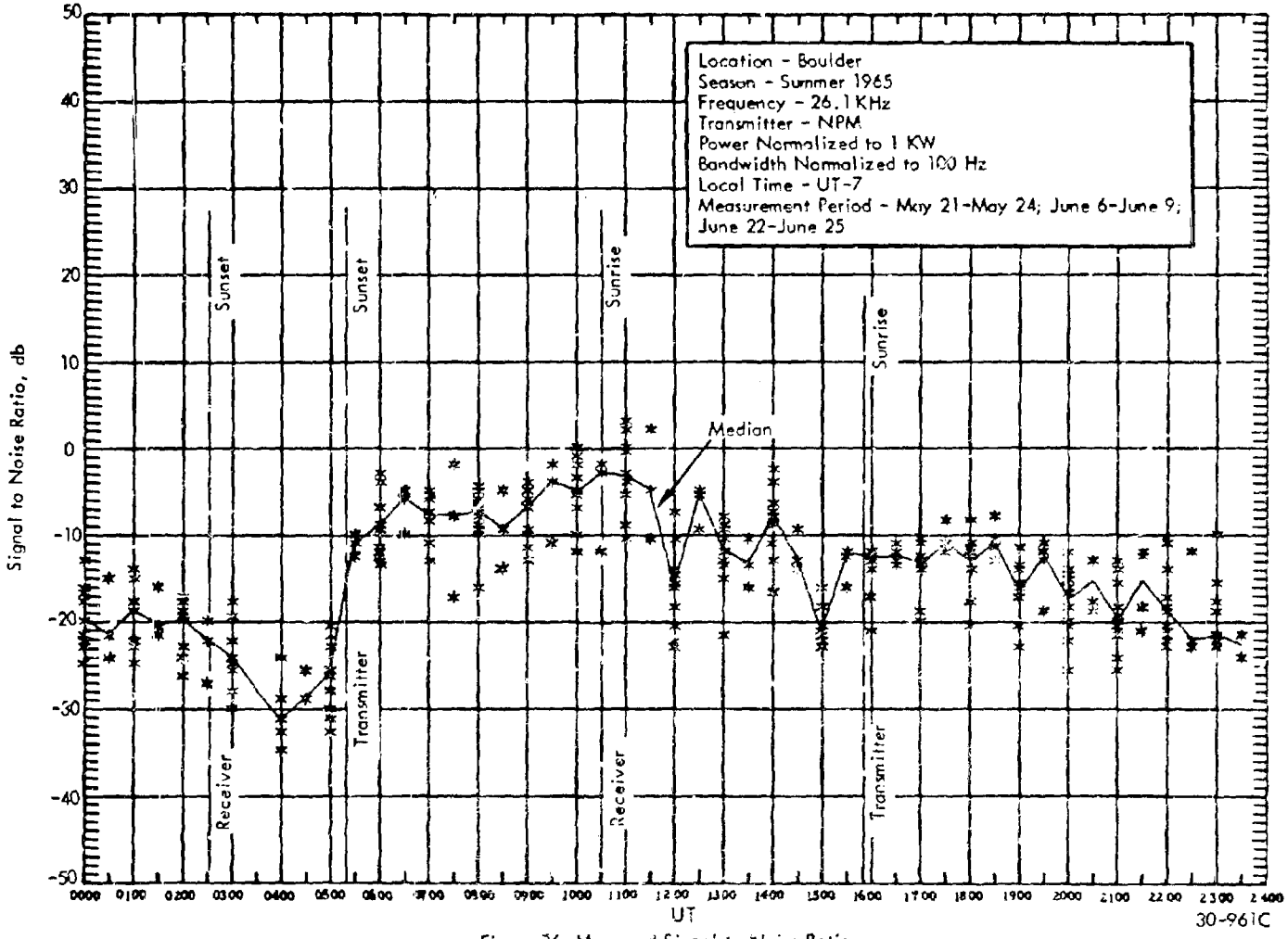

Figure 96 Measured Signal to Noise Ratio

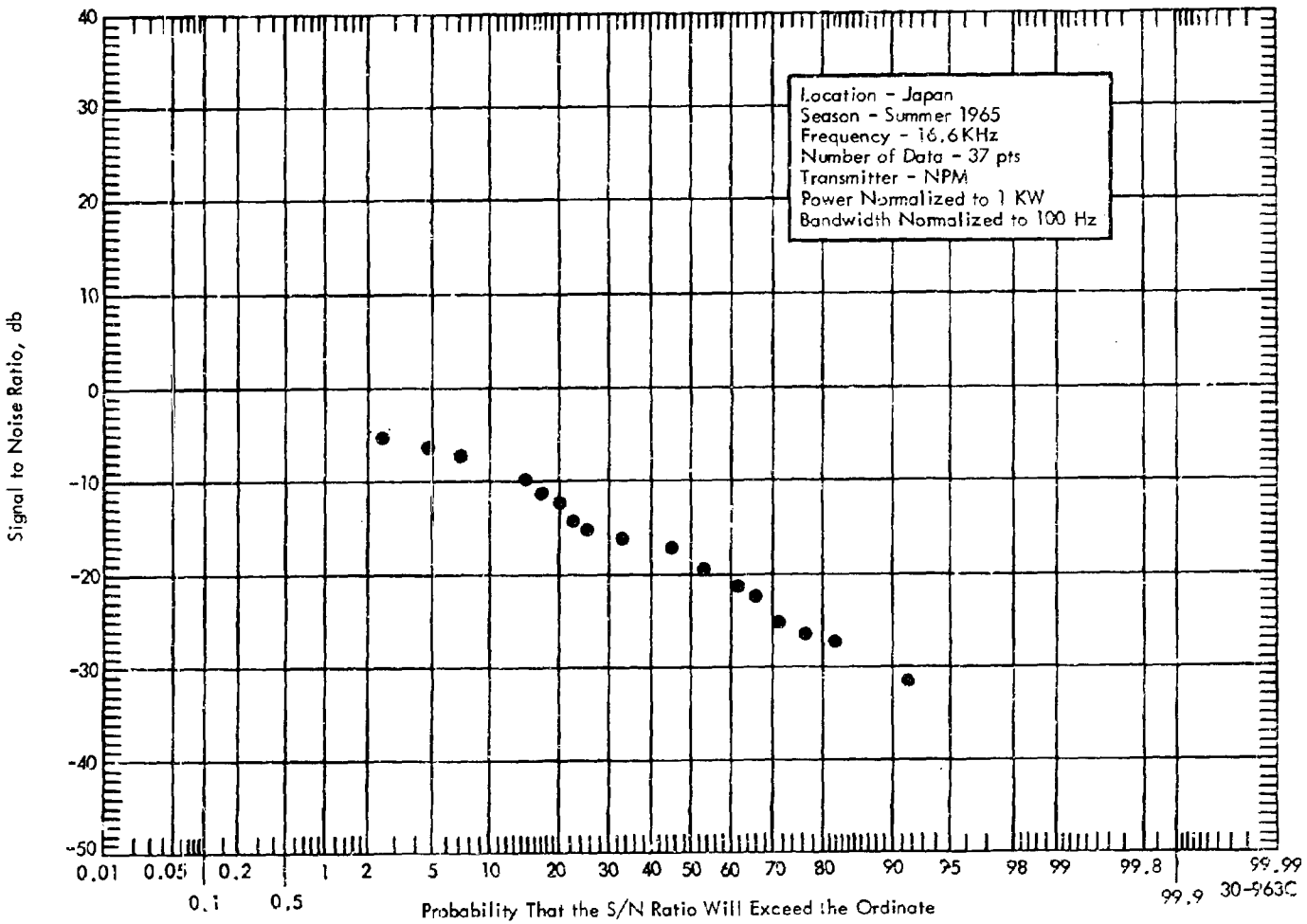

Figure 97 Cumulative Distribution of Measured Signal to Noise Ratio

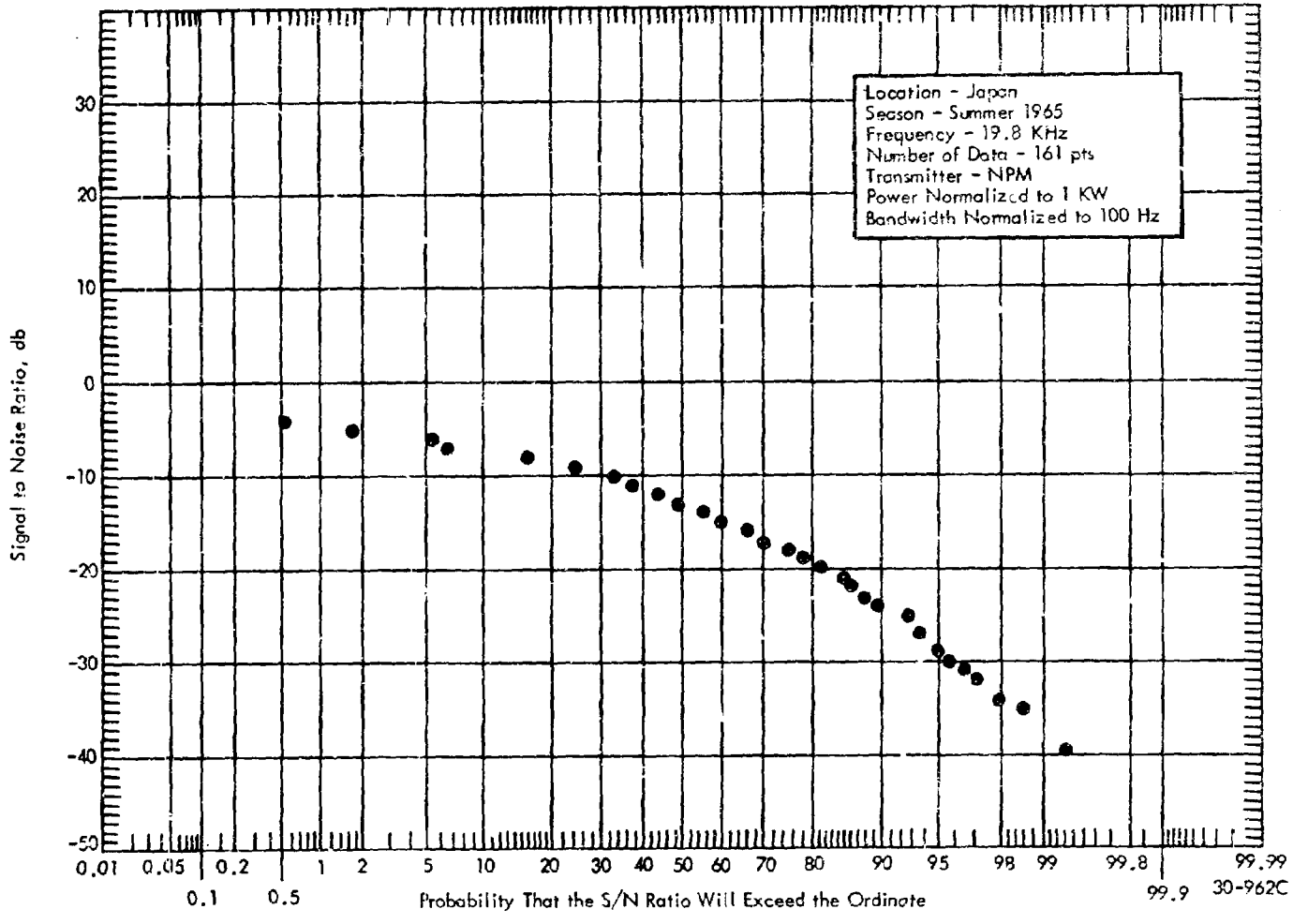

Figure 98 Cumulative Distribution of Measured Signal to Noise Ratio

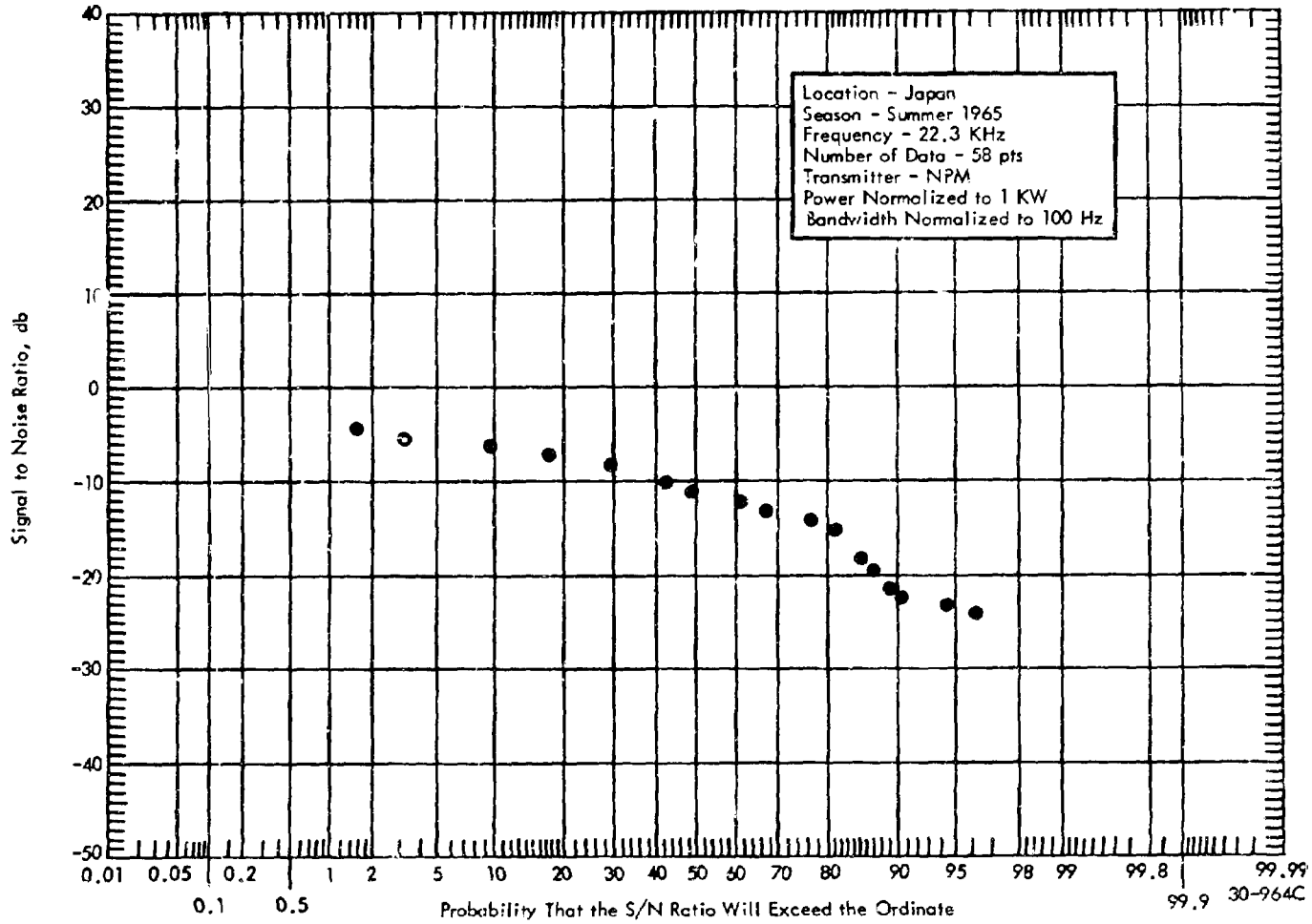

Figure 99 Cumulative Distribution of Measured Signal to Noise Ratio

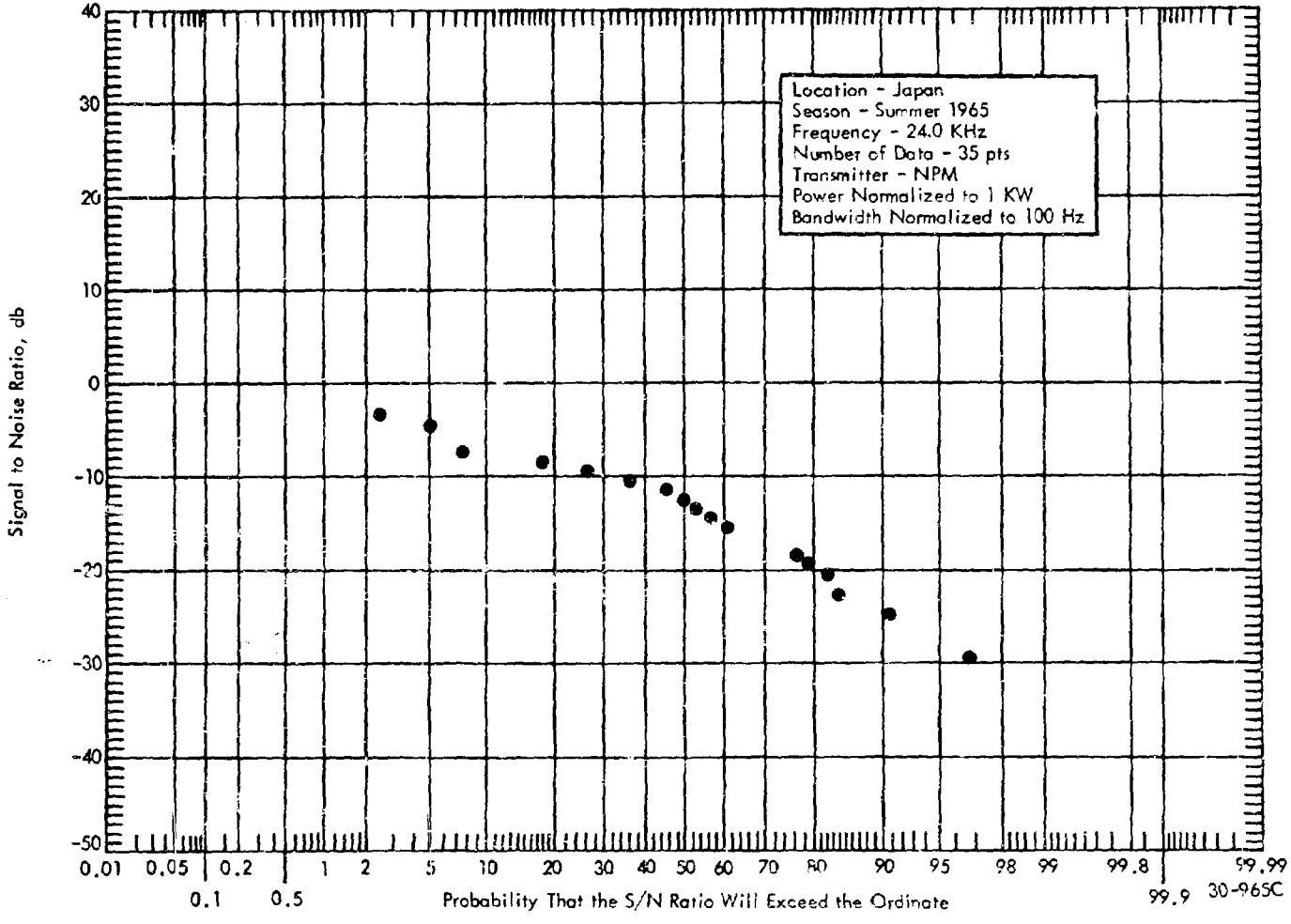

Figure 100 Cumulative Distribution of Measured Signal to Noise Ratio

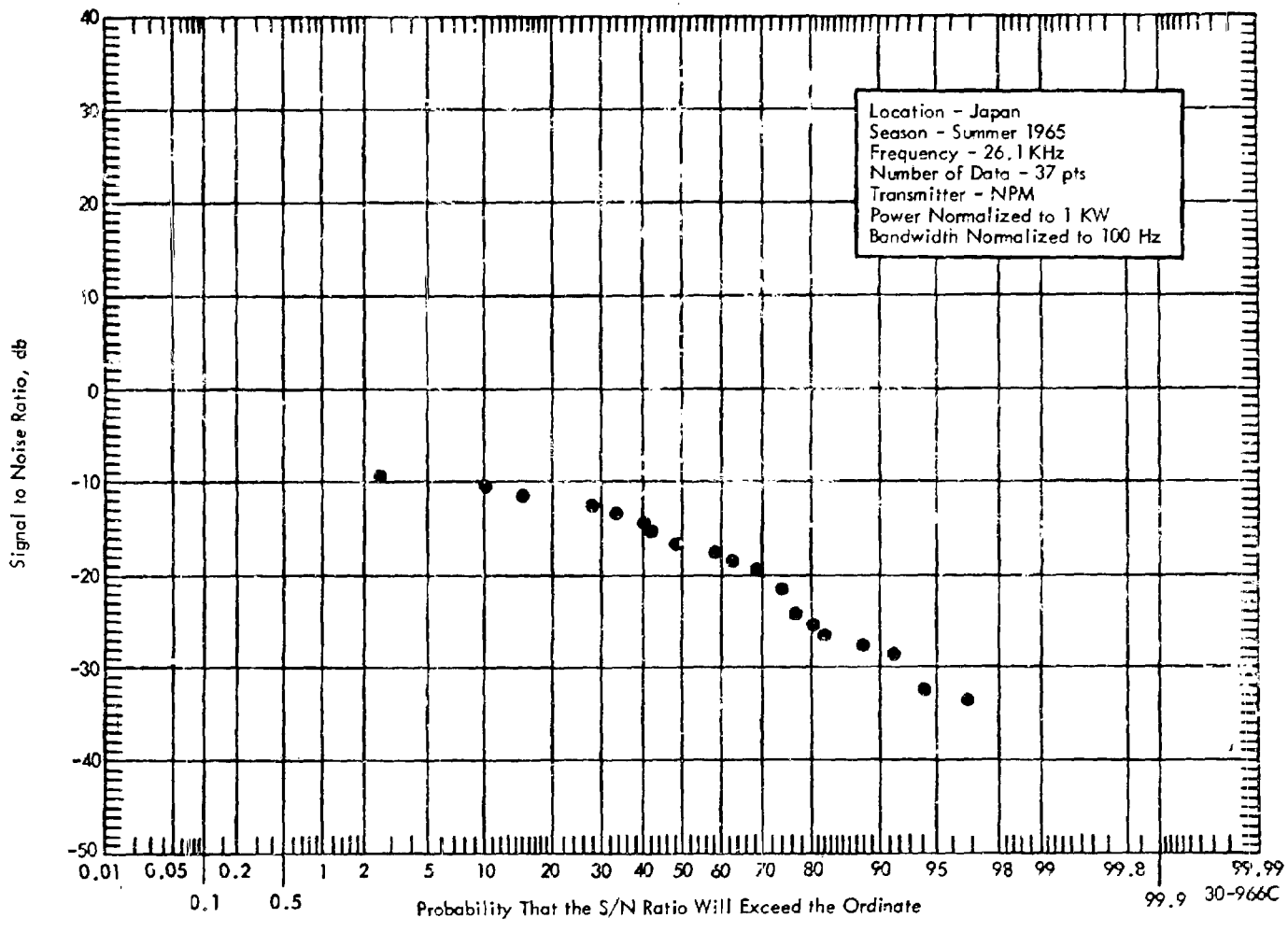

Figure 101 Cumulative Distribution of Measured Signal to Noise Ratio

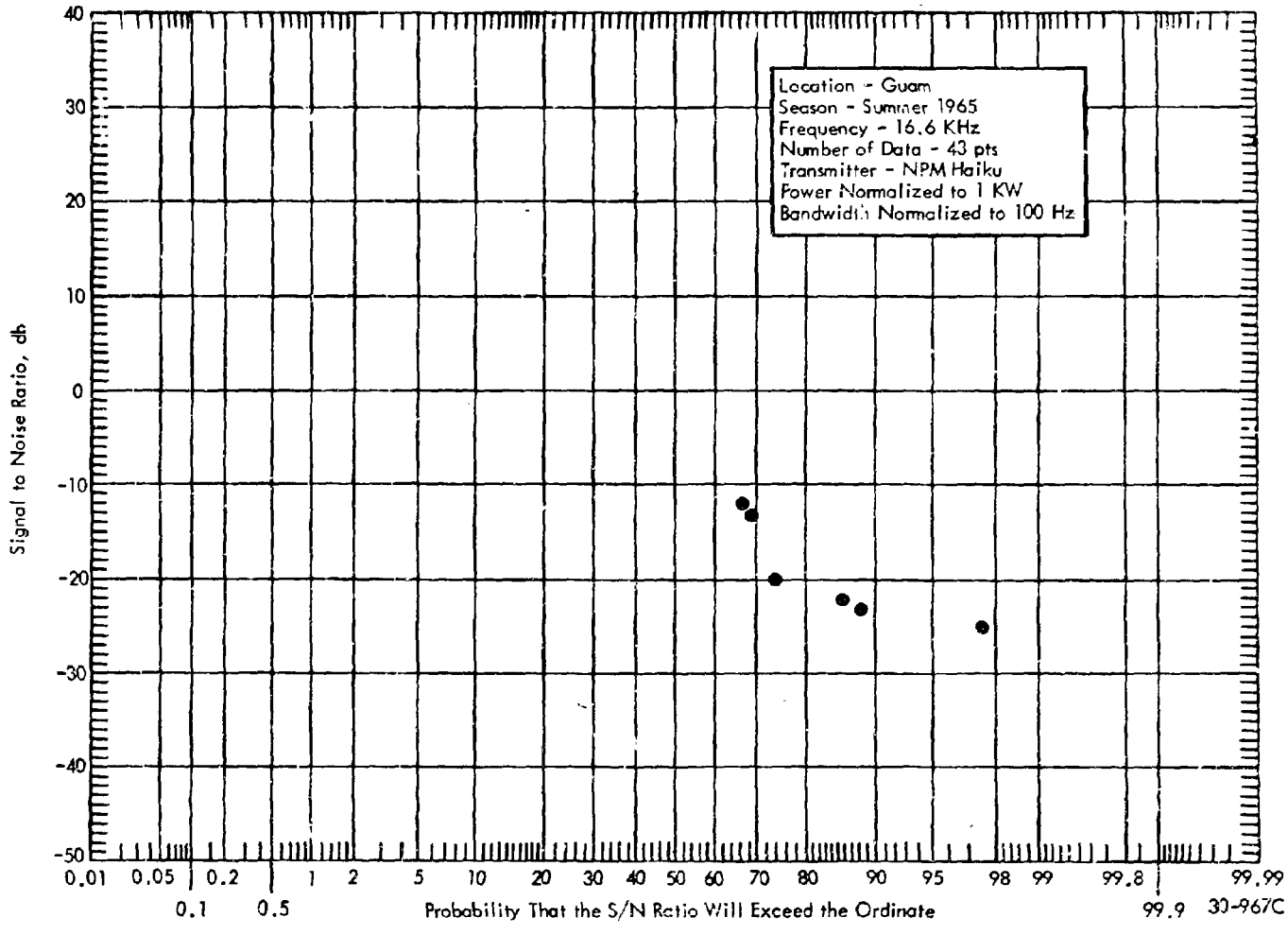

Figure 102 Cumulative Distribution of Measured Signal to Noise Ratio

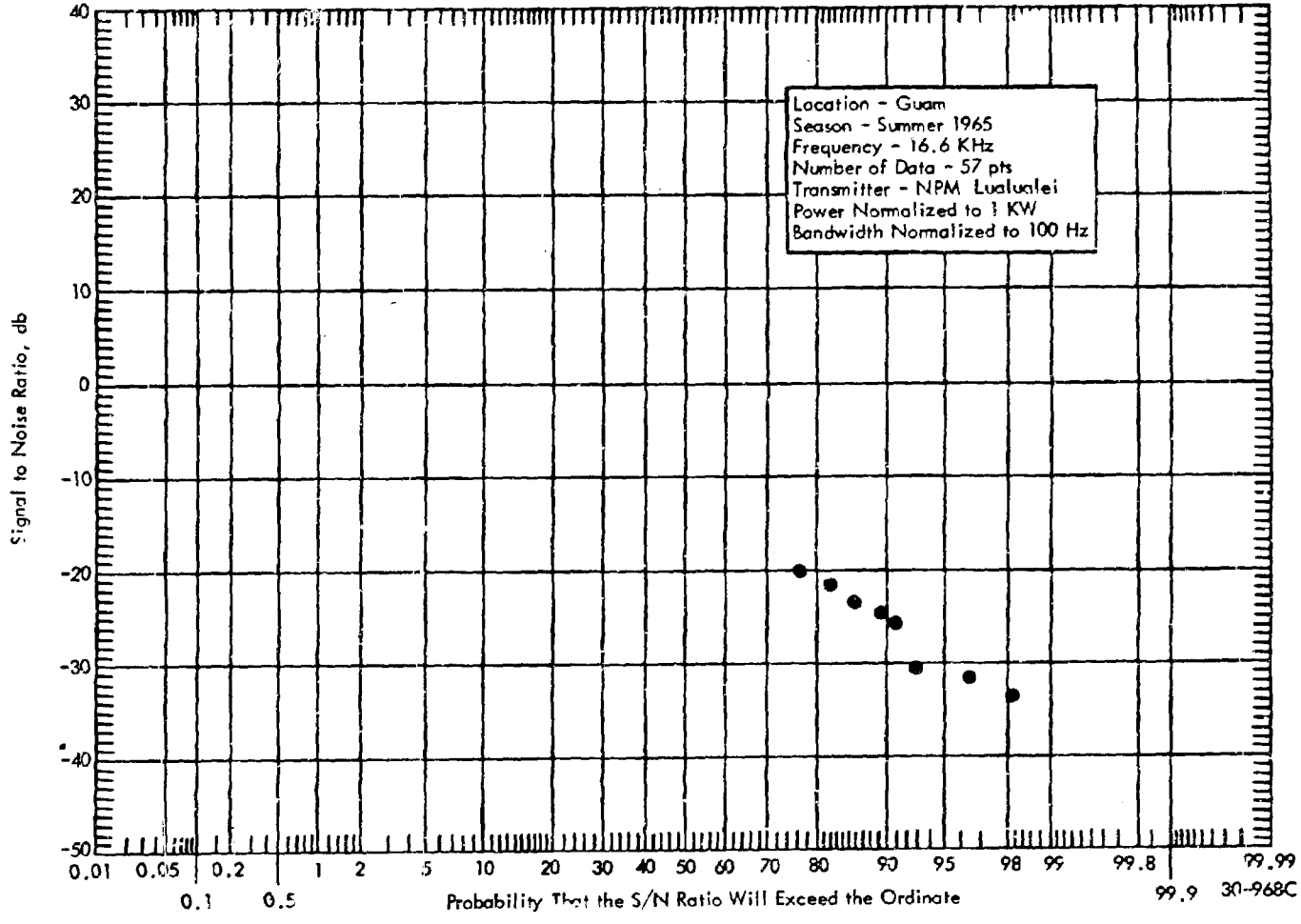

Figure 103 Cumulative Distribution of Measured Signal to Noise Ratio

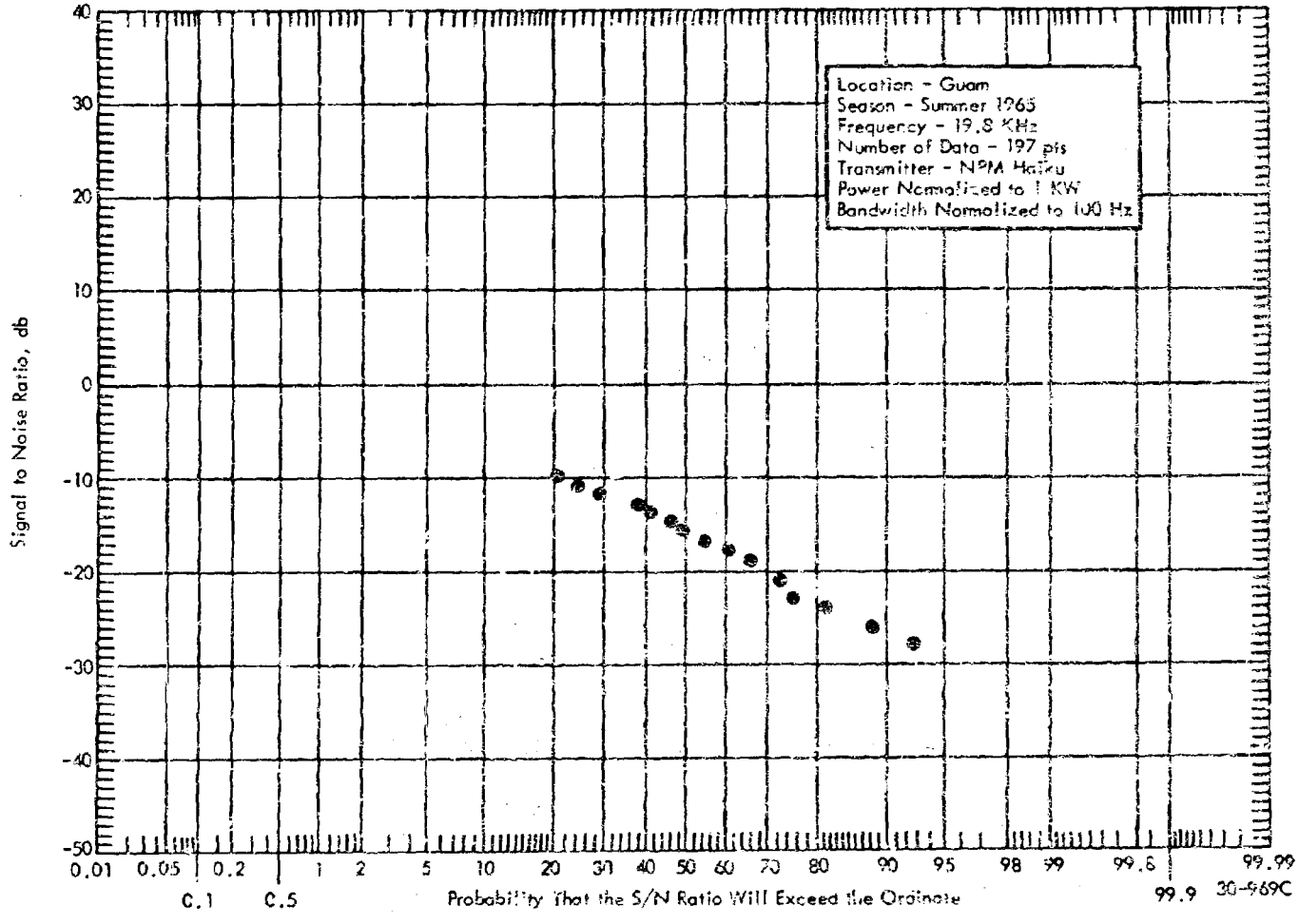

Figure 104 Cumulative Distribution of Measured Signal to Noise Ratio

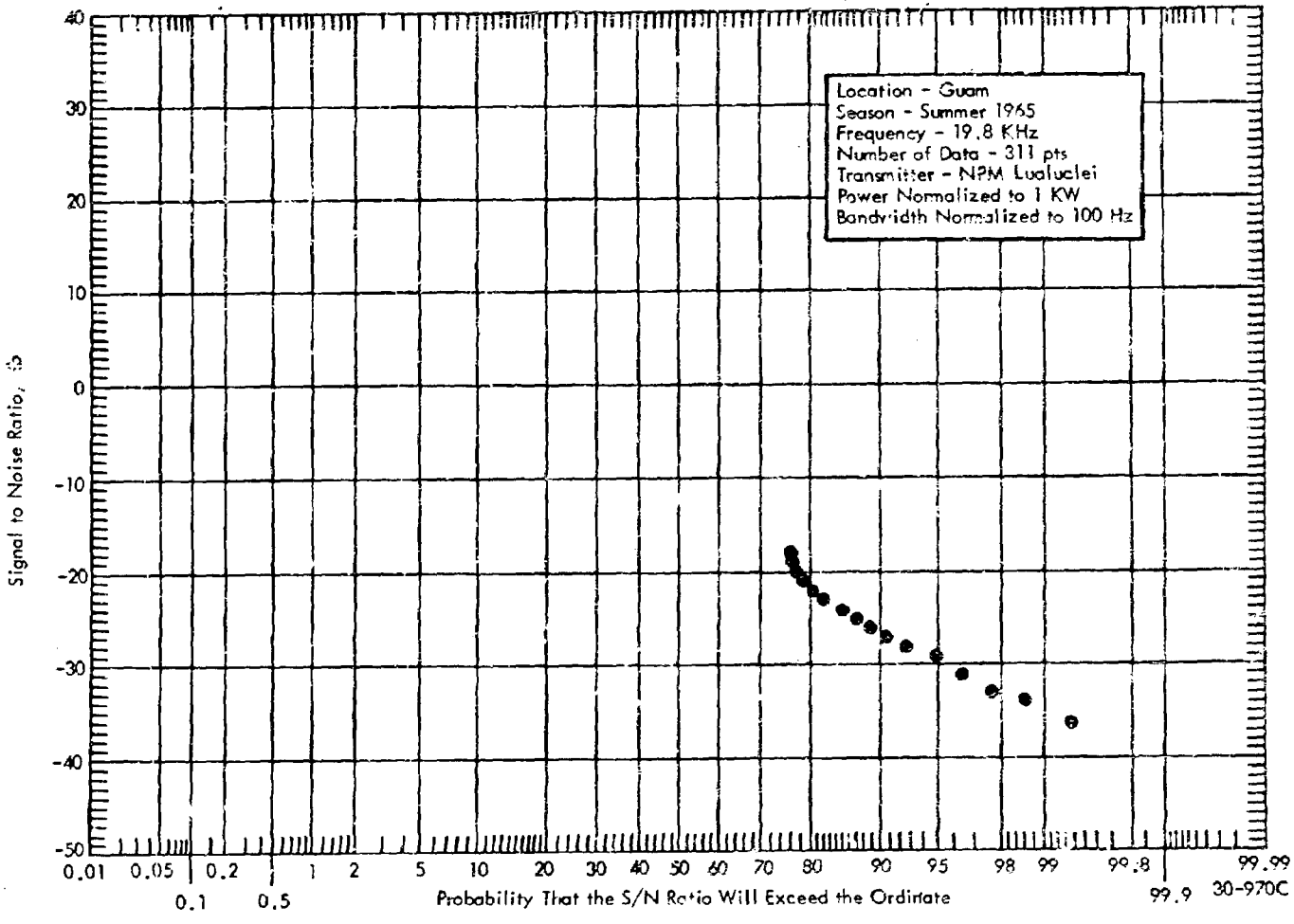

Figure 105 Cumulative Distribution of Measured Signal to Noise Ratio

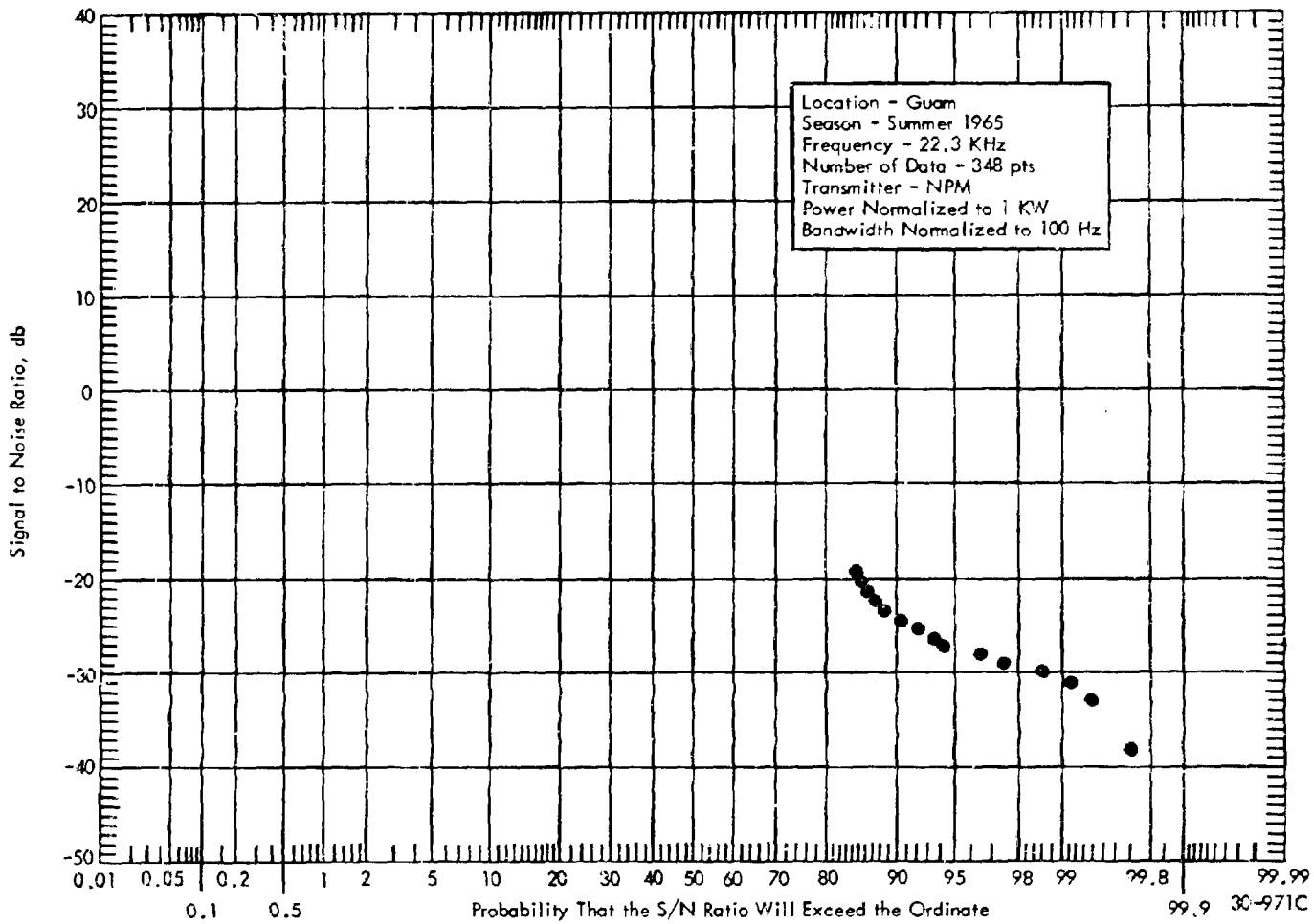

Figure 106 Cumulative Distribution of Meas ured Signal to Noise Ratio

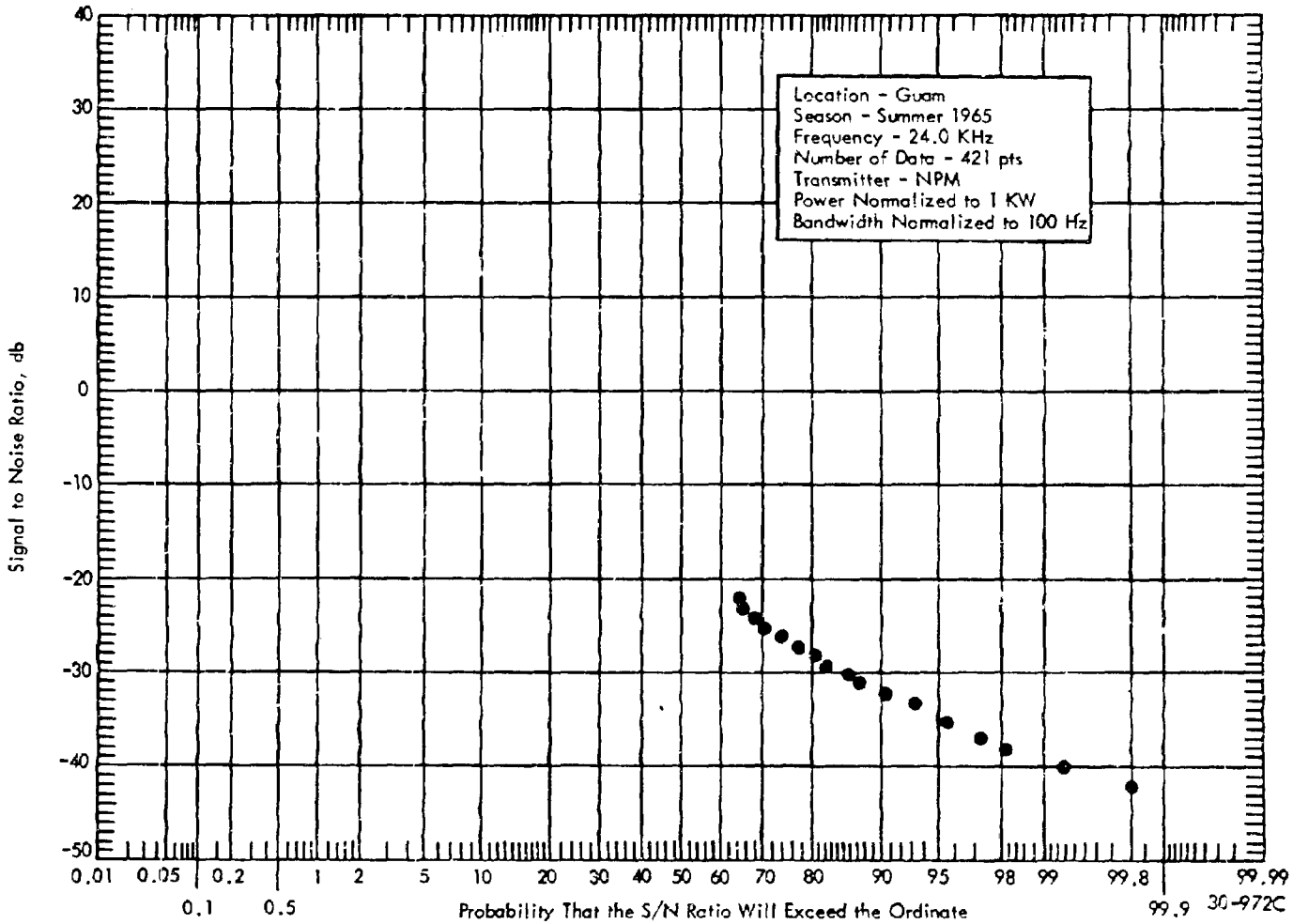

Figure 107 Cumulative Distribution of Measured Signal to Noise Ratio

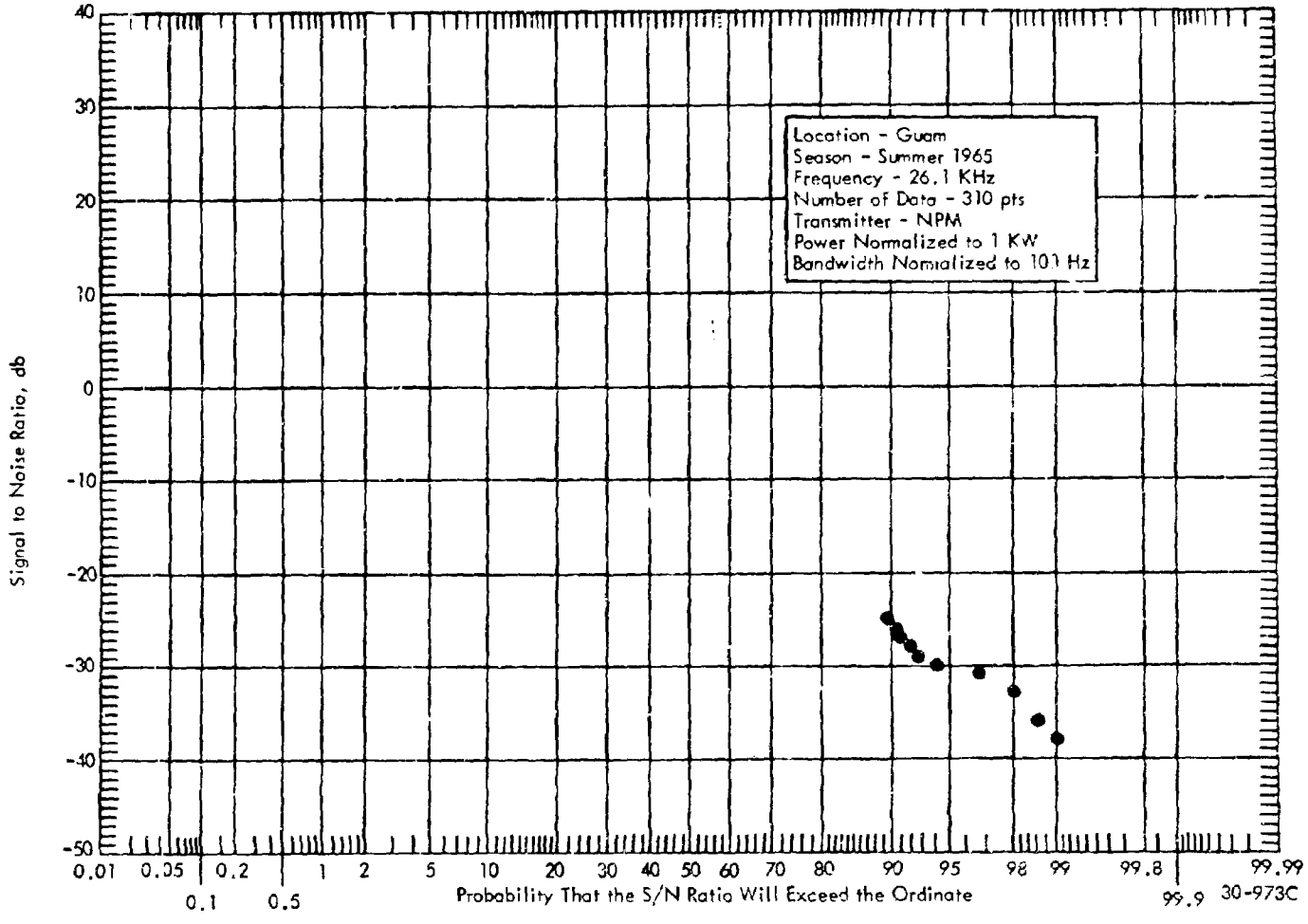

Figure 108 Cumulative Distribution of Measured Signal to Noise Ratio

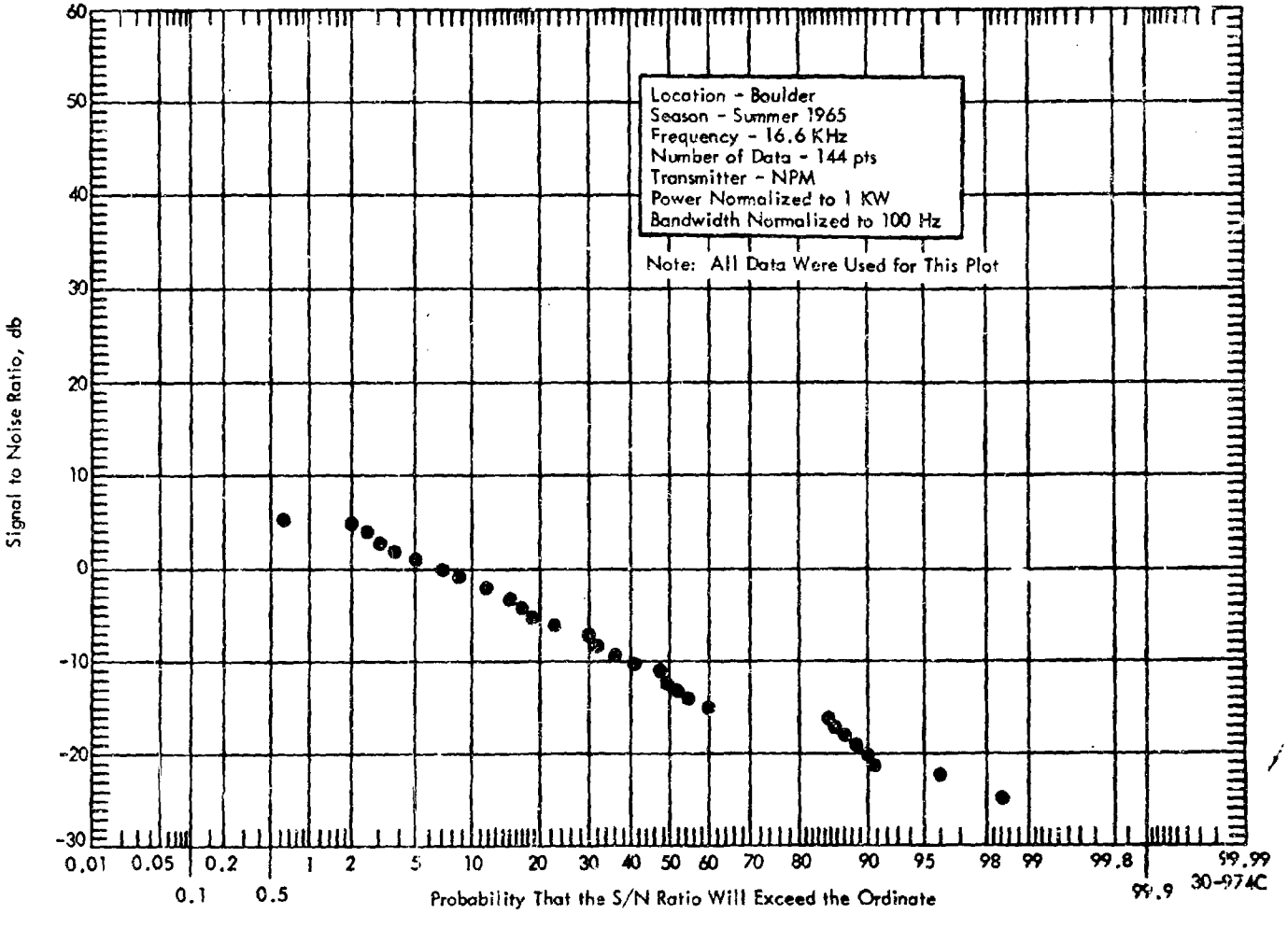

Figure 109 Cumulative Distribution of Measured Signal to Noise Ratio

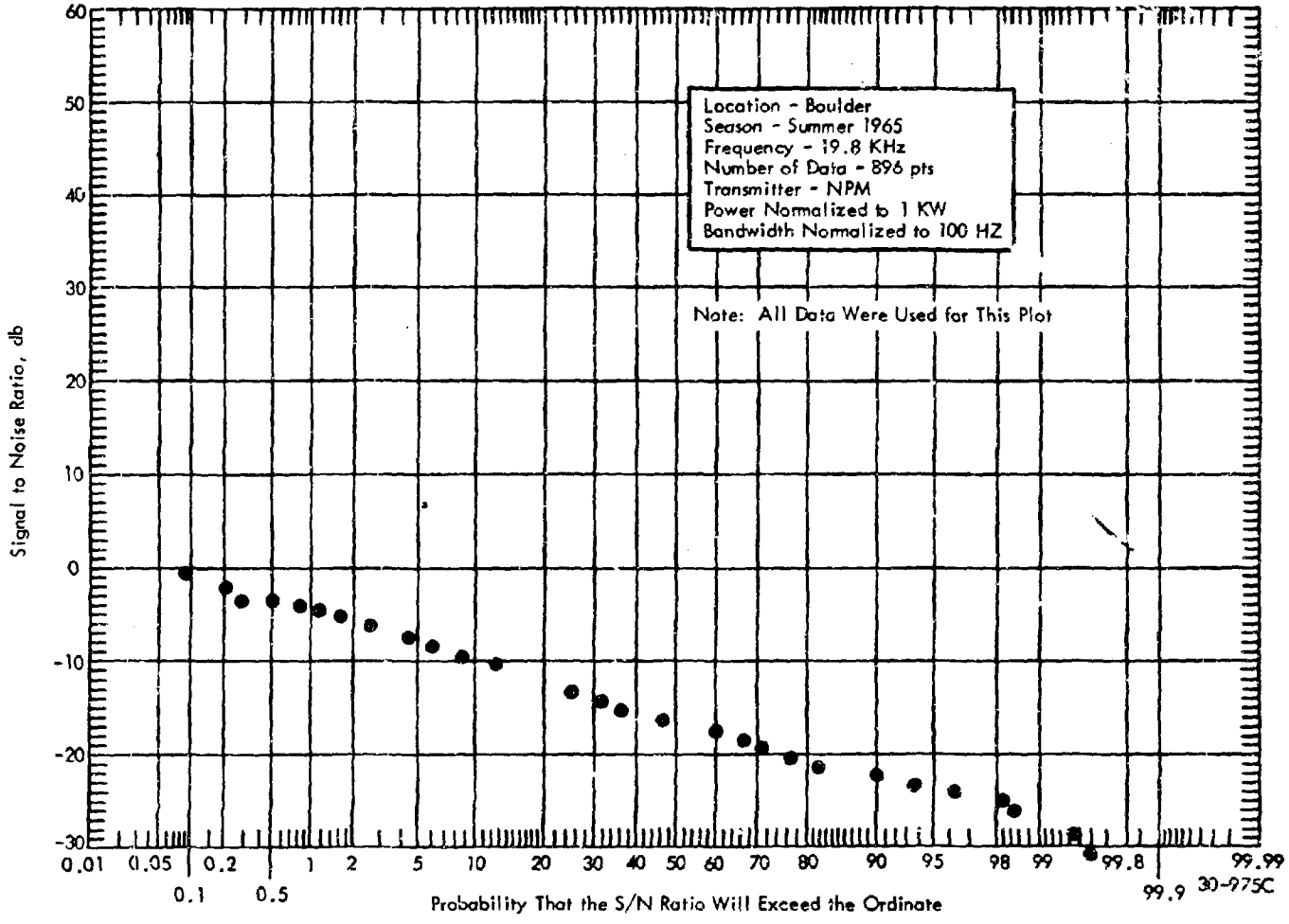

Figure 110 Cumulative Distribution of Measured Signal to Noise Ratio

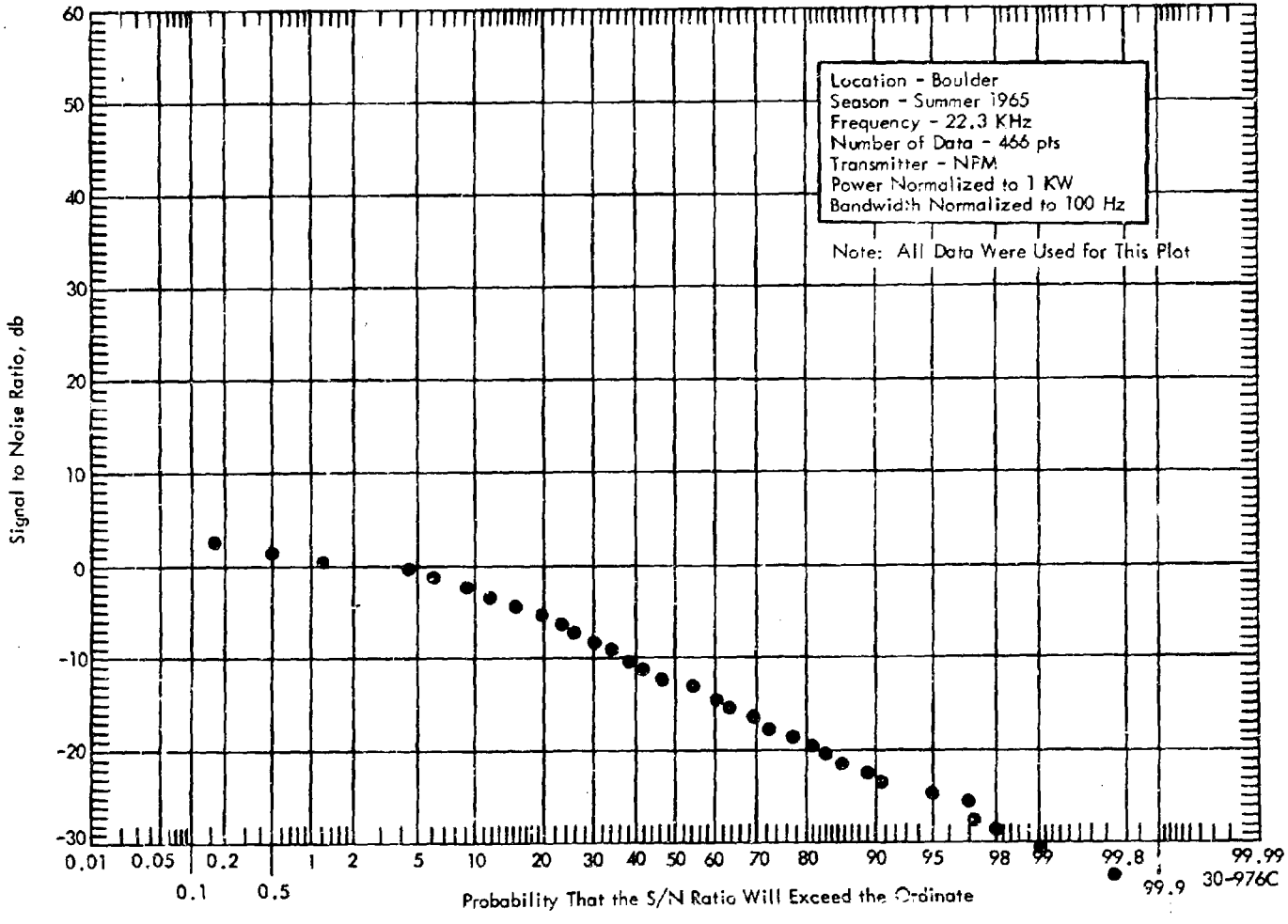

Figure 111 Cumulative Distribution of Measured Signal to Noise Ratio

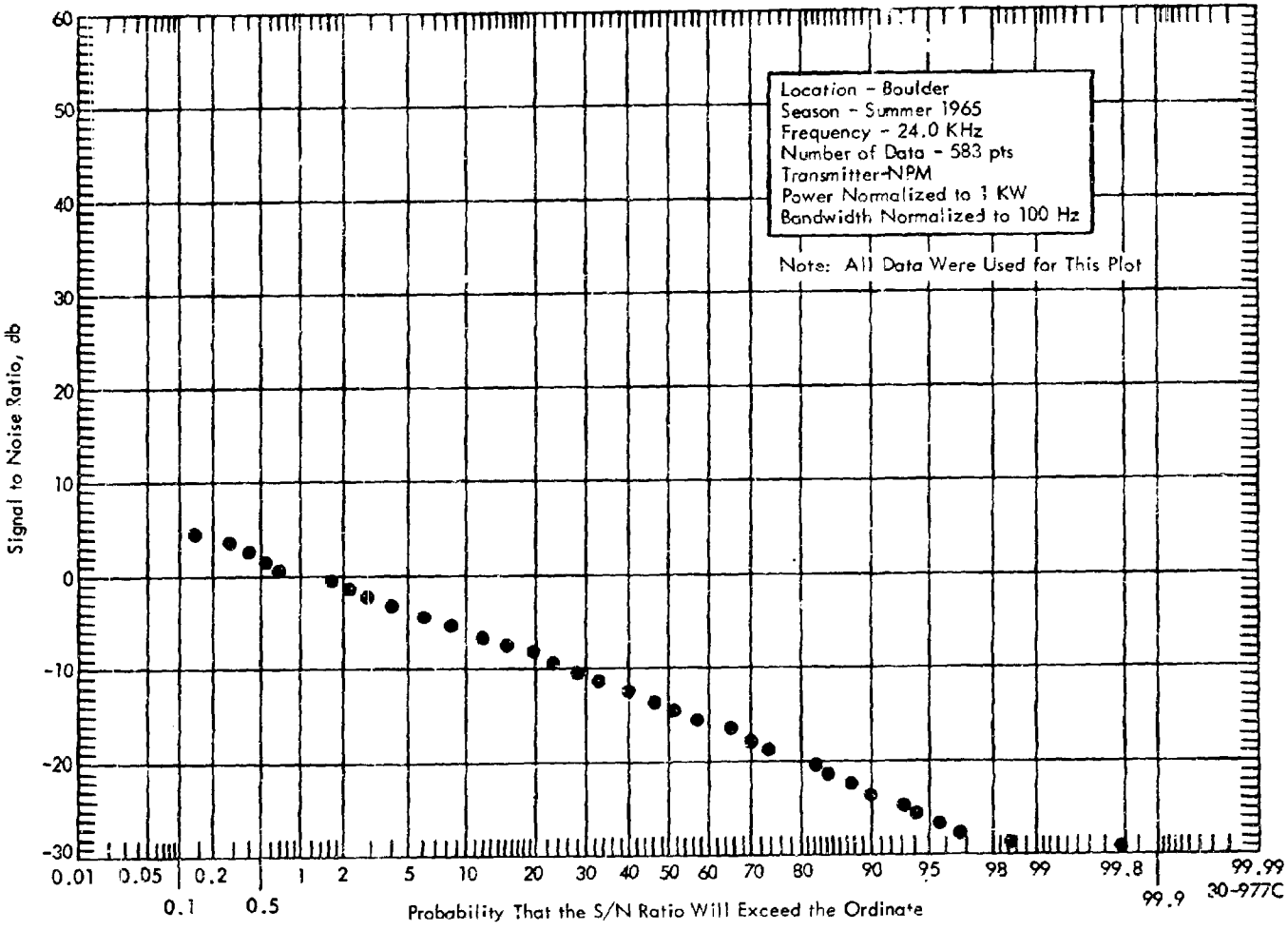

Figure 112 Cumulative Distribution of Measured Signal to Noise Ratio

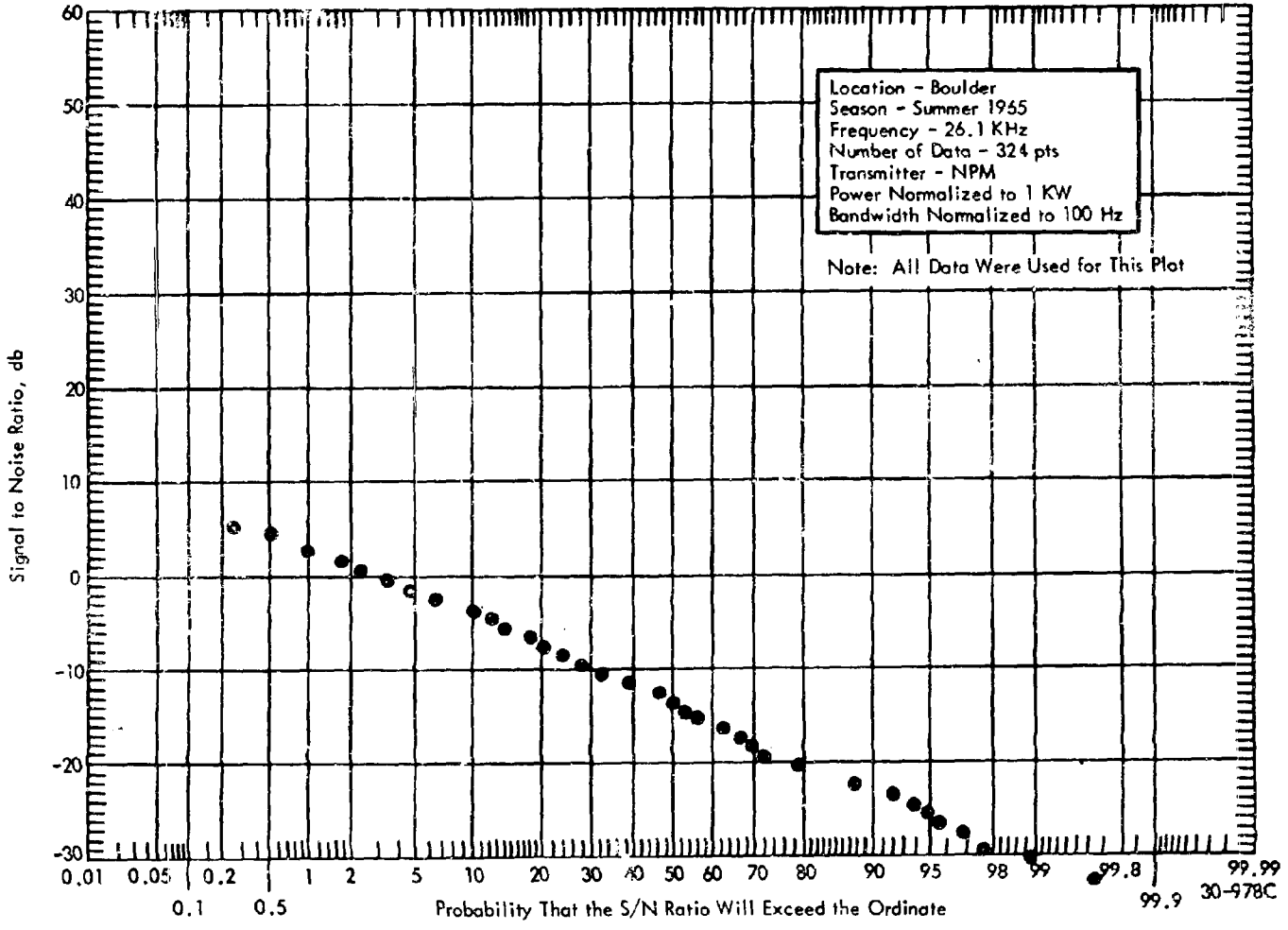

Figure 113 Cumulative Distribution of Measured Signal to Noise Ratio

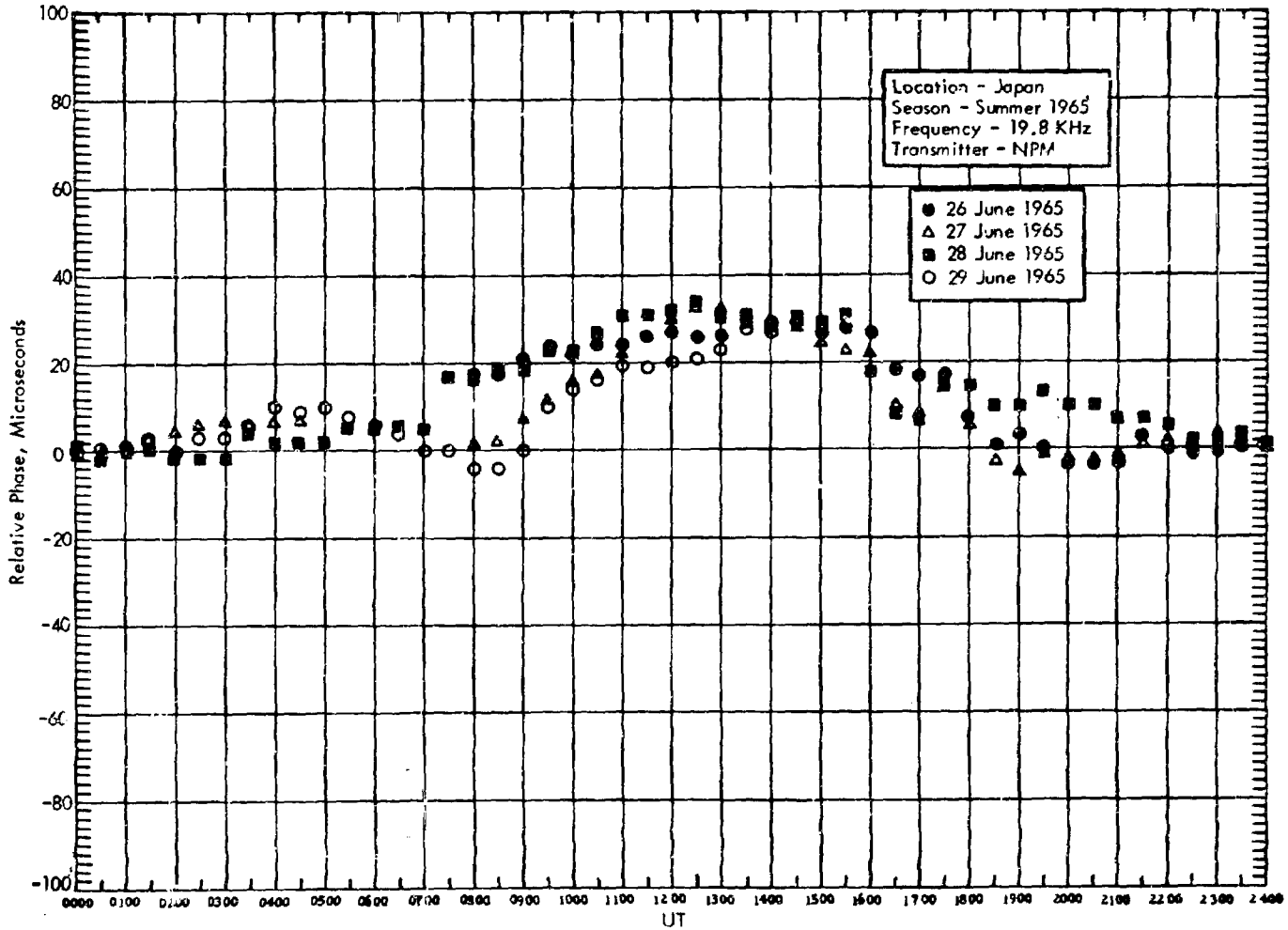

Figure 114 Diurnal Variation of Phase

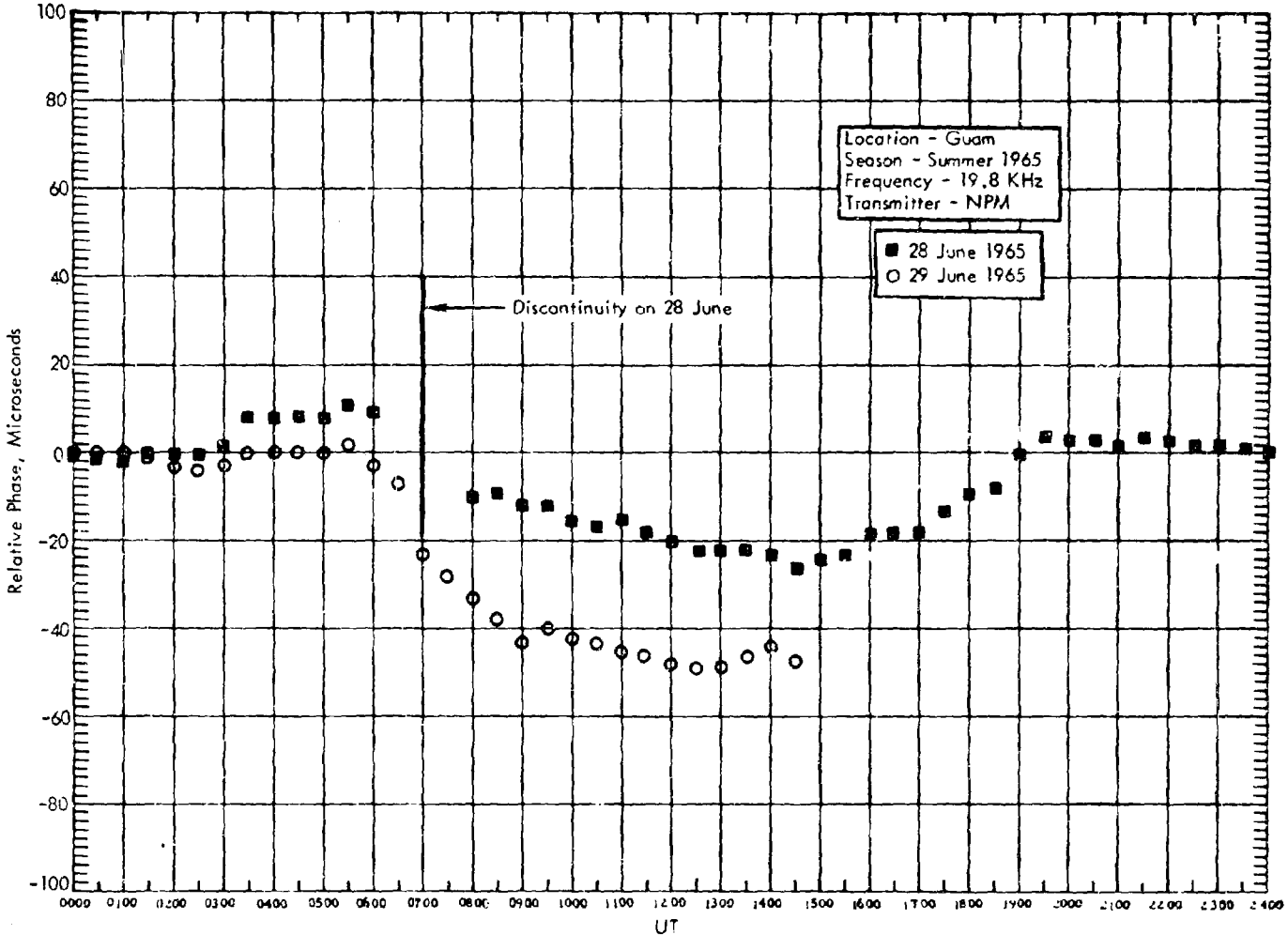

Figure 115 Diurnal Variation of Phase

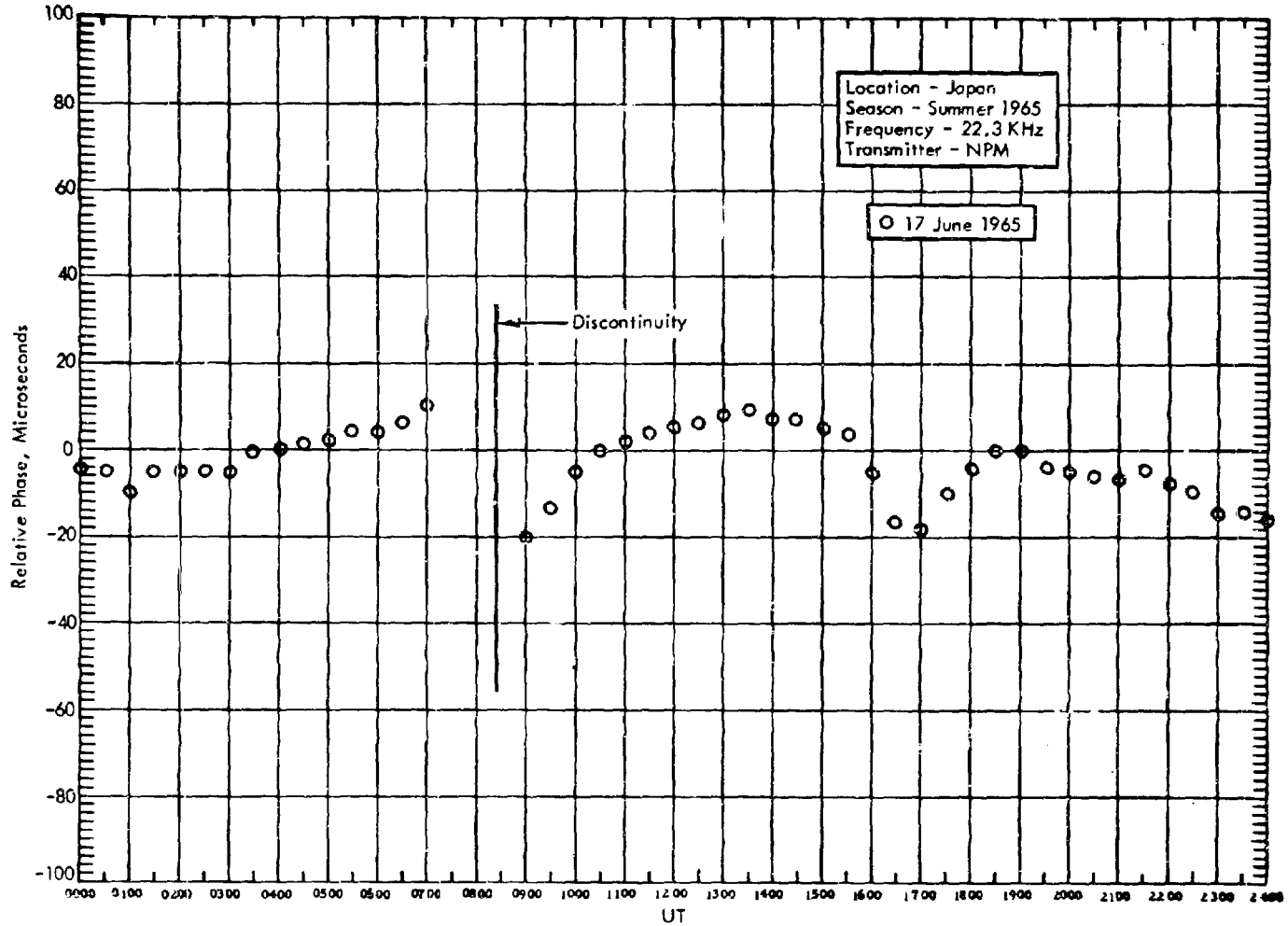

Figure 116 Diurnal Variation of Phase

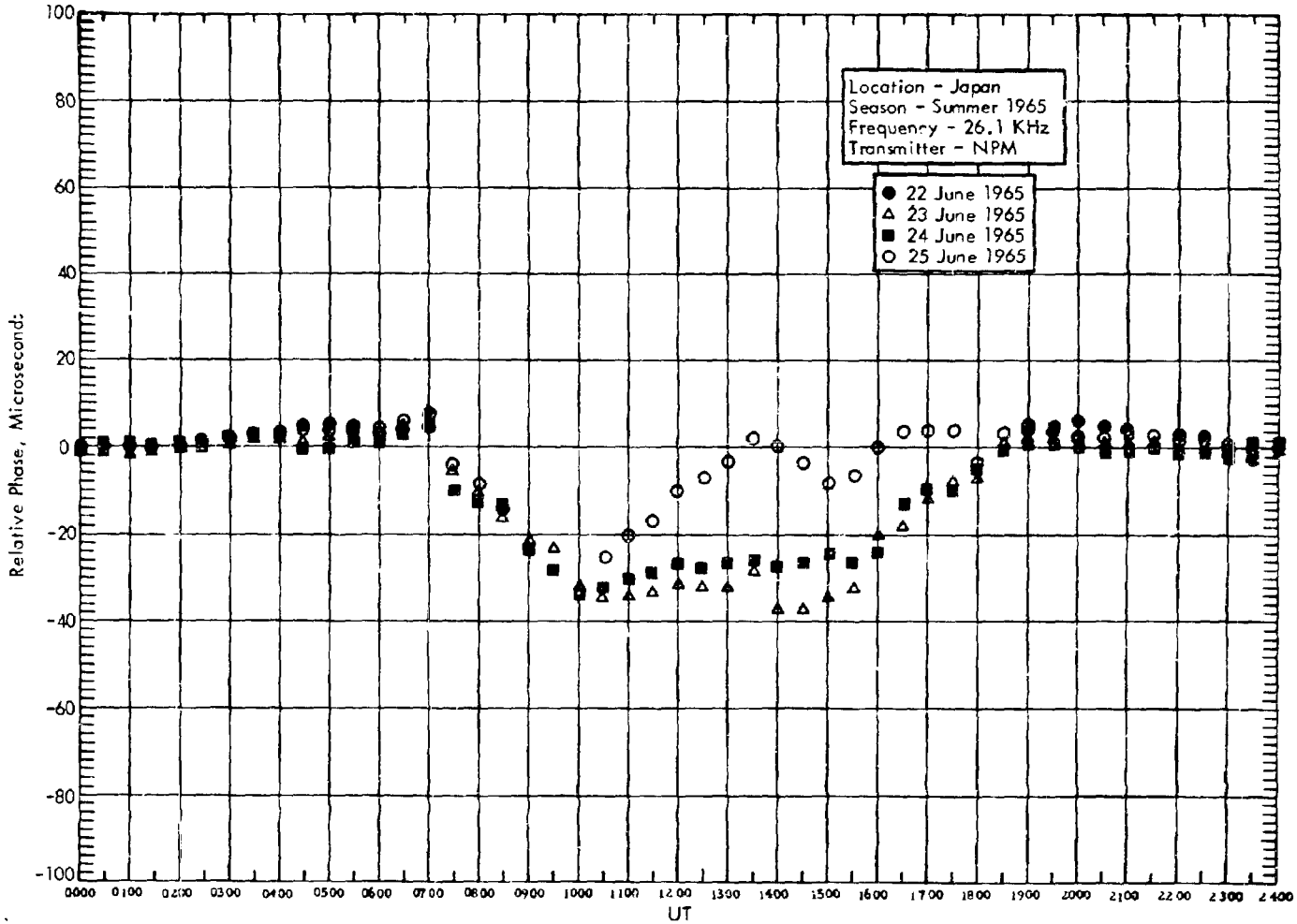

Figure 117 Diurnal Variation of Phase

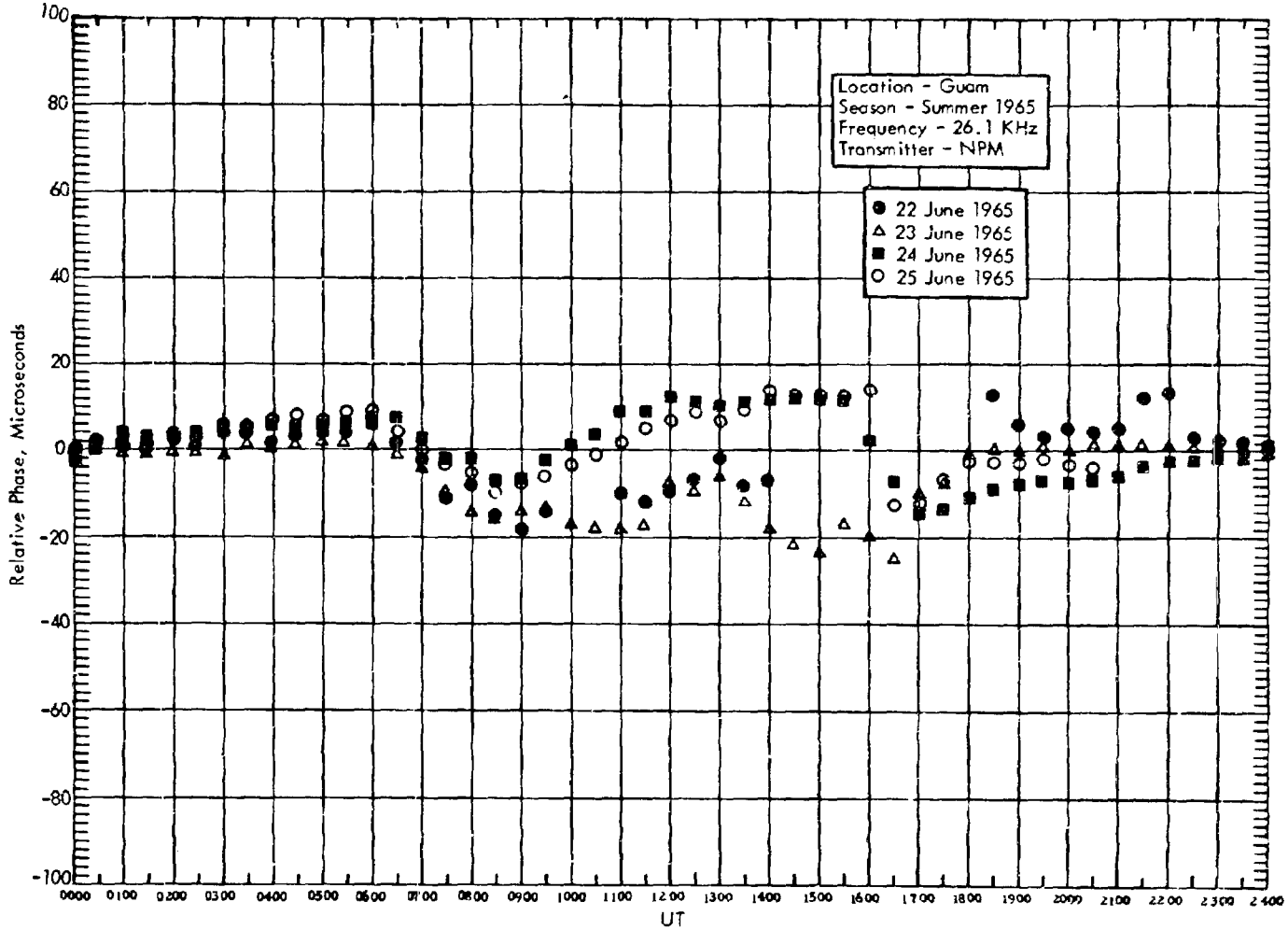

Figure 118 Diurnal Variation of Phase

APPENDIX A
INTERIM REPORT ERRATA

During the final analysis of the Pacific test data, a number of errors were discovered in the preliminary analysis. Compiled herein is an errata list which may be used to correct the interim reports (released during the summer of 1965).

I BOULDER

1. All of the signal and noise data must be raised by 1.5 db.
2. June 6 through June 9 (26.1 kHz) - subtract 9.7 db.

II GUAM

Due to the narrow bandwidth of the receiver used to measure field intensities of the signal and atmospheric noise field intensities at Guam, much of the noise data obtained at that site is inaccurate. It is suggested that all of the atmospheric noise levels for Guam which were given in the interim reports be considered suspect. The data which was accurate or suitable for correction has been re-tabulated and will be available along with all other tabulated data from the Bureau of Ships and the Naval Research Laboratory.

A. Data Changes

1. May 17 through May 20 (24.0 kHz) - subtract 20 db;
2. May 22 0100 hours (26.1 kHz) - subtract 1.5 db;
3. May 24 2100 hours (26.1 kHz) - subtract 10 db;
4. May 29 2330 through May 30 0300 hours (22.3 kHz) - add 10 db;
5. June 5 1630 through 1930 hours (24.0 kHz) - add 10 db;
6. June 8 2300 through 2400 hours (26.1 kHz) - add 10 db;
7. June 10 2200 hours (19.8 kHz) - add 4.5 db;
8. June 14 2200 hours (22.3 kHz) - add 2.0 db;

9. June 15 2200 hours (22.3 kHz) - add 3.5 db;
10. July 4 2300 hours (16.6 kHz) - add 2.0 db;
11. July 11 2200 hours (19.8 kHz) - subtract 6.0 db.

B. Data to be Deleted

1. May 18 2300 hours (24.0 kHz);
2. May 21 2400 hours (26.1 kHz);
3. May 24 0030 through 1030 and 2130 hours (26.1 kHz);
4. May 29 2200 and 2230 hours (22.3 kHz);
5. May 30 2300 hours (22.3 kHz);
6. June 4 2230 through June 5 0100 hours (24.0 kHz);
7. June 5 0300 and 0330 hours (24.0 kHz);
8. June 5 2000 through 2400 hours (24.0 kHz);
9. June 4 1800 through June 5 0400 hours (19.8 kHz);
10. June 7 0100 hours (26.1 kHz);
11. June 28 0400 hours (19.8 kHz).

III JAPAN

All of the Japan noise data except the Amplitude Probability Distributions as presented in the interim reports must be lowered by 10.1 db. The tables of signal data for Japan in the interim reports did not contain the measurements made on the half hour period. These tables have been re-tabulated and will be available, if needed from the Bureau of Ships and the Naval Research Laboratory.

A. Data Changes

1. May 17 through May 20 (24.0 kHz) - add 3.0 db;
2. May 17 through May 20 (19.8 kHz) - add 4.6 db;
3. May 21 through May 24 (26.1 kHz) - add 2.4 db;
4. May 21 through May 27 (19.8 kHz) - subtract 9.4 db;
5. May 25 through May 28 (24.0 kHz) - add 3.0 db;

6. May 29 through May 31 0600 hours (22.3 kHz) - add 3.6 db;
7. June 1 0300 hours (22.3 kHz) - add 10.0 db;
8. June 2 0700 through June 3 1800 hours (19.8 kHz) - add 3.0 db;
9. June 8 0900 through June 9 2400 hours (19.9 kHz) - subtract 8.0 db;
10. June 13 0100 through June 15 1200 hours (16.6 kHz) - subtract 10.0 db;
11. June 18 0200 through 0700 hours (24.0 kHz) - subtract 10.0 db;
12. June 18 0200 and 0900 hours (24.0 kHz) - subtract 20.0 db;
13. June 22 1900 through June 24 1000 hours (26.1 kHz) - subtract 10.0 db;
14. July 2 0000 hours (22.3 kHz) - add 10.0 db.

B. Data to be Deleted

1. May 28 0030 through June 2 0700 hours (19.8 kHz).

APPENDIX B

RADIATION RESISTANCE

Roland D. Croghan

During the period of time between June 4 and June 10, 1965, field strength measurements were taken on the transmitter signals from the Lualualei and Haiku Naval VLF Transmitters located on the Island of Oahu, Hawaii. The purpose of the measurements was to calculate the radiation resistance, as a function of frequency, of both the Lualualei and Haiku transmitters. All field strength measurements were taken so that the distance from the transmitter, d, was $\lambda/2 < d < 52$ km (this range is within the distance where the radiation fields vary inversely with distance over homogeneous ground of expected worst-case conductivity).

The actual sites of measurement are shown on Figure B-1. The majority of the sites shown were measuring sites used by NRL personnel in previous radiation resistance measurements. DECO Electronics duplicated the majority of these measuring locations; in addition, three new measuring sites were added.

During the measurements Haiku operated on the frequencies of 16.6 and 19.8 kHz. During normal operation a CW signal was transmitted at reduced power. At scheduled times the power was increased for three minutes followed by three minutes of off-time. Lualualei transmitted during this period on frequencies of 19.8, 24.0 and 26.1 kHz. Transmissions during normal operation were both ICW and FSK. At scheduled times a three minute CW signal was transmitted followed by three minutes of off-time.

The block diagram in Figure B-2 shows the measuring equipment used to measure the radiated component of the magnetic field. A loop was used with a calibration box followed by a tuning and amplifier section to

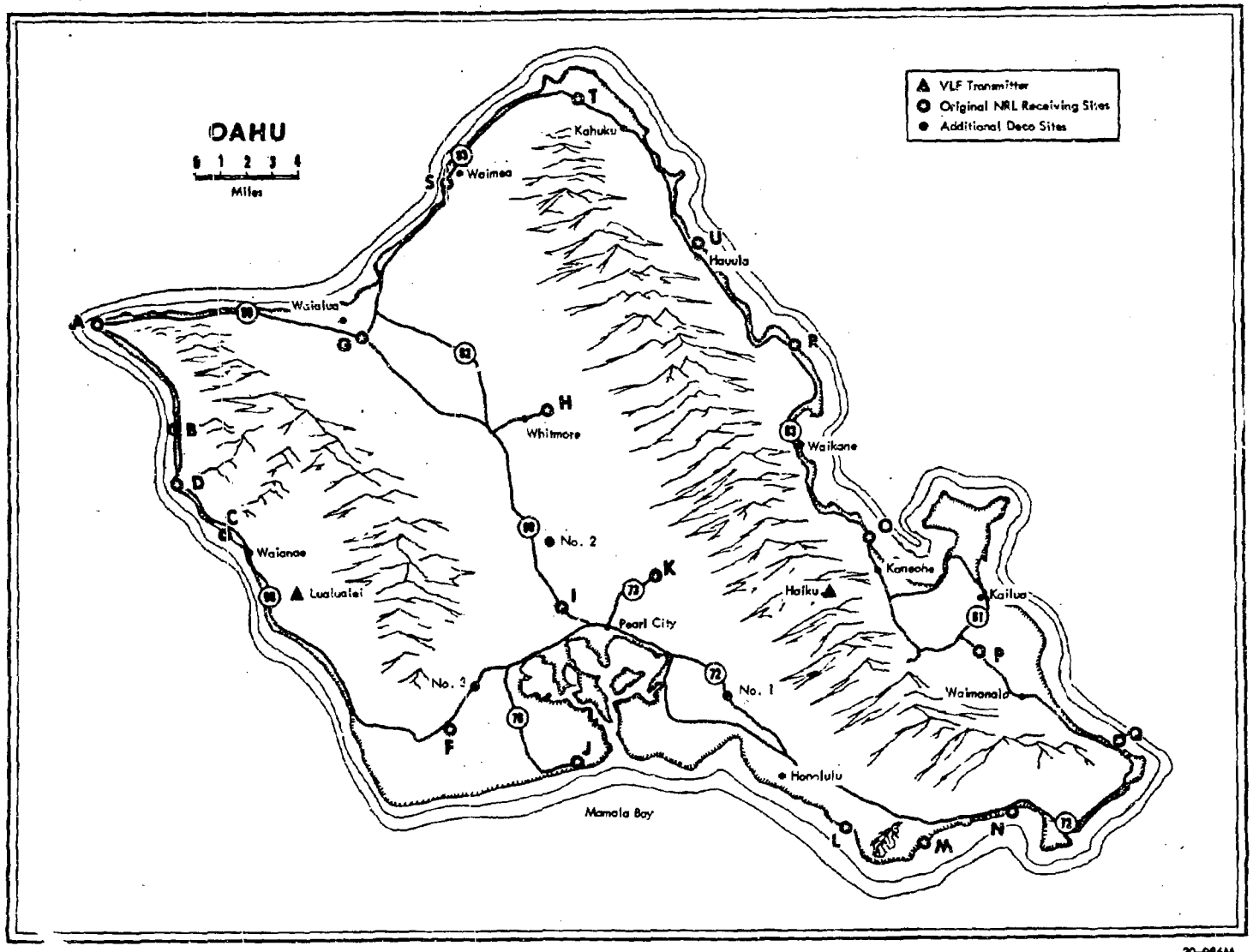

30-986M

Figure B-1 Measured Sites and VLF Transmitter Locations

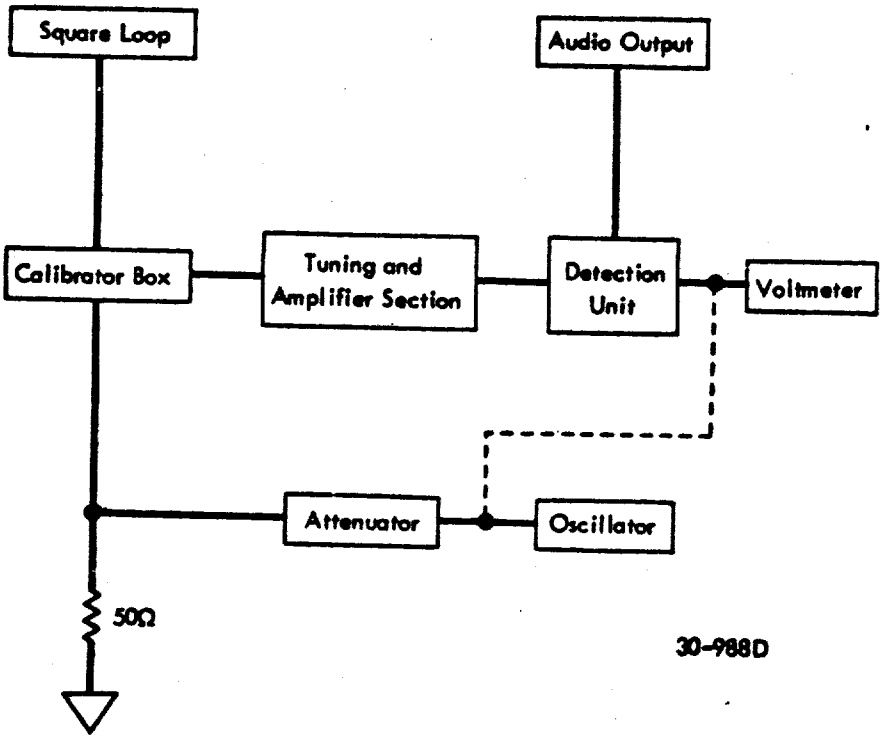

Figure B-2 Field Strength Measuring System

discriminate between the transmitted signals of Lualualei and Haiku. Additional tuning was provided in the detection unit along with two methods of detection. Besides a direct reading voltmeter, audio slide-back detection was available.

All measurements except two were taken when the transmitters were on CW transmission (the two were when Lualualei was on FSK). After tuning on the signal and maximizing the signal with the loop, an output voltage was read. During the off period a calibrated signal in db relative to 1 μv/m from the oscillator was injected to match the voltmeter reading. The resultant values of field strength are shown in Tables I and II respectively, for Lualualei and Haiku. The field strengths have been normalized to the indicated antenna currents. The data is also shown in Figures B-3 and B-4 where the field strength is plotted as a function of distance and frequency. The spread in the data as shown on the figures from an inverse distance line can be contibuted to the nonhomogeneity of the ground, causing ground impedance discontinuities which affects the magnitude of the field. The best inverse distance line fit to the data can be used with the following equation to derive the radiated power for the reference antenna current;

$$P_r \left| \text{db rel. 1 kw} \right| = E_g \left| \text{db rel. 1 } \mu\text{v/m} \right| - 109.5 + 20 \log d \left| \text{km} \right| . \quad \text{(B-1)}$$

The radiation resistance is then

$$R_r \left| \text{ohms} \right| = \frac{P_r}{I^2} \quad \frac{\left| \text{watts} \right|}{\left| \text{amperes}^2 \right|} \quad \text{(B-2)}$$

where I is the reference base antenna current. The resulting values of radiation resistance are shown in Table III.

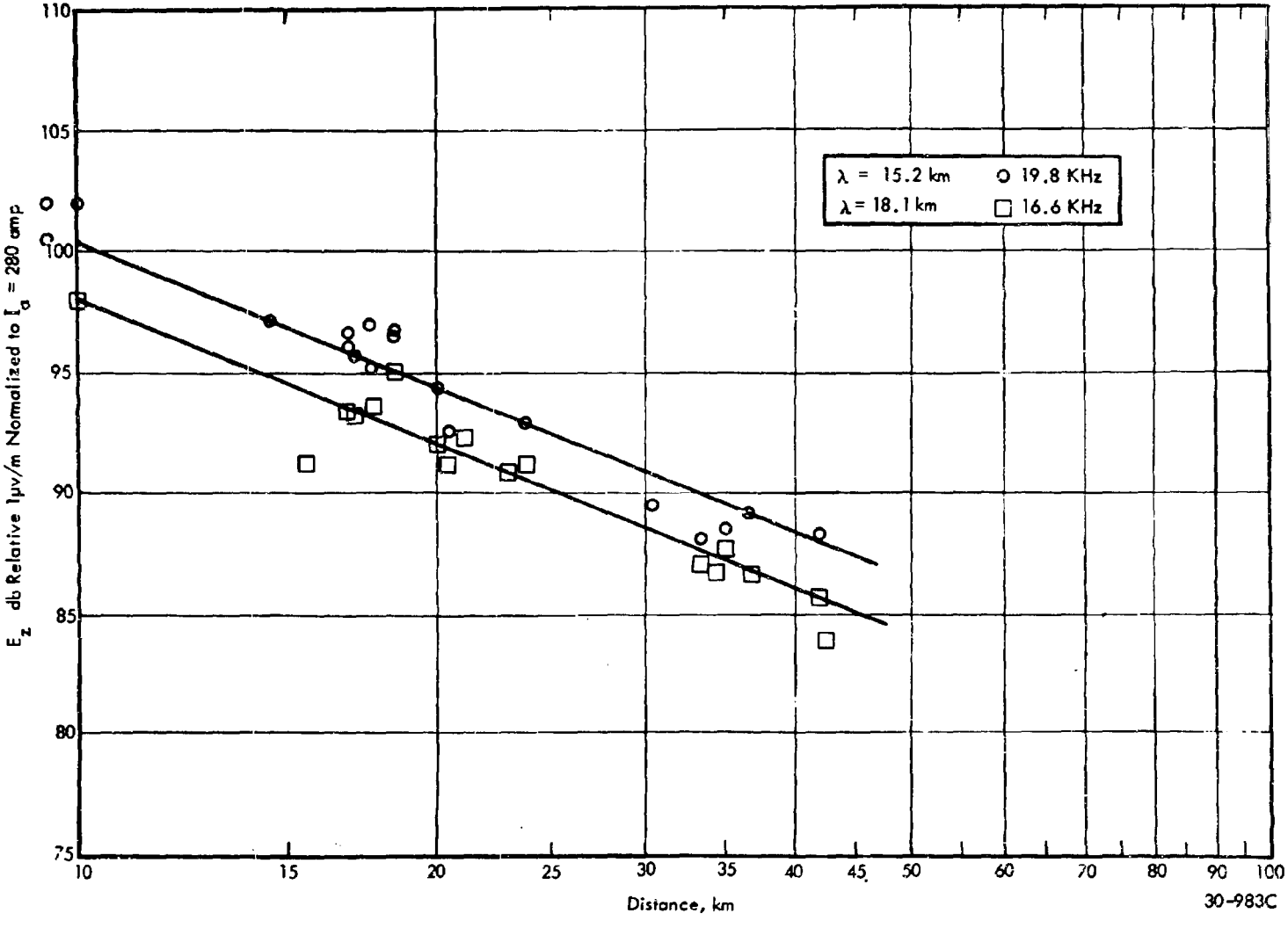

Figure B-3 Normalized Field Strengths of the Haiku Transmitter

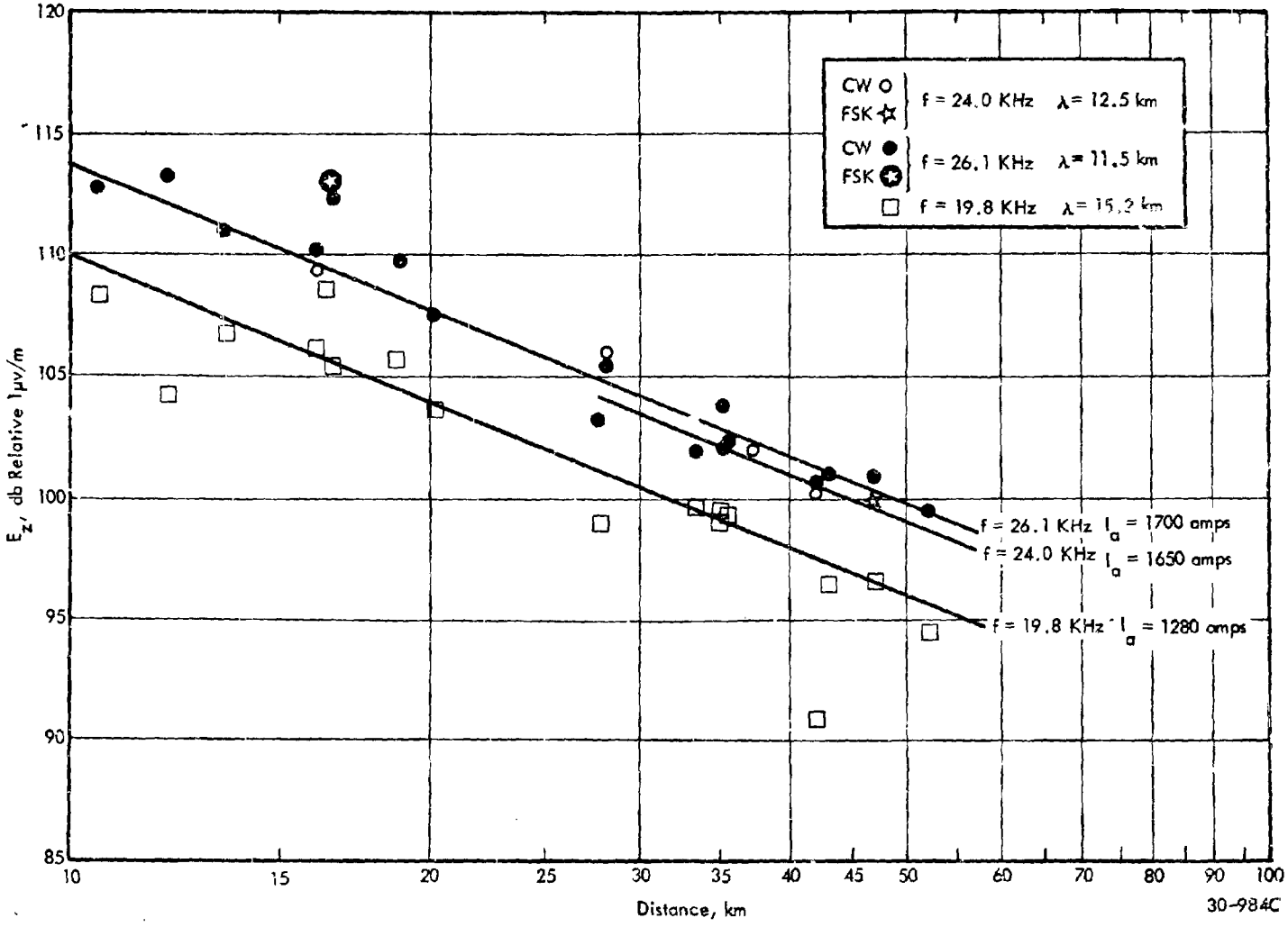

Figure B-4 Field Strength of the Lualualei Transmitter

TABLE I

LUALUALEI

Date 1965	Time † HT	Frequency kHz	Location	Distance km	Normalized Current Amperes	E_z, dB 1 μv/m
6/4	1225	24.0	1	28.0	1650	105.9
	1525	24.0	2	16.1		109.3
6/5	0955	24.0	L	37.0		101.9
	1137	24.0	M	42.0		100.2
	1318	24.0	N	47.0		99.8
	1553	26.1	O	52.0	1700	99.5
	1623	26.1	N	47.0		100.9
	1727	26.1	M	42.0		100.6
6/6	1731	26.1	J	20.1		107.5
	1926	26.1	I	16.6		112.4
6/7	0856	26.1	2	16.1		110.1
	0924	26.1	H	18.8		109.7
	0956	26.1	G	16.4		112.9
	1055	26.1	S	27.8		103.2
	1126	26.1	T	35.4		102.3
	1155	26.1	U	33.3		101.8
	1354	26.1	R	35.0		102.0
	1455	26.1	Q	35.1		103.8
	1526	26.1	P	42.8		101.0
6/9	0854	26.1	1	28.0		105.4
	0958	26.1	3	12.1		113.2
	1255	26.1	D	10.6		112.7
	1324	26.1	B	13.4		110.9
	1530	19.8	B	13.4	1280	106.6
	1555	19.8	D	10.6		108.1
	1651	19.8	C (1 mi east)	6.0		111.6
	1753	19.8	3	12.1		104.2
	1857	19.8	J	20.1		103.5
6/10	0857	19.8	I	16.6		105.3
	0929	19.8	2	16.1		106.1
	0956	19.8	H	18.8		105.6
	1055	19.8	G	16.4		108.5
	1128	19.8	S	27.8		98.9
	1159	19.8	T	35.4		99.3
	1256	19.8	U	33.3		99.6
	1330	19.8	R	35.0		99.4
	1457	19.8	Q	35.1		98.9
	1529	19.8	P	42.8		96.4
	1556	19.8	O	52.0		94.4
	1658	19.8	N	47.0		96.6
	1729	19.8	M	42.0		90.0

† For GMT Time, add 10 hours.

TABLE II

HAIKU

Date 1965	Time † HT	Frequency kHz	Location	Distance km	Normalized Current Amperes	E_z, dB 1 μv/m
6/4	1136	19.8	1	9.4	280	101.9
	1455	19.8	2	18.5		96.8
6/5	1032	19.8	L	14.5		97.2
	1203	19.8	M	16.9		96.7
	1325	19.8	N	17.7		96.9
	1440	19.8	O	20.4		92.5
	1628	19.8	N	17.7		95.1
	1723	19.8	M	16.9		96.0
6/6	1612	19.8	F 1.4 mi. Wjunc	30.3		89.5
	1738	19.8	J	20.0		94.3
	1915	19.8	I	17.1		95.6
6/7	0815	19.8	2	18.5		96.5
	1006	19.8	G	33.3		88.1
	1033	19.8	S	35.0		88.6
	1115	19.8	T	34.4		
	1159	19.8	U	23.0		
	1330	19.8	R	15.6		
	1443	19.8	Q	3.7		107.8
	1530	19.8	P	10.0		101.9
6/9	0835	19.8	1	9.4		100.5
	0951	19.8	3	23.8		93.0
	1151	19.8	C 1 mi. east	36.7		88.6
	1234	19.8	D	41.9		88.3
	1544	16.6	B	42.4	280	83.9
	1606	16.6	D	41.9		85.7
	1656	16.6	C 1 mi. east	36.7		86.6
	1743	16.6	3	23.8		91.2
	1820	16.6	J	20.0		92.0
6/10	0817	16.6	I	17.1		93.2
	0916	16.6	2	18.5		95.0
	1001	16.6	H	21.1		92.3
	1035	16.6	G	33.3		87.1
	1134	16.6	S	35.0		87.1
	1201	16.6	T	34.4		86.7
	1259	16.6	U	23.0		90.9
	1321	16.6	R	15.6		91.2
	1440	16.6	Q	3.7		106.4
	1533	16.6	P	10.0		98.0
	1600	16.6	O	20.4		91.2
	1701	16.6	N	17.7		93.5
	1721	16.6	M	16.9		93.3

† For GMT Time, add 10 hours.

It should be noted that very few data points are available for 24 kHz, so R_r should not be weighted as heavy as the 19.8 and 26.1 kHz data. The above data were supplied to NRL to average with their measurements for determining the average effective height. The effective height of the antennas as a function of radiation resistance is:

$$h_e = \frac{\lambda_o}{\pi} \left(\frac{R_r}{160} \right)^{1/2} \qquad \text{(B-3)}$$

where h_e is the effective height in meters and λ_o is the wavelength in meters.

TABLE III

Station	Frequency kHz	Radiation Resistance ohms
Lualualei	19.8	0.068
	24.0	0.082
	26.1	0.0914
Haiku	16.6	0.119
	19.8	0.161

APPENDIX C

METHODS OF DATA REDUCTION

Donald L. Stone

The initial data from each of the three receiver stations was reduced differently due to the difference in the receiving equipment used. The signal data taken at Boulder, using the URM-6, was contaminated with atmospheric noise when the signal-to-noise-ratio was low. The Tracor receiver which was used in Japan had a bandwidth narrow enough that an uncontaminated signal amplitude was measured. The noise data from Japan was obtained with a HP 302-A receiver in connection with an automatic frequency selecting instrument. The data taken in Guam with the HP 302-A was similar to the URM-6 data and was reduced in the same manner.

All of the scaled data was punched onto tabulating cards for computer processing. All of the field intensities, means, medians, standard deviations and probabilities were computed by a CDC 3600 digital computer and plotted on a EAI 3440 Data Plotter with the exception of the Guam signal-to-noise-ratios and the phase plots. The formulas used are discussed in the following sections.

SIGNAL

All data was scaled from the EA strip charts in db relative to 1 microvolt. The contaminated signal data was first converted to microvolts and the signal computed by the following formula:

$$E_s = \sqrt{E_{sn}^2 - E_n^2} \qquad \text{(C-1)}$$

where:

E_s is the signal in μv,

E_{sn} is the contaminated signal in μv, and

E_n is the noise in μv.

The signal was then converted to db relative to 1 μv and the field intensity computed by the following:

$$E_s' = E_s + K_1 \qquad \text{(C-2)}$$

where:

E_s' is the signal field intensity in db relative to 1 μv/m,

E_s is the signal in db relative to 1 μv, and

K_1 is a constant including effective height.

NOISE

The noise field intensity was computed by the following:

$$E_n' = E_n + K_2 \qquad \text{(C-3)}$$

where:

E_n' is the noise field intensity in db realtive to 1 μv/m for a specified bandwidth,

E_n is the average noise in db relative to 1 μv, and

K_2 is a constant which included the effective height, bandwidth factors, and average to rms conversion factor.

SIGNAL-TO-NOISE-RATIO

The signal-to-noise-ratios for Boulder and Guam were computed by the following:

$$S/N = E_s' - E_n' \qquad \text{(C-4)}$$

where:

S/N is the signal-to-noise-ratio in db for the specified bandwidth.

Since the automatic noise equipment at Japan did not measure the atmospheric noise at the same frequencies as the signal transmissions, an interpolated noise level was used to compute the signal-to-noise-ratios. For example, the noise level for 16.6 kHz was linearly interpolated from the values of noise measured at 10 kHz and 20 kHz. To minimize the error of this method, the only noise data used was that taken within 1/2 hour of the particular signal measurement and a separate interpolated noise value was used for each signal measurement.

MEDIANS

To compute the median of an array of data the array was first numerically ordered. (An array of data was defined as any group of signal data, noise data, etc.) The median value of the array was then defined as follows, if N, the number of data, was odd

$$\text{median} = X_{(N+1)/2} \qquad \text{(C-5)}$$

however if N was even

$$\text{median} = \frac{X_{N/2} + X_{N/2+1}}{2} \qquad \text{(C-6)}$$

where:

X is an element of the array.

STANDARD DEVIATIONS

To compute the standard deviation of an array of data the arithmetic mean of the voltage (not the log of the voltage) must be computed using the equation

$$\bar{X} = \frac{1}{N} \sum_{i=1}^{N} X_i \qquad \text{(C-7)}$$

where:

$\bar{X}$ is the mean,

X_i is an element of the array,

N is the total number of elements,

$i = 1, 2, 3 \ldots\ldots N.$

The standard deviation was then computed using

$$\sigma^2 = \sum_{i=1}^{N} (X_i - \bar{X})^2 \qquad \text{(C-8)}$$

where:

σ is the standard deviation, and the other symbols as defined above expressed in db.

CUMULATIVE PROBABILITY DISTRIBUTIONS

To compute the probability that a given level was exceeded in an array of data, the array was first numerically ordered. The probability for a given level was then computed using

$$P_i = \frac{100\,(N - K_i)}{N + 1} \qquad \text{(C-9)}$$

where:

P_i is the probability, in percent, for the ith db level,

K_i is the number of elements of the array that have a magnitude less than the ith db level, and

N is the total number of elements in the array.

Since the noise measurements in Guam were generally inaccurate for large S/N ratios, it was impossible to accurately establish signal-to-noise-ratios greater than 20 db in a 7 Hz bandwidth. For ratios less than 20 db, cumulative probability distributions were manually computed and plotted using equation C-9.

One of the more important aspects of the data reduction was the elimination of bad data. Any data or calibration which was suspect for any reason was thrown out. Calibrations were made in the field with several antennas and instruments a number of times during the measurement period. Some of the equipment was also calibrated upon its return to Boulder. The excellent agreement of these many checks, and the elimination of data when there was not agreement, has given us high confidence in the results from this program.

APPENDIX D

CALCULATION OF FIELD STRENGTH VS. DISTANCE

Garner and Rhoads of NRL computed the variation of field strength with distance from 0.5 to 10.0 megameters, taking into account the 1st, 2nd and 3rd order waveguide modes for all distances. This was done for ionosphere heights of 70 and 90 km. Figures D-1 to D-4 present the results of their computations for the frequencies 19.8, 22.3, 24.0 and 26.1 kHz. These figures are included for comparison with the measured fields and are discussed in Section 4.1.

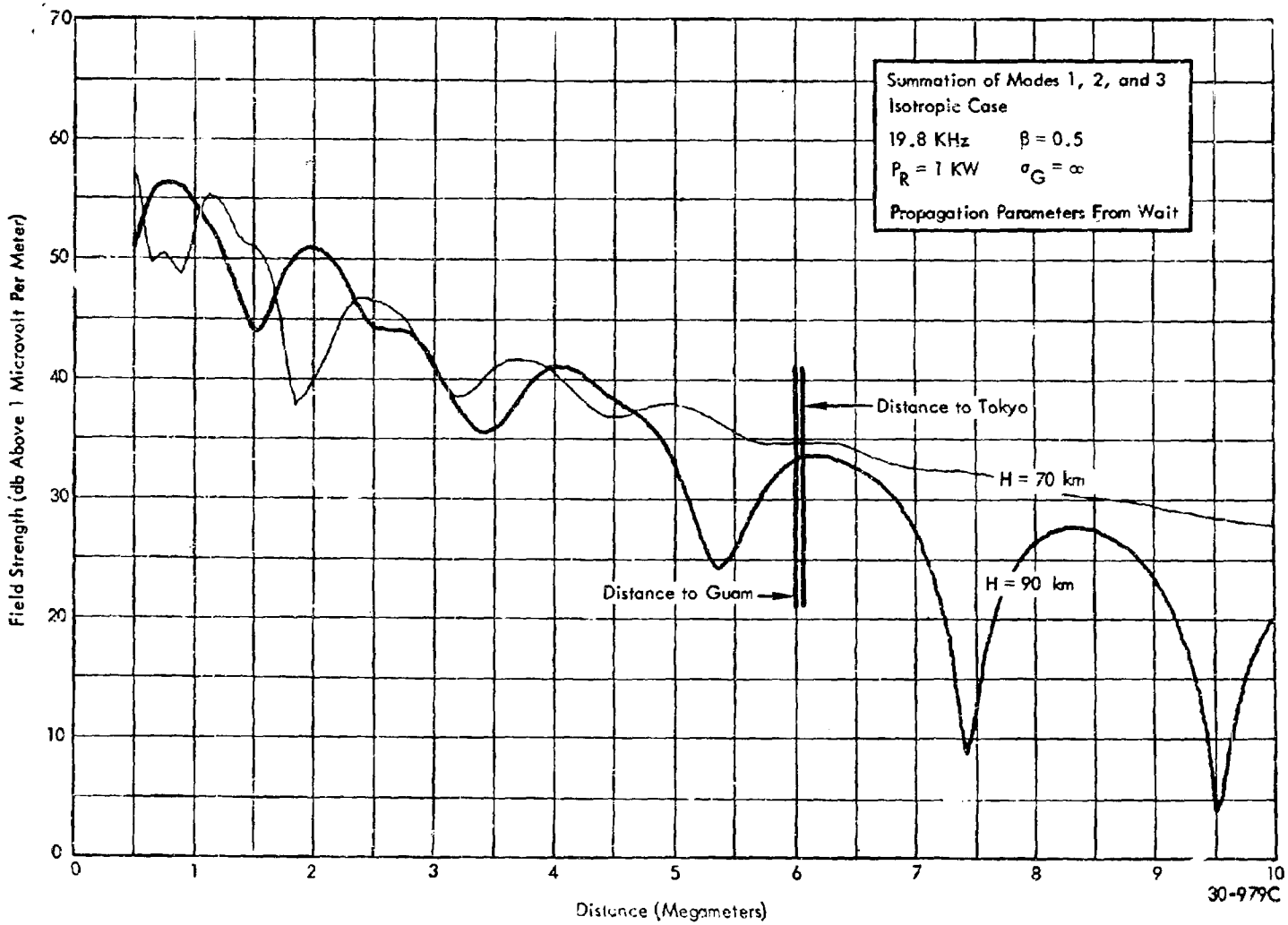

Figure D-1 Computed Field Strength

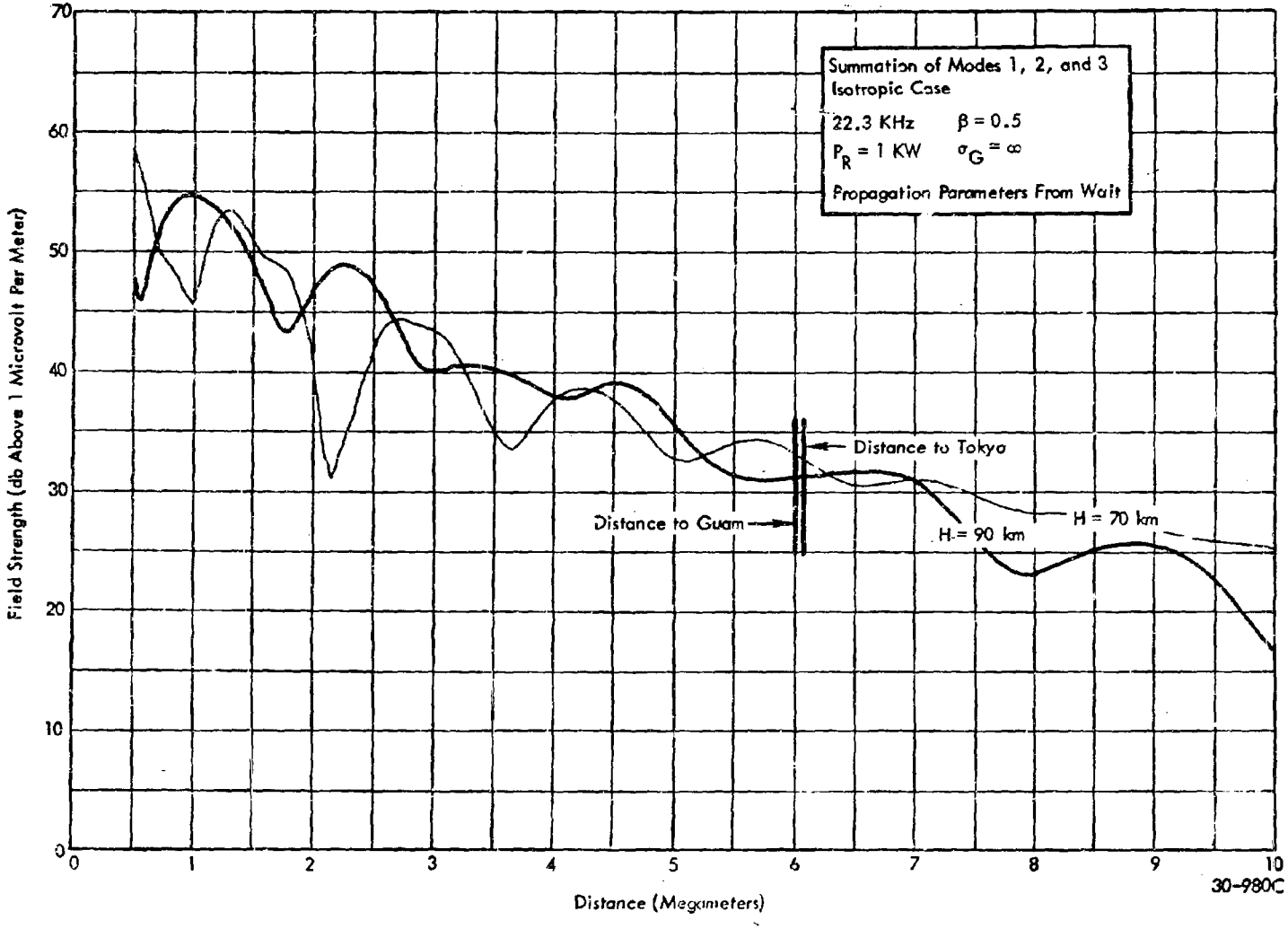

Figure D-2 Computed Field Strength

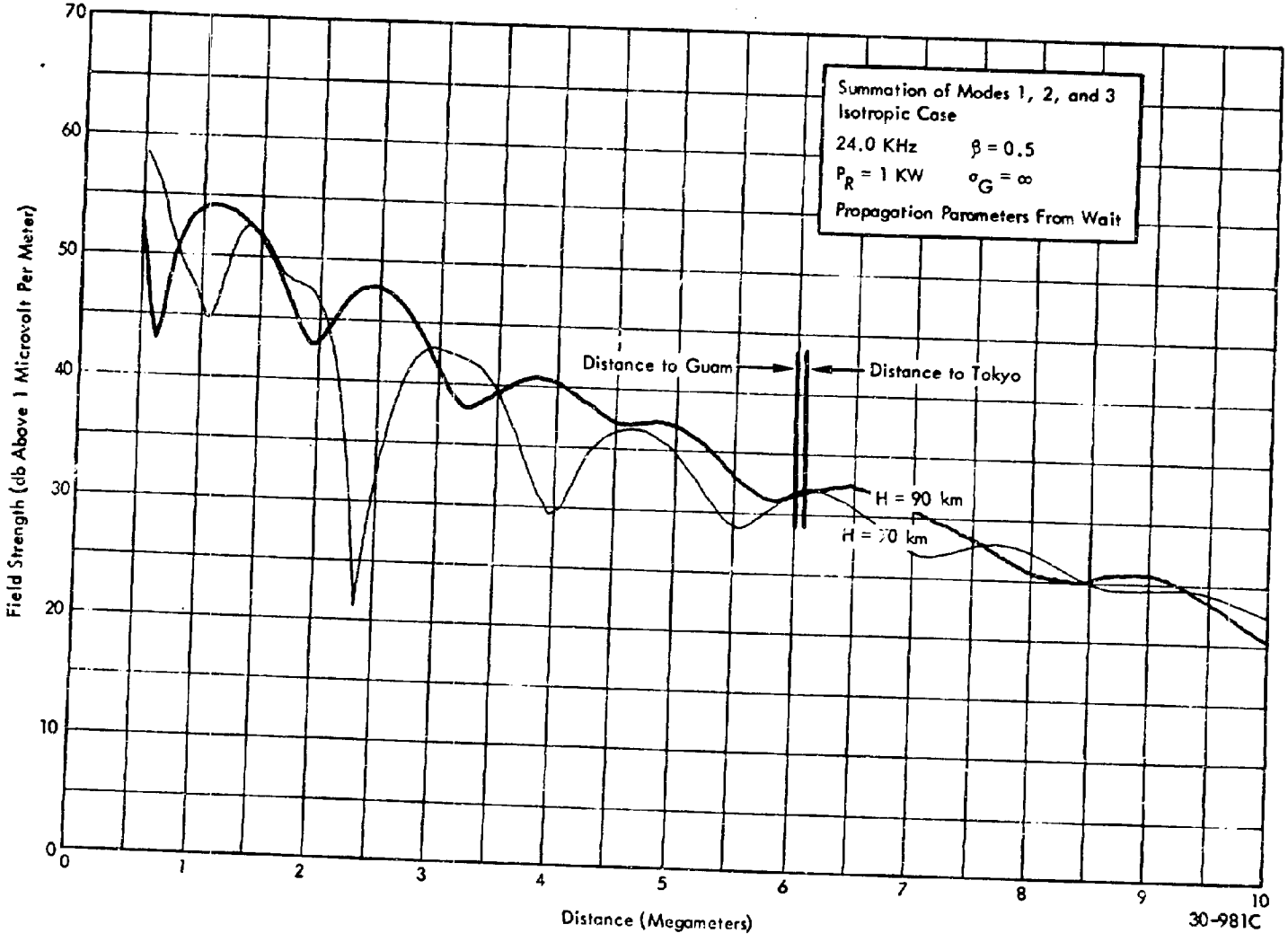

Figure D-3 Computed Field Strength

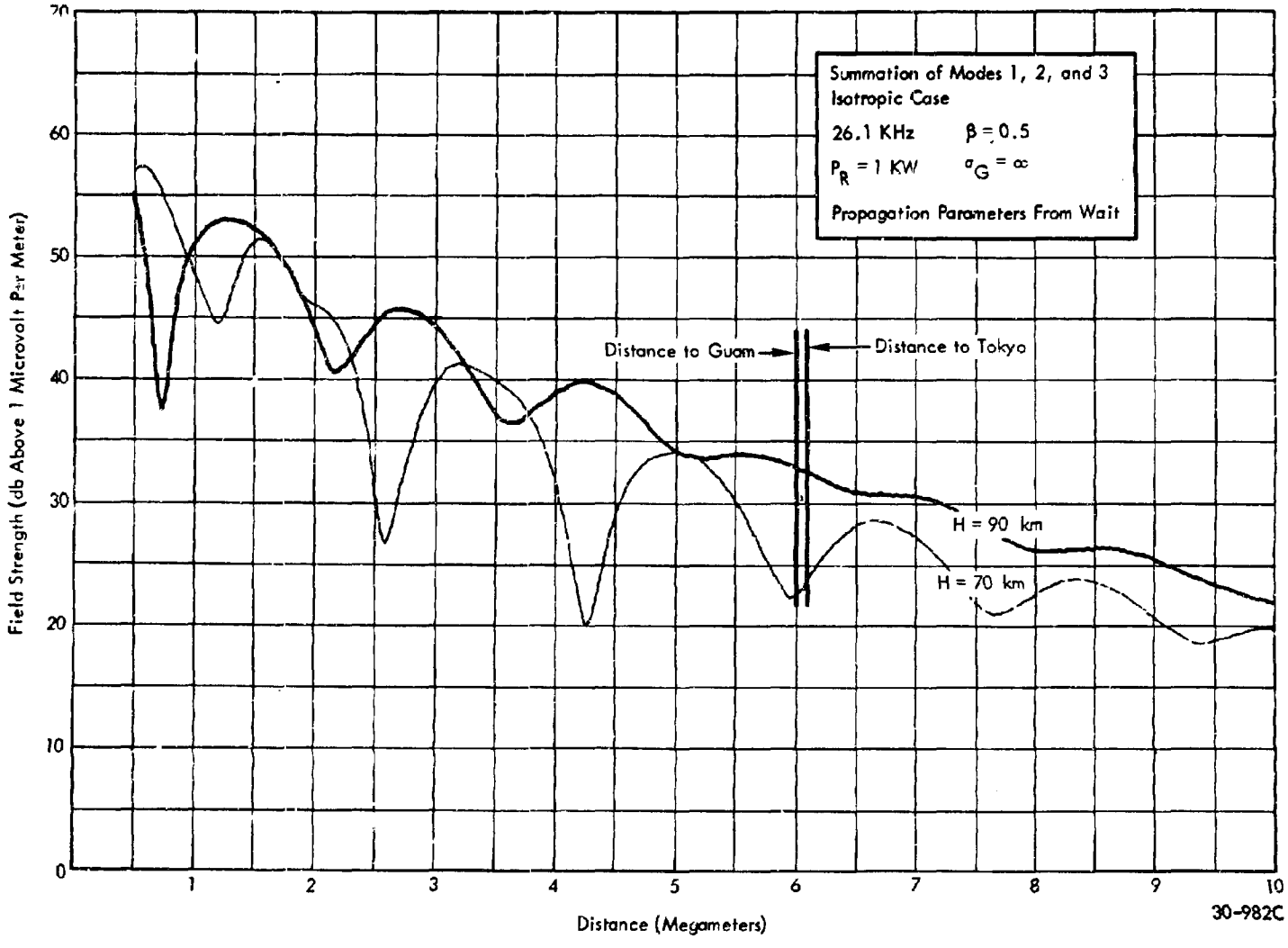

Figure D-4 Computed Field Strength

DECO 30-F-12
DECO Electronics, Inc., Boulder Division
VLF PROPAGATION AND NOISE MEASUREMENTS IN THE PACIFIC.
E. L. Maxwell, March 1966, 150 pp, graphs, appendices. Contract NOnr 3387(00)
Nr 371-580 Dated 15 December 1960

During May, June and July of 1965, the received field intensity from both VLF stations on Oahu Island, Hawaii were measured at Tokyo, Japan; Guam; and Boulder, Colorado. Atmospheric noise field intensities were also measured at all three sites and relative phase variations of the received signals were measured at Japan and Guam. This program presented a unique opportunity to study VLF propagation, since the paths from Oahu to Guam and Japan were almost the same length and were both all sea paths. The availability of two transmitters on Oahu which permitted simultaneous measurements at two VLF frequencies over the same path was also a unique opportunity. The results of this measurement program are presented in a number of ways in this report to afford maximum opportunity to study the propagation and atmospheric noise conditions.

The results show 22.3 and 24.0 kHz to be the best frequencies of those measured for the Oahu to Guam and Japan paths. Significantly, the diurnal variations of field intensity were very repeatable even during sunset and sunrise transition times which indicates that better predictions of VLF field intensities may be possible with an improved propagation model.

Means, medians, standard deviations, cumulative probabilities and diurnal variations of signal, noise and signal-to-noise-ratios have been computed, plotted and tabulated for all frequencies and for four hour time blocks and twenty-four hour periods. In addition, continuous plots of signal data for Japan and Guam are presented.

I Maxwell, E. L.
II DECO 30-F-12

DECO

DECO 30-F-12
DECO Electronics, Inc., Boulder Division
VLF PROPAGATION AND NOISE MEASUREMENTS IN THE PACIFIC.
E. L. Maxwell, March 1966, 150 pp, graphs, appendices. Contract NOnr 3387(00)
Nr 371-580 Dated 15 December 1960

During May, June and July of 1965, the received field intensity from both VLF stations on Oahu Island, Hawaii were measured at Tokyo, Japan; Guam; and Boulder, Colorado. Atmospheric noise field intensities were also measured at all three sites and relative phase variations of the received signals were measured at Japan and Guam. This program presented a unique opportunity to study VLF propagation, since the paths from Oahu to Guam and Japan were almost the same length and were both all sea paths. The availability of two transmitters on Oahu which permitted simultaneous measurements at two VLF frequencies over the same path was also a unique opportunity. The results of this measurement program are presented in a number of ways in this report to afford maximum opportunity to study the propagation and atmospheric noise conditions.

The results show 22.3 and 24.0 kHz to be the best frequencies of those measured for the Oahu to Guam and Japan paths. Significantly, the diurnal variations of field intensity were very repeatable even during sunset and sunrise transition times which indicates that better predictions of VLF field intensities may be possible with an improved propagation model.

Means, medians, standard deviations, cumulative probabilities and diurnal variations of signal, noise and signal-to-noise-ratios have been computed, plotted and tabulated for all frequencies and for four hour time blocks and twenty-four hour periods. In addition, continuous plots of signal data for Japan and Guam are presented.

I Maxwell, E. L.
II DECO 30-F-12

DECO

DECO 30-F-12
DECO Electronics, Inc., Boulder Division
VLF PROPAGATION AND NOISE MEASUREMENTS IN THE PACIFIC.
E. L. Maxwell, March 1966, 150 pp, graphs, appendices. Contract NOnr 3387(00)
Nr 371-580 Dated 15 December 1960

During May, June and July of 1965, the received field intensity from both VLF stations on Oahu Island, Hawaii were measured at Tokyo, Japan; Guam; and Boulder, Colorado. Atmospheric noise field intensities were also measured at all three sites and relative phase variations of the received signals were measured at Japan and Guam. This program presented a unique opportunity to study VLF propagation, since the paths from Oahu to Guam and Japan were almost the same length and were both all sea paths. The availability of two transmitters on Oahu which permitted simultaneous measurements at two VLF frequencies over the same path was also a unique opportunity. The results of this measurement program are presented in a number of ways in this report to afford maximum opportunity to study the propagation and atmospheric noise conditions.

The results show 22.3 and 24.0 kHz to be the best frequencies of those measured for the Oahu to Guam and Japan paths. Significantly, the diurnal variations of field intensity were very repeatable even during sunset and sunrise transition times which indicates that better predictions of VLF field intensities may be possible with an improved propagation model.

Means, medians, standard deviations, cumulative probabilities and diurnal variations of signal, noise and signal-to-noise-ratios have been computed, plotted and tabulated for all frequencies and for four hour time blocks and twenty-four hour periods. In addition, continuous plots of signal data for Japan and Guam are presented.

I Maxwell, E. L.
II DECO 30-F-12

DECO

DECO 30-F-12
DECO Electronics, Inc., Boulder Division
VLF PROPAGATION AND NOISE MEASUREMENTS IN THE PACIFIC.
E. L. Maxwell, March 1966, 150 pp, graphs, appendices. Contract NOnr 3387(00)
Nr 371-580 Dated 15 December 1960

During May, June and July of 1965, the received field intensity from both VLF stations on Oahu Island, Hawaii were measured at Tokyo, Japan; Guam; and Boulder, Colorado. Atmospheric noise field intensities were also measured at all three sites and relative phase variations of the received signals were measured at Japan and Guam. This program presented a unique opportunity to study VLF propagation, since the paths from Oahu to Guam and Japan were almost the same length and were both all sea paths. The availability of two transmitters on Oahu which permitted simultaneous measurements at two VLF frequencies over the same path was also a unique opportunity. The results of this measurement program are presented in a number of ways in this report to afford maximum opportunity to study the propagation and atmospheric noise conditions.

The results show 22.3 and 24.0 kHz to be the best frequencies of those measured for the Oahu to Guam and Japan paths. Significantly, the diurnal variations of field intensity were very repeatable even during sunset and sunrise transition times which indicates that better predictions of VLF field intensities may be possible with an improved propagation model.

Means, medians, standard deviations, cumulative probabilities and diurnal variations of signal, noise and signal-to-noise-ratios have been computed, plotted and tabulated for all frequencies and for four hour time blocks and twenty-four hour periods. In addition, continuous plots of signal data for Japan and Guam are presented.

I Maxwell, E. L.
II DECO 30-F-12

DECO